Author:
Claxton, Amanda Jane

Title:
Modelling water flow and chemical transport through floodplain systems

Modelling water flow and chemical transport through floodplain systems

Amanda Jane Claxton

A dissertation submitted to the University Of Bristol in accordance with the requirements of the degree of Doctor of Philosophy in the Faculty of Science.

School of Geographical Sciences, August 2002.

87 500 words

Abstract

This study uses a fieldwork-modelling research methodology to investigate hydrological pathways and chemical transport in floodplains and riparian zones, which occupy a key position in the landscape at the catchment-river interface. A numerical model is developed (ESTEL2D-SUBIEF2D) that is capable of modelling subsurface water and chemical movement at a high spatial and temporal resolution. The model is used in conjunction with data from two field sites (a lowland floodplain on the River Severn, UK, and a headwater riparian zone on Sleepers River, USA), and with hypothetical tracers, to quantify the effect of a range of factors on the operation of hydrological and biogeochemical processes in floodplain systems.

This study shows the relative importance of river and hillslope inputs of water and chemicals to the floodplain, and how the scale of hydrological event (overbank flow, bankfull flow and low flow) affects the interaction of these sources. For example, in the case of an overbank flood event, hillslope inputs can be held back by the steep hydraulic gradient induced by flood water for up to 10 days. A comparison of headwater and lowland floodplains is attempted for the first time and indicates that different hydrological processes operate in these two environments. This implies that results from existing smaller scale riparian zone studies cannot simply be 'scaled up' to larger, lowland floodplain zones.

The operation of the denitrification process within the floodplain is investigated as a relevant example of the more general transport modelling capability of the numerical code. This supports and extends the results of previous studies which have suggested that denitrification in the floodplain may be fundamentally limited by the interaction of hydrological processes and carbon availability. This comprehensive exploration of the full range of subsurface flow pathways through the floodplain highlights the importance of an understanding of hydrological pathways as critical to understanding chemical transport within the floodplain system.

Acknowledgements

First, I would like to thank my supervisors in Bristol, Paul Bates and Malcolm Anderson, for all their help and sound guidance throughout my studies. I would also like to thank Tim Burt in Durham for his comments and advice on the denitrification work. From the geography department, I would like to thank Ed Thomas and Dave Kilham for their assistance with everything computer-related, and Dave King for his help with the Severn field site equipment.

From the hydrology group, I must thank Mike Stewart, Roland Parrott, Catherine Wilson, Paul Wilkinson, Matt Horritt, Kate Marks, Thorsten Stoesser, Hannah Cloke, James Blake and JP Renaud, who have provided lots of day-to-day support and advice. Special thanks to Roland, Hannah and James, who all succumbed at some point to the promise of pasties from Much Wenlock and accompanied me on the many Severn field site trips.

I would like to thank Jeff McDonnell for giving me the opportunity to visit Oregon State University, and for accommodating me in the Department of Forest Engineering. In particular, I must thank Brian McGlynn at OSU, for providing access to the Sleepers River field dataset and for answering endless questions about it! I am also very grateful to Kendall, Jan, Petra, Dana, Kevin, Ilja and Tracie, for making my stay in Corvallis so enjoyable and so memorable.

I would like to say a special thank you to Hannah and JP for lots of assistance with the modelling work, for all their support, particularly when things were not going so well, and for the many excellent meals and glasses of homemade wine! Outside work, I would like to thank my housemate, Andy, for his great company, and Rob, Russ, Rachel and Stuart for their hospitality on my many visits to Sheffield. Thanks also to the ex-Beehive Roaders for beers, parties and festivals, and for not talking about floodplains! I also owe a great deal to Paul, who has been there for me through the highs and lows with lots of love and support.

Finally, I would like to thank my family, and above all my parents, Gill and Chris, as none of this would have been possible without their unfailing support and encouragement in everything I have chosen to do.

AUTHOR'S DECLARATION

I declare that the work in this dissertation was carried out in accordance with the Regulations of the University of Bristol. The work is original except where indicated by special reference in the text and no part of the dissertation has been submitted for any other degree.

Any views expressed in the dissertation are those of the author and in no way represent those of the University Of Bristol.

The dissertation has not been presented to any other University for examination either in the United Kingdom or overseas.

SIGNED: A. Claxton

DATE: 14th March 2003

Contents

List of Figures

List of Tables

1 Introduction

Floodplains have for millenia been preferred sites for human habitation, due to the proximity of water supply, fertile land for agriculture, and navigable waterways for trading (Marriott, 1998; Petts, 1998). Improvements in flood protection and land drainage techniques aimed at improving agricultural land and protecting people and property from flooding have led to extensive modification of floodplains worldwide (Bailey, 1998; Gardiner, 1998; Holmes, 1998). This has resulted in the loss of valuable habitat and reduced the ability of floodplains to perform their natural functions, which include:

- storage of floodwater giving flood defence benefit downstream;
- reduced risk of bank erosion;
- nutrient transformation and retention reducing loading from diffuse sources;
- potential for efficient aquifer recharge (after Holmes, 1998 and Maltby *et al.*, 1998).

In this chapter, an assessment of the need for an understanding of floodplain hydrological and chemical transport processes will be presented, followed by a brief outline of the thesis. This chapter will begin with an evaluation of the relevant terminology.

1.1 Terminology

The topic of floodplain water and chemical transport, which forms the focus of the present research, has been studied by a number of diverse yet interrelated subject areas, including ecology and hydrology in particular. The description of floodplain processes by different research communities has led to a slightly ambiguous terminology with regard to the near-stream area. Words such as riparian zone, floodplain, buffer zone and hyporheic zone are all used in this context, often interchangeably.

The term 'floodplain' is generally used in a geomorphological sense to describe the area beside a river that is inundated when the river floods. The term 'riparian zone' is derived from the Latin word *ripa*, meaning bank and shoreline (Gold and Kellogg, 1997) and was first used to refer specifically to the ribbon of deciduous plants that occurs along stream

banks (Stanford, 1998). The use of the term 'floodplain' is more generally associated with lowland rivers, and the term 'riparian zone' with headwater streams, although several researchers now use 'riparian zone' interchangeably with 'floodplain' in describing the near stream zone in headwater environments (Pinay and Burt, 2001).

The term 'hyporheic zone' is also used extensively in the near-stream literature. It may be defined as a subsurface region in unconfined, near-stream aquifers where mixing of stream water and groundwater occurs (Triska *et al.*, 1989, Wondzell and Swanson, 1999), although a range of definitions have been suggested for this term (Correll, 2000). The hyporheic interstices are functionally a part of both the fluvial and groundwater ecosystems (Brunke and Gonser, 1997). Ecotones such as this, which form a boundary between two ecosystems, are important regulators of the movement of energy and material through catchments, acting as both conduits and barriers.

Riparian buffer zones are areas of trees, shrubs or perennial grass located adjacent to streams, lakes, ponds and wetlands. Buffer zones are implemented as an environmental pollution remediation strategy, with the aim of preventing erosion, trapping sediments and nutrients from field runoff to protect water quality, and improving wildlife habitats (USDA-NRCS, 2000). They are a subset of the wider phenomenon of conservation buffers: "areas or strips of land maintained in permanent vegetation to help control pollutants and manage other environmental problems" (USDA-NRCS, 2000). Such conservation buffers (in this wider sense) may be located not only along streams, or around lakes and wetlands, but also within fields or at field edges.

1.2 The need for an understanding of floodplain processes

Very few papers on the water quality effects of riparian buffer zones were published before the 1970s (Correll, 1997). Research in this area began with a consideration of surface flow processes, and the scientific study of subsurface chemical movement through floodplains has been developing since the 1980s (Hedin *et al.*, 1998). In addition, although the longitudinal patterns and processes along river courses have long been recognised, it is only in the past two decades that the importance of interactive pathways in the lateral and vertical directions has been identified (Stanford and Ward, 1993).

From an ecological standpoint the dynamic convergence of aquifer-riverine components adds physical heterogeneity and functional complexity to floodplain landscapes, and they can thus sustain exceptionally high biodiversity (Stanford and Ward, 1993). Processes in the hyporheic zone appear to exert major influences on riverine species richness, bioproduction, and mass transfer of available materials and biota; as an ecotone or boundary, the hyporheic zone may modify or control the flow of material or energy between adjacent systems

(Hakenkamp *et al.*, 1993). Microbial transformation and transport of solutes in groundwaters has been shown to be an important source of nutrients for channel flora in streams and rivers (Stanford and Ward, 1993). From the hydrological viewpoint, the prevalence of surface and groundwater interactions in the floodplain region also gives these areas a central place in the hydrological cycle (Pusch *et al.*, 1998). The importance of viewing streams and groundwater as integrated components of a hydrological continuum is increasingly recognised (Brunke and Gonser, 1997).

Ultimately, the ecology and hydrology of near-stream environments are intimately linked, and each discipline is increasingly coming to recognise the necessity of the other for a holistic understanding of the near-stream environment. For example, geomorphological and groundwater controls are increasingly emphasised in studies of near-stream ecology (Stanford, 1998). Groundwater-surface water interactions exert major control on structural and functional attributes of stream ecosystems (Ward *et al.*, 1999) and any changes to the exchange processes that connect running waters to their surroundings will affect the ecological integrity of subterranean and surface water environments (Brunke and Gonser, 1997). In many river valleys, anthropic encroachment and human-induced change has occurred across floodplains and within river channels to the point where connectivity between these ecosystem subunits has probably been severed completely (Stanford and Ward, 1993). An improved understanding of the connectivity between channel, hyporheic and riparian attributes of river ecosystems will be an important step in any attempts at restoration of these systems.

Attitudes to floodplain areas are changing towards consideration of the possible negative impacts of floodplain development on surface and subsurface water, and there has been renewed interest in the broader ecological function of floodplain areas (Burt *et al.*, 1998). In particular, the concept that floodplains may have potential for controlling water-based pollution, particularly diffuse pollution from agricultural land (Dils and Heathwaite, 1996), and for conservation and catchment biodiversity (Norris, 1993; Haycock *et al.*, 1997; Burt *et al.*, 1998; Maltby *et al.*, 1998), has been the impetus for much of the research into floodplain chemical transport. Most of this work has focused on nutrients, sediments and pesticides. While point source pollution has been tackled with some success in recent years, non-point source pollution remains difficult to control because it is spatially ill-defined, and the principle contaminants are delivered to the stream environment along various dynamic pathways (Haycock *et al.*, 1997; Verchot *et al.*, 1998). The soil-stream interface is a crucial control point for nutrient fluxes between terrestrial and aquatic ecosystems because this area has unusually high potential for biogeochemical transformations (Dahm *et al.*, 1998; Hedin *et al.*, 1998).

Although the retention of nutrients within riparian buffer strips has been reported in numerous locations globally, the role of the riparian zone in regulating chemical movement remains unclear and has proved difficult to quantify (Haycock and Pinay, 1993; Cey *et al.*, 1999).

> There are now over 700 publications on the water quality functions of riparian buffers...and new studies are being published at an accelerating rate. However, our knowledge of the functions of these buffers is in many ways inadequate. This is an increasingly important problem, since in many parts of the world riparian buffers have become an important part of environmental landscape planning for watershed planning.
>
> (Correll, 2000)

Riparian buffers have indeed been implemented as part of environmental pollution management strategies. To date, one of the most notable schemes involving riparian buffers is the National Conservation Buffer Initiative, launched in April 1997 by the United States Department of Agriculture (USDA). The aim of this scheme is to help agricultural producers and other landowners install two million miles of conservation buffers throughout the United States by the year 2002, to protect soil, air and water quality, and improve fish and wildlife habitat (NRCS, 1997). The scheme has been supported by nine federal agencies, the National Conservation Buffer Council (consisting of seven private sector firms), and more than 75 non-profit agricultural and environmental organisations, collectively termed the National Conservation Buffer Team. Financial incentives are available to landowners who sign up to the initiative. This is clearly a very significant scheme, and illustrates the way in which many public and regulatory agencies have accepted the scientific conclusion as to the value of riparian buffers for protecting water quality. In many ways, the demand for information and utilisation of the practice is advancing faster than the science (Gilliam *et al.*, 1997).

Development and implementation of successful control strategies depends on knowledge of the solute source areas and the transport pathways involved (Withers and Jarvis, 1998), but guidelines for buffer zone establishment remain vague. Conflict about the optimal use of these areas is likely to increase in the near future (Bren, 1993), and the economic cost of returning floodplains to a more 'natural' condition may be high (Withers and Jarvis, 1998). Buffer zones require maintenance and management, and may take valuable agricultural land out of production, so there may be tremendous resistance by landowners to installing a 5-30 m buffer (guidelines vary), where no vegetated buffer currently exists. A sound understanding of physical processes on which to base management decisions is therefore of critical importance.

A restrictive feature of floodplain/riparian zone research to date is that it has tended to concentrate on upland streams, with relatively few studies of lowland rivers. The reasons for this are clear; small experimental catchments are used because they generally require less instrumentation to characterise the system behaviour, and it is easier to gain a 'whole-catchment' perspective from which to develop process understanding. However, with the great diversity of near-stream environments in upland and lowland situations, it is perhaps unrealistic to expect that a mere 'scaling-up' of upland riparian zone processes will accurately represent processes in the larger, lowland floodplain configuration. It is reasonable to expect that there may be process differences between these two extremes, but the current lack of lowland floodplain research makes it very difficult to quantify this notion.

Most studies of the near-stream environment have been conducted in the field; there are fewer examples of studies where a numerical modelling approach has been used. Current models are often constrained by their assumptions, which are unsuited to modelling the near-stream zone, or they do not have the capacity for modelling chemical transport in addition to saturated-unsaturated water movement. However, the growing recognition of the great spatial and temporal variability of floodplains has resulted in the realisation that field studies alone may be insufficient to unravel the underlying processes (Jolly *et al.*, 1998). The application of a suitable numerical model (or a combined fieldwork-modelling approach) to the investigation of floodplain water and chemical transport problems is a technique that may enhance interpretation of field data, and provide an opportunity for scenario testing which may offer new insights into process operation.

1.3 Thesis outline

This work will focus on developing a numerical code specifically suitable for modelling subsurface hydrological processes and chemical transport in both headwater and lowland systems. The application of this model will enable identification of the effect of a range of controlling factors on process operation in this dynamic environment, in a way that has hitherto not been possible.

Chapter 2 presents the research context from which this study has arisen. In reviewing the current state of floodplain water and chemical transport research, particular consideration is given to the field and modelling techniques used in previous studies, and the advantages and disadvantages of particular approaches. This provides the justification for the research gap that is to be pursued during the course of this study. The particular aims, objectives and research methodology that are employed to investigate this research gap are then presented.

Chapter 3 describes the development of the numerical model, implemented in two stages: stage one involves the development of a conceptual model, describing how the system is

believed to operate, and stage two (the numerical model development) involves establishing how the conceptual model will be expressed in mathematical terms, and how the resulting set of equations will be solved. The model performance is then initially evaluated against an analytical solution.

Chapter 4 covers the development of further model features that are required before the model can be implemented in the near-stream environment. The first is an ability to simulate complete saturation within the variably saturated model domain, which involves a consideration of the mechanisms which effect changes in the stored fluid mass of the soil. The second is the ability to account for a seepage boundary condition. The assumptions and capabilities of the final numerical model are presented.

Chapter 5 explores issues surrounding the testing of physically-based models, in terms of verification, optimisation, sensitivity analysis, calibration and validation. A model testing strategy suitable for this study is identified, along with the final field site selection. The results of the model tests are then presented and analysed. The assessment process is carried out with the aim of establishing confidence in the operation of the model, so that it can be taken forward to the next stage of hypothesis testing.

Chapter 6 looks at the process inferences that can be drawn from the model assessment results presented in Chapter 5. The factors controlling hydrological and chemical transport processes operating in floodplain environments are then explored more fully using a hypothetical (conservative) tracer to investigate specific hypotheses.

Chapter 7 explores the potential of the model to look at the importance of a range of controlling factors on chemical transport and transformation (of a non-conservative tracer) in the near-stream environment. This focuses on the denitrification process, as a relevant example of the more general chemical transport modelling capability of the numerical code. Mathematical equations used to model the denitrification process are reviewed, and the denitrification formulation chosen for this study is presented. This part of the model is then subjected to a model assessment procedure before being used in a series of hypothetical scenarios.

The thesis ends with a summary showing how the work in this study has responded to the research gap identified in Chapter 2. This includes a discussion of the major achievements and limitations of the work, and the identification of avenues for further research.

1.4 Chapter summary

The soil-stream interface is perhaps the most obvious and important control point along paths of nutrient flux from terrestrial to aquatic ecosystems. It has an unusually high

potential for biogeochemical transformations, and it can intercept and rapidly transfer nutrients from the surrounding terrestrial watershed to the aquatic environment (Hedin *et al.*, 1998). Floodplains and riparian zones therefore form transitional boundaries between terrestrial and aquatic ecosystems, and occupy an important position at the catchment-river interface.

The key position occupied by floodplains within the landscape means that any modification of this zone has the potential for repercussions in flood routing, the movement of biota between land and water ecosystems, and the transfer of water, sediment, and chemicals (including nutrients and pesticides) to water courses, resulting in impacts on stream and drinking water quality. Management of this zone, particularly if implemented as part of a buffer zone initiative, may also have associated economic costs, both as a result of the extra demands for maintenance, and as a consequence of taking valuable agricultural land out of production.

Despite their importance, floodplain hydrological and chemical transport processes are relatively poorly understood. The fact that the study of floodplain processes has fallen between standard academic divisions may have contributed to the lack of a holistic approach to floodplain research, with each subject area considering separate parts of the floodplain system in isolation. Although this situation is beginning to change, such a holistic viewpoint has yet to be explored in detail.

2 Floodplain Hydrological and Chemical Transport Processes

Chapter 1 has illustrated the need for an understanding of floodplain hydrological and chemical transport processes, highlighting the critical position that floodplains occupy at the catchment-river interface, and the potential environmental and economic consequences involved in development and management of floodplain landscapes.

Chapter 2 aims to develop the specific aims and objectives to be investigated during this project. In order to achieve this, the context of the wider subject of floodplain hydrological and chemical transport processes will be explored in some detail, with consideration of the methods employed to explore this subject to date, the current state of process knowledge, and areas which require further investigation.

2.1 Development of floodplain water flow and chemical transport research

This section aims to explore how previous studies have contributed to the field of floodplain hydrological and chemical transport research. The history of this subject can be conveniently broken down into four main phases of related investigation: bank storage research, hillslope-channel connection research, hyporheic zone (surface-groundwater interaction) research, and buffer zone research. Each of these topics will be presented in terms of a description of the research area and its importance, the approach that researchers have taken in terms of fieldwork and modelling, and how knowledge of the subject is currently limited.

2.1.1 Bank storage research

River channels have long been thought of as conduits for water and chemical transport, but until the 1950s little serious consideration had been given to how they interacted with the surrounding landscape. Identification of the bank storage phenomenon was perhaps the first time that this interaction was recognised. In many cases, the bed and banks of river channels are composed of permeable sediments through which water can be transmitted. Depending

on the local hydraulic gradient, water may travel from the channel into the surrounding floodplain, or from the floodplain into the channel. When the river stage rises above the level of the water-table in the floodplain during flood events, a net flux of water into the floodplain is induced (Whiting and Pomeranets, 1997). This water is stored temporarily and then released during river flow recession as the river level drops but floodplain water-tables remain high (Figure 2.1). This process and the volume of water that is stored and released from the channel bed and banks is called bank storage (Todd, 1955). Bank storage is a significant hydrological process, as it can reduce and delay the flood peak of a river, and can contribute substantial discharge to rivers during baseflow (Squillace, 1996).

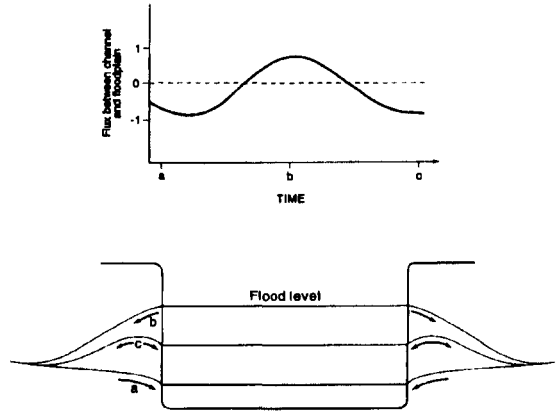

Figure 2.1 The bank storage process. At time (a) the river is receiving baseflow, at time (b) a flood peak is passing and flow is induced into the banks, and at time (c) the peak has passed and the bank-storage wedge is draining (from Burt et al., *2002).*

As well as the implications for hydraulic routing, this process also has important physical, chemical and ecological consequences for river systems (Whiting and Pomeranets, 1997). Baseflow generated by the bank storage process may play a role in sustaining riparian vegetation and aquatic organisms, increasing habitat diversity. In addition, bank storage affords an opportunity for transforming and immobilising chemicals, including nutrients and pollutants, transported by river water (Peterjohn and Correll, 1984).

A combined strategy of numerical modelling and fieldwork has been employed in two recent studies of the bank storage phenomenon. Squillace (1996) constructed a transient two-dimensional groundwater flow model to quantify the movement of bank storage water, using the US Geological Survey's modular finite-difference groundwater flow model MODFLOW. This modelling work was combined with a field study of bank storage water in Iowa, USA. The area represented by the model was a 320 m-long cross-section through the floodplain from the hillslope to the river channel, extending to a depth of 30 m (Figure 2.2). The

calibrated model indicated that a 2 m rise in river stage caused bank storage water to move horizontally at least 30 m into the floodplain aquifer, and vertically about 4 m below the river bed. It also illustrated that bank storage water moving through the river bed can be a significant portion of the total bank storage, at least in the case of this wide and shallow river. This study was restricted to a two dimensional representation only, and the influence of down-valley flow across the floodplain was not considered. Groundwater discharge was only to the river, and recharge could occur from the river, precipitation, and an ephemeral stream. No hillslope inputs were considered, but this was justified in this case by the presence of very low permeability sediments at the hillslope boundary of the floodplain.

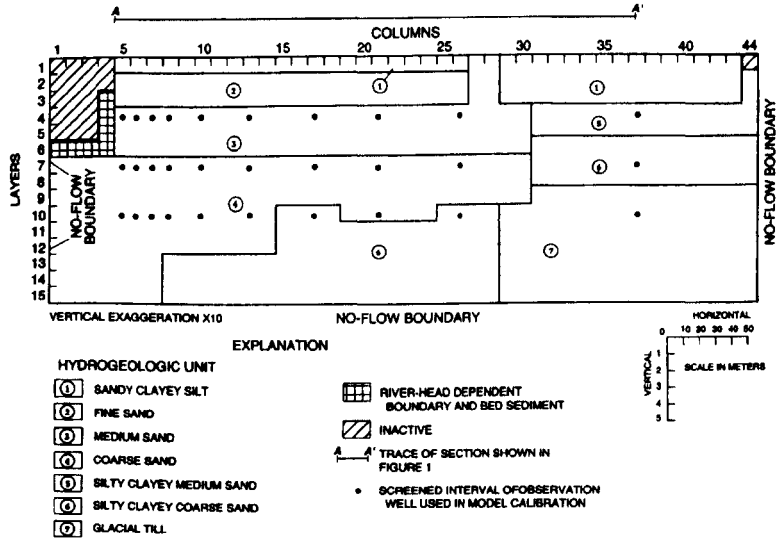

Figure 2.2 Domain used for the MODFLOW bank storage flow modelling study, showing model grid, extent, and simulated hydrogeologic units (from Squillace, 1996).

Whiting and Pomeranets (1997) modelled the response of floodplain flow to rapid changes in water stage in a river channel. In tackling this problem they recognised an important limitation of many of the widely known groundwater modelling packages such as MODFLOW when applied to the near-stream area. As these models are designed to model extensive regions they make use of the simplifying Dupuit-Forcheimer assumptions, which state that head is constant along any vertical and the hydraulic gradient is equal to the slope of the free surface. This decreases the complexity of the model, but makes it unsuitable for use in situations where the free surface is significantly sloped, as occurs in near-stream areas when river stage is changing rapidly (Whiting and Pomeranets, 1997). Consequently, they developed an exact, traditional model describing time-dependent unconfined saturated groundwater flow, WaTab2D, solved using finite-element techniques. This study indicated

that the amount of water stored in the banks, and thus potentially available for release, is greater in valleys that are wide, with channels that are deep, and where the floodplain material is coarse. The time frame over which water in bank storage contributes to baseflow is dependent on hydraulic conductivity, specific yield, width of the valley, and water-table drop. This will clearly impact upon water residence time and therefore chemical transport and transformation in the floodplain and the channel.

While these investigations have been valuable in quantifying the timing and extent of the bank storage process they are limited in several ways. There has been little consideration of the impact of down-valley, three-dimensional flow processes. The studies have also been restricted to in-bank flow events and do not consider the hydrological or chemical implications of overbank flow, or interactions with other water sources external to the river channel (for example, inputs of water from adjacent hillslopes). Where models have been used, their utility is sometimes compromised by the limiting assumptions that have to be made when representing this highly spatially variable and temporally dynamic environment.

2.1.2 Hillslope-channel connection research

Since the 1970s, hillslope hydrological research has been concerned with investigating the flow processes within the soil and over the soil surface responsible for generating and controlling runoff to river channels from the wider catchment (Anderson and Burt, 1990). A number of different routes by which hillslope water can reach the river channel have been identified. These hydrological pathways are important in terms of controlling the timing and peak rate of runoff, and also the chemical characteristics of input water (Burt, 1997).

The prevailing conceptual model of hillslope hydrological flow pathways is illustrated in Figure 2.3. Within this framework, several physical components of the hillslope discharge in response to a rain event are identified: infiltration-excess overland flow, saturation-excess overland flow, return flow, saturated subsurface flow, and groundwater flow. The processes that deliver stormflow are found to vary with factors such as topography, soil properties, and rainfall characteristics, and indirectly with climate, vegetation, and land use (Dunne, 1978). It is evident that this conceptual model includes no formal representation of the floodplain and its effects on streamflow generation and runoff processes.

Part of the reason for this lack of consideration of floodplain influences is that much of this research has concentrated on headwater basins, particularly in humid agricultural landscapes, where slopes directly adjoin the channel (Hill, 1996; Burt, 1997). These catchments provide a more manageable research environment and provide the opportunity for a whole-catchment perspective. However, this has the result that hydrological theories of runoff generation have been developed for a narrow range of environments, with a limited range of data sets, and

the effect of floodplains on these theories has not been fully investigated. If the runoff flow path and chemistry from hillslopes can be modified by floodplains before reaching the river, then clearly hillslope hydrological processes are only part of the explanation of streamflow generation and river water quality.

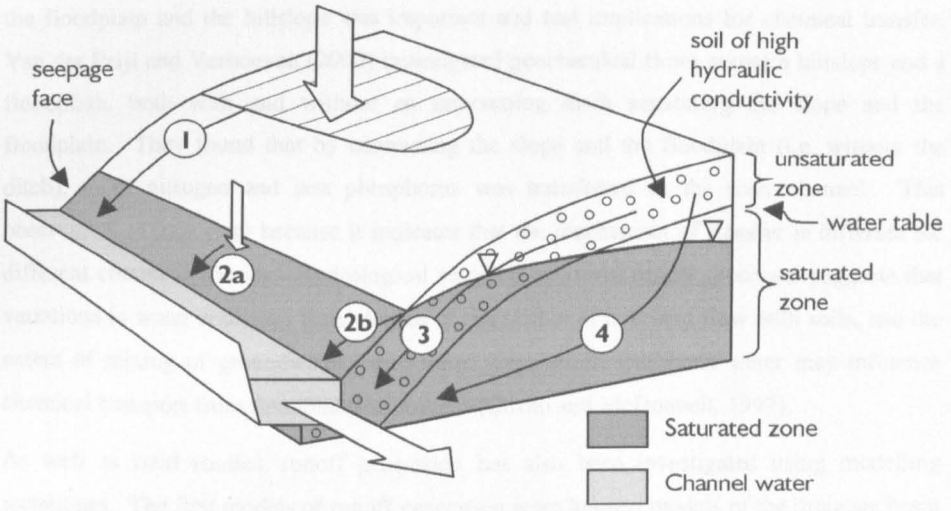

Figure 2.3 Conceptual model of hillslope hydrological processes, showing the hydrological pathways involved in the delivery of rainfall to a stream channel. 1. Infiltration-excess overland flow. 2. Saturation-excess overland flow: 2a. direct runoff; 2b. return flow. 3. Subsurface stormflow. 4. Groundwater flow (from Burt and Haycock, 1996).

Studies of hillslope-channel connections that include a floodplain have really only developed during the 1990s. When a floodplain is introduced to the streamflow generation problem, two factors become important; understanding the entry of runoff on to the floodplain (external flow pathways, including contributions from hillslopes in the form of overland storm flow and subsurface contributions, and contributions from the river channel, in the form of overbank flood flow and subsurface bank storage), and understanding the hydrological processes of the floodplain itself (internal flow pathways). The few studies on this subject consider different aspects of this flow system. Haycock and Pinay (1993) conducted a field study of groundwater nitrate dynamics at two sites in southern England and investigated subsurface water flow and nitrate contributions from the hillslope to the floodplain. Haycock and Burt (1993) considered that flow contributions to the floodplain might come from three possible sources; the hillslope, the stream, and down-valley water movement from the upstream edge of the floodplain. Flows from the floodplain to the river channel may take the form of overland flow (where springs emerge near the base of the hillslope), and subsurface flow, where water flows up through the floodplain soil and enters the stream directly as bed and bank seepage (Hill, 1996).

The nature of the connection between the hillslope and the channel clearly has implications for the chemical characteristics of floodplain and river water (Correll, 1997), and this has recently been the subject of several studies. Heppell *et al.* (1999) looked at the hydrological routes and controls on leaching of a herbicide from an agricultural clay hillslope to the adjacent ephemeral stream. Where a floodplain was present, hydrological connectivity of the floodplain and the hillslope was important and had implications for chemical transfer. Van der Peijl and Verhoeven (2000) investigated geochemical flows across a hillslope and a floodplain, both with and without an intervening ditch separating the slope and the floodplain. They found that by connecting the slope and the floodplain (i.e. without the ditch), more nitrogen and less phosphorus was transferred to the river channel. This observation is important because it indicates that the mechanism of transfer is different for different chemical species. Hydrological research on storm runoff processes suggests that variations in water residence time, degree of interaction of overland flow with soils, and the extent of mixing of groundwater, unsaturated zone water, and event water may influence chemical transport from floodplains to streams (Cirmo and McDonnell, 1997).

As well as field studies, runoff generation has also been investigated using modelling techniques. The first models of runoff generation were lumped models of the drainage basin (Flügel and Smith, 1999). However, the 1970s and 1980s saw the development of physically based distributed models, which have the capability of forecasting the spatial pattern of hydrological conditions within a catchment as well as the discharge outflow. Hillslope hydrologists were able to take advantage of this advance to improve representation of heterogeneous hillslope-channel connections in order to investigate the nature of runoff generation processes in more detail. Freeze (1978) presented a mathematical model of hillslope-channel hydrological processes, which consisted of three separate models of subsurface flow, overland flow, and channel flow. At this early stage, however, no consideration was given to the effect of an intervening floodplain. Another example of hillslope-channel hydrological modelling is the Variable Source Area Simulator (VSAS), which addresses the dynamic nature of the surface and subsurface flow of the contributing drainage area to a river channel (Troendle, 1985). More recent modelling efforts have included an integrated process study and model simulation of the hydrological dynamics of hillslope drainage by Flügel and Smith (1999). However, this study was still restricted to steep, mountainous catchments where hillslopes directly adjoin the channel, and the model took no account of the feedback from the water level in the adjacent channel. Despite the development of the mathematics for physically-based modelling of streamflow generation in the 1970s, very few hillslope hydrological flow path models have been developed to date (Flügel and Smith, 1999).

Within models of watershed hydrological processes, hillslope-channel connections and floodplain flow processes have mostly been crudely treated as the model structure and grid scale fail to capture key flood flow attributes (Anderson *et al.*, 1996). For example, in SHETRAN, a model of basin scale hydrological processes developed from the Système Hydrologique Européen (SHE) model (Abbott *et al.*, 1986a), channel reaches are represented in one dimension only (Figure 2.4). In addition, the channel system is represented only on the boundaries of the grid squares with dimensions of the order of 100 by 100 m, resulting in a very poor resolution of the channel system and associated floodplain areas (Parkin *et al.*, 1996).

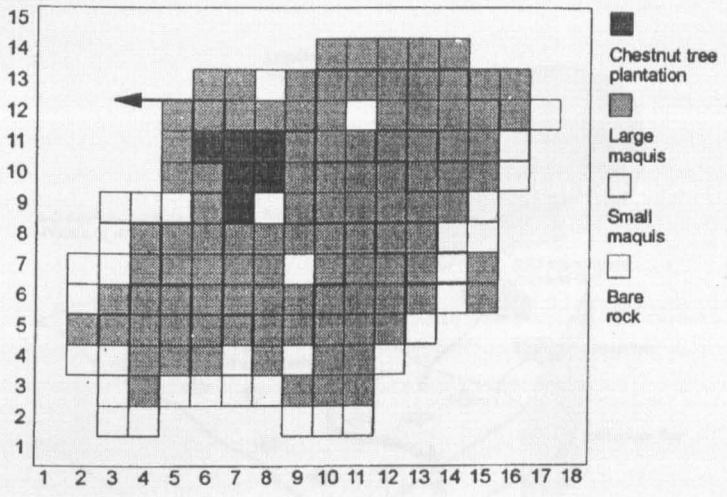

Figure 2.4 SHETRAN grid network and channel system for the Rimbaud catchment, showing also the modelled vegetation distribution (from Parkin et al., *1996).*

The current generation of two dimensional hydraulic models (RMA-2, TELEMAC2D) enable the channel to be resolved separately from the floodplain (Bates *et al.*, 1997) and offer a much greater resolution of floodplain surface flow processes than had been available with the SHE model (Gee *et al.*, 1990). However, modelling with RMA-2 and TELEMAC2D is restricted to surface floodplain and channel flow only, presuming zero-flux conditions at the hillslope boundary of the floodplain, and zero-flux across the channel bed, banks and floodplain surface. The next stage in model development has been to relax these zero-flux boundary conditions, by coupling TELEMAC2D with other models that can provide the necessary inputs. Price (1997) combined TELEMAC2D (a 2D finite element hydraulic model), with a 1D infiltration model. This was extended by Bates *et al.* (1996) who combined TELEMAC2D with a pseudo 3D hillslope hydrological flow path model and

the 1D infiltration model, in order to relax the second zero-flux boundary at the hillslope-floodplain interface.

The latest modelling effort in this area was undertaken by Stewart *et al.* (1999), who combined a two-dimensional floodplain hydraulic model with a lumped catchment runoff model, a hillslope hydrological flow path model, and a one-dimensional floodplain infiltration model, illustrated schematically in Figure 2.5. This approach examined overbank flood flows and overland hillslope inputs, but no consideration was given to linkages between the hillslope and floodplain subsurface components, and there was only a unidirectional flux from the hillslope to the channel. Rainfall on to the floodplain was also not considered.

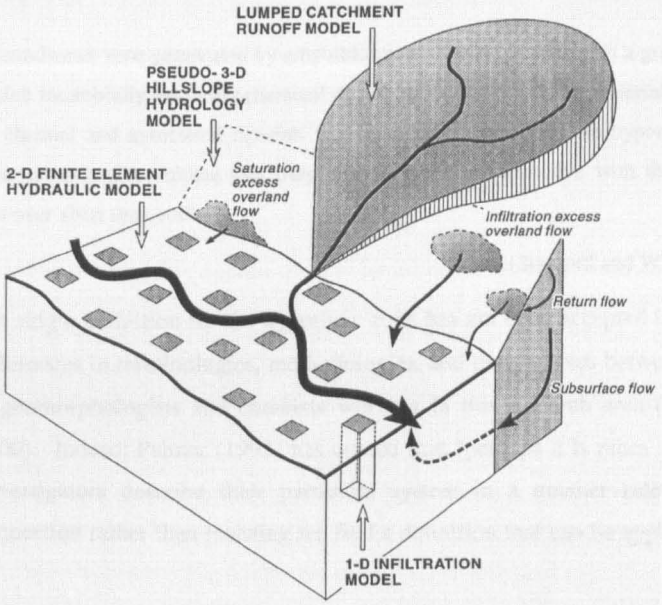

Figure 2.5 Schematic representation of the combined hydrological/hydraulic model (Stewart et al., *1999).*

A consequence of the extensive, reach-scale nature of these coupled hydrological-hydraulic modelling studies has been a lack of sufficient data with which to validate model results. Although these simulations have helped constrain estimates of water fluxes, they have not led to an improved process understanding. However, they have demonstrated that process complexity has hitherto been subsumed in the calibration procedure (Bates *et al.,* 1996), and have led to the recognition of a need for a subsurface hydrological floodplain model.

It seems that the influence of floodplains in relation to hillslope-channel connections is only starting to be explored in detail. Although research has been conducted on various aspects of

the hillslope-floodplain-channel system, there has been little attempt to bring all the potential water and chemical flow pathways together in one study at a scale that would allow sufficiently detailed analysis.

2.1.3 Hyporheic zone and surface-groundwater interactions research

This section can be broadly described as looking at the study of the interaction of surface water and groundwater. This somewhat all-encompassing initial standpoint emphasises that there is as yet no general agreement on what constitutes a hyporheic zone. Triska *et al.* (1990), stated that the hyporheic zone may be defined by the penetration of river water into fluvial deposits within the active channel and laterally and vertically through floodplain substrata. Stanford and Ward (1993) state three different ways of defining the hyporheic zone:

> ...it is a groundwater zone penetrated by amphibiontic stream organisms; it is a groundwater zone in which microbially mediated chemical dynamics exert controls on material cycles in the active channel and associated riparian vegetation; and physically the hyporheic zone includes the groundwater volume that may be hydraulically interactive with the channel hydrograph over short time scales.
>
> (Stanford and Ward, 1993)

The fact that a single definition for the hyporheic zone has not been accepted is due in large part to the differences in terminologies, methodologies, and perspectives between biologists, hydrologists, geomorphologists and chemists working in this research area (White, 1993; Woessner, 2000). Indeed, Palmer (1993) has argued that "perhaps it is more worthwhile to insist that investigators describe their particular system in a manner relevant to their experimental question rather than insisting we find a definition that can be applied across all streams".

The study of surface-groundwater interactions is closely related to hyporheic zone research. However, Harvey and Wagner (2000) describe the two fields as being subtly different, hyporheic interactions involving repeated interaction of surface and groundwater, while surface-groundwater interactions involve groundwater flow paths that enter or leave the channel only once. It is quite likely that this distinction is not always made clear in the literature. Although the discussion presented here will concentrate on the interaction of streams and rivers with a contiguous alluvial aquifer, it should be recognised that types of surface water involved in surface-groundwater interactions may also include lakes, wetlands and oceans (Winter, 1995).

Interactions between the stream and surrounding catchment have traditionally been viewed as unidirectional. The stream is effectively a pipe receiving water and solutes from the

catchment, but the pipe functions purely as the conduit for transport. For many studies of stream ecology, these ideas of compartmentalised zones and processes may provide a sufficient context for interpretation (Bencala, 1993). An alternative, more holistic, approach views the stream as an integral part of the catchment, and focuses on the dynamic, bidirectional nature of connections within the system. Adopting this viewpoint moves away from the idea of there being a physical spatial zone defined and identified as the 'hyporheic zone'. Instead, the part of the continuum that contains water of both surface and subsurface origin becomes the dynamic hydrological connection between streams and catchments (Bencala, 1993). This approach also recognises the idea that lotic systems are active along three spatial dimensions. The longitudinal dimension has long been acknowledged, but it is only in more recent work that the importance of interactive pathways in the lateral and vertical directions has been recognised (Triska *et al.*, 1990, White, 1993).

Prior to the 1980s, work on the hyporheic zone was largely led by ecologists, but the contemporary era of hyporheic zone research, stimulated by the work of Hynes (1983), has focused attention on the need for integration of groundwater hydrology and stream ecology. This ongoing process of integrating academic disciplines is advancing understanding of the influence of hydrological processes on hyporheic ecological communities and processes (Valett *et al.*, 1993). Surface-groundwater interactions exert a major control on structural and functional attributes of stream ecosystems (Ward *et al.*, 1999), adding physical heterogeneity and functional complexity to floodplain landscapes and sustaining exceptionally high biodiversity (Stanford and Ward, 1988, 1993). This region can be regarded as a crucial point in the landscape for controlling lateral chemical fluxes between uplands and aquatic ecosystems (Dahm *et al.*, 1998), and as hyporheic flow can process a large percentage of the total volume of river flow along a river channel (Fernald *et al.*, 2000), it has the potential to have a substantial impact upon river water quality.

This recognition of streams and groundwater as integrated components of a hydrological continuum has led to the appreciation that human impacts on terrestrial and aquatic systems may lead to reductions in the exchange processes that connect streams to their surroundings, and thus diminish the ecological integrity of both surface and subsurface water environments (Brunke and Gonser, 1997). Understanding how water within the alluvial aquifer and water within the stream channel interact is critical to efforts attempting to protect both groundwater and surface water resources (Woessner, 2000).

There has been a great deal of field work carried out in this area of study, using a wide variety of techniques, the measurements from which are regularly interpreted using mathematical hydrological models. Groundwater inflow and outflow can be determined from stream-flow discharge measurements, which offer a straightforward and efficient

means to constrain net groundwater fluxes. Determination of hyporheic exchange fluxes involves use of one of the following methods: Darcy-groundwater-flux calculations from measurements of water levels in wells, piezometers and piezometer nests; direct measurements of water fluxes across the streambed using devices such as seepage meters; or tracer based approaches (using introduced or environmental tracers).

The Darcy approach uses two-dimensional contour maps of hydraulic head, estimates of hydraulic conductivity of the near-channel sediment, and the basic governing equations for groundwater flow in order to calculate groundwater fluxes across a streambed (Harvey and Wagner, 2000). Wondzell and Swanson (1996), and Wroblicky *et al.* (1998) used MODFLOW to calculate hyporheic fluxes, and Harvey and Bencala (1993) used a finite difference modelling approach to the same problem. Hydraulic measurements and the flow pathways inferred from them indicate that streambed fluxes can be directed both into and out of the channel and that the direction of the flux can be affected by streambed topography and channel features such as meander bends (Harvey and Wagner, 2000). Inevitably there are uncertainties associated with this approach, particularly with selecting an appropriate number and distribution of monitoring locations to characterise the flow system, and also with characterising the hydraulic conductivity of the streambed sediments.

The use of seepage meters for direct measurement of hydrologic fluxes across the streambed is a relatively new approach (Wroblicky *et al.*, 1998). Whilst they have been tested extensively in test tanks and lakes, their performance in a stream environment has not been so thoroughly evaluated (Harvey and Wagner, 2000).

Tracer based studies may use naturally occurring tracers, such as water temperature (e.g. White *et al.*, 1987), or introduced tracers, such as chloride or bromide (e.g. Triska *et al.*, 1993), as an indication of hyporheic flow pathways. Hill and Lymburner (1998) confirmed that the extent of stream-groundwater exchanges can be successfully estimated using naturally occurring background conservative ions as a tracer technique. They delineated the hyporheic zone using a chemical mixing equation based on differences in background stream and groundwater chloride concentrations. In a typical introduced stream tracer experiment, the non-reactive solute tracer is injected into the stream at a constant rate, and concentrations of the tracer are monitored over time at several points downstream. A simple one-dimensional model for in-stream tracer transport is then used to simulate the field data, thereby linking the field measurements to advection and longitudinal dispersion in the channel, groundwater inflow, and hydrologic retention (storage) in surface or subsurface zones (Harvey and Wagner, 2000). While tracer experiments provide a good method for characterising the cumulative effects of storage processes in catchments, only certain timescales and dimensions of hyporheic processes are accessible through stream-tracer

experimentation, as illustrated in Figure 2.6. In fact, any particular method of investigation is likely to provide insight into only a limited subset of the entire spectrum of hyporheic flow paths that are present.

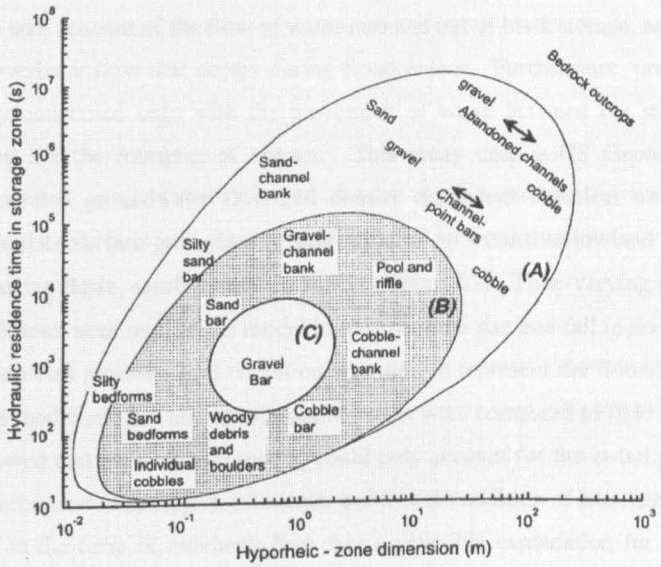

Figure 2.6 Spatial and temporal domain of hyporheic interactions and relation to roughness features in channels. The part of the domain with longer timescales and larger spatial scales of hyporheic interactions (A) is generally inaccessible to detection by stream tracers. The region that is typically accessible by stream tracers is shown by B. Region C shows a typical window of detection for a single tracer experiment (from Harvey and Wagner, 2000).

The use of these alternative techniques highlights the importance of scale considerations in surface-groundwater research. Hydrological exchange processes in alluvial floodplains occur along several major pathways operating at different scales (Sear *et al.*, 1999; Ward *et al.*, 1999; Zijl, 1999). Scales of near-channel hyporheic exchange may range from centimetres to tens of metres depending on bed geometry and hydraulic potentials (Woessner, 2000). On a wider surface-groundwater interaction scale, flow paths from the wider catchment to the river may be composed of local groundwater flow through the floodplain, and/or regional groundwater flow by-passing the floodplain (van Lanen and Dijksma, 1999). It is important to understand the position of the floodplain in relation to local and regional flow systems as differences in the residence time and in the environment encountered by groundwater travelling by various hydrologic pathways within the floodplain may also have implications for stream and groundwater chemistry (Hill, 1996; Duff and Triska, 2000). The restriction of the majority of studies to riparian zones of low order

streams in humid landscapes (Winter, 1995; Stanley and Jones, 2000) may have had a significant impact on the scale of hyporheic flow paths that have been identified to date.

A recent modelling study by Jolly *et al.* (1998) has aimed to explore the impact of flooding on salt transport processes to streams. This research recognised that previous models had tended only to take account of the flow of water into and out of bank storage, not considering the effect of overbank flow that occurs during flood events. Furthermore, previous studies were primarily concerned only with the movement of water between the stream and the floodplain, and not the transport of solutes. This study used a US Geological Survey saturated-unsaturated groundwater flow and density dependent chemical transport model SUTRA to simulate surface-groundwater interaction in an extensive lowland floodplain in the Murray-Darling Basin, south-eastern Australia (Figure 2.7). Time-varying pressure head boundary conditions were used in the model to represent the rise and fall in river and stream levels, and a constant pressure head condition was used to represent the floodplain-hillslope boundary. The modelled flow and salt transport results were compared to field observations. This study showed that bank storage mixing could only account for the initial period of salt concentration recession following flood events, and that the addition of localised recharge on the floodplain in the form of overbank flow was a plausible explanation for the later salt recessions. The flood event was shown to have a significant effect on solute transport, and the mechanism of water transfer between the river channel and the floodplain was also shown to have an important effect on solute residence time.

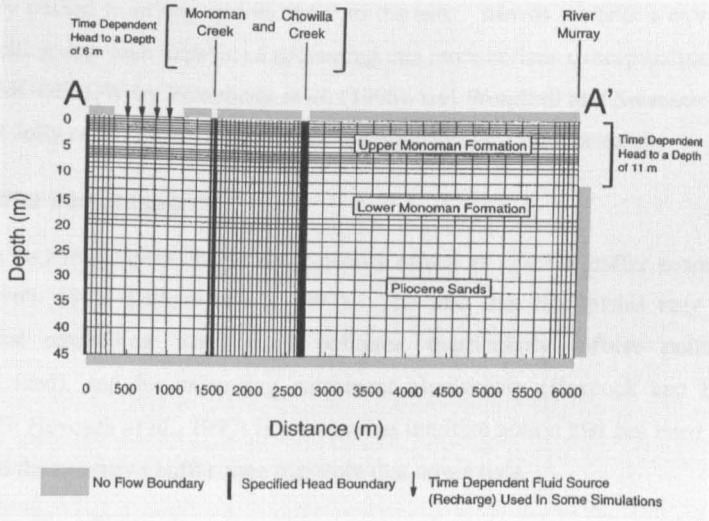

Figure 2.7 Model mesh and boundary conditions of the simulated cross section in the SUTRA floodplain flow study (from Jolly et al., *1998).*

Chakka and Munster (1997) used another US Geological Survey model known as VS2DT (Variably Saturated Two Dimensional Transport) to simulate macropore transport of agricultural chemicals through a clay soil to the underlying sand and gravel aquifer at a research site on the Brazos River floodplain, USA. VS2DT was then used to simulate flow through a variably saturated floodplain aquifer in direct hydraulic connection with the adjacent river. The model solves the Richards' equation for groundwater flow and the advection-dispersion equation for chemical transport in both saturated and unsaturated conditions, using two-dimensional finite difference methods. This model also permits inputs from surface runoff rainfall events, but overbank flow conditions were not simulated in this study.

A major challenge facing experimental research in the hyporheic zone is the determination of the relative importance of surface water versus groundwater inputs on hyporheic processes, and the effect of local conditions (Palmer, 1993). Current knowledge of hyporheic zone effects on stream chemistry is limited by a failure to understand the hydrogeological setting of floodplains and integrate hydrology with the chemistry and biology of these complex environments (Hill, 2000). Comparative research on the role of hillslope, floodplain, hyporheic zone and in-stream environments in regulating stream chemistry is limited and has only been conducted in a narrow range of watersheds (Hill, 2000). The view of Bencala (1993) that we can move away from compartmentalising the surface water-catchment interaction remains primarily theoretical. The notion of storage zones has created a climate of thought that encourages partitioning of the system, where water and solutes are conceptually passed from one system 'box' to the next. Moves towards a more physically based modelling approach capable of addressing this more holistic conceptualisation, such as the use of MODFLOW by Wroblicky *et al.* (1998), and Wondzell and Swanson (1998), and the study of Jolly *et al.* (1998), may provide the direction for future research.

2.1.4 Buffer zone research

There were very few papers on the water quality effects of riparian buffer zones before the 1970s (Correll, 1997; Gilliam *et al.*, 1997). The idea that floodplains may have great potential for controlling water-based pollution (particularly diffuse pollution from agricultural land), and for enhancing catchment biodiversity (Haycock and Burt, 1993; Norris, 1993; Haycock *et al.*, 1997) is a somewhat intuitive notion that has been the driving force behind the extensive buffer zone literature that now exists.

Research into this subject is important because mitigating non-point source pollution is more problematic than dealing with point source pollution (Verchot *et al.*, 1998). Diffuse pollution is spatially ill defined and the principal contaminants are delivered to the stream

environment along various dynamic pathways (Haycock *et al.*, 1997). Development and implementation of successful control strategies depends on knowledge of the source areas and transport pathways involved. In addition, implementing a buffer zone as a pollution management option has an economic cost (Withers and Jarvis, 1998), so the scientific basis for this procedure should be firmly established.

Most of this research has focused on the transport and transformation of agricultural nutrients and pesticides, including nitrogen and phosphorus. The type of hydrological pathway studied is often dependent on the particular chemical under consideration, as the dominant transport pathways are different for different chemical species (e.g. subsurface water flow paths for nitrate transport, and surface water flow paths for phosphate transport). It is unlikely that retention of all chemical species can be maximised in the same environment, with the implication that management options to reduce the loss of one chemical may conflict with those intended to reduce the loss of another (Haycock *et al.*, 1997; Withers and Jarvis, 1998).

Correll (2000) stated that one indication of the immaturity of riparian buffer research is the lack of a successful, well-tested simulation model. The few models that have been developed have been motivated by the need to provide appropriate design specification for buffer zones for management purposes. An early attempt to model buffer zone processes was made by Chescheir *et al.* (1987), who developed a modelling approach to determine the pollutant removal effectiveness of wetland buffer zones which receive pumped agricultural drainage water. The behaviour of five nutrients was investigated, including nitrate. The water flow through the drained agricultural areas was modelled using a field scale water management model DRAINMOD to provide estimates of the pumped applications to the wetland buffer. The water flow through the buffer area itself was simulated using a wetland model for overland flow, with no consideration of subsurface flow processes. Nitrate removal was considered to be by denitrification, and a subroutine was added to calculate nutrient removal based on a first order decay equation:

$$c = c_b + (c_i - c_b)e^{jr} \qquad 2.1$$

where c is the nutrient concentration in a water unit [M L^{-3}], c_i is the initial nutrient concentration in water pumped on to the filter [M L^{-3}], c_b is the background nutrient concentration [M L^{-3}], j is a decay constant [$-T^{-1}$], and r is the residence time of the water unit on the filter [T].

The model was tested using field hydrological and nutrient data. The timing and magnitude of the simulated water movement was found to compare well with observations, but chemical data showed that the model was least accurate in the prediction of nitrate removal,

which was underestimated. This was thought to be because environmental factors such as temperature were not included in the decay constant.

Phillips (1989) also approached the modelling of the floodplain environment from a chemical buffering perspective, in an attempt to provide guidelines for establishing riparian buffer dimensions. The ability of riparian soil types to assimilate upland runoff was compared using the Riparian Buffer Delineation Equation (RBDE). This model compared the effectiveness of a given buffer to that of a reference buffer, for a given imposed flow. For this analysis it was assumed that buffer effectiveness is directly related to the time it takes water to pass through the buffer. Chemical concentration over time was described by first-order kinetics in the form of a negative exponential model:

$$\frac{c_t}{c_i} = e^{-jt} \qquad 2.2$$

where c_i [M L^{-3}] and c_t [M L^{-3}] are concentrations initially and at time t [T], and j is a rate coefficient [$-T^{-1}$]. The model is based on retention time and is applicable to non-conservative pollutants.

Phillips (1989) and Chescheir *et al.* (1987) tackled the problem of buffer zone effectiveness in essentially the same way, both assuming that the residence time of a nutrient on the filter area was the controlling factor in the amount of nutrient decay, and that non-conservative nutrient decay followed first order reaction kinetics. However, the assumption of first order kinetics, empirical fitting of rate coefficients, and lack of consideration of environmental factors such as temperature, soil moisture concentration and aeration lead to problems with this approach. Rate coefficients obtained from laboratory studies are only effective rate constants, so they include the effects of all parameters influencing the chemical transformation process such as pH, available carbon, oxygen concentration and temperature (in the case of denitrification). Some authors have attempted to account for the influence of environmental factors on the rate of denitrification, including Selim and Iskander (1981) who treated the rate coefficients for nitrogen transformations as variables rather than constants. In addition, the idea of calculating residence time is, once again, effectively compartmentalising the system and moving solute from one notional 'box' to another.

One more recent modelling example, the Riparian Ecosystem Management Model (REMM) has been developed as a tool to determine the effectiveness of riparian buffers in controlling non-point source pollutants from agricultural fields (Williams *et al.*, 2000). REMM is a daily time step simulation model which models a buffer as a three zone system. Each zone can be assigned a separate geometry, soil conditions, chemical concentrations and vegetation characteristics. The model then simulates surface and subsurface runoff, evapotranspiration,

erosion and sediment transport, plant growth, and nutrient cycling. REMM is a much more comprehensive model than those developed by Chescheir *et al.* (1987) and Phillips (1989), incorporating several chemical species, varying buffer zone characteristics, and both surface and subsurface flow and solute transport. The use of REMM to design buffers has the potential to provide a systematic way to look at how different buffer characteristics affect the movement of pollutants from agricultural land to streams, but the model has not yet been tested under a wide variety of buffer conditions.

2.1.5 Factors controlling floodplain water movement and chemical transport

Studies within the buffer zone literature in particular tend to concentrate on determining the factors at each site that affect floodplain hydrological processes and biogeochemical properties, but studies from other fields of near-stream research also investigate controlling factors. These factors are discussed here under separate headings, but it should be appreciated that many of them are interdependent. An indication of these interrelationships is given in Figure 2.8.

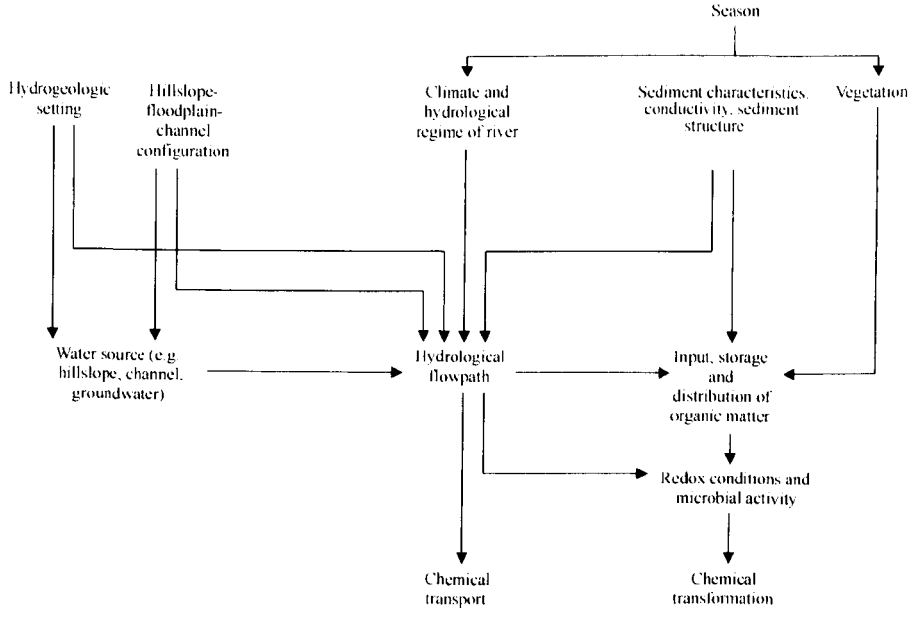

Figure 2.8 Factors controlling the transport and transformation of chemicals in floodplain environments.

2.1.5.1 Vegetation

Some studies have looked at the relative merits of different types of vegetation cover for their nitrate buffering capabilities. Addy *et al.* (1999) compared forested and mowed buffer

zones on poorly drained soils and found no significant difference in groundwater nitrate removal rates between the two types of vegetation. This study highlighted the need to consider the relative importance of vegetation cover versus other site characteristics. Haycock and Pinay (1993) compared nitrate transport and transformation under grass and poplar cover during the winter months at two floodplain sites in southern England. The poplar-vegetated riparian zone was more effective in absorbing nitrate in groundwater flow than the grass vegetated site; it was postulated that this was due to the carbon contributed to the soil microbial biomass by the above-ground biomass. There is a growing consensus that rather than being directly influential (i.e. affecting chemical concentrations by uptake), vegetation has an indirect effect on subsoil processes by contributing organic matter (Spruill and Galeone, 2000) which influences microbial activity (Pusch *et al.*, 1998). Seasonal changes in vegetation cover may influence the supply rate of organic substances at different times of year, and hence the potential for biochemical transformations.

2.1.5.2 Organic carbon content

Biogeochemical processes in riparian zones are frequently mediated by soils with low oxidation-reduction (redox) potential, which directly affects the types of chemical reactions and microbial communities present (Dwire *et al.*, 2000). Redox potential is influenced by soil organic carbon content (along with soil moisture content, texture, temperature and dissolved oxygen), which provides a source of electron acceptors for a range of biogeochemically important redox processes. A study by Hedin *et al.* (1998) showed that redox gradients provided the dominant control on forms of inorganic-N within soil-stream interfaces of Smith Creek. This indicated how a mechanistic and predictive understanding of stream riparian zone biogeochemistry can be enhanced by considering how microbial communities interact with variations in the supply of electron donors and acceptors (Hedin *et al.*, 1998), including soil organic carbon.

Several studies have observed that the distribution of organic carbon in the subsurface environment is somewhat patchy, and that this may result in so called 'hotspots' of microbial activity (Groffman *et al.*, 1996). This observation has implications for the design of field studies, which should take into account the irregular distribution of organic carbon in order to avoid incorrect estimation of the potential of a site for biogeochemical transformations. Modelling efforts also need to be able to represent spatial heterogeneity in organic carbon content and associated chemical transformation potential.

2.1.5.3 Hydrogeological setting

The hydrogeological setting of a near-stream zone, including the topography and underlying geological configuration, and the position of the stream channel within the fluvial plain

(Woessner, 2000), represent major controls on the opportunity for groundwater to interact with the riparian zone (Inamdar *et al.*, 2000). Gold *et al.* (2000) evaluate the role of landscape setting in riparian groundwater nitrate removal, which can influence hydrological linkages between uplands and riparian zones as well as groundwater flow path, retention time, and nitrate transformation rates within riparian ecosystems. Topographical features at a range of scales may be influential on hydrological and chemical transport processes. Hill *et al.* (1998) found that complex vertical and horizontal stream-subsurface water exchanges between the streambed and the floodplain of an agricultural stream in Ontario, Canada were controlled by stream channel riffle-pool units.

Studies of nitrate transport and transformation in riparian zones tend to have been largely restricted to sites with a simple geological arrangement of a shallow permeable buffer zone underlain by an impermeable layer (Cooper, 1990; Haycock and Burt, 1993; Haycock and Pinay, 1993; Jordan *et al.*, 1993; Hill, 1996; Hill 2000), where significant vertical flow is prohibited. Under this configuration, groundwater flows at a shallow depth above relatively impermeable clay or till, and any chemicals transported in the groundwater have the opportunity to react with the near-surface floodplain sediments. Very few studies have considered more complex hydrogeological environments. As chemical transport and transformation is heavily dependent on the hydrological flow paths which are strongly controlled by hydrogeological setting, the notion of floodplains acting as buffer zones may have more restricted applicability than has been inferred on the basis of studies to date.

2.1.5.4 Soil stratigraphy and hydraulic characteristics

Sedimentary structures form a dynamic framework that controls subsurface flow and the vertical and horizontal exchange of water between channels and floodplains (Huggenberger *et al.*, 1998). Soil characteristics, such as hydraulic conductivity, are of fundamental importance for the exchange processes between ecological systems and have a marked effect on hydrological residence time, redox conditions, and flow pathways (Hendricks, 1993; Brunke and Gonser, 1997; Dahm *et al.*, 1998). Morrice *et al.* (1997) looked at three headwater streams in west and north-central New Mexico, USA, with associated catchments of contrasting lithology, alluvial grain size, and hydraulic conductivities. Their results suggested that hydraulic transport and associated retention of nutrients are affected by these characteristics. Wroblicky *et al.* (1998) also compared streams in catchments with alluvial sediments derived from materials of different parent lithology. Pinay *et al.* (2000), in an investigation of the microbial denitrification process in alluvial soils, found a significant relationship between denitrification rates in the floodplain soils and their texture.

Grimaldi and Chaplot (2000) studied the effect of geological substratum on the downstream variation in nitrate contents during baseflow conditions in two small streams of northwestern France. The grain-size distribution and permeability of the materials making up the hyporheic zone could explain the contrast in behaviour between the stream flowing on granite and the stream flowing on schist. They concluded that the relationship between permeability and denitrification is complex. A hyporheic zone with low permeability limits the input of stream waters towards denitrifying sites and the return of denitrified water towards the stream. However, high permeability is not necessarily favourable to nitrate removal, because although it allows the transfer of stream water nitrate as far as the denitrifying sites, at the same time it brings about a reoxygenation of this environment. This reduces the residence time of water and nitrate and limits the effectiveness of nitrate removal from streams through processes in the near-stream environment. Chestnut and McDowell (2000) also looked at the effect of riparian and hyporheic sediment hydraulic characteristics on carbon and nitrogen dynamics. They found significant spatial heterogeneity in the hydrologic and chemical properties of near-stream zone sediments, and found that hydraulic conductivity explained much of the variation in dissolved organic carbon concentrations, with the highest concentrations occurring in sites having low conductivity.

In addition, it is likely that distinct sediment structures will be present in the floodplain, potentially in the form of buried channel deposits. As well as having different hydraulic characteristics, these features may well be prime locations for organic carbon and enhanced biogeochemical transformation processes. Once again this indicates that chemical activity may be restricted to distinct sediment structures within the floodplain, and all areas of the floodplain may not be equally active in chemical transformation processes (Haycock and Burt, 1993). This has implications for measuring processes in the field as, for example, microcosm studies of denitrification potential may miss groundwater transformations that occur within microsites (Gold *et al.*, 1998).

2.1.5.5 Hydrological regime

Several issues relating to hydrological regime are relevant to near-stream flow and transport processes, including the effect of river stage, hydrograph response and extreme hydrological events, external hydrological links to floodplains, and seasonal influences.

The flow, transport and exchange of groundwater and chemicals in the fluvial plain is controlled by the relation of stream stage to the adjacent groundwater hydraulic gradients (Woessner, 2000). Fluctuations in the water-table elevation and the extent of surface saturation in the floodplain, associated with changes in the stage of the hydrograph, drive spatial and temporal heterogeneity in soil redox conditions (Dwire *et al.*, 2000).

The magnitude of external hydrological connections between the floodplain and the hillslope or the stream control the input of chemical constituents, such as nitrogen and dissolved oxygen, to the near-stream zone (Duff and Triska, 2000). Devito *et al.* (1996) carried out a study of groundwater-surface water interactions in two conifer swamps located in headwater catchments with contrasting till depth. Differences in upland-wetland connections resulted in contrasting hydrologic regimes in the two swamps. Both swamps were hydrologically connected to the uplands during the winter season when there were large upland water inputs, and had a similar hydrological characteristics of a high water-table, rapid storm response, and predominance of saturated overland flow. However, during the summer months upland water inputs were absent in the catchment with shallow till, resulting in cessation of baseflow and a lower water-table that varied in response to precipitation. In the catchment with deeper till, upland water inputs continued throughout the summer, sustaining baseflow and maintaining the level of the water-table.

Overbank flood events can provide a pathway for significant surficial deposition of suspended organic and mineral matter (Brunet *et al.*, 1994). Flood events can also play a significant role in regulating subsurface hydrological and chemical processes, directly affecting nutrient cycling in alluvial soils by controlling the duration of oxic and anoxic phases (Pinay *et al.*, 2000). The nature of the flooding conditions can also be important. Sánchez Pérez *et al.* (1999) found that in flooded conditions, nitrate removal was dependent on the duration of flooding, and the nature of alternating periods of wet and dry conditions in the near-stream zone, which control the equilibrium between the various nitrogen species. The hydrological mechanism of inundation will be affected by the antecedent moisture content of the floodplain prior to the flooding event, influencing the degree of mixing of river water and local water, with associated implications for chemical transport. Mertes (1997) demonstrated this phenomenon on the extensive floodplain of the River Amazon.

Seasonality effects may also be superimposed on these factors. Seasonal changes in temperature, stream discharge, and hydrological connectivity between the hillslope, the floodplain, and the stream, may affect biogeochemical patterns in groundwater-surface water interactions (Hendricks and White, 1995). Field monitoring of groundwater levels and stream stage in a study by Wroblicky *et al.* (1998) indicated systematic variation in the orientation of the groundwater system relative to the stream in response to seasonal changes in precipitation, snow cover, and stream flow.

2.1.6 Further issues in floodplain research

The focus on the idea that floodplains can act as buffer zones has perhaps prevented a more general consideration of how water and chemicals move through floodplains, and whether

floodplains can be both a source, as well as a sink, of water and chemicals, depending on the local conditions. For example, research in agricultural catchments suggests that some riparian zones function as a sink for phosphorus during base flow, whereas others are seasonal sources (Hill, 2000). The variable source area concept of stream flow generation indicates that riparian zones can be a potential source of runoff during storm events, particularly where subsurface storm flow on hillslopes emerges on to the floodplain as saturation-excess overland flow. Once floodplains become sufficiently wide, they may become an important source of runoff in their own right, as well as continuing to provide a conduit for slope drainage to the river (Burt, 1997).

Much of the focus on floodplains as a sink for chemicals has been on nitrogen transformations, and denitrification in particular. The studies of Addy *et al.* (1999) and Cey *et al.* (1999) both found conditions conducive to denitrification, either in the riparian zone or at depth near the field-riparian zone boundary. Mengis *et al.* (1999) used a comprehensive multiple geochemical and isotopic approach to assess groundwater nitrate transport and transformation processes in a riparian zone at Strawberry Creek, near Waterloo, Canada. Their experiment confirmed that denitrification was occurring in the riparian zone and contributed to an observed drop in nitrate concentration along the groundwater flow path through the riparian zone.

In contrast, Stanford and Ward (1993) found predominantly oxic conditions in the hyporheic zone of the alluvial aquifers of Flathead River, Montana, USA. Nitrate concentrations were often more than an order of magnitude higher in the aquifers than in the channel, indicating that nitrification is probably an important process in these aquifers. Ohrui and Mitchell (1998) also found high nitrification rates in the near-stream zone of two small, forested watersheds in Japan.

2.1.7 Summary of previous research and identification of a research gap

Research into floodplain hydrological processes and chemical transport has developed in several academic disciplines, and within distinct research spheres, each with a focus on a different aspect of the floodplain hydrological and chemical transport system. Bank storage research was really the first time that interaction between a river channel and the adjoining floodplain had been considered. At the same time, research into hillslope-channel connections was developing, with a particular emphasis on storm flow generation, but was generally limited to headwater catchments with little or no significant floodplain. The more comprehensive field of hyporheic zone research advanced the concept of bank storage by starting to explore the consequences of surface-groundwater interactions for the chemical

Table 2.1 Summary of floodplain hydrological and chemical transport research

Research area		Bank storage	Hillslope-channel	Hyporheic zone	Buffer zone
Flow pathway	*River to floodplain*	Subsurface flow only.	Subsurface flow only.	Subsurface flow and one overbank flow modelling study by Jolly *et al.* (1998).	Not considered.
	Floodplain to river	Subsurface flow only.	Surface and subsurface stormflow.	Subsurface flow only.	Overland flow and subsurface flow.
	Hillslope to floodplain	Not considered.	Surface and subsurface stormflow.	Not considered.	Overland flow and subsurface flow.
	Floodplain to hillslope	Not considered.	Subsurface flow only.	Not considered.	Not considered.
Landscape setting		Headwater and lowland.	Headwater only, floodplain not often included.	Headwater and occasional lowland studies.	Usually headwater only, also generally a simple geological setting.
Dimensions*		2D transverse cross-section.	Usually 2D transverse cross-section, some consideration of down-valley flow.	Usually 2D cross-section, either longitudinal or transverse, some 2D plan view studies.	2D transverse cross-section or 2D plan view (psuedo-3D maps of water table elevation).
Chemical transport		No direct studies.	Studies of herbicide transport and nutrient transport.	Salt transport, agricultural chemicals.	Agricultural chemicals, nutrients.
Examples of models used		WaTab2D, MODFLOW	HILLS; watershed hydrology models e.g. SHE	SUTRA, MODFLOW, VS2DT	REMM
Model limitations		Models restricted by limiting assumptions in highly dynamic situations, no chemical transport component.	Low resolution representation of near-stream zone in watershed hydrology models; floodplains not explicitly represented in current applications of hillslope hydrology models.	Models restricted by limiting assumptions in highly dynamic situations, and not always suitable for extensive unsaturated flow modelling.	Models generally designed for management purposes; not so suitable for exploring process interaction.

* Transverse cross-section means across the channel
Longitudinal cross-section means along the channel

and ecological quality of riverine systems. This appreciation of the chemical quality effects of floodplains has influenced a relatively recent interest in the management use of near-stream areas for buffering watercourses from chemical inputs from the surrounding catchment. A summary of these four research areas is given in Table 2.1.

Previous investigations of floodplain hydrological processes indicate that the distribution and rates of nutrient cycling processes within the near-stream zone are linked to interdependencies between hydrological, chemical and biological processes (Valett *et al.*, 1996; Dahm *et al.*, 1998), but that hydrological processes in particular are the key to understanding chemical transport and transformation processes (Cooper, 1990; Burt, 1997; Correll, 1997; Gilliam *et al.*, 1997; Hill, 1997). The flow path of water influences chemical input (Haycock and Burt, 1993; Burt, 1997) as well as the degree of interaction of water and chemicals from different sources within the near-stream zone (Hill, 2000). Further to this, hydrological factors such as hydraulic gradient, water-table position, and water retention characteristics of sediments affect riparian zone water and chemical residence time and spatial distribution (Gold and Kellogg, 1997), redox conditions, vegetation dynamics, and microbial processes. Many of the key chemical transformation processes are bacterially mediated, but the opportunity for these bacterial processes to influence contaminant levels is highly dependent on the hydrological behaviour of the floodplain, and the source and transportation of chemical species (Haycock *et al.*, 1997).

Most studies of chemical transport suffer from a lack of hydrological data to couple to the chemical data. There is thus a need to ensure that hydrological budgets are complete so that chemical budgets are based on a sound foundation (Haycock *et al.*, 1997). As it is usually an inadequate understanding of hydrological processes that limits quantitative understanding of the results (Correll, 1997), it may be appropriate to focus the bulk of future research efforts on the hydrological aspects of the system. The understanding of the hydrological characteristics of the near-stream zone can then form a template for the successful interpretation of chemical transport and transformation processes (Hill, 1996).

This field of research is at quite an early stage, and the interrelationship of the factors affecting floodplain hydrological and chemical transport processes have made it difficult to draw general conclusions about the effect of individual factors, particularly as studies have remained quite site specific. The great spatial and temporal variability of stream-aquifer interactions where the river has an adjacent floodplain dictates that field studies are often insufficient to unravel the underlying processes (Jolly *et al.*, 1998), particularly under extreme hydrological conditions. In this context, the use of a combined fieldwork-modelling strategy is a powerful methodology.

Simulation models test our ability to synthesise our knowledge of the functioning of natural systems (Correll, 2000); the very process of model construction forces the organisation of ideas about how a system works into a coherent structure (Tanji, 1982), and can highlight areas where process understanding is currently weak. In addition, models can enhance interpretations of field data (Tychon *et al.*, 1999) and can be used in a propositional sense to test hypotheses (Beven, 2000; Bates and Anderson, 2001; Morton and Suárez, 2001). With models it may be possible to gain a broader view with the purpose of detecting common patterns among sets of climatic and landscape conditions. Models provide an opportunity to study combinations of conditions that have not yet been encountered in field studies (Gold and Kellogg, 1997). Scenario testing on this scale would be extremely expensive and time consuming to undertake in the field, and it would be difficult to account for the effect of all the controlling factors. Models can also provide a useful and efficient method of directing future fieldwork efforts.

Current models of floodplain hydrological and chemical transport processes are, however, constrained by their assumptions, which are unsuited to modelling near-stream environments during flood events when vertical hydraulic gradients may be significant (e.g. the Dupuit-Forcheimer assumptions of MODFLOW). Also, not all of the models described deal with chemical transport (e.g. MODFLOW, Squillace, 1996 and WaTab2D, Whiting and Pomeranets, 1997). SUTRA is primarily intended for two-dimensional simulation of flow, and either solute or energy transport in saturated variable-density systems. As such, SUTRA's numerical algorithms are not appropriate for the non-linearities of unsaturated flow, and it is not an economical tool for extensive unsaturated flow modelling (Voss, 1984). The VS2DT model is more appropriate in this sense, but the finite difference formulation for solving the governing equations may be unsuitable for rapidly evolving boundary conditions, as occur during flood events. Models such as REMM have been specifically designed for management purposes. While the simplifying model assumptions introduced make them ideal for this objective, they do not have the time resolution or explicit process representation needed for exploring process interaction in floodplain environments, particularly under rapidly changing boundary conditions.

Field data are an important feature of a fieldwork-modelling research methodology. The use of suitable field data to support the modelling results promotes confidence in the conclusions drawn from the study. While such a study may initially be based around specific sites for model testing purposes, once there is confidence in the model's ability to represent the system the specification of the system parameters can be changed to explore a wider spectrum of scenarios. Careful evaluation and recognition of the assumptions and limitations of both modelling and fieldwork is also important.

The need to expand the study of floodplain hydrological and chemical transport processes beyond individual sites is propounded below:

> While we know that exchange of water between surface water and ground water is an important regulator of system biogeochemistry and ecology, we do not know how the parameters change across streams. This broader perspective is important not only for generalisations about subsurface processes but, more fundamentally, for advancing our conceptual models of streams.
>
> (Stanley and Jones, 2000)

Field site selection is therefore important if any attempt is to be made to incorporate a spectrum of floodplain types. Cross-site comparisons are currently restricted to headwater streams, and "an obvious need in the pursuit of general models of exchange is to improve our understanding of the hydrology and ecology of subsurface and exchange processes in larger channels" (Stanley and Jones, 2000). It would therefore be instructive to explore the behaviour of lowland floodplains, which have received relatively little attention.

There are clearly many uncertainties over processes of water and chemical movement through floodplain systems, and the relative importance of different factors affecting these processes. Most studies that have assessed the capacity of the near-stream zone for chemical removal have treated the system as a black box and have not provided insight into the hydrological and chemical transformation processes that produce different patterns of chemical distribution. Previous research has been limited in terms of the characteristics of the field sites which have been investigated, mostly limited to headwater catchments and only exploring part of the whole spectrum of internal and external flow paths that may exist in the floodplain. It has also been limited by the 'compartmentalised' conceptualisation of the hillslope-floodplain-channel system. Whilst a fieldwork-modelling strategy is a sound methodology with which to explore process interaction in this highly dynamic region, as yet no model has been developed which would be suitable for this function.

2.2 Research proposal

This section will present the specific research aims that will be pursued during the course of this project. A suitable strategy for achieving these aims will also be discussed.

2.2.1 Research aims

The aims of the study are twofold:

1. To develop a model of subsurface hydrological and chemical transport processes through both headwater and lowland floodplain systems.

2. To use this model to advance process understanding, quantifying the effect of a range of factors on the operation of hydrological and biogeochemical processes in floodplain systems.

The following specific hypotheses will be addressed in order to fulfil these aims:

a. The scale of the hydrological event (overbank flood, bankfull flood and low flow event) controls floodplain water and solute source, flow path and residence time.

b. The scale of the floodplain zone (headwater riparian zone versus lowland floodplain) controls floodplain water and solute source, flow path and residence time.

c. Other factors (such as carbon content and distribution, temperature and soil hydraulic characteristics) are important in controlling solute transport and transformation.

This work is therefore focused on delivering a numerical code specifically suitable for modelling hydrological processes and associated chemical transport in floodplain systems. This will enable identification of the combination of factors or thresholds of factors that determine whether certain processes operate in this environment, in a way that has not hitherto been possible.

2.2.2 Methodological summary

The outline of the fieldwork-modelling strategy is presented below. The model development process will follow standard procedures of development and testing.

1. Define the problem and identify the processes that are believed to determine the movement of water and chemicals in floodplain systems, and factors that may affect the operation of these processes.

2. Develop a hydrological and chemical transport model for application to the floodplain environment at a high spatial and temporal resolution, capable of representing the processes identified in (1).

3. Investigate sensitivity of the model to parameters such as the soil hydraulic characteristics, and structural parameters such as the mesh resolution and time step.

4. Validate the hydrological dynamics of the model using data from dedicated floodplain monitoring programmes.

5. Investigate floodplain hydrological and biogeochemical dynamics through further model development and use a range of hypothetical scenarios to investigate the hypotheses outlined in Section 2.2.1 above.

2.3 Chapter summary

There is a clear scientific and management need to understand water movement and chemical transport through floodplains. An understanding of hydrological processes is the key to understanding chemical transport and transformation processes, but the details of hydrological pathways and chemical transport in the near-stream zone are not yet well known, in part because previous approaches to floodplain hydrology have developed along rather narrow lines. It seems timely that a more all-encompassing overview of the subject should be attempted, not restricted by the demand to find an answer to the question 'How wide should a buffer zone be?'

The originality of this study lies in the development of a model specifically suitable for studying the movement of water and chemicals within the floodplain, taking into account the rapidly changing conditions that are characteristic of flood events, and capable of representing water and chemicals derived from both hillslope and riverine sources. This floodplain hydrological and chemical transport model, combined with a dedicated floodplain monitoring system, will be an important development in its own right, but will also represent a significant opportunity to contribute towards process understanding in this subject area by tackling questions which have not previously been addressed and which cannot realistically be answered by field studies alone.

3 Developing the Initial Model Platform

Chapter 2 has considered how the study of floodplain hydrological and chemical transport processes has previously been approached, and where the state of process knowledge currently lies. A series of aims have been identified which will address current research gaps using a combined fieldwork-modelling methodology. Having recognised the lack of a suitable model with which to address current issues in floodplain hydrological and chemical transport research, the next important step is to develop such a scheme.

This chapter will be concerned with the model development process, which can be divided into two stages. The first stage entails the development of a conceptual model, which is a description of how the system is believed to operate. The second stage, numerical model development, involves establishing how the conceptual model will be expressed in mathematical terms, and how the resulting set of equations will be solved. This chapter will conclude with some initial model simulations.

3.1 Conceptual model

For a model to have any chance of representing reality, it must include relevant processes within an adequate structure (Lane and Richards, 2001). At the same time, to make the solution possible, it is common to introduce simplifying assumptions. These are commonly assumptions about the spatial dimensionality of the problem, the temporal scale of the problem, and the necessary processes for inclusion in the model. Stating and evaluating these assumptions is critical for defining the applicable limits of a particular model. A definition of the conceptual model of floodplain hydrological and chemical transport processes can be developed from the information presented in the previous chapter.

The following discussion of floodplain flow representation concentrates on the cross-sectional hillslope-floodplain-channel view, rather than the alternative plan view. Employing only a one-dimensional (1D) vertical or horizontal representation of floodplain subsurface flow would not be a suitable way to conceptualise the floodplain environment in this study, given the recognition that water exchanges may occur both horizontally between the channel banks into the floodplain and also vertically between the floodplain and the

channel bed. It is therefore clear that a two- or three-dimensional (2D or 3D) representation is essential. 3D flow processes have been identified in some floodplain situations, for example Haycock and Burt (1993), where a significant sedimentological feature on the floodplain contributed strongly to groundwater flow in a down valley direction, in addition to flow perpendicular to the river channel. 3D hydrological representation may present a solution that more accurately considers the 3D structure of floodplain flow, but the trade off is a much more computationally expensive modelling process. With this in mind, the benefits of 3D flow representation as compared to 2D are yet to be established, particularly in the case of floodplains with simple sedimentological structures and/or where down valley flow is not so pronounced. For example, in the study by Hedin *et al.* (1998), the steepest changes in chemical concentrations across the floodplain were observed in a direction perpendicular to the stream. Therefore, while recognising the possibility that down valley flow may occur to some extent, it is assumed in this study that the dominant flow processes can be adequately represented by a 2D, transverse cross-sectional modelling strategy. This conceptual model of floodplain hydrological processes is illustrated in Figure 3.1.

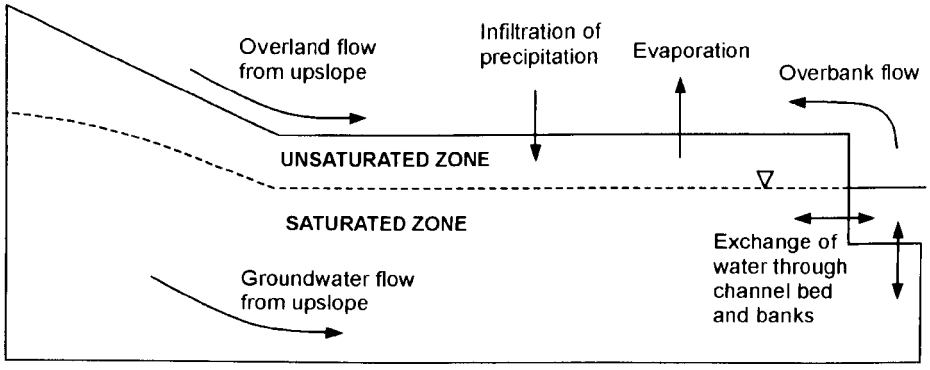

Figure 3.1 2D conceptual model of floodplain hydrological processes.

When developing the conceptual model of subsurface floodplain hydrological processes, the nature of the soil structure should be taken into consideration. Two flow domains have been recognised within the soil system: the micropore domain (soil matrix), where water movement is driven by capilliarity and potential flow forces, and the macropore domain, where water movement is primarily driven by gravity. Macropores are large openings or voids in the soil which may be holes created by soil fauna (such as earthworms), holes generated by plant roots, cracks and fissures caused by soil drying and shrinkage, and natural soil pipes formed due the erosive nature of subsurface water flow (Beven and Germann, 1982). In the presence of macropores, soil water flow will not adequately be described by equations based on Darcy's law, since the assumptions of homogeneous soil hydraulic

properties and a well-defined hydraulic gradient will no longer apply (Beven and Germann, 1982).

In examining the mechanisms by which stream flow responds to precipitation, macropores have been proposed as an important route by which storm water can be delivered quickly to the stream (the 'macropore' flow hypothesis; Bonell, 1998). The high velocity of macropore subsurface flow means that water arriving at the stream channel by this route would almost certainly be 'new' water (i.e. water generated by the current storm event), rather than 'old' water (i.e. water that was stored in the catchment prior to the storm event). However, field experiments using natural isotope tracers increasingly appear to support the view that 'old' water dominates the storm runoff hydrograph, even in areas where the existence of macropores is well documented. Diffuse subsurface flow, including both shallow throughflow and deeper groundwater flow, may offer a more plausible basis for explaining stream flow response to precipitation (the 'displacement' flow hypothesis; Bonell, 1998).

Further work is required to in order to fully understand the behaviour of flows in macropores. Considerable uncertainty exists over the conditions (for example soil type, climate, land use, and rainfall rate) under which macropore flow may be important in contributing to the rapid movement of water through soils (Bonell, 1998). The existence of macropores is not in itself evidence of a significant role in the runoff process.

Some models have adopted a two domain approach to modelling matrix and macropore flow (Bonell, 1998). However, a continuum of pore sizes will often exist within the soil, which may invalidate the two-domain representation. There is a need for a coherent theory of flow through structural soils that would make the macropore domain concept redundant (Beven and Germann, 1982).

On balance, inclusion of macropore representation within the model is not justified, for the following reasons:

- There is no clear consensus on the role that macropore flow plays in contributing to the routing of precipitation through the soil to the stream channel.
- There is uncertainty over the circumstances under which macropore flow may be important.
- Much is still unknown about the way macropores operate hydrologically, including both the nature of macropore flows, and how they interact with the surrounding matrix under different flow conditions.

- As a result, there is no clear modelling approach to the representation of macropore flow, and such models that do exist "cannot easily be applied under field conditions and [remain] largely of value to theoretical or laboratory studies" (Bonell, 1998).

Exploring ways to incorporate an appropriate representation of macropore flow would be distracting from the stated aim of this thesis, and it is felt that adding such a component to the model would introduce unwarranted complexity. Unless the modelling exercise is aimed specifically at exploring the effects of macropore flow on subsurface flow processes, this assumption to neglect the representation of macropore flow is common among subsurface hydrological modelling studies (e.g. Hanschke and Baird, 2001).

As the aim of this study is specifically to investigate *subsurface* water flow paths and chemical transport, surface flow processes such as channel flow, overbank inundation of the floodplain and overland flow will not be modelled explicitly. However, the potential of surface flow processes to impact upon subsurface flow paths will certainly need to be considered. This will be accomplished by using measurements of surface flow processes, such as channel flow and overbank flow, as part of the dynamic boundary condition specification for the subsurface flow model. For example, an explicit representation of overbank flow will not be incorporated in the model, but the presence of ponded water on the floodplain will be allowed to influence subsurface flow patterns by the use of a specified head boundary condition along the length of the affected boundary, with a value that corresponds to the depth of ponded water.

The pattern of water and chemical movement through floodplain systems is believed to be highly spatially and temporally dynamic. The wide variation in the level of the floodplain water-table at different times of year, and the associated variation in the proportions of the saturated and unsaturated zones mean that the model must be capable of simulating variably saturated conditions. In addition to this, there will potentially be periods (during high flow and overbank flow events) when the entire domain is saturated, and the model should be able to cope with these situations too. Few variably saturated flow models adequately model a fully saturated domain, because most variably saturated models do not take into account any compression properties of the soil or fluid. In this case, a change in stored fluid mass is only possible through changes in saturation of the voids; there can be no change in storage due to deformation of the porous media or expansion of the fluid. When the domain being simulated is saturated or very close to full saturation there is no change in storage over time (the capacity is zero), and the Richards' equation is reduced to a steady state condition. Therefore, instead of a fully transient simulation, such a model simply calculates a series of steady state simulations according to the new boundary conditions given at each time step. This phenomenon was recognised by Narasimhan (1979) who stated that "under certain

boundary conditions, neglecting deformation with the onset of moisture suction can cause the transient equation to break down". The introduction of a storage coefficient to the selected variably saturated flow model may therefore be necessary to cope with this problem.

It is also envisaged that some mechanism will need to be available in the model for simulating a seepage face condition. This will be necessary in instances where subsurface flow causes saturation of the soil to the ground surface. This may happen because of a break in slope that reduces the hydraulic gradient (i.e. at the intersection of the floodplain and the toe of the hillslope), or because the ground intersects a free water surface such as a stream (i.e. at the intersection of the channel and the floodplain/riparian zone) (Ogden and Watts, 2000). The seepage face capability is not commonly incorporated in groundwater flow models.

In summary, this conceptual model implies that the numerical model will have to be capable of coping with high spatial and temporal variability. It should allow a 2D cross-sectional representation of the floodplain system, as illustrated in Figure 3.1, and be capable of representing both saturated and unsaturated conditions within the model domain, including an appropriate development of transient flow under conditions of complete saturation. The boundary condition options available in the model will need to be capable of simulating a seepage face condition. Macropore flow and surface flow processes will not be represented. In order to keep the model as simple as possible, the conceptual model described in this section incorporates those elements of the system that have been identified as being of key importance, while at the same time neglecting those elements (such as macropore flow) that are less fundamental.

3.2 Numerical implementation

In this section the process of translating the conceptual model into a distributed, physically-based model will be discussed. This involves establishing equations to describe the relevant processes and selecting the most appropriate numerical method for solving these governing equations. A review of currently available models will be followed by the criteria that will guide model selection for this study. This will be followed by a description of the chosen model and identification of those areas where its capabilities need to be further enhanced to give the process representation identified above.

Distributed physically-based models are so called because the model is based on an understanding of the physics of the processes in operation, in this case the physics of water and solute movement through porous media in variably saturated conditions. Physically-based models are necessarily distributed because the equations on which they are defined generally involve one or more space co-ordinates (Beven, 1985). They therefore have the

capability of forecasting the spatial pattern of hydrological conditions (such as flow depths and velocity values) within the computational domain as well as simple outflows and bulk storage volumes (Beven, 1989; Grayson *et al.*, 1992). This attribute makes them an especially attractive choice for modelling the movement of pollutants and sediments and the effects of spatially variable inputs and outputs, and these are considered research areas that offer the greatest potential for the application of distributed models (Beven, 1985; Stewart *et al.*, 1998).

Several concerns about physically-based modelling have been raised, and a common criticism is that these models are often overparameterised. Overparameterisation facilitates a good fit of model predictions to field observations that might engender false confidence in the results (Christophersen *et al.*, 1993). Alternatively, a model that consists of many parameters may be seen as advantageous in a research context, as it permits a researcher to test a range of scenarios. It is thus emphasised here that the model developed during this study will not be used for making exact predictions of future responses of this hydrological system (akin to the use of models as management tools). Rather, it is to be used as a research tool, contributing to an understanding of floodplain processes by the development and testing of theories and hypotheses. This is a similar rationale to that propounded by other model developers (Voss, 1984; Addiscott and Wagenet, 1985; Grayson *et al.*, 1992). Under these circumstances, the use of a physically-based model in this study is appropriate.

A mathematical model consists of a set of equations that, subject to certain assumptions, describe physical processes (Mercer and Faust, 1980). The descriptive equations for physically-based models are in general non-linear partial differential equations that cannot be solved analytically for cases of practical interest. Solutions must then be found using approximate numerical methods (Wang and Anderson, 1992; Beven, 1985). Numerical methods are based on subdividing the flow region into finite segments bounded and represented by a series of nodal points at which a solution is obtained. So, the continuous differential equation for groundwater flow, defining hydraulic head everywhere in an aquifer, is replaced by a finite number of algebraic equations that define the hydraulic head at specific points. The system of algebraic equations can then be solved using iterative techniques or by direct matrix methods. Numerical models have proved to be flexible in the range of initial and boundary conditions for water and solute they can accommodate; numerical approximations are possible for complex, compressible, nonhomogeneous and anisotropic flow regions having various boundary configurations (Feddes *et al.*, 1988).

A variety of numerical methods are available, including finite difference, finite element and finite volume, all of which involve some form of discretisation of the space co-ordinates, and also, for transient models, of the time ordinate. Solutions are then found for the points or

nodes defined by the space-time discretisation (Beven, 1985). The most widely used methods in groundwater flow modelling are finite difference and finite element; a comparison of their attributes is presented in Table 3.1. Given the highly dynamic nature of the floodplain environment, and the need to incorporate solute transport into the model, the finite element technique seems to be superior for this investigation.

Table 3.1 A comparison of finite difference and finite element numerical solutions (after Wang and Anderson, 1982; Beven 1985; Nielsen et al., 1986; Feddes et al., 1988).

Finite difference method	**Finite element method**
Usually implemented with rectangular cells.	Implemented with a variety of element types, including triangular elements.
Head is defined only at the nodal points themselves.	Interpolation functions are used to define the potential throughout the problem domain, within each element.
More difficult to vary nodal spacing.	Easier to vary nodal spacing; more realistic representation of heterogeneous or anisotropic media.
Cannot deal very well with complex geometries of flow regions, exhibits slow convergence, and it is difficult to treat moving boundary conditions.	Capable of solving complex flow geometries, non-linear and time-dependent boundary conditions, and a high flexibility in following rapid soil water movement, such as near soil surface or wetting fronts. Also useful for solving coupled problems, such as contaminant transport.
Mesh is simpler to construct; simple and efficient in treating the time derivatives.	More time-consuming and laborious preparation of the solution mesh, although software now exists to overcome this limitation.

3.2.1 Review of available models and model selection

Water quality models attempt to simulate changes in the concentration of pollutants as they move through the environment (James, 1993), and need to take into account the properties of different solutes. Conservative substances are inert, and their concentration remains unchanged except by transport phenomena (advection and dispersion). However, for most pollutants, physical, chemical and biological processes also cause changes in their concentration (James, 1993). Reviews of approaches to solute transport modelling are presented by Steele (1985) and Spitz and Moreno (1996) (groundwater quality modelling), Addiscott and Wagenet (1985) (solute leaching in soils) and Nielsen *et al.* (1986) (solute transport processes in the unsaturated zone).

A description of a selection of the available solute transport models is presented in Table 3.2, in order of increasing dimensionality. These models vary in the number of dimensions they represent, the range of chemical transport processes and geochemical reactions included, in the numerical discretisation method employed (finite difference or finite element) and in

their cost and availability. The basic model criteria identified for modelling water flow and chemical movement through the floodplain system can be summarised as follows:

(i) 2D formulation to represent the dominant flow processes.

(ii) Finite element discretisation to cope with rapid soil water and chemical movement during simulation of flood events.

(iii) Designed specifically for variably saturated conditions.

(iv) The transformation of chemicals within the floodplain depends on chemical reactions. The choice of equations to describe the geochemistry of the floodplain will depend on which chemicals are selected for study in this investigation. The model should be flexible in the chemical reaction equations the user can incorporate.

In addition, the following attributes should either be present in the model, or there should be potential for them to be incorporated:

(v) Capable of simulating extensive areas of saturated soil within the domain.

(vi) Capable of simulating a seepage boundary condition.

If requirements (v) and (vi) cannot be met, the source code of the model should be available to allow development of suitable model features.

Models that conform to the basic criteria (see Table 3.2) are BioF&T-2D, SEEP-W, ESTEL2D and SUBIEF2D, HYDRUS-2D, and VAM2D. SUTRA is not included in this list as it was primarily developed for simulation of 2D flow and either solute or energy transport in saturated variable-density systems, while unsaturated flow and transport processes were included to allow simulation of some unsaturated problems (Ataie-Ashtiani *et al.*, 1999).

The highlighted models are broadly similar but vary in details of solver techniques, model assumptions, and the method of linking the hydrological and solute transport sections of the model. In most solute transport models developed to date, the flow and solute transport equations are uncoupled (or 'weakly' coupled) in the sense that a simultaneous solution is not required, as it is assumed that changes in concentration do not affect the flow field (Anderson, 1979). An important exception to this is the case of density-dependent flow, where changes in concentration affect the density of the water and hence the velocity distribution. In this case, it is necessary to iterate between the flow equation and the transport equation; this is referred to as 'strong' coupling (e.g. SUTRA). As far as can be deduced from the available model documentation, none of the models that conform to the basic criteria also fulfil both of the additional model criteria. Only SEEP-W, VAM2D and HYDRUS-2D incorporate the seepage boundary condition, but none of the models seems to account for changes in storage when a fully saturated zone develops in the model domain.

Table 3.2 Selection of available solute transport models

Model	Developer/ Supplier	Description	Numerical discritisation[1]	Saturated/ unsaturated	Hydrology	Solute transport	Geochemistry options	Computer system
Chemflo	US EPA[2]	Simulates water and chemical movement.	1D FD	Unsaturated	Water movement modelled using Richards' equation.	Chemical transport modelled using the convection-dispersion equation.	None.	PC
PESTAN	US EPA	Transport of organic solutes through the vadose zone to groundwater.	1D analytical solution.	Unsaturated	The model is based on a closed-form analytical solution of the advective-dispersive-reactive transport equation. Steady-state flow conditions are assumed.		First-order degradation.	PC
PRZM2	US EPA	Pesticide transport and transformation down through the crop root and vadose zone to the water table.	1D FD/FE	Unsaturated	VADOFT 1D FE module simulates flow in unconfined, variably saturated porous media. Daily time step.	PRZM 1D FD model simulating transport and transformation of the parent compound and up to two daughter species.	Incorporates volatilization and vapour phase transport in soils and microbial transformation.	PC
SWIMv2	CSIRO[3] Australia.	Designed to address soil water and solute balance issues of production and land management.	1D	Saturated and unsaturated	Richards' equation for water flow through vertical soil profile. Time step may vary from seconds to years.	Convection-dispersion equation for solute transport.	Equation for reactive solutes is available: need to specify the adsorption isotherm.	PC
VLEACH	US EPA	Vadose zone leaching model describing the movement of an organic contaminant between three phases.	1D FD	Unsaturated	Initially, VLEACH calculates the equilibrium distribution of contaminant mass between the liquid, gas and sorbed phases. Transport processes are then simulated; vertical transport by advection in the liquid phase and gaseous diffusion in the vapour phase. Assumes the vadose zone is in a steady-state condition with respect to water movement. The contaminant is not subjected to in situ production or degradation.		Model is based on equilibrium reactions between phases.	PC

Table 3.2 continued

Model	Developer/ Supplier	Description	Numerical discritisation[1]	Saturated/ unsaturated	Hydrology	Solute transport	Geochemistry options	Computer system
VS2DT	USGS[4]	Flow and solute transport in variably saturated, single phase flow in porous media.	1D columns, 2D vertical cross sections and 3D cylinders, FD.	Saturated and unsaturated	Nonlinear water flow equation (based on total hydraulic head).	The derivation of the advection-dispersion solute transport equation is based on conservation of mass and Fick's law.	Solute source/sink terms include first-order decay, equilibrium partitioning to the solid phase and ion exchange.	PC
BioF&T-2D	DAEM[5]	Biodegradation, flow and transport.	2D or 3D FE	Saturated and unsaturated	Flow and transport in the unsaturated zone is modelled either in 1D vertical or in 2D planar or radial symmetric vertical sections or in full 3D. The flow and transport in the saturated zone are modelled as 2D areal or a 3D phenomenon. Incorporates convection, dispersion, diffusion.		Adsorption, desorption and biodegradation.	PC
CTRAN/W	GEO-SLOPE International Ltd	Contaminant transport and migration analysis model.	2D FE	Saturated and unsaturated	SEEP/W module computes the water flow velocity, water content and water flux.	CTRAN/W has a SOLVE function to analyse advection dispersion processes; TRACK function to model advection only.	Optional losses due to adsorption and decay.	PC
ESTEL2D and SUBIEF2D	LNH-EDF[6] and University of Bristol	Finite-element model of saturated-unsaturated flow through porous media.	2D FE	Saturated and unsaturated	Richards' equation describes flow through porous media; solved to give either pressure head or pressure head and moisture content.	SUBIEF module has potential to be linked with ESTEL; solves the advection-dispersion equation.	User defined geochemical reactions can be incorporated within SUBIEF.	UNIX workstation.
FLOWNET/ TRANS	Waterloo Hydrogeologic, Inc.	Cross-sectional steady-state groundwater flow and transport model.	2D FE	Saturated	Solves the steady-state saturated flow equation using the dual formulation of hydraulic potentials and stream functions.	Solves the contaminant transport problem using the standard 2D equation for advective-dispersive transport.	Includes first order decay and retardation.	PC
FLOWPATH II	Waterloo Hydrogeologic, Inc.	Groundwater flow, remediation and wellhead protection model.	2D	Saturated	Designed for simulating 2D groundwater flow and contaminant transport in unconfined, confined and leaky aquifers.		Adsorption is assumed to be uniform for the entire model domain.	PC

Table 3.2 continued

Model	Developer/ Supplier	Description	Numerical discritisation[1]	Saturated/ unsaturated	Hydrology	Solute transport	Geochemistry options	Computer system
HYDRUS2D/ SWMS-2D	USDA Salinity Laboratory	2D water flow and solute transport	2D FE	Saturated and unsaturated	Numerically solves the Richards' equation for saturated-unsaturated water flow and the Fickian-based advection-dispersion equation for solute transport.		Includes provisions for linear equilibrium adsorption, zero-order production, and first-order degradation.	PC
MOC	USGS	2D solute transport and dispersion in groundwater.	2D FD	Saturated	The model couples the groundwater flow equation with the solute transport equation to simulate convective transport, hydrodynamic dispersion and mixing from fluid sources.		Incorporates first-order irreversible rate reaction, reversible equilibrium controlled sorption and reversible equilibrium controlled ion exchange.	PC
SUTRA	USGS	Simulation model for saturated-unsaturated fluid-density dependent groundwater flow with transport or chemically-reactive single species solute transport.	2D hybrid FE and integrated FD.	Saturated and unsaturated	Fluid density dependent saturated or unsaturated groundwater flow.	Transport of a solute in groundwater, or transport of thermal energy in the groundwater and solid matrix of the aquifer.	Solute may be subject to equilibrium adsorption on the porous matrix and both first order and zero order production and decay.	PC
VAM2D	Scientific Software Group	Simulates transient or steady-state flow and contaminant transport in porous media.	2D FE	Saturated and unsaturated	Unsaturated-saturated flow equation is solved using the Galerkin method with an iterative scheme. Hysteresis effects in the water retention curve can be simulated.	The contaminant transport option can account for advection and hydrodynamic dispersion.	The transport option can account for equilibrium sorption and first-order degradation.	PC

Table 3.2 continued

Model	Developer/ Supplier	Description	Numerical discritisation[1]	Saturated/ unsaturated	Hydrology	Solute transport	Geochemistry options	Computer system
3DFEMFAT	Scientific Software Group	Flow and transport.	3D FE	Saturated and unsaturated	The generalised Richards' equation and Darcy's law governing pressure distribution and water flow in saturated-unsaturated media.	Transport equation is derived based on the principle of conservation of mass.	Three adsorption models (linear isotherm, nonlinear Langmuir and Freundlich isotherms) in the transport module.	PC or any workstation.
ChemPath	BASELINE Concept	3D groundwater solute transport model.	3D flow lines.	Saturated	ChemPath is designed to take the groundwater flow solution from a groundwater model in the form of pathlines and solve the contaminant transport problem along these solute pathlines instead of the 2 or 3D mesh or grid.		Can include zero and first order decay; linear, Langmuir and Freundlich equilibrium and kinetic sorption and two site sorption.	PC
HST3D	USGS	Simulation of heat and solute transport in 3D groundwater flow systems.	3D FD	Saturated	Saturated groundwater flow equation is a combination of the conservation of total fluid mass and Darcy's law.	Heat transport equation from the conservation of enthalpy for the fluid and porous medium; solute transport equation from the conservation of mass for a single solute species.	Solute species may decay and adsorb onto he porous medium.	PC
HYDROGEO CHEM	Yeh and Tripathi (1991).	Hydrologic transport and geochemical reaction model.	3D FE	Saturated and unsaturated	The generalised Richards' equation and Darcy's law governing pressure distribution and water flow within saturated-unsaturated media.	Transport equations covering advection, dispersion and diffusion.	Aqueous complexation, adsorption/desorption, ion-exchange, precipitation/dissolution, redox and acid-base reactions.	PC or any workstation.

Table 3.2 continued

Model	Developer/ Supplier	Description	Numerical discritisation[1]	Saturated/ unsaturated	Hydrology	Solute transport	Geochemistry options	Computer system
HYDROGEO CHEM2	Modified from Yeh and Tripathi (1991).	Reactive chemical transport controlled by kinetic and equilibrium reactions.	3D FE	Saturated and unsaturated	As above.	Transport module designed to simulate transport of aqueous components and mass balance of absorbent components and ion-exchange sites: includes advection, dispersion/diffusion and slight deformation.	Geochemical reaction module includes nine types of kinetic and equilibrium reactions.	PC or any workstation.
KYSPILL	American Institute of Hydrology	Groundwater pollution forecasting system for modelling contaminant plumes. Primarily a forecasting tool.	3D dispersion in soils; 2D propagation in aquifers.	Saturated and unsaturated	Implements new stable semi-analytical solutions of the coupled flow and transport equations. Assumes the Dupuit simplifications to describe the groundwater flow are valid.		Linear kinetic adsorption isotherm; first order degradation process for biological, radioactive or chemical decay.	PC
MODFLOWT	USGS	An enhanced version of MODFLOW for simulating 3D contaminant transport.	3D FD	Saturated	Groundwater flow data sets created using MODFLOW.	Simulates transport of one or more miscible species through advection and dispersion.	Adsorption and decay.	PC
MT3D	S. S. Papadopulos and Associates, Inc.	A modular 3D groundwater solute transport model.	3D	Saturated	Linked with the groundwater flow simulator, MODFLOW.	Models advection, anisotropic dispersion.	Models first-order decay and production reactions and linear and nonlinear sorption.	PC

[1] FD = finite difference; FE = finite element.
[2] United States Environmental Protection Agency.
[3] Commonwealth Scientific and Industrial Research Organisation.
[4] United States Geological Survey.
[5] Draper Aden Environmental Modeling.
[6] Laboratoire National d'Hydraulique d'Électricité de France.

The ESTEL2D model confers the advantages of permitting the more accurate spatial representation of soil types within the model domain and incorporates recent advances in the numerical analysis of the Richards' unsaturated flow equation (Desitter *et al.*, 2000). Both the ESTEL2D and SUBIEF2D models have been developed by Laboratoire National d'Hydraulique d'Électricité de France (LNH-EDF) in collaboration with the University of Bristol, so they also have the advantage of easily accessible in-house expertise, as well as access to the model source code. SUBIEF2D also allows great flexibility in the geochemistry it can incorporate. The user can implement any suitable chemical reaction equation through a water quality file or incorporate an existing geochemical model to describe the requisite chemical reactions. Both ESTEL2D and SUBIEF2D are part of the TELEMAC suite of water and chemical transport models. SUBIEF2D is currently designed for use with a 2D surface water hydraulic modelling code, TELEMAC2D, but potential exists for it to be adapted for use with the ESTEL2D subsurface hydrological model, as all these models are based on the same architecture and finite element libraries.

The ESTEL2D model, in conjunction with the SUBIEF2D model, has been selected for use in this study because it meets all the basic criteria and it has the additional benefits outlined above. It also has the potential for the implementation of an appropriate method to account for zones of complete saturation in the model, and for implementing a seepage boundary condition. By beginning this study with a thorough investigation of hydrological processes using the ESTEL2D model and only later incorporating the chemical transport aspect with the SUBIEF2D model, a deliberate attempt is made to prioritise the modelling to reflect the opinion of many researchers, highlighted in the previous chapter, that "perhaps the single most important key to understanding a solute-transport problem is the development of an accurate definition (or model) of the flow system" (Konikow and Patten, 1985).

The potential for coupling ESTEL2D and SUBIEF2D has been mentioned in a study by Lucille *et al.* (2000). However, their work was concerned with coupling transport (SUBIEF2D) with a geochemical model (CHESS), not coupling transport with a hydrological model. In addition, the Lucille *et al.* (2000) study only considered fully saturated, steady state cases. The full implications of a variable moisture content, and how this should be implemented in the SUBIEF2D model, were not explored.

3.2.2 Description of model formulation

The following section will describe the ESTEL2D and SUBIEF2D models, the mathematical equations on which they are based, and the procedure for running a model simulation.

Assuming a fluid of constant density and viscosity, the governing equation for variably saturated flow through incompressible porous media can be derived by combining the

momentum equation (Darcy's law) with the mass conservation equation. The resulting equation, referred to as the Richards' equation, can be expressed using either the pressure head (h), the moisture content (θ) or a combination of the two (the 'mixed' form) as the unknown variable. The mixed form of the Richards' equation may be given as:

$$\frac{\partial \theta}{\partial t} - \underline{\nabla} \cdot K(h)\underline{\nabla} h - \frac{\partial K}{\partial z} = 0 \qquad 3.1$$

where t is the time [T], θ is the volumetric moisture content [L^3 L^{-3}], h is the pressure head [L], K is the hydraulic conductivity tensor [L T^{-1}], and z is the elevation [L]. When solved numerically, the mixed form of the Richards' equation has been shown to lead to significant improvements in the solution mass conservation properties when compared to the alternative θ-based and h-based formulations (Celia *et al.*, 1990).

In unsaturated conditions both the moisture content (θ) and the hydraulic conductivity (K) are not constant, but are dependent on the pressure head (h). In order to solve Richards' equation, the constitutive relations between the dependent variable (pressure head) and the nonlinear terms (moisture content, moisture capacity, and conductivity) must therefore be specified. First, the relationship between moisture content and pressure head is provided by the soil water retention curve. To define the soil water retention curve, the effective saturation is first defined as:

$$S_e = \frac{\theta - \theta_s}{\theta_s - \theta_r} \qquad 3.2$$

where S_e is the effective saturation, θ_r is the residual saturation [L^3 L^{-3}], and θ_s is the saturated moisture content [L^3 L^{-3}].

Neglecting any hysteresis effect, the soil water retention curve takes the form of a relationship between S_e and h that increases from the residual saturation θ_r to the saturated moisture content θ_s. A number of soil water retention models are included in the code including the van Genuchten (van Genuchten, 1980) and Brooks and Corey (Brooks and Corey, 1964) relationships. ESTEL2D does not yet incorporate hysteresis as to do so would add great complexity to the model. There is no need for a separate expression relating moisture capacity and pressure head, as this relation will follow by differentiating the moisture content-pressure head function.

A second relationship is required that describes the manner in which hydraulic conductivity decreases with moisture content. Hydraulic conductivity can be decomposed as the product of a relative conductivity, which is pressure head (or moisture content) dependent, and a saturated conductivity tensor:

$$\underline{\underline{K}} = k_r \underline{\underline{K}}_{sat} \qquad 3.3$$

where $\underline{\underline{K}}$ is the hydraulic conductivity [L T^{-1}], k_r is the relative conductivity ($0< k_r<1$), and $\underline{\underline{K}}_{sat}$ is the saturated conductivity tensor [L T^{-1}]. The relative conductivity tends to decrease to a null value when the soil dries and is therefore an increasing function of h. It is common practice to use a conductivity-pressure head relationship that is derived from the moisture content-pressure head function, using some physically based approach such as the distribution of pore sizes. In this way, the number of fitting parameters in the constitutive relations is kept to a minimum (Paniconi *et al.*, 1991).

Boundary conditions refer to conditions specified at the edges of the flow domain (Beven, 1985). Three main types of boundary conditions can be defined within ESTEL2D: Dirichlet condition (pressure head is specified), Neuman condition (flux is specified) and Cauchy condition (flux is a function of a dependent variable) (Feddes *et al.*, 1988). At infiltration boundaries the boundary condition may change during the simulation from a specified flux boundary when the surface is unsaturated (precipitation rate), to a fixed head boundary as water starts to pond on the surface.

When transient soil water flow is modelled, initial conditions must be defined; within ESTEL2D these are values of pressure head at each nodal point within the model domain (Feddes *et al.*, 1988). They describe the state of the hydrological system in terms of moisture contents and subsurface hydraulic potentials at a time $t = 0$ from which the simulation starts. The initial head distribution can be obtained by solving a steady state problem. Alternatively, the initial heads can be generated based on knowledge of the initial water-table distribution or initial soil saturation deficits. A water-table depth or soil moisture deficit can be converted into a vertical pressure head distribution using, for example, a hydrostatic assumption (Paniconi and Wood, 1993). It may take a significant period of start-up time in the simulation before the forecasts of the model no longer depend significantly on the specified initial conditions (Beven, 1985).

Solution of the above equation system in time and space is achieved by finite element numerical methods. The time discretisation for the Richards' equation is defined using the modified Picard iterative scheme; this is a widely used procedure, robust and simple to implement, but it has been known to fail or converge slowly (Celia *et al.*, 1990; Paniconi and Putti, 1994). The finite element spatial discretisation in ESTEL2D is defined using the Galerkin variational formulation. The governing equations are solved to give the pressure head, from which values of hydraulic head, Darcian velocity and moisture content can subsequently be derived using additional relationships.

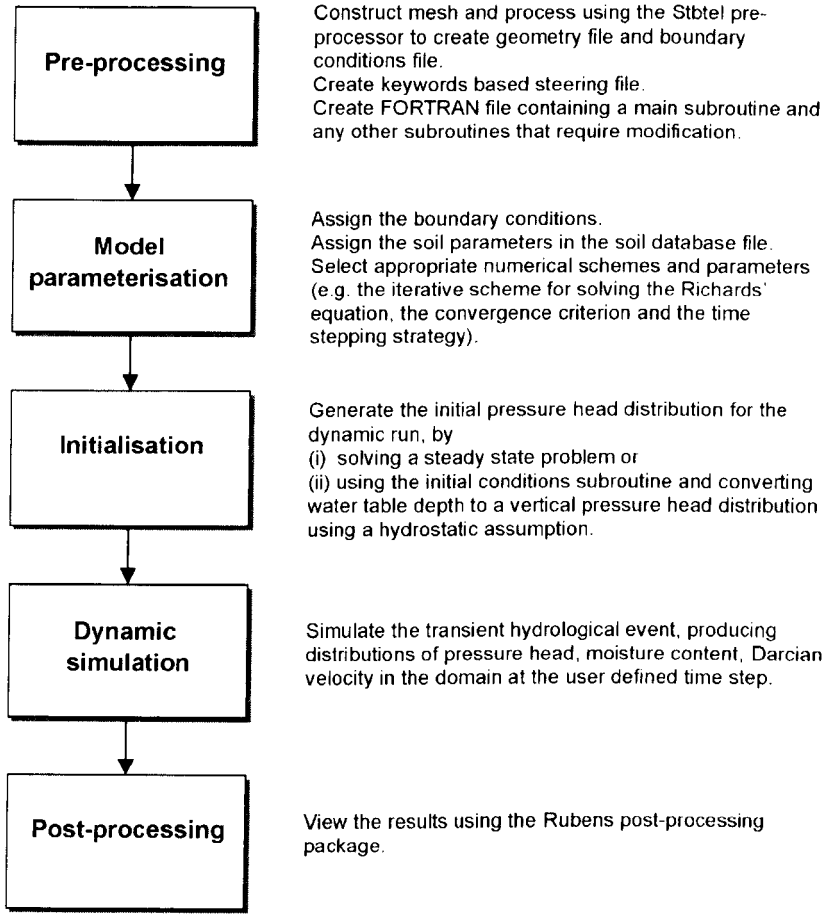

Figure 3.2 Procedure for running an ESTEL2D simulation

Two convergence criteria are available as standard in the ESTEL2D model: a relative convergence criterion, and the Huang convergence criterion. In addition to these, a further, modified Huang convergence criterion has been developed for this study. The relative convergence criterion involves both an absolute error and a relative error as follows:

$$|dh| \leq \delta_r |h| + \delta_a \qquad 3.4$$

where dh is the change in pressure head, h, between two iterations [L], δ_r is the relative tolerance, and δ_a is the absolute tolerance [L]. Equation 3.4 shows that the relative part can become large in comparison with the absolute part when the absolute value of the pressure head is high, making this a less strict criterion under these circumstances. Huang *et al.* (1996) introduced a criterion based on the capacity:

$$C|dh| \leq \delta_c \qquad 3.5$$

where C is the moisture capacity, and δ_c is the Huang tolerance. This has the advantage of allowing a relatively large error for regions where the soil is dry but changes in the water content are still small. However, this criterion is only valid in unsaturated conditions. Wherever the domain is saturated, the capacity is zero (without the storage parameter), with the result that the test for convergence will always be true (the left-hand side of Equation 3.5 will always be zero). A modification of the Huang convergence criterion has therefore been implemented in ESTEL2D that is applicable in both saturated and unsaturated conditions. Where the domain is unsaturated, the standard Huang criterion (Equation 3.5) is maintained. Where the domain is saturated, the criterion is modified as follows:

$$|dh| \leq \delta_c \varphi \qquad \text{when } C = 0 \qquad 3.6$$

where φ is an additional parameter with a value greater than one that is implemented to make the convergence criterion less strict in the saturated zone. The greatest accuracy is therefore maintained in the unsaturated zone where the capacity can change rapidly for a small change in pressure head.

A more detailed discussion of the governing equations, finite element discretisation and time discretisation used in ESTEL2D is contained in Desitter (1998) and Desitter *et al.* (2000). The stages involved in running an ESTEL2D simulation are illustrated in Figure 3.2.

The equation solved in SUBIEF2D is an advection-dispersion equation, designed for sediment and solute transport in open channel flow. This is introduced briefly below, but will be considered in more detail in Section 3.5 where the procedure for coupling the models is discussed.

Changes in chemical concentration can occur within a dynamic groundwater system primarily as a result of three processes: advective transport, hydrodynamic dispersion and sources and sinks (Konikow and Patten, 1985). Advective transport (also commonly referred to in the literature as convection) refers to the transport of solutes due to water moving and carrying solute with it. Hydrodynamic dispersion causes a spreading of the solute about the average direction of water flow. Source/sink terms can be divided into two general categories: solute mass introduced to or removed from the domain by fluid sources and sinks, and mass introduced or removed by chemical reactions occurring within the water (e.g. radioactive decay) or between the water and the solid phase (e.g. adsorption and desorption). The first two processes are described mathematically by the advection-dispersion equation. SUBIEF2D solves the following transport equation (Moulin and Ben Slama, 1998):

$$\frac{\partial c}{\partial t} = \frac{1}{H}\underline{\nabla}\cdot\left(\underline{\underline{D'}}H\underline{\nabla}c\right) - v.\underline{\nabla}c \qquad 3.7$$

where v is the flow velocity [L T^{-1}], H is the depth of water flow [L], c is the concentration of tracer [M L^{-3}] and D' is the dispersion coefficient [L^2 T^{-1}]. The model also includes the facility for simulating the erosion and deposition of a particulate tracer.

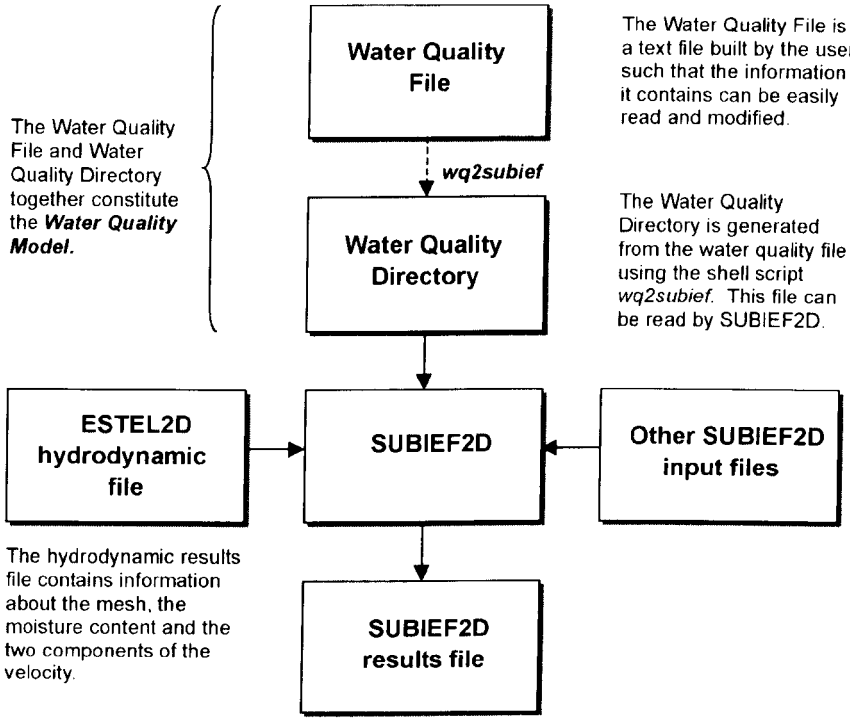

Figure 3.3 Organisation chart of a SUBIEF2D simulation.

Boundary conditions are imposed in SUBIEF2D by specifying for each tracer the type of boundary condition (set concentration at a fluid border, free concentration at a fluid border, or an impermeable boundary condition), and the values of the imposed concentrations. The type of boundary condition is obviously partly dependent on the boundary conditions implied by the fluid dynamics in the hydrodynamic results file. The imposed concentrations are implemented through the use of an input file that allows the user to define different boundary concentrations for different areas of the mesh, and the time period over which these boundary conditions apply. Initial tracer concentrations, which may vary in different areas of the mesh, are set in another user defined input file. In addition, a source points input file allows the user to define the characteristics of solute outfalls located inside the computational domain. To solve the governing equations, three advection schemes are

available: the Method of Characteristics, the SUPG scheme, and the PSI scheme. The properties of these solver schemes will be explored during the model assessment procedure.

The organisation of the SUBIEF2D model is illustrated in Figure 3.3. More information on the governing equations of SUBIEF2D, the model structure and model use can be found in Moulin and Gailhard (1996).

In a groundwater flow study, the sediment erosion and deposition capability of the SUBIEF2D model will no longer be relevant. The implementation of the advection-dispersion equation may also need to be altered. These and other issues will need to be explored when attempting to couple the ESTEL2D and SUBIEF2D model codes.

3.3 Initial coupling of SUBIEF2D and ESTEL2D

SUBIEF2D was designed to work with a hydrodynamic results file from the TELEMAC2D surface water hydraulic code. To assess the potential for adapting SUBIEF2D for use with the subsurface hydrological processes of ESTEL2D first required an understanding of how the model operated with TELEMAC2D. It was then possible to identify the parts of the model that could remain unchanged, the parts that were specific to TELEMAC2D use and needed to be omitted or modified, and new pieces of code that were necessary.

A review of the SUBIEF2D model operation with TELEMAC2D hydrodynamic files highlighted three main areas that needed careful consideration before SUBIEF2D could be used with an ESTEL2D hydrodynamic file. These three areas are the mesh specification, the treatment of erosion and deposition, and the implementation of the advection-dispersion equation.

3.3.1 Mesh specification

When used with a TELEMAC2D hydrodynamic file, the SUBIEF2D code expects to receive a 2D mesh in plan view, but with a value of bottom elevation associated with each node, giving a pseudo-3D representation of the domain. The inclusion of bottom elevation permits erosion and deposition of the bed to be calculated when a particulate tracer is used. The meshes used in ESTEL2D applications are 2D but represent a vertical cross-sectional view, rather than a plan view, of the domain. The notion of a bed elevation in the sense of the TELEMAC2D case is therefore inappropriate, and a meaningful physical interpretation of this variable in the ESTEL2D case is not immediately obvious. This issue is considered further in the discussion of the modelling of erosion and deposition.

The 2D vertical cross-sectional mesh of ESTEL2D can be used with the SUBIEF2D code by setting the bottom elevation to zero everywhere in the domain. This is done automatically

by the SUBIEF2D code if there is no bottom topography file and if no bottom elevation is given in the hydrodynamic results file (as is the case with ESTEL2D hydrodynamic results files).

3.3.2 Erosion and deposition

SUBIEF2D is designed to model the movement of tracers in both dissolved and suspended form. In the latter case, SUBIEF2D can calculate their settling on the bottom and their return to suspension through erosion. SUBIEF2D therefore includes several variables that pertain specifically to particulate (sediment), rather than dissolved, chemical transport.

The way sediment transport is modelled in the original SUBIEF2D code was quite specific to surface water flow situations, given the inclusion of parameters such as a friction coefficient. Modelling subsurface sediment transport would require more careful consideration of the physical meaning of some of the SUBIEF2D variables for an ESTEL2D case and possibly extensive modification of the code. This would also involve tackling more thoroughly the issue of whether the notions of bed elevation and bed concentration have real physical parallels in an ESTEL2D case, or if a totally new approach is needed. In fact, the transport of particulate tracers in subsurface flow is a relatively neglected area of interest in hydrological modelling and this phenomenon is rarely included in subsurface chemical transport models, although they may include chemical adsorption on to stationary sediments i.e. the soil matrix. It was therefore felt sufficient for this study to consider only dissolved tracers, and not the transport of sediment. This involved a more straightforward application of the SUBIEF2D code in its original form.

It was not immediately obvious how SUBIEF2D made the distinction between a dissolved chemical and a suspended particle, as there is no separate water quality file to describe a particulate tracer as opposed to a dissolved tracer. It appeared that three external parameters were important to this issue; settling velocity of the state variable, critical velocity for deposition of the state variable, and critical velocity for erosion of the state variable. If these variables are not assigned a value by the user in the water quality file they are given default values; the settling velocity and deposition velocity are set artificially low (to zero) and the erosion velocity is set artificially high (1×10^{6} m s^{-1}), which effectively means that the dissolved tracer will never settle and the 'bottom' will never erode. This is effectively the definition of a dissolved tracer. For a dissolved tracer in an ESTEL2D case, it is therefore acceptable to leave these three parameters set at their default values.

Further SUBIEF2D model parameters that needed consideration before the code could be used with an ESTEL2D results file are listed in Table 3.3. It was felt that these could present difficulties for an ESTEL2D case, where a dissolved tracer is used and where modification

of the 'bed' is not desired. These variables mostly relate to erosion and deposition of the tracer and associated modifications of the bed. The SUBIEF2D code was thoroughly checked for every subroutine where these particulate tracer-related parameters are used. It was possible to establish that they are irrelevant in the case of an ESTEL2D hydrodynamic file, and importantly, that if they are left at their default values they will pose no problems for the computation.

Table 3.3 SUBIEF2D sediment related model parameters.

Parameter	Default	Description	Comments
Bottom concentration	500 g l^{-1}	Used to set the concentration of the layer of sediment settled at the bed for each of the tracers.	In the ESTEL2D case where the bed elevation is set to zero and isn't modified over time, this variable should become irrelevant, as it is describing the concentration of a deposit of zero thickness. It can be left at the default value with no computational problems.
Critical evolution ratio	0.05	This number is the admissible maximum ratio between bottom evolution and water depth.	In the ESTEL2D case where the bed doesn't evolve, this variable becomes irrelevant and can be left as the default value with no computational problems arising.
Law of bottom friction	2	Used to select the law of bottom friction, Chezy (1) or Strickler (2).	In SUBIEF2D the friction coefficient plays a role in the calculation of the shear velocity at the bed. This velocity in part determines settling and erosion. As there is no erosion or deposition, this variable becomes irrelevant and can be left at the default value.
Friction coefficient	50	Sets the value of the Chezy or Strickler coefficient.	As the friction law is irrelevant, so is the value of the friction coefficient. It can be left at the default value as it doesn't play any part in the computation.
Partheniades constant	0.00002	Determines the value of the constant involved in the Partheniades erosion law.	As there is no erosion and deposition, this variable is irrelevant.
Variable settling velocities	No	Allows the user to define a settling velocity at each point of the mesh for each state variable.	For an ESTEL2D simulation, this logical variable should be left at the default setting of false.

One final check of what is happening at the 'bed' in terms of erosion and deposition when SUBIEF2D was used with an ESTEL2D results file was performed by checking the evolution of the bottom elevation and bed evolution variables which are printed in the SUBIEF2D results file. In all simulations where the settling, erosion and deposition velocities were given their default values listed above, the bed elevation remained at zero

and bed evolution was also zero at all points in time. In summary, it appears that there is no direct way to establish that a tracer is dissolved rather than particulate, but by leaving the erosion and deposition water quality parameters at their default values, and by setting the bed topography to zero, this will automatically ensure that the tracer is treated as dissolved.

3.3.3 Implementation of the advection-dispersion equation

This section will provide a more thorough account of the theory of solute transport through porous media. This review will enable a suitable form of the advection-dispersion equation to be implemented in the revised version of the SUBIEF2D model. The necessary modifications to the code will be described at the end of this section in two parts, the first describing the treatment of advection in SUBIEF2D and the second describing the treatment of dispersion.

3.3.3.1 Theory of solute transport in porous media

A summary of the phenomena that affect solute transport is illustrated in Figure 3.4. The following discussion will look at each of these phenomena in turn. Some of these expressions are used interchangeably in the literature, but in an attempt to clarify the nomenclature, the terms used throughout this report will be consistent with the terms used in the diagram.

Chemical mass transport results from the operation of two phenomena: advection and hydrodynamic dispersion. Advection is the process by which solutes are transported due to the bulk motion of the flowing water. Owing to advection, non-reactive solutes are carried at an average rate equal to the average linear velocity of the water (or volumetric flow rate per unit area of connected pore space), v [L T^{-1}], where $v = q/n$, q [L T^{-1}] being the specific discharge (Darcy velocity) and n [dimensionless] the porosity. The advection process is sometimes called convection, a term that is more correctly reserved for use in discussion of thermally driven groundwater flow (Anderson, 1979).

As flow takes place through a porous medium, a mass of solute (tracer) in the flow will gradually spread out and occupy an ever-increasing portion of the flow domain, beyond the region it is expected to occupy according to the advective hydraulics of the flow system alone. This spreading phenomenon is called hydrodynamic dispersion (also referred to as dispersion or miscible displacement) in a porous medium. As a result of this process, some of the water molecules and solute molecules travel more rapidly than the average linear velocity and some travel more slowly. The solute therefore spreads out in the direction of flow and declines in concentration (Freeze and Cherry, 1979). If initially a tracer-labelled liquid occupies a separate region, with an abrupt interface separating it from an unlabelled

liquid, this interface does not remain an abrupt one, the location of which may be determined by the average velocity expressed by Darcy's law. Instead, an ever-widening transition zone is created, across which the tracer concentration varies from that of the tracer liquid to that of the unmarked liquid (Bear, 1972).

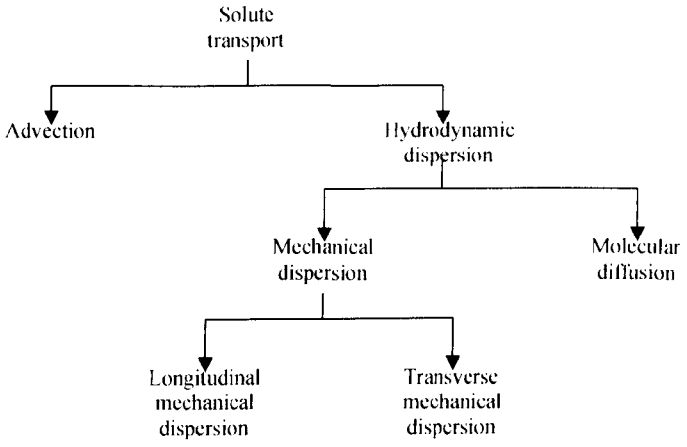

Figure 3.4 Summary diagram of the relationship between phenomena affecting solute transport.

Hydrodynamic dispersion occurs as a result of two processes (see Figure 3.4): firstly, mechanical mixing (mechanical dispersion) during fluid advection, and secondly, molecular diffusion due to the thermal-kinetic energy of the solute particles. Logically, if mechanical dispersion is to be incorporated in the advection-dispersion equation, it should be reflected in the velocity term (Domenico and Schwartz, 1990). Unfortunately, it has not been possible to do this in a simple way. Instead, the coefficient of hydrodynamic dispersion has been introduced to incorporate the combined effect of molecular diffusion and mechanical dispersion (in one dimension):

$$D_x' = D_x + D^* \qquad 3.8$$

where D_x' is the coefficient of hydrodynamic dispersion in the x direction $[L^2\ T^{-1}]$, D_x is the coefficient of mechanical dispersion in the x direction $[L^2\ T^{-1}]$ and D^* $[L^2\ T^{-1}]$ is the coefficient of molecular diffusion for the solute in the porous medium. The justification for treating dispersion in this manner is purely a practical one and stems from the fact that the macroscopic outcome is the same for both diffusion and mechanical dispersion (Domenico and Schwartz, 1990). The actual physical processes, however, are entirely different.

Mechanical dispersion is caused by three mechanisms (on a microscopic scale). The first occurs in individual pore channels because molecules travel at different velocities at

different points across the channel due to the drag exerted on the fluid by the roughness of the pore surfaces. The second process is caused by the difference in pore sizes along the flow paths followed by the water molecules; because of differences in surface area and roughness relative to the volume of water in individual pore channels, different pore channels have different bulk fluid velocities. The third dispersive process is related to the tortuosity, branching and interfingering of pore channels (Freeze and Cherry, 1979). The coefficient of mechanical dispersion, D_x, can be described in the following terms:

$$D_x = \alpha_x v_x \qquad 3.9$$

where α_x [L] is a characteristic property of the porous medium known as dynamic dispersivity, or simply as dispersivity, and v_x [L T^{-1}] is the average linear velocity in the x direction (Bear, 1972). In the case of isotropic media, this equation may be extended to give the following relationships (Bear, 1972):

$$D_L = \alpha_L v \qquad \text{and} \qquad D_T = \alpha_T v \qquad 3.10$$

where α_L is the longitudinal, α_T the transverse dispersivity [L] and v is the average linear velocity [L T^{-1}]. It should be noted that the process of mechanical dispersion is directionally dependent (anisotropic) even though the porous medium is isotropic with respect to textural properties and hydraulic conductivity. Dispersion is stronger in the direction of flow (the longitudinal dispersion) than in directions normal to the flow line (transverse dispersion), so the tracer will spread faster in the flow direction than in directions perpendicular to it (Dullien, 1979; Freeze and Cherry, 1979). In practice, this means that a_L will have a greater value than a_T.

With regard to the molecular diffusion coefficient, it has been recognised that there is a distinction to be made between the diffusion coefficient of a given ion in open water (bulk diffusion coefficient), and the diffusion coefficient of a given ion in porous media (the effective or apparent diffusion coefficient). For example, the hydrodynamic dispersion coefficient D' [L^2 T^{-1}] in Nielsen *et al.* (1986) and Padilla *et al.* (1999) is described in the following terms:

$$D' = D_0\tau + \gamma|v|^{\eta} \qquad 3.11$$

where D_0 is the bulk diffusion coefficient [L^2 T^{-1}], τ is the tortuosity factor [dimensionless], v is the pore water velocity [L T^{-1}] and γ and η are empirical constants where $\eta \sim 1$ and γ is the dispersivity [L]. In this example, $D_0\tau$ is the effective diffusion coefficient, D^* [L^2 T^{-1}] of

Equation 3.8. Freeze and Cherry (1979) also describe the diffusion coefficient in a similar way:

$$D^* = \omega D_0 \qquad 3.12$$

where D^* is the effective diffusion coefficient [$L^2\ T^{-1}$], D_0 is the bulk diffusion coefficient of a given ion [$L^2\ T^{-1}$] and ω is an empirical coefficient that "takes into account the effect of the solid phase of the porous medium on the diffusion" (Freeze and Cherry, 1979). ω has a value less than 1 and is typically between 0.5 and 0.01. This coefficient is analogous to tortuosity as described in the Nielsen *et al.* (1986) example. When looking at examples in the literature, it is therefore important to establish whether a given diffusion coefficient refers to the bulk diffusion coefficient of a chemical species, typically in the range 1 x 10^{-9} to 2 x 10^{-9} $m^2\ s^{-1}$ (Freeze and Cherry, 1979), or the effective diffusion coefficient. The effective diffusion coefficient is smaller than the bulk diffusion coefficient because the ions follow longer paths of diffusion, caused by the presence of the particles in the solid matrix (tortuosity).

The principal differential equation that describes the transport of dissolved reactive constituents in saturated isotropic porous media is known as the advection-dispersion equation (Biggar and Nielsen (1976), one dimensional, steady state case):

$$\frac{\partial c}{\partial t} = D' \frac{\partial^2 c}{\partial x_d^{\,2}} - v \frac{\partial c}{\partial x_d} \qquad 3.13$$

where c is the solute concentration [$M\ L^{-3}$], D' is the coefficient of hydrodynamic dispersion [$L^2\ T^{-1}$], v is the average pore water velocity [$L\ T^{-1}$] and x_d is soil depth [L]. The first term in this equation describes solute transport due to hydrodynamic dispersion, and the second term describes solute transport due to advection.

For unsaturated flow, the dispersivity and the coefficient of molecular diffusion in the porous medium will depend on the saturation (Bear and Verruijt, 1987). Different authors describe different ways to include the moisture content function in the equation. Dagan and Bresler (1979) presented the following equation where mechanical dispersion and molecular diffusion are treated separately and it is only the mechanical dispersion coefficient that is affected by moisture content, not the whole hydrodynamic dispersion coefficient (in one dimension):

$$\frac{\partial c}{\partial t} = D^* \frac{\partial^2 c}{\partial z^2} + \frac{1}{\theta} \frac{\partial}{\partial z} \left(\theta D \frac{\partial c}{\partial z} \right) - v \frac{\partial c}{\partial z} \qquad 3.14$$

where c is the solute concentration [M L^{-3}], θ is the volumetric water content [L^3 L^{-3}], z is the vertical coordinate [L], D is the mechanical dispersion coefficient [L^2 T^{-1}], D^* is the effective molecular diffusivity [L^2 T^{-1}] and v is the pore velocity (average linear velocity) [L T^{-1}]. A rough approximation for D^* is $2/3D_0$, where D_0 is the diffusivity in the solution phase. $D = \alpha_L v$ in which α_L [L] is the dispersivity for longitudinal dispersion.

The advection-dispersion equation as presented in the original, surface water transport version of SUBIEF2D is as follows (Moulin and Ben Slama, 1998):

$$\frac{\partial c}{\partial t} = \frac{1}{H}\underline{\nabla} \cdot \left(\underline{\underline{D'}} H \underline{\nabla} c\right) - v.\underline{\nabla} c \qquad 3.15$$

where v is the flow velocity [L T^{-1}], H is the depth of water flow [L], c is the concentration of tracer [M L^{-3}] and D' is the dispersion coefficient [L^2 T^{-1}]. In this case, unlike Equation 3.14, the mechanical dispersion and molecular diffusion are treated together in one coefficient, and therefore both are affected by the value of water content.

The equation for surface water solute transport is directly analogous to the equation for solute transport through porous media. As the two equations are based on the same governing principles, the coupling procedure for the two models should not require any major alterations to the SUBIEF2D model code. However, the following issues, which relate to subtle differences between the surface and subsurface transport equations, will be explored in more detail:

(i) incorporation of the Darcian flow velocity variable for subsurface solute transport;

(ii) the relationship between water depth in the surface transport equation and moisture content in the subsurface transport equation;

(iii) the relationship between the form of the dispersion coefficient for surface water transport and the hydrodynamic dispersion coefficient in the subsurface transport equation.

3.3.3.2 Advection in SUBIEF2D

To calculate the transport of a tracer from a TELEMAC2D simulation, SUBIEF2D takes values of velocity in the X and Y directions and height of water from the TELEMAC2D hydrodynamic results file. In an ESTEL2D case, the equivalent variables that are needed to solve the advection-dispersion equation are velocity in the X and Y directions and moisture content. All the other values in the hydrodynamic results file are not used.

The use of velocities from an ESTEL2D simulation is directly comparable to the use of velocities from a TELEMAC2D simulation, although some modifications are necessary in

the ESTEL2D case. The Darcian velocity from the hydrodynamic ESTEL2D results file is a macroscopic value which describes the flow through a unit cross-sectional area of the soil, including solids and pore spaces; the actual velocity of the water will overall be greater because water really only flows through pore spaces, not through the solid phase of the soil. For a SUBIEF2D simulation with an ESTEL2D results file the Darcian velocity values have to be changed to values of average linear velocity. A modification has thus been made to the SUBIEF2D code to divide the Darcian velocity by the moisture content. The values of moisture content are calculated by ESTEL2D and stored in the hydrodynamic results file.

In an ESTEL2D case, moisture content is used instead of water height. These variables are described in different terms; water height is described in units of length, whereas volumetric moisture content is a dimensionless variable. However, they both constitute a measure of the amount of water available for chemical transport, so there is a straightforward way to use moisture content in the place of water depth for the ESTEL2D case. The two can be seen to be directly interchangeable in the following example where the ESTEL2D case is seen as a special version of the TELEMAC2D case (Figure 3.5). In each case, the psuedo-3D model calculates the volume of water V_W [L^3] in an element by multiplying the cross-sectional area of the element A [L^2], by the water depth H [L]. The water depth is composed of the porosity n, the percentage saturation S and the depth of the element d [L], in effect a measure of the capacity of the element for holding water:

$$V_W = AH \qquad \text{where } H = nSd \qquad 3.16$$

For an element of unit depth (d = 1 m) and cross-sectional area 10 m^2, in the TELEMAC2D case n = 1 and S = 1, so H = 1 and V_W = 10 m^3.

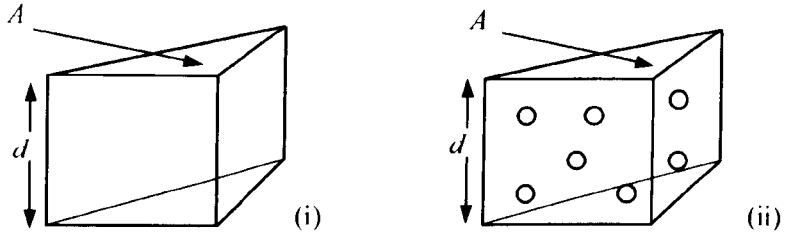

Figure 3.5 (i) TELEMAC2D element and (ii) ESTEL2D element.

In the ESTEL2D case, n is always some value less than 1 (e.g. n = 0.5), because part of the element is occupied by soil. If the soil is completely saturated S = 1, so H = 0.5 and V_W = 5.0 m^3. If the soil is not fully saturated $S \leq 1$ (e.g. S = 0.8), in which case H = 0.4 and V_W = 4.0 m^3.

So, anywhere in the SUBIEF2D model code where water depth is used, for an ESTEL2D case the moisture content is used directly instead. The fact that moisture content has dimensions of cubic metres of water per cubic metre, rather than metres (as for water depth), causes no conflicts of dimensionality in the governing equation (see Equation 3.15).

SUBIEF2D simulations with TELEMAC2D results files can suffer from computational problems in areas of the domain where the water depth tends to zero. This should not be a problem for simulations with ESTEL2D results files because the moisture content of soil will never become zero; it always has a residual value, θ_r, as defined in the ESTEL2D soil database file (and see Equation 3.2).

3.3.3.3 Dispersion in SUBIEF2D

In the unmodified version of the model, the hydrodynamic dispersion coefficient (the equivalent of the velocity diffusivity for a TELEMAC2D case) is calculated in one of three ways:

(i) the dispersion coefficients given in the steering file are used as constants;

(ii) the dispersion coefficients given in the steering file are used in the Euler formula;

(iii) the dispersion values are taken from the TELEMAC2D simulation results file.

In subsurface chemical transport, hydrodynamic dispersion comprises two phenomena; mechanical dispersion and molecular diffusion. A new equation has therefore been programmed into the model (as a replacement for option (ii), the Euler formula), which takes both of these components into account:

$$D_L = \alpha_L v + D^* \qquad 3.17$$

$$D_T = \alpha_T v + D^* \qquad 3.18$$

where D_L and D_T are the longitudinal and transverse coefficients of hydrodynamic dispersion [$L^2\ T^{-1}$], respectively, α_L and α_T are the longitudinal and transverse dispersivities [L], respectively, D^* is the effective molecular diffusion coefficient [$L^2\ T^{-1}$], and v is the average pore water velocity [$L\ T^{-1}$]. As much of the chemical transport work in this study is likely to be theoretical, and values of these parameters will have to be established from literature sources rather than direct measurement, it is preferable to restrict the number of parameters to this simple definition. Therefore, tortuosity is not given as a separate variable; it is assumed to be subsumed in the effective molecular diffusion coefficient.

With this modified version of the code, the values for the longitudinal and transversal dispersivities (α_L and α_T respectively) are defined by the user in the input file in order to calculate the hydrodynamic dispersion coefficient according to the Equations 3.17 and 3.18.

3.4 Initial coupled model runs

After the implementation of the SUBIEF2D changes needed to use an ESTEL2D hydrodynamic results file, the model underwent preliminary tests. This involved comparing the results of a numerical simulation with the analytical solution of a simplified solute transport problem. The aim of these tests was to verify that the coupling procedure had been implemented satisfactorily.

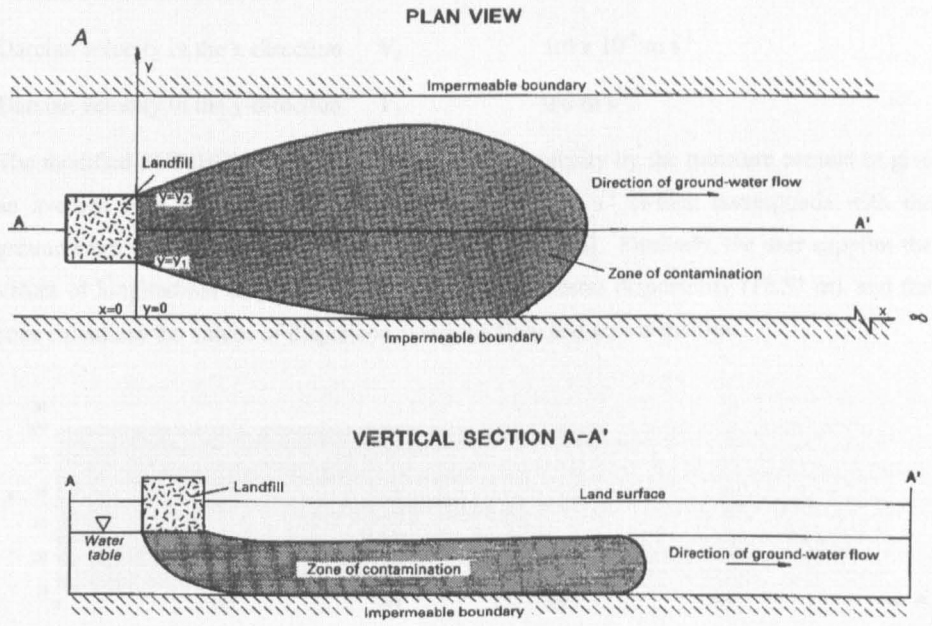

Figure 3.6 Schematic diagram of analytical test case domain (from Wexler, 1992).

Analytical solutions to a range of 1D, 2D and 3D solute transport problems have been compiled into a set of computer programs by the US Geological Survey (Wexler, 1992). An example from the resulting software, ANALGWST, was used to test the revised SUBIEF2D model. The example used here is an idealised semi-infinite, finite width aquifer with a finite width (or 'strip') continuous solute source (illustrated in Figure 3.6). This system has a Dirichlet source boundary condition (specified solute concentration) and zero flux Neumann boundary conditions on the lateral boundaries. The initial conditions are specified such that initial solute concentrations everywhere in the domain are zero. In addition, the following assumptions are employed:

(i) Fluid is of constant density and viscosity.

(ii) Flow is in x-direction only, and velocity is constant.

(iii) The moisture content and longitudinal and transverse dispersion coefficients (D_L, D_T) are constant.

The model variables for this example are given in Table 3.4. The pattern of solute concentration calculated by the analytical solution is output after 25 days and 50 days.

The corresponding numerical solution has also been calculated using SUBIEF2D and an artificially constructed ESTEL2D hydrodynamic results file. The ESTEL2D results file contains three variables, each with a constant value:

Volumetric moisture content	θ	0.4 $m^3 m^{-3}$
Darcian velocity in the x-direction	V_x	1.4 x 10^{-6} m s^{-1}
Darcian velocity in the y-direction	V_y	0.0 m s^{-1}

The modified SUBIEF2D code divides the Darcian velocity by the moisture content to give an average pore water velocity value of 3.5 x 10^{-6} m s^{-1} (which corresponds with the groundwater velocity value input to the analytical solution). Similarly, the user supplies the values of longitudinal dispersivity (57.14 m) and transverse dispersivity (18.57 m), and the code calculates the values of dispersion along the flow and across the flow.

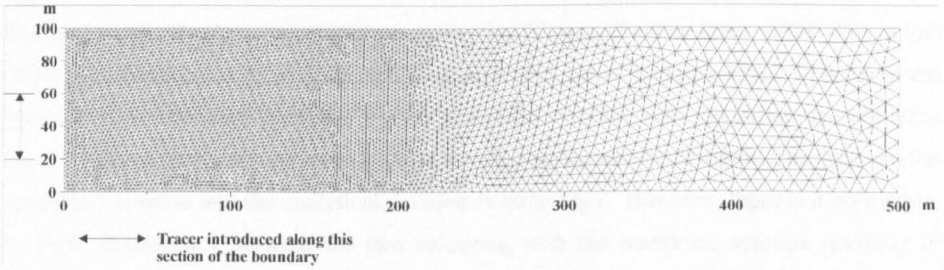

Figure 3.7 Finite element mesh for analytical test case, indicating inflow strip of imposed solute concentration (between y = 20 m and y = 60 m).

A finite element mesh has been constructed according to the dimensions used in the analytical case (Figure 3.7). The domain therefore has a finite width of 100 m. 'Semi-infinite' implies that the outflow boundary of the system being simulated is far enough away from the solute source that the boundary will not affect solute concentrations within the area of interest (Wexler, 1992). The finite element mesh has therefore been specified with a much greater length (500 m) than the distance that the solute would be transported in 50 days given the parameter values in Table 3.4 (approximately 150 m). As no solute transport is

expected in the portion of the mesh furthest from the solute source, the elements in this area of the domain have a much coarser resolution. At this stage, tests of the effect of the model structural parameters have not yet been carried out. To circumvent potential problems with the numerical solution, these initial model runs have therefore used a high spatial and temporal resolution (2.5 m elements, rising to 10 m elements in the low resolution section of the mesh, and a 200 second timestep).

Table 3.4 Model variables for the analytical test case.

Parameter		**Value**
Aquifer width	W	100 m
Lower limit of solute source	Y_1	20 m
Upper limit of solute source	Y_2	60 m
Groundwater velocity	V_x	3.5×10^{-6} m s^{-1}
Longitudinal dispersivity	α_L	57.14 m
Transverse dispersivity	α_T	18.57 m
Solute concentration at source	c_0	100 mg l^{-1}
From the values given above, the following terms are obtained:		
Dispersion in x-direction	D_L	2.0×10^{-4} m^2 s^{-1}
Dispersion in y-direction	D_T	6.5×10^{-5} m^2 s^{-1}

Figure 3.8a shows the distribution of the tracer in the domain after 50 days. Figure 3.8b shows a profile of solute concentration, again after 50 days of solute input, taken along a line that passes through y = 40 m (indicated by the line and arrow in Figure 3.8a). This compares the solute concentration predicted by the analytical solution with the solute concentration obtained using the numerical simulation. Overall, the degree of correspondence between the numerical solution and the analytical solution is quite high. However, there is a noticeable, if small, discrepancy between the two solutions, with the numerical solution resulting in slightly higher concentrations along the profile in comparison with the analytical solution.

As a further investigation, two more values of constant velocity were tested, which were half (1.75×10^{-6} m s^{-1}) and double (7.0×10^{-6} m s^{-1}) the velocity already examined (3.5×10^{-6} m s^{-1}), all with an input solute concentration of 100 mg l^{-1}. The results of these simulations are illustrated in Figure 3.9. These simulations show a similar result to that illustrated in Figure 3.8b; a fairly good correspondence between the numerical and analytical solutions, but a slightly higher concentration resulting from the numerical solution. The discrepancy appears to grow slightly as the velocity increases.

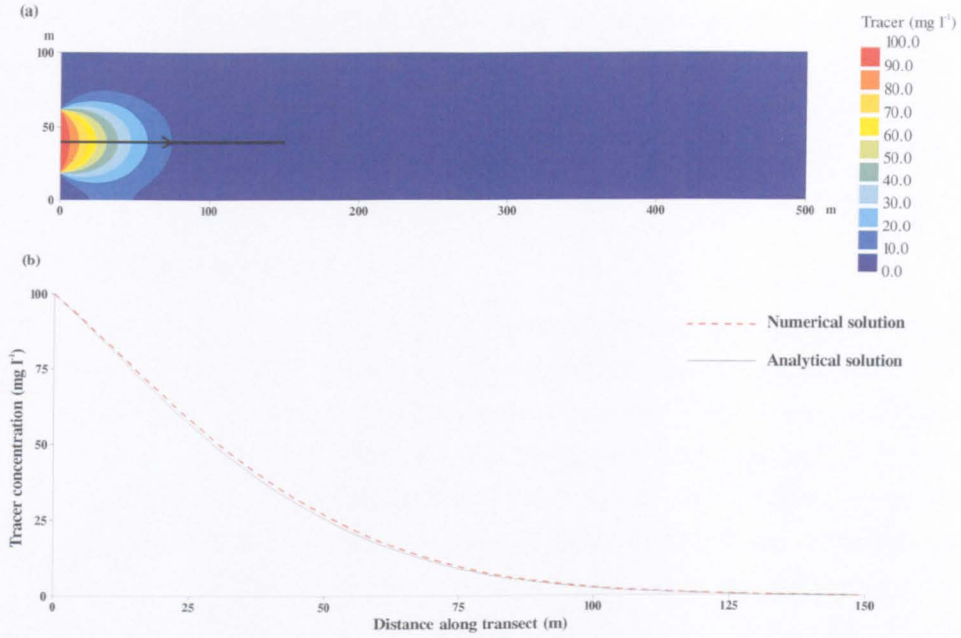

Figure 3.8 Comparison of numerical solution and analytical solution, with an inflow solute concentration of 100 mg l^{-1}. a) Distribution of solute after 50 days. b) Profile of solute concentration after 50 days, at y = 40 m.

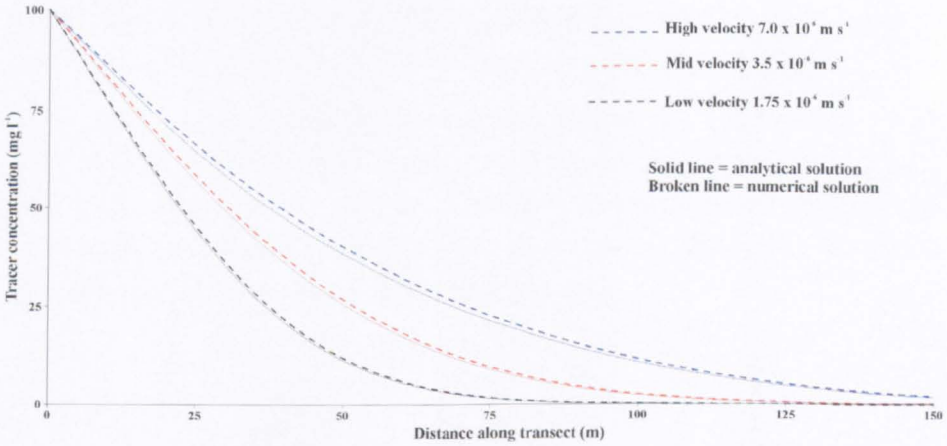

Figure 3.9 Comparison of numerical solution (broken line) and analytical solution (solid line) for three different velocity values: 7.0 x 10^{-6}, 3.5 x 10^{-6} and 1.75 x 10^{-6} m s^{-1}.

Numerical solutions of the advection-dispersion equation commonly suffer from inaccuracies in the solution, including oscillations in the computed concentration profile, and numerical errors that cause a smearing of the concentration front (numerical dispersion). It is likely to be this kind of phenomenon that is resulting in the observed discrepancy between the analytical solution and the numerical simulation reported here. The accuracy and errors

of the numerical solution will be subject to a much more comprehensive assessment during the model optimisation procedure in a Chapter 5. In general, the comparison of the numerical solution with an analytical solution has established that the computer program actually carries out the logical processes expected of it. The SUBIEF2D code has been successfully modified for use with ESTEL2D results files.

3.5 Chapter summary

During this chapter, a preliminary version of a hydrological and chemical transport model has been developed which will be capable of addressing current research questions in floodplain hydrological and chemical transport process research. Firstly, a conceptual model of how the floodplain system is believed to operate was developed, based upon research to date in this field. Available numerical models were reviewed, and a decision was made to base the model development around two existing models, ESTEL2D and SUBIEF2D, as they fulfil the basic technical criteria for successful modelling of this complex, dynamic environment. A description of these models was followed by a detailed exploration of the changes which had to be made to the SUBIEF2D model code in order to model solute transport in porous media. Once these changes had been implemented, the numerical model was subjected to tests against an analytical solution of the advection-dispersion equation. This has revealed that the chemical transport computer code is working as intended, and that the changes that have been made to the code have been implemented satisfactorily.

This chapter has also identified two additional features that are necessary for the implementation of the conceptual model of floodplain hydrological processes outlined in Section 3.1. These attributes are the seepage face boundary condition, and the thorough treatment of changes in stored fluid mass under fully saturated conditions. The development of these features will be the subject of the following chapter.

4 Further Model Developments

Chapter 3 was concerned with the selection and description of the ESTEL2D and SUBIEF2D models, which will provide the basis on which to construct a model of floodplain hydrological and chemical transport processes. The initial coupling of these two models was described and implemented, along with some comparisons to an analytical solution, which indicated that the model is working as intended.

However, as pointed out in the description of the model criteria, the coupled model requires some extra features before it can successfully be implemented in the hillslope-floodplain-channel environment. The first is an ability to simulate periods of complete saturation within the model domain, which will involve a consideration of the mechanisms which effect changes in the stored fluid mass of the soil. The second is the ability to account for a seepage boundary condition, which will be necessary to model cases appropriately where hillslope throughflow discharges onto the floodplain surface at the hillslope-floodplain interface, or in areas of the floodplain directly adjacent to the stream channel. The development of these two features in the ESTEL2D part of the newly coupled model will form the subject of this chapter.

4.1 Accounting for mechanisms of change in water storage

The intended application of ESTEL2D to the dynamic floodplain environment demands that the model should include a way to account for the phenomenon of storage. In order to develop an appropriate solution, the literature on this subject will be reviewed, and whether and how other variably saturated models incorporate storage properties will also be considered.

4.1.1 Review of storage properties of porous media

This section aims to draw together some of the work that has been carried out in this subject area. Research by Narasimhan in the late 1970s is particularly relevant, as he was specifically concerned with the importance of the treatment of water storage in saturated-unsaturated flow modelling. Since that time there has been relatively little exploration of the topic, although work continues to develop on the closely related topics of soil deformation

and fluid flow through deforming porous media. In order to set other modelling approaches in context, this review begins with a description of the alternative formulations of the Richards' equation as implemented in ESTEL2D, and an overview of their relative merits.

In the modelling of unsaturated-saturated flow processes several alternatives exist for solving numerically the governing balance equations with their non-linear constitutive relationships. The Darcy equation of fluid motion and the fluid mass conservation equation form the physical basis. In the context of unsaturated flow the basic formulation involves both the fluid pressure head h and the saturation S as unknown variables. For these two unknowns only one balance equation, the basic Richards' equation, is available. To close the mathematical model one constitutive relationship in the form of the capillary pressure head-saturation function (moisture characteristic curve) is additionally needed to convert one variable to the other (and vice versa). Consequently, the modeller has to decide between primary and secondary variables. Depending on such a choice, different modelling approaches result which are mathematically equivalent in the continuous formulation, but their discrete analogs are different (Diersch and Perrochet, 1999). Three forms of the unsaturated flow equation can be derived:

(i) the pressure based (h)-form, where the primary variable is the pressure head (or the hydraulic head; Celia *et al.*, 1990):

$$C(h)\frac{\partial h}{\partial t} - \underline{\nabla}\cdot K(h)\underline{\nabla}h - \frac{\partial K}{\partial z} = 0 \qquad 4.1$$

where h is pressure head [L], $C(h) \equiv d\theta/dh$ is the specific moisture capacity function [L^{-1}], $K(h)$ is the unsaturated hydraulic conductivity [$L\,T^{-1}$], and z is elevation [L].

(ii) the saturation-based (S)-form, where the saturation or the moisture content, θ [dimensionless] is chosen as the primary variable,

$$\frac{\partial \theta}{\partial t} - \underline{\nabla}\cdot K(\theta)\underline{\nabla}\left(\frac{\theta}{C}\right) - \frac{\partial K}{\partial z} = 0 \qquad 4.2$$

(iii) the mixed (h-S)-form, where both variables are employed and, in solving the discrete equation system, the pressure head is actually used as the primary variable (Celia *et al.*, 1990):

$$\frac{\partial \theta}{\partial t} - \underline{\nabla}\cdot K(h)\underline{\nabla}h - \frac{\partial K}{\partial z} = 0 \qquad 4.3$$

Each of the three different forms has advantages and drawbacks. The h-based form can be used for both saturated and unsaturated soils. The pressure head variable is unique and continuous. But it has been shown that the h-based form can produce significant global mass

balance errors unless very small time steps are used (Diersch and Perrochet, 1999). In addition, the *h*-based equation may become very difficult to solve when the soil is extremely dry. It is therefore best suited to soils of moderate to high saturation (Narasimhan and Witherspoon, 1977). Some of these difficulties are avoided when using the mixed-form schemes that possess much better properties with respect to accurate mass conservative solutions (Diersch and Perrochet, 1999). Numerical schemes based on the *S*-form of the Richards' equation are restricted to unsaturated flow conditions because the saturation variable is not unique for saturated regions, where the soil-water diffusivity goes to infinity (in Equation 4.2, there would be a division by zero when $C = 0$) and a pressure-saturation relationship no longer exists. However, such a saturation-based algorithm can result in significantly improved performances compared to pressure based methods, especially when applied to very dry heterogeneous soils (Diersch and Perrochet, 1999).

It is the mechanism by which the change in stored fluid mass takes place that is the subject of this discussion and which will prove crucial to obtaining a transient simulation. In ESTEL2D, changes in stored fluid mass with time can only take place as a result of changes in saturation of the soil voids. The nature of the soil water retention models used means that a change in pressure head will only result in a change in saturation when the medium is unsaturated. As soon as the pressure head reaches a critical value the moisture content reaches saturation and, critically, no changes in water storage can occur ($d\theta/dt = 0$; $d\theta/dh = 0$). As this review will demonstrate, changes in stored fluid mass can in fact occur by other mechanisms, in addition to changes due to saturation of the voids accounted for by the ESTEL2D model (and many other saturated-unsaturated flow models).

The fundamental feature that distinguishes transient fluid flow from the steady state case is the phenomenon of change in stored fluid mass (Narasimhan, 1979). The principal physical phenomena that govern change in storage in the saturated zone, on one hand, and the unsaturated zone on the other, are basically different; the former is dominated by change in void volume, and the latter by change in saturation. In unifying saturated-unsaturated flow it is therefore essential to consider the mechanism of change in storage. Prior to the work of Narasimhan in 1979, very limited attention had been given to a careful treatment of the phenomenon of groundwater storage in unifying saturated-unsaturated flow. One reason for this may have been that soil physicists generally neglect deformation in the partially saturated soil while hydrogeologists and soil engineers devote their attention primarily to purely saturated flow.

The mass of fluid stored in a finite volume of a porous medium is given by (Narasimhan, 1979):

$$M_w = V_v \rho_w S \qquad 4.4$$

From empirical observations it is well known that volume of voids V_v [L^3], fluid density ρ_w [$M\ L^{-3}$], and saturation S [dimensionless] are all functions of the average fluid pressure head h [L] over the volume element. The change in the quantity of fluid mass stored in the volume element, as the average pressure head changes, can be quantified by means of the parameter 'fluid mass capacity' defined by (Narasimhan, 1979):

$$M_c = \frac{dM_w}{dh} = \rho_w S \frac{dV_v}{dh} + V_v S \frac{d\rho_w}{dh} + V_v \rho_w \frac{dS}{dh} \qquad 4.5$$

This is equivalent to the specific moisture capacity function, $C(h)$ in Equation 4.1 which describes the change in moisture content due to a change in saturation of the soil voids. In Equation 4.5 the mechanism for that change has been expanded into three distinct phenomena causing a change in the stored fluid mass: $\rho_w S\ dV_v/dh$ is deformation of skeletal matrix, $V_v S\ d\rho_w/dh$ is expansion of fluid, and $V_v \rho_w\ dS/dh$ is desaturation of voids. In the form of the Richards' equation used in ESTEL2D, the only mechanism available to account for a change in moisture content is desaturation of the voids.

Incidentally, in saturated flow models only the first two terms on the right hand side of Equation 4.5 will be considered as desaturation of the voids is not an option available to create changes in fluid storage (Domenico and Schwartz, 1990).

In shallow groundwater systems subject to small or moderate changes in h (e.g. floodplain areas adjacent to river channels), the expansivity of water, $d\rho_w/dh$, is relatively small in comparison with the deformability or the desaturability of the voids and hence can be neglected with justification. Under this circumstance, when the volume element is fully saturated, the dominant mechanism controlling change in storage is dV_v/dh (Narasimhan, 1979). When the volume element is partially saturated, it is customary in the soil physics literature to treat the soil skeleton as rigid, and since $d\rho_w/dh$ is neglected, the soil mechanism controlling change in storage is dS/dh. However, making dS/dh the only cause of release of water from storage in partially saturated soils has been known to lead to conceptual difficulties either when the soil is very close to full saturation, or when it is fully saturated, but has negative pressure head (as is the case in the capillary fringe above the water-table) (Narasimhan, 1979). The pressure head has to drop below the air entry value h_A of the soil in order that desaturation can be initiated. It is obvious that in the range $h_A < h < 0$, $dS/dh = 0$, implying that if the soil is assumed to be rigid, the volume element cannot change its storage and hence cannot partake in transient fluid flow.

Thus it is clear that for a proper unification of the saturated and unsaturated zones it is necessary to take into account the deformation of the porous medium in the partially saturated zone. In the light of Equation 4.5 this amounts to the evaluation of the quantity dV_f/dh when $h < 0$.

It seems that there are two general approaches to taking account of the deformation of the porous medium. The first is synthesised from independent estimates of fluid compressibility, matrix compressibility, and matrix desaturability in accordance with existing stress levels and pore pressure at the location of interest, and may therefore change over time. The second is a lumped parameter (storage coefficient or specific storage) incorporating fluid compressibility as well as matrix porosity and compressibility.

4.1.2 Approach based on the theory of consolidation

The model reported in Narasimhan and Witherspoon (1977, 1978), Narasimhan *et al.* (1978) and Narasimhan (1979) simulates saturated-unsaturated groundwater flow in which the deformation of the soil skeleton is handled according to Terzaghi's (1925, cited in Narasimhan, 1979) one-dimensional consolidation theory. This model contains an example of the first type of storage parameter, which is not a constant coefficient but changes according to the ambient pressure and effective stress levels. The following summary of the theory of consolidation is taken from Narasimhan (1979).

A porous medium deforms in response to changes in its skeletal stresses. Therefore the role of h in causing the change in void volume of an element depends on how change in h causes the skeletal stresses to change.

In general, change in volume occurs due to three-dimensional changes in skeletal stresses. However, if the stresses acting on the boundary of the region of fluid flow remain constant, then one could make certain simplifying assumptions with regard to the relationship between h and skeletal stresses, and conveniently avoid the effort needed for solving the three-dimensional stress-strain equation. Terzaghi (1925) proposed the one-dimensional theory of soil consolidation, and introduced the concept of effective stress, which denotes the stresses effectively acting on the soil skeleton:

$$\sigma' = \sigma - \gamma_w h \qquad 4.6$$

where σ' and σ denote effective stress and total vertical stress [M L^{-1} T^{-2}], respectively, and γ_w is the specific weight of water [M L^{-2} T^{-2}]. Assuming that σ, the total stress, remains constant with time, then any change, Δh, in pressure head is fully converted to an equivalent effective stress.

Although Terzaghi's concept has proved to be valid in a multitude of field studies related to saturated soils, soil engineers have found that Equation 4.6 does not strictly hold for partially saturated soils. Experience shows that in such soils, only part of the pressure head is convertible to effective stress. To take this into account, Bishop (1960, cited in Narasimhan and Kanehiro, 1980) proposed a modification to Equation 4.6 by introducing a parameter χ:

$$\sigma' = \sigma - \chi \gamma_w h \qquad 4.7$$

where $0 \leq \chi \leq 1$. The reason why h is not fully convertible to mechanical stresses in a partially saturated soil is because as saturation decreases, the surface area of the soil grains, over which the fluid exerts its pressure, also decreases. Hence χ is a function of saturation. The $\chi(S)$ function will vary from soil to soil, depending on the pore size distribution.

The change in stored fluid mass in Equation 4.5 can be written:

$$\rho_w S \frac{dV_v}{dh} = -\rho_w S \gamma_w \frac{dV_v}{d\sigma'} \frac{d\sigma'}{dh} \qquad 4.8$$

Using Equation 4.7 and assuming a constant total stress in the soil:

$$\frac{d\sigma'}{dh} = -\gamma_w \frac{d(\chi h)}{dh} = -\gamma_w \left(\chi + h \frac{d\chi}{dh} \right) \qquad 4.9$$

the following definition for the deformation of the skeletal matrix may then be obtained:

$$\rho_w S \frac{dV_v}{dh} = -\rho_w S \gamma_w \chi^* \frac{dV_v}{d\sigma'} \qquad 4.10$$

where χ^* is equivalent to the expression on the right hand side of Equation 4.9. To evaluate change in fluid mass in the volume element due to deformation it is therefore necessary to know the relationship between the change in void volume and the change in effective stress for the material composing the volume element. In the soil mechanics literature, experimental data on soil deformation are usually presented in the form of a plot of void ratio, e, as a function of effective stress, σ'. Equivalently, since e is uniquely related to porosity, n, the same data could be presented in the form of a plot with n as a function of σ'. Either the e versus σ' or the n versus σ' relationship can be used to evaluate $dV_v/d\sigma'$.

If the volume element is defined to have a fixed volume of solids, V_s, and the solid grains are assumed to be incompressible, then:

$$-\frac{dV_v}{d\sigma'} = -V_s \frac{d(V_v / V_s)}{d\sigma'} = -V_s \frac{de}{d\sigma'} = V_s a_v \qquad 4.11$$

where a_v is called the coefficient of compressibility [L T^2 M^{-1}]. If the volume element is defined to always have a constant bulk volume, V [L^3], then:

$$-\frac{dV_v}{d\sigma'} = -V\frac{dn}{d\sigma'} = Vm_v \qquad 4.12$$

where m_v is the coefficient of volumetric compressibility [L T^2 M^{-1}]. In view of Equations 4.10, 4.11, and 4.12, the fluid mass capacity of the volume element Equation 4.5 may now be written as:

$$M_c = V_s\left[\rho_w S\gamma_w\chi * a_v + eS\frac{d\rho_w}{dh} + e\rho_w\frac{dS}{dh}\right] \qquad 4.13$$

for a volume element with constant V_s; or

$$M_c = V\left[\rho_w S\gamma_w\chi * m_v + nS\frac{d\rho_w}{dh} + n\rho_w\frac{dS}{dh}\right] \qquad 4.14$$

for a volume element with constant bulk volume, V.

4.1.3 Lumped parameter approach

The saturated-unsaturated models of Cooley (1971), Freeze (1971), Neuman (1973), and Vauclin *et al.* (1975) include flow in both the saturated and the unsaturated domains, but these researchers do not treat in detail the fundamental stress-strain relationships of the porous medium in response to changes in pore water pressure. Nor do they consider the variation in the permeability of the porous medium in response to changes in effective stress. They incorporate examples of the second approach to taking account of the deformation of the porous medium. Considering Equation 4.5, a single lumped storage parameter, which does not explicitly account for deformation of the soil matrix, provides a way of incorporating changes in stored fluid mass due to the deformation of the skeletal matrix and the expansivity of water. Neuman (1973) used this approach to incorporating storage in a saturated-unsaturated model. The Richards' equation then becomes:

$$\underline{\nabla}.K(h)\underline{\nabla}(h+z) = n\frac{\partial S}{\partial t} + S.S_s\frac{\partial h}{\partial t} \qquad 4.15$$

where K is the hydraulic conductivity tensor [L T^{-1}], S is the saturation [dimensionless], h is the pressure head [L] and n is the porosity [dimensionless]. The specific storage, S_s [L^{-1}], is defined as a coefficient:

$$S_s = \rho_w gn(\alpha + \beta) \qquad 4.16$$

where ρ_w is the density of water [M L^{-3}], g is the acceleration due to gravity [L T^{-2}], β is the compressibility of water [L T^2 M^{-1}] and α is the compressibility of the formation [L T^2 M^{-1}]. This is a lumped parameter incorporating fluid compressibility as well as matrix porosity and compressibility. In the examples given in Neuman (1973), the value of S_s is set to zero, from which it can be deduced that in order to obtain a transient model simulation, the soil water conditions in this case must have been unsaturated.

Diersch and Perrochet (1999) suggest a slightly different form for the storage parameter known as specific pressure storativity [L T^2 M^{-1}]:

$$S_{op} = n\beta + (1-n)\alpha \qquad 4.17$$

where β is water compressibility [L T^2 M^{-1}], α is soil compressibility [L T^2 M^{-1}], and n is the porosity.

The specific pressure storativity S_{op} [L T^2 M^{-1}] is the volume of water released from saturated pore storage due to a unit drop in fluid pressure per total solid matrix plus pore volume. Note that specific storage, S_s [L^{-1}] (which when multiplied by confined aquifer thickness gives the storage coefficient [L]), is related to S_{op} as $S_s = \rho_w.g.S_{op}$, where g is gravitational acceleration [L T^{-2}]. Specific storage, S_s, expresses the volume of water released from pore storage due to a unit drop in piezometric head.

Since matrix compressibility is often a function of the effective stress in shallow clays and fine-grained sediments, the storage coefficient as it is defined and used in hydrogeology should be applied only to relatively rigid sediments that are subject to small variations in pore pressure over which the specific storage is reasonably constant. Because many aquifers satisfy these conditions, the use of a constant storage coefficient to characterise them is valid and useful. The specific storage has the advantage of being directly determinable from various types of well test data (Narasimhan and Kanehiro, 1980).

4.1.4 Approaches to the storage parameter in commercially available saturated-unsaturated models

The models that have been investigated in this section are all saturated-unsaturated flow models. The aim of this investigation was to determine whether these models incorporate a storage parameter of some kind, and if so, how it has been defined and implemented, using examples from the literature where they are available. The models are 3DFEMWATER (Yeh and Ward, 1980) and SUTRA (Voss, 1984).

4.1.4.1 3DFEMWATER

The user manual of 3DFEMWATER (Yeh and Ward, 1980) states that "due to the relatively small influence of compressibility on water capacity in the unsaturated zone (with respect to the drainage potential), soil and water compressibility have been ignored in the storage term." This has been interpreted as applying to the unsaturated zone only, as later the manual refers specifically to the saturated component of flow. The equation governing saturated flow represents a limiting case of the Richards' equation where the relative hydraulic conductivity is a constant equal to 1.0 and the water capacity (change in storage) is a constant equal to the specific yield for an unconfined aquifer, or specific storage for a confined aquifer i.e. not equal to zero. This is a simple coefficient of the second type of storage parameter discussed in this report (Section 4.1.3).

4.1.4.2 SUTRA

Although SUTRA is a saturated-unsaturated flow model, its numerical algorithms are not specialised for the non-linearities of unsaturated flow and it is therefore not an economical tool for extensive unsaturated flow modelling (Voss, 1984). However, the model does deal explicitly with the saturated component of flow, including the changes in storage due to soil and water compressibility that are necessary to simulate transient flow.

The fluid mass balance is a calculation of how the amount of fluid mass contained within the void spaces of the solid matrix changes with time. In a particular volume of solid matrix and void space, the total fluid mass may change with time due to ambient groundwater inflows or outflows, injection or withdrawal wells, changes in fluid density caused by changing temperature or concentration, or changes in saturation (which may arise due to changes in the soil skeleton). In SUTRA, the fluid mass balance is expressed as:

$$\frac{\partial(eS\rho_w)}{\partial t} = \left(S.\rho_w S_{op} + e\rho_w \frac{\partial S}{\partial p} \right) \frac{\partial p}{\partial t} + \left(eS \frac{\partial \rho_w}{\partial U} \right) \frac{\partial U}{\partial t} \qquad 4.18$$

where p is the pressure, and U represents solute concentration or temperature. In ESTEL2D, the last term on the right-hand side of Equation 4.18 is not included as density dependent flow is not considered. S_{op} is the specific pressure storativity, expressed using the same equation as that used by Diersch and Perrochet (1999) (Equation 4.17).

The user has to specify such parameters as water compressibility β and soil compressibility α, porosity n, and hydraulic conductivity K. The specific pressure storativity S_{op} is calculated by the model using Equation 4.17. An example of SUTRA use, and the kind of values of S_{op} that may be encountered, is provided by Jolly *et al.* (1998). They used values of the

parameters α and β of 3 x10^{-8} Pa^{-1} and 4.5 x 10^{-10} Pa^{-1} respectively. Then for two soils of different porosity, the value of S_{op} was calculated as shown in Table 4.1.

Table 4.1 Examples of specific pressure storativity and specific storage calculations and values.

Soil type	Porosity, n	Specific pressure storativity, S_{op} (Pa^{-1}) $= (1-n)\alpha+n\beta$	Specific storage, S_s (m^{-1}) $= \rho_w g S_{op}$*
1	0.3	$= (0.7 \times 3 \times 10^{-8}) + (0.3 \times 4.5 \times 10^{-10})$	$= 1000 \times 9.80665 \times 2.1 \times 10^{-8}$
		$= 2.1 \times 10^{-8}$	$= 2.06 \times 10^{-4}$
2	0.6	$= (0.4 \times 3 \times 10^{-8}) + (0.6 \times 4.5 \times 10^{-10})$	$= 1000 \times 9.80665 \times 1.2 \times 10^{-8}$
		$= 1.2 \times 10^{-8}$	$= 1.18 \times 10^{-4}$

* ρ_w is the density of water (1000 kg m^{-3}) and g is the acceleration due to gravity (9.80665 m s^{-2}).

This review has demonstrated that groundwater storage has an important role to play in unifying saturated-unsaturated flow. Storage properties can be incorporated into a saturated-unsaturated model in the form of a storage parameter, which may be a simple lumped coefficient (specific storage or specific pressure storativity), or a more complex parameter that takes into account the influence of effective stress on the soil matrix and the fluid. Either way, the storage parameter reflects the idea that under both saturated and unsaturated conditions, small changes in water storage are possible due to the compressibility of the soil matrix and the fluid.

4.1.5 Incorporating a storage parameter in ESTEL2D

Currently, the soil water retention models used in ESTEL2D only permit changes in water content as a result of changes in saturation, dS/dh. No changes in moisture content due to other forms of storage (expansion of the fluid $d\rho_w/dh$ or compression of the soil matrix dV_s/dh) are considered. Initially, the storage properties which result from soil and fluid compressibility, and which need to be included to create the transient simulation under fully saturated conditions, will be incorporated in the capacity calculation of ESTEL2D in the form of a simple lumped coefficient (i.e. the second type of storage specification). It is not justifiable to incorporate the more complicated approach (based on the theory of consolidation), as the amount of information that would be needed to parameterise the storage would be well beyond the level of information that is currently available to the model user.

Given the values of soil and fluid compressibility from the literature, a simple storage coefficient will be defined according to Equation 4.16. In practice it may be necessary to calibrate this parameter, but this review has at least established its physical basis. As the

storage parameter is essentially designed to permit changes in capacity *dθ/dh* under conditions of positive soil water pressure, it will be incorporated into the model code as a small value added to the specific moisture capacity as already calculated by the model. For the model user, this will involve the specification of a value of specific storage in the soil database.

This storage parameter will be enough to permit a transient simulation by ensuring that changes in storage will always be possible, even under fully saturated conditions. It will have a negligible effect on capacity when the soil is unsaturated; its effects will only be noticeable when the soil reaches full saturation. The effect of this model parameter will be explored during the model assessment process in Chapter 5.

4.2 Accounting for a seepage boundary condition

A complication in modelling unconfined groundwater flow is the need to simulate seepage flow when the water-table intersects the land surface (Romano *et al.*, 1999). Even when groundwater seepage is not apparent in the field, the existence of a seepage face is necessary to provide a physical transition between a phreatic surface and an equipotential boundary when the water-table approaches a surface water body. Incorporating a seepage boundary condition in a subsurface hydrological model is an interesting problem because the boundary condition along a slope containing a seepage face is a function of the dependent variable h and cannot be known a priori (Rulon *et al.*, 1985). This will therefore involve some kind of iterative procedure that moves the position of the seepage face until a convergence criterion is satisfied.

4.2.1 Approaches to modelling a seepage face

A seepage-face is an external boundary of the saturated zone where flux is directed outward and there is atmospheric pressure along that boundary (Ataie-Ashtiani *et al.*, 1999). During the iterative solution, atmospheric pressure is maintained for all nodes along the seepage face and they are treated as Dirichlet nodes with the prescribed pressure head $h = 0$. All nodes above the seepage face are specified as no-flux nodes, and are maintained with negative pressures. An iterative technique for locating the seepage face initially proposed by Rubin (1968) and Neuman (1973) has since been used and developed by Cooley (1983), Rulon *et al.* (1985) and Ataie-Ashtiani *et al.* (1999). This iterative technique is outlined below:

> The position of the seepage face is initially guessed. Then, for the first iteration, the value of h is set equal to zero along the seepage face and this segment of the slope is treated as a prescribed h boundary. Then, the nodal flux per unit area Q is set equal to zero along the unsaturated portion of the slope and this segment is treated as a prescribed flux boundary. The

> flow equation is then solved with the expectation that (1) the newly calculated values of Q will indicate that flow is directed out of the slope only along the prescribed h segment and (2) the newly calculated values of h will be negative only where Q was previously set equal to zero. If these expectations are not met, the boundary conditions at the errant nodes are redefined to agree with the new solution. This procedure is repeated until the solution converges.
>
> (Rulon *et al.*, 1985)

In order for the solution to converge, the modification of the boundary condition should proceed sequentially from node to node, beginning at the saturated end of the seepage face (i.e. the lowest point of the seepage face).

Rulon *et al.* (1985) approached the seepage face problem by defining a seepage face boundary on a slope (DE), and an infiltration boundary (CD) (Figure 4.1). The infiltration boundary and the seepage face boundary may contain both prescribed flux and prescribed h segments. Where the water-table intersects the infiltration boundary (CD), h is set to zero. The remainder of the boundary is unsaturated so that the flux is prescribed equal to the rainfall rate. Similarly, those portions of the seepage face boundary (DE) that contain a seepage face will have h set equal to zero; those portions that remain unsaturated will have the flux set equal to zero.

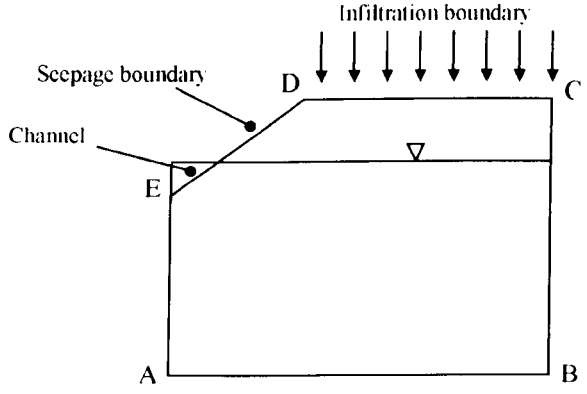

Figure 4.1 Implementation of a seepage face boundary condition (after Rulon et al., 1985).

Rulon *et al.* (1985) implemented a modification of the Neuman scheme to allow for the development of more than one seepage face. However, their implementation was still restricted in several ways. First, a major problem with this approach is that the boundary is divided into a section where a seepage face may develop (DE), and a separate section where infiltration is permitted (CD). Therefore, a node that is located on the seepage face boundary cannot be part of the infiltration boundary. Rainfall must be restricted to the flat, upland

surface and infiltration cannot be modelled along the slope. Secondly, the model does not take into account the interactions between the subsurface flow system and changes in the stream level; in effect, the location of the lowest point in the seepage face boundary is fixed. Thirdly, although this implementation allows the development of multiple seepage faces on one slope, it does not allow the development of seepage faces on more than one slope. This restricts the geometry of the hydrological systems that can be modelled. In addition, there is no mechanism to route water discharging across the seepage face. The model assumes that overland flow or evapotranspiration immediately removes water leaving the seepage face.

The two-dimensional, saturated, steady-state groundwater flow model FLONET, provides an example where the potential seepage face boundary also permits infiltration at nodes where the pressure head is negative. The seepage face boundary is effectively defined as the whole of the top boundary CE in Figure 4.1. The seepage face is treated as a system-dependent prescribed head boundary where the hydraulic head equals the elevation (and therefore the pressure head, $h = 0$). The remaining nodes along the boundary that can potentially become seepage nodes continue to accept recharge and are part of the prescribed flux boundary. The lengths of these two boundary segments are continually adjusted during the iterative process until flow is inward (into the domain) in areas where the water-table lies below ground surface and the pressure head is zero where seepage (outflow) occurs (Romano *et al.*, 1999).

4.2.2 Incorporating seepage in ESTEL2D

The seepage face boundary condition has been implemented in ESTEL2D by J. -P. Renaud. The iterative scheme has been based on the example of Rulon *et al.* (1985), with several modifications. First, the restriction placed on the boundary conditions whereby a node that is located on the seepage face boundary cannot be part of the infiltration boundary, has been lifted. This effectively means that the whole of the top boundary (CE in Figure 4.1) is a system-dependent boundary condition. Nodes that are part of the seepage face are still specified as $h = 0$, but unsaturated nodes above the seepage face may be specified with a positive flux value.

Secondly, the potential for multiple seepage face development is retained but extended to include multiple seepage development on two slopes. This extends the range of hillslope-channel geometries that can be modelled to include, for example, seepage face development on slopes on both sides of a stream channel (Figure 4.2). The user specifies the potential seepage faces by stating the top and bottom node for seepage face one (e.g. A and B in Figure 4.2), and the top and bottom node for seepage face two (e.g. C and B in Figure 4.2). Multiple seepage faces may still develop along each of these designated boundaries. The

iterative procedure then works by moving one node on seepage face one, followed by one node on seepage face two.

Thirdly, the new seepage face scheme can simulate a dynamic interaction between the seepage face and the river channel as river stage changes over the course of a simulation. This is carried out by checking for the location of specified head nodes at the bottom of the seepage face, which denote the river stage. For the example in Figure 4.2, the code would begin checking for river stage nodes at point B, working sequentially up the boundary towards the top (A) until reaching the first node which is not specified head (B_1). This node will be temporarily labelled as the new bottom node for this seepage face boundary, and if there are two slopes in which seepage faces may develop, this process is repeated for the second slope.

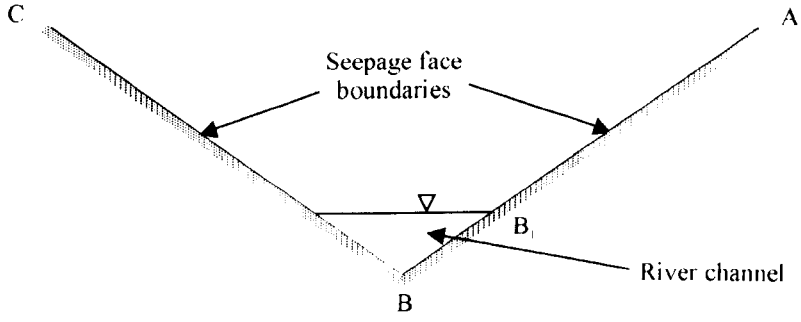

Figure 4.2 Implementation of double seepage face boundary in ESTEL2D.

A further modification was made to the iterative scheme in order to reduce the computation time for the simulation. For each new time step, the position of the seepage face at the previous time step is retained and used as the initial condition for the new time step. This reduces the number of iterations of the seepage face scheme needed to achieve convergence.

4.3 Assumptions and utility of the final model

The model now has all the essential features that were deemed necessary to model the floodplain hydrological and chemical transport environment outlined in Section 3.1. At this stage it is worth summarising the assumptions on which the model is based that must be taken into consideration when using this model for any particular application. The major capabilities of the newly developed model will also be highlighted.

4.3.1 Major assumptions

(i) Water movement is described by Darcy's law and the Richards' equation, flow is laminar and isothermal, chemical gradients are neglected, and the air phase is continuous.

(ii) There is no hysteresis in the soil water functions.

(iii) Flow is only within the soil matrix; flow through macropores is not explicitly modelled.

(iv) Water is the only flowing fluid phase (i.e. the air phase is assumed to be inactive). The soil matrix is considered slightly compressible.

(v) Gradients of fluid density, viscosity and temperature do not affect the velocity distribution, and fluid properties are independent of concentrations of solutes.

(vi) Injected solutes are miscible with flowing fluid and Fick's law governs dispersive transport in the porous medium.

(vii) The hydrodynamic dispersion coefficient is defined as the sum of the coefficients of mechanical dispersion and molecular diffusion. The medium dispersivity is assumed to correspond to that of an isotropic medium, where α_L and α_T are the longitudinal and transverse dispersivities, respectively.

(viii) Water and solute flow can be described by a two-dimensional representation.

4.3.2 Major capabilities

(i) The model can represent a range of boundary conditions, including a seepage face.

(ii) It incorporates a unifying treatment of the saturated and unsaturated zones in the form of a specific storage parameter.

(iii) The finite-element formulation is capable of simulating highly spatially and temporally variable boundary conditions, and complex topography.

(iv) The model can represent a distribution of spatially variable soil types. Anisotropy can be easily incorporated within the hydraulic conductivity term.

(v) The user can incorporate any chemical transformation equations needed in a separate user defined input file.

4.4 Chapter summary

This chapter has discussed important developments that are needed in the combined ESTEL2D-SUBIEF2D model in order to simulate particular aspects of floodplain

hydrological processes. Previous approaches to these developments have been reviewed, and suitable methods for implementing these developments have been applied to the ESTEL2D model. Thus, at this stage, the complete model platform has been obtained, fulfilling stage two of the research methodology outlined in Section 2.2.2, namely to develop a hydrological and chemical transport model for application to the floodplain environment at a high spatial and temporal resolution. The model now contains all the elements that were deemed necessary in the conceptual model of floodplain hydrological and chemical transport processes described at the start of Chapter 3. The following chapter will be concerned with the stages three and four of the research methodology, which involve investigating the sensitivity of the model to structural, soil hydraulic and chemical transport parameters, and validating the hydrological dynamics of the model using data from dedicated floodplain monitoring programmes.

5 Model Assessment

Chapter 4 was concerned with the further developments to the numerical model that is to be used to explore hydrological and chemical transport processes operating in the floodplain environment. At this stage, therefore, all the parts of the code needed to implement the conceptualisation of the floodplain system have been developed. Initial model runs and comparisons with an analytical solution in Chapter 3 indicate that the computer code provides an accurate solution to the governing partial differential equations for a particular boundary value problem. However, a much more comprehensive programme of model testing must be undertaken in order to explore model sensitivity, calibration and validation issues. An improved understanding of the way the model reacts to changes in model parameters and boundary conditions will permit increased confidence in the model results, and confidence in the intended use of the model for scenario testing.

Chapter 5 will begin by exploring the issues surrounding the testing of physically-based models, followed by the statement of a model testing strategy suitable for this study. The field site requirements for model assessment will be outlined, along with the final field site selection. The results of the model tests will then be presented.

5.1 Context of model assessment

A model is a simplification of reality. All natural environmental systems are far too complex to describe in totality. In fact, if the natural environment could be described totally, this would obviate the need for a model at all. This simplification is a strength because it permits the modeller to reduce the system to its most essential features, including only the behaviour of the real system which is relevant for the application in mind (Howes and Anderson, 1988). However, this same facet can be seen as a weakness, as it introduces the possibility that the model does not include the correct process representation, which may undermine confidence in the model results. Of course, the doubt over whether the correct processes are implemented is an inevitable consequence of the fact that we do not have perfect knowledge of the system. Unless we are just to dismiss the recognised benefits of modelling in terms of helping to organise our thinking, and their use for investigating and interpreting the detailed causal mechanisms of various processes, the way to approach this problem is to try to

increase confidence in the model's ability to represent the natural system. This can be achieved through a careful application of a well devised model testing strategy.

> Evaluation is a methodology for establishing the suitability and relevance of a computer simulation model for a particular application and for assessing the level of confidence associated with the information derived from the model.
>
> (Howes and Anderson, 1988)

All scientific knowledge is provisional (Oreskes and Belitz, 2001). However, there are particular aspects of numerical simulation models that exacerbate the problem of uncertainty to a degree that may be substantially greater than in some other forms of scientific endeavour. These features are non-uniqueness (more than one model configuration may produce the same output), the problem of temporal and spatial divergence (although the model may accurately reproduce available observation data, there is no guarantee that it will perform at an equal level when applied over a different spatial or temporal scale), and the subjectivity of model assessment (the subjectivity of our judgements of what constitutes a good fit). This highlights the importance of model assessment.

The literature of model assessment is littered with inconsistencies over the usage of terms, so at this point, a consideration of terminology and semantics is essential (Roache, 1998). A particularly strong view, that models cannot be verified or validated, has developed from considerations of the philosophy of science (Konikow and Bredehoeft, 1992; Oreskes *et al.*, 1994). These authors argue that the word 'verify' means an assertion or establishment of truth, and it is impossible to demonstrate the truth of any proposition, except in a closed system.

> Verification and validation of numerical models of natural systems is impossible. This is because natural systems are never closed and because model results are always non-unique. Models can be confirmed by the demonstration of agreement between observation and prediction, but confirmation is inherently partial...models are representations, useful for guiding further study but not susceptible to proof.
>
> (Oreskes *et al.*, 1994)

The term validation denotes the establishment of legitimacy (Oreskes *et al.*, 1994). Konikow and Bredehoeft (1992) pointed out that the term is used misleadingly to suggest that the model is an accurate representation of physical reality. However, under the strict conditions outlined above, it has been established that this is not even a theoretical possibility. Konikow and Bredehoeft (1992) therefore stated that the process of comparing model results to observations might be more accurately termed 'history matching'.

A model is "both an embodiment of a hypothesis and the numerical experiment to facilitate hypothesis testing" (Bates and Anderson, 2001). Numerical models are basically a form of scientific hypothesis. A model cannot be proved true, in the same way that scientific hypotheses can never logically be verified (Oreskes *et al.*, 1994). Even falsification may be practically impossible.

> The level of complexity in models of environmental systems is such that falsification is: (i) dependent upon what criteria we set as necessary for falsification; (ii) inevitable, given the complexity of the real world that is being modelled; and (iii) of no real use unless it can inform the modeller of exactly why the model is failing.
>
> (Lane and Richards, 2001)

The very fact that models apply simplifying assumptions means that there will almost always be some evidence with which they are not consistent (Morton and Suárez, 2001).

These arguments and conundrums have led some authors to the conclusion that the terms verification and validation, with their connotations of truth, are inappropriate, and an alternative language of 'confirmation' has been developed to account for this difficulty. In the context of model testing, laboratory tests and field data are forms of confirmation. A theory or law (or model representing the theory or law) can be 'confirmed' by these observations, and the greater the number and diversity of confirming observations, the more probable it is that the conceptualisation embodied in the model is not flawed. But confirming observations can never demonstrate that the theory is true, they only support its probability. No matter how much data we have, there will always be the possibility that more than one theory can explain the available observations.

An alternative viewpoint in this debate is that the terms verification and validation have acquired special disciplinary meaning (Rykiel, 1994; Roache, 1998). Roache (1998) criticised Oreskes *et al.* (1994) for trying to define verification and validation according to common use (i.e. a dictionary definition). He argued that the technical meaning of terms are defined independent of common use, and in a specific technical context. Within this framework, he makes clear the essential distinction between verification and validation. Verification is 'solving the equations right' and validation is 'solving the right equations'. Verification is seen to be essentially an activity in mathematics, and validation is essentially an activity in science. An additional argument is that these terms will continue to be used, so it is perhaps better to state clearly what is meant by these terms than to adopt an entirely new terminology, which may also encounter problems with ambiguous definitions. Rykiel (1994) stated that modellers should take the lead in asserting the restrictions and limitations of models:

(i) make clear that verification and validation are used in a technical sense;

(ii) if necessary, don't use terms if they are likely to be misunderstood and create a false sense of truth rather than consensus;

(iii) take care to specify the context of the model;

(iv) use model acceptability and performance indices rather than simple declarations of validation to describe the results of model testing.

In fact, the two schools of thought are not as far apart as they at first seem; both are advocating a more probabilistic based approach to model assessment (in the sense that 'truth' cannot be obtained, so 'confirmation' of a theory is a more realistic goal). From the more formalised standpoint of philosophy of science (e.g. Oreskes *et al.*, 1994) the strict definitions of validation and verification are seen to be inappropriate, so a new language is proposed in order to adopt the more probabilistic framework. From the more applied perspective (e.g. Roache, 1998), the definitions of verification and validation are seen to have acquired special meanings that already incorporate these probability connotations, through the use of clarifying phrases within the definitions. This debate will hopefully clarify the usefulness of models as it will provide a clearer appreciation of the utility and limitations of models among both model users and those who make use of model results. The importance of communicating the meaning of terms used in model assessment to reduce confusion is a clear message from this discussion.

Model evaluation procedures should be carefully considered. As physically-based models are complex, there is not the time or the facilities to examine every mode of behaviour under all possible combinations of conditions. The assessment of a model must necessarily be made from a limited number of experimental frames (Sargent, 1982), and the selection of these experimental frames will influence the utility of the conclusions that can be drawn regarding the model operation. As model confirmation is a matter of degree, the more diverse and wide ranging strategies employed to assess model performance, the better the position attained from which to support the probability that the model is not flawed. Lane and Richards (2001) argue that some of these assessment strategies may seem less rigorous, but only because more formal procedures are precluded by the complex nature of these models. The potential sources of model error are wide ranging (Morel-Seytoux, 2001): conceptual errors in the description of the system to be modelled; errors in the model equations; parameter estimation errors; input and data errors; and numerical solution errors. A wide range of assessment techniques will be needed to explore all these potential sources of error, including, but not limited to, comparing predicted and observed results.

The overall process undertaken in this chapter is termed a model assessment procedure (Lane and Richards, 2001). Some authors use validation to refer to the whole model assessment process; this use is avoided here. The terms verification and validation will be used, with the recognition that they must be defined with appropriate precision. A model testing strategy may involve the following five stages: verification, optimisation, sensitivity and/or uncertainty analysis, calibration, and validation, each of which will be outlined in this section.

5.1.1 Verification

The comparison of numerical code results with analytical solutions is a critical step in code development as the failure of a numerical code to reproduce an analytical solution indicates some problem with the program. It involves ensuring that the computer carries out procedures as the programmer intended, and that the program is consistent with the functionality of the mathematical model (Howes and Anderson, 1988; Refsgaard and Knudsen, 1996). This stage basically assesses the ability of a generic model to give an accurate solution to the governing equations. However, even if a numerical solution matches an analytical solution, this says nothing about the correspondence of either one to reality (Oreskes *et al.*, 1994). In addition, analytical solutions only provide a test for those cases defined by the assumptions made to allow analytical solutions to be reached. Oreskes *et al.* (1994) therefore suggested that the practice of comparing numerical and analytical solutions is best referred to as bench-marking. However, in a technical context bench-marking is often used with the more specific meaning of code-to-code comparison (Roache, 1998).

5.1.2 Optimisation

Model optimisation involves checking the sensitivity of the model results to model structural parameters, and then adjusting these parameters in such a way as to minimise the computation time needed for a simulation, without compromising the accuracy and stability of the model results. Typically this involves an investigation of the effect of model element size, time step, and numerical solver on the model output, with the investigator making a decision about which aspects of the model output to compare. An example of this approach is the work of Rogers *et al.* (1985) who illustrated the effect of changing grid spacing and time steps on peak flow predictions of the Institute of Hydrology Distributed Model (IHDM) of watershed hydrological processes.

5.1.3 Sensitivity analysis and uncertainty analysis

5.1.3.1 The concept

For a physically based computer simulation model, sensitivity and uncertainty analyses provide excellent quantitative methods of analysing a simulation model (Howes and Anderson, 1988). Sensitivity analysis is used to analyse the internal mathematical response of a model by determining how small changes in input parameters are translated into variations in model outputs, and does not require comparison to a data set. A sensitivity analysis can be used to (from Howes and Anderson, 1988):

(i) demonstrate that in response to representative variation of model input and parameter values, theoretically realistic model behaviour is experienced. For example, an increase in hydraulic conductivity, with all other parameters held constant, should theoretically increase the flux of water through the system. This theoretical expectation should be reflected in the model behaviour.

(ii) illustrate the model to be sufficiently sensitive to represent actual variation in the prototype system.

(iii) identify those model parameters or inputs to which the model is most sensitive. The implication of this is that parameters to which the simulations are most sensitive need to be evaluated with relatively high accuracy. Therefore, the greatest effort can be directed towards the determination of suitable values for these parameters (Anderson and Rogers, 1987). Other parameters can potentially be evaluated using data available in the literature (Bathurst, 1986).

Uncertainty analysis attempts to determine the probabilistic uncertainty associated with a given model output. Sensitivity analysis and uncertainty analysis are therefore conceptually similar, and they both allow the modeller to explore the effects of uncertainty from the following sources:

(i) uncertainty in the conceptual model, reflected in the inability of the simulation model to represent the system's physical behaviour;

(ii) uncertainties resulting from an inability to quantify accurately the model input parameters (including boundary conditions), a failure to capture natural parameter variability due to unsampled temporal and areal variations, and the discrepancy between point measurements and the spatially distributed model (Melching, 1994).

In the majority of cases, sufficient parameter measurements may not be available due to the high cost of in situ acquisition. Where they are available they may be imprecise due to measurement errors and there may be uncertainties associated with their spatial and temporal

variations (Bronstert, 1999; Freissinet *et al.*, 1999). This will produce a corresponding level of uncertainty in the simulations. Several researchers have therefore advocated the importance of viewing the parameters as defined by some (unknown) statistical distribution rather than as fixed values truly characteristic of an area (Abbott *et al.*, 1986b; Binley and Beven, 1989; Konikow and Patten, 1985; Gold and Kellogg, 1997).

Parameterising soil hydraulic properties is one of the most challenging aspects of subsurface hydrological modelling. A range of field, laboratory and statistical techniques are available to estimate soil hydraulic properties such as hydraulic conductivity and the soil moisture retention curve. In many cases obtaining field data, or even laboratory data, about these parameters can be prohibitively expensive, time consuming and laborious. It can be difficult to ensure spatially and temporally representative sampling in a way that is commensurate with the distributed nature of the model, as measurements are often only made at the point scale.

> ...measured parameter values do not integrate the response of the "elemental" area, and there is an inconsistency in scale between that used in measurement of field variables and the way in which they are applied in models.
>
> Grayson *et al.*, 1992

Approaches to field measurement are therefore being sought which provide distributed estimates of soil parameters, of which ground penetrating radar technology is one example. This can provide high resolution information on the nature and distribution of sediments within the shallow subsurface of soils (Huggenberger *et al.*, 1998; Steenhuis *et al.*, 1998; Davis *et al.*, 1999). However, the application of these methods is currently at an early stage and the full scope of their use and limitations is yet to be established.

5.1.3.2 The methodology

Sensitivity analysis

Sensitivity analysis at a basic level involves modifying each input parameter within a defined range of values, solving the governing equations, and observing the impact of the perturbation on the resulting solution (Freissinet *et al.*, 1999), known as the factor perturbation approach. In conducting a sensitivity analysis, the modeller has two basic decisions to make: which parameters to vary and which output variables to inspect (Bates *et al.*, 1997).

In terms of model input, perturbation factors can be chosen by the modeller (deterministic) or from a probability distribution (stochastic). The deterministic approach may take the form of a so called relative sensitivity coefficient, which looks at the change in some model

performance measure per unit fractional change (in percentage terms), of a parameter (Miller *et al.*, 1976).

A simple sensitivity analysis, performed to highlight the effects of varying any single parameter on model outcome, does not generate a sense of the interaction of the input parameters on the expected outcomes (Addiscott and Wagenet, 1985), and may not capture all aspects of model behaviour (Anderson and Rogers, 1987). Ideally, therefore, more parameters should be varied simultaneously to create a more comprehensive picture of model behaviour. The effect of changing two parameters simultaneously can be shown by producing a response surface showing some expression of output difference as a function of the values of the two parameters (Harlin and Kung, 1992). If more than two parameters are varied at a time the output information becomes much more difficult to present and interpret.

An example of the complexity of model sensitivity to a given parameter is shown in the research of Bathurst (1986). This study of the sensitivity of the SHE model of catchment hydrological processes revealed that the model output was more sensitive to saturated moisture content values than the saturated vertical conductivity. However, the influence of these parameters also depended on how much of the catchment was saturated, and the relative importance of the sensitivity of each of these parameters therefore varied between hydrological events.

Uncertainty analysis

The most commonly used uncertainty analysis methodologies can be classified as 'statistical sampling' methods (Fressinet *et al.*, 1999). They require the definition of some stochastic strategy to sample the parameter space (the vector space spanned by all possible combinations of parameter values, Hornberger and Spear, 1981) and generate a set of simulations. The schemes used include:

(i) Monte Carlo methods (e.g. Kuczera and Parent, 1998), which involve making repeated simulations using randomly generated parameter combinations.

(ii) Latin Hypercube Simulation, a stratified sampling approach which has been shown to converge more quickly than the random sampling employed in Monte Carlo simulations (Melching, 1994), but the accuracy of which is still a function of the number of samples.

(iii) Rosenblueth's Point Estimation Method, involving 2^n simulations, where n is the number of parameters. Thus, while this method is quite efficient for problems with a small number of uncertain basic variables, the computational requirements can be similar to Monte Carlo simulations when n reaches 10 to 15.

In the Monte Carlo method selected input variables are represented by a probability distribution function (PDF) rather than by a single value. A series of simulations is then executed. In each simulation the input is obtained from a random selection of values based on the PDF of each variable, and the mean, standard deviation and other statistical properties of the predicted outputs are obtained (Gold and Kellogg, 1997). The Generalised Likelihood Uncertainty Estimation (GLUE) framework of Beven and Binley (1992) and the Metropolis algorithm (Kuczera and Parent, 1998) are both based on the Monte Carlo approach. The GLUE procedure is based on the premise that a range of different sets of model parameter values may be equally likely as simulators of a catchment (Beven and Binley, 1992). Since its inception, this methodology has been used by a number of researchers within the hydrological sciences community (e.g. Aronica *et al.*, 1998; Lamb *et al.*, 1998). Apart from these statistical sampling methods, other methods of analysing uncertainty include first-order uncertainty analysis, Bayesian methods, and the fuzzy-set approach (Fressinet *et al.*, 1999).

5.1.3.3 Summary of approaches to sensitivity and uncertainty analysis

The approach to model sensitivity and uncertainty analysis must be considered carefully. There is a trade-off to be made between the time taken to perform the analysis, and the benefit gained from it in terms of improved undertanding of the model behaviour. In conducting a comprehensive uncertainty analysis, the number of simulations (and therefore the computer time) necessary to achieve an accurate estimate of uncertainty may become prohibitive (Harlin and Kung, 1992; Melching, 1994). There is also an issue of whether a Monte Carlo based sampling approach such as GLUE can represent faithfully the prior knowledge of the catchment and previous experience of the model that the modeller can bring to a particular application (O'Connell and Todini, 1996). In addition, Miller *et al.* (1976) argue that as the model increases in complexity, the source of the most important error may remain in just a few mechanisms or submodels, so that practical uncertainty in model predictions is associated with a much smaller number of parameters than would be expected, given the apparent complexity of the model. A very detailed uncertainty analysis may therefore be considered unnecessary, particularly when the model is not to be used for prediction.

A deterministic sensitivity analysis shows the response of the model to absolute values of different input parameters, and often provides sufficient information to give an indication of how the model behaves (Watts, 1997). However, even without a comprehensive uncertainty analysis, model assessment need not end with a simple sensitivity analysis. For example, Bates *et al.* (1997) adopted an approach whereby an initial stage of single-parameter sensitivity analysis was carried out, indicating the two most influential parameters. By then

going on to study the effect of varying these two parameters simultaneously they were able to investigate almost the full range of model responses. In a similar way, Smith (1998) tested a physically-based model in the first instance by comparing a simple measure of model output from a single-parameter sensitivity analysis. He then took the most sensitive parameter from this analysis and subjected it to an analysis that considered a more complex, spatially distributed, measure of model output.

Sensitivity analysis should perhaps then be viewed as a process that involves increasingly detailed analysis on those aspects of the model that appear to exert the most influence over model results.

5.1.4 Calibration

Once the simulation model has been tested to satisfactory standards, application requires that suitable initial parameter values for the system be specified. These values are derived from measurement of the prototype system (Howes and Anderson, 1988). The main aim in calibrating a model is to obtain a unique parameter set which is in some sense physically realistic. The main problem that is experienced is an inability to obtain such a solution (Howes and Anderson, 1988).

In principle, the parameter values of a physically based model should not need to be calibrated as they are based on physical measurements. In practice, some calibration is required, as the number of measured values may be insufficient, and measured values are often obtained at the point scale and may not be representative of the grid scale to which the model parameters are applied (Abbott *et al.*, 1986b). Calibration is concerned with searching a parameter space, in a similar way to sensitivity and uncertainty analysis. The parameter space of a physically based model can be huge, so the situation arises where more than one set of calibration parameters may fit the available data (Beven, 1989; Bates *et al.*, 1992; Bates *et al.*, 1997; Stewart *et al.*, 1998). However, a large amount of *a priori* information and knowledge is used in formulating and parameterising a physically based model for a particular catchment. This information is a function of the available knowledge of the values of physically based parameters for factors such as vegetation type and soil type; of the informal information available on catchment response; and the base of knowledge and experience which the modeller brings to the parameterisation process. This greatly reduces the space for physically realistic and consistent parameter values (O'Connell and Todini, 1996).

The possibility of alternative but physically acceptable parameterisations, consistent with the available information, giving rise to the same set of responses, can be further reduced by increasing the dimensionality of the measurement space. For example, if only outflow

measurements are used then the possibility of non-unique parameterisations becomes more likely. However, if multiple measurements are available, particularly measurements internal to the model domain, on soil physical properties, moisture contents and tensions in the unsaturated zone, groundwater levels, and so on, this further enhances the prospects of a unique and physically realistic parameterisation of a catchment (O'Connell and Todini, 1996). This type of analysis allows a distributed model to be used to its highest potential and is of particular importance if a second model, such as a chemical transport model, is to be initialised using hydrodynamic results (Bates *et al.*, 1997).

The knowledge gained from the sensitivity analysis can be used to guide the calibration process. In applying the IHDM to an upland catchment in Wales, Binley *et al.* (1991) used sensitivity analysis results to reduce the parameter calibration problem. In their example, this meant that only four parameters were calibrated by comparing observed and simulated discharges, while the other parameters required were fixed on the basis of field estimates.

5.1.5 Validation

In principle, validation is "substantiation that a computerized model within its domain of applicability possesses a satisfactory range of accuracy consistent with the intended application of the model" (Schlesinger *et al.*, 1979). In practice, this often involves a process of comparing model output with actual historical data for that range of conditions which are relevant in the context of the proposed model application, but using a different data set to that used for model calibration. This permits an assessment of the practical or theoretical significance of disparities between the behaviour of the real system and the computer simulation model. In association with these comparisons, those conditions beyond the model's range of application must also be clearly defined (Howes and Anderson, 1988). Refsgaard (2001) and Refsgaard and Knudsen (1996) refer to this as site-specific validation, not to be confused with a more general validation of a model code, which will never be possible. An assessment of the goodness of fit of the model's behaviour to the measured system may be achieved by application of various graphical and numerical comparisons.

If there is not a good agreement between the model results and the measurements of the real system, this may imply one (or more) of the following causes:

(i) Numerical errors in the solution (although these will have been explored to some extent in model optimisation).

(ii) Errors in the conceptualisation of the system, or the way this conceptualisation has been implemented. This includes neglecting relevant processes as well as representing inappropriate ones. For example, using Darcy's law where significant

macropore flow is present, or using a 2D representation where significant flow or transport occurs in the third dimension.

(iii) Errors in the field measurements.

This last point is particularly interesting because it is often assumed that field measurements are the reality to which the model results are compared. In fact, field measurements can be subject to error in a similar way to models; assumptions (which are not always acknowledged) made during the design of measurement apparatus, research design (e.g. sampling), data analysis and reduction, mean that the representation of reality achieved by field data can be highly approximate.

> There is no fundamental reason to suppose that the empirical, observed data describe or represent reality with any greater accuracy or precision than the model's predictions.
>
> (Lane and Richards, 2001)

Whilst this may be a somewhat controversial statement, it at least demonstrates the importance of stating the margin of error associated with field measurements.

Comparison with independent check data does not help us to understand why a model is invalid. It could be due to any one of the reasons suggested above. However, this is why validation is not carried out in isolation; the rest of the model assessment process should have given a good indication of numerical errors, and a feeling for the sensitivity of the model to parameter changes and boundary condition specification. This, coupled with a good understanding of the limitations of the field data, should make it possible to narrow down the likely explanations for why the model doesn't provide a good fit.

It is important to point out that discrepancies between the model output and field observations are not something to be avoided at all costs. Progress comes not from determining the predictive success of a model, but more from understanding and investigating those situations where the model fails in a variety of different ways (Kirkby, 1994).

Of course, even if the model produces a good fit to the field measurements, it is still perfectly possible that one or more of the above errors is present (the idea that the model might produce the right results for the wrong reasons, Beven, 1989). The capacity to mimic data is not evidence that the underlying processes have been captured, and therefore not evidence of predictive capacity (Oreskes and Belitz, 2001).

> Consistency is not equivalent to either accuracy or validity, and a lack of invalidation is not equivalent to validation.
>
> (Konikow, 1992)

However, the use of diverse sets of field data, at different scales of increasing complexity, and comparisons with measurements of the internal behaviour of the model system, all help to build confidence and increase the probability that the model is not flawed.

5.2 Fieldsite selection and description

5.2.1 Justification of fieldsite choice

In order to obtain a high confidence in the model, it is necessary to compare the model's and the system's behaviour under different sets of conditions. The design of such 'experimental frames' is crucial (Howes and Anderson, 1988). Part of this design involves choosing appropriate field datasets with which to test the model results. To provide a firm basis for selecting appropriate fieldsites for this study it is necessary to evaluate the spectrum of floodplains that can be identified in the field. However, the development of a classification of floodplain types within the wider literature is at an early stage, so this discussion will be framed in the context of more general classifications of general hillslope-channel interactions.

5.2.1.1 Classifications of floodplain types

Classification systems have long been used to assign river segments and areas of land into classes within which attributes are sufficiently homogeneous to provide a framework for research (Quinn *et al.*, 2000). Classifications of hillslope-channel interactions seem to have developed in terms of landscape development, and the river continuum concept, both of which will be examined here. The landscape development classification is not primarily concerned with contemporary processes such as hydrological interactions, but it provides a starting point for exploring this issue.

The 'landscape development' classification of hillslope-channel units is primarily concerned with the transport of sediment between the hillslope and the channel, and the way that the form of the hillslope-channel profile adjusts over time in response to feedback mechanisms between the two. For example, hillslopes influence stream behaviour in that they represent source areas for water and sediment that are supplied to streams and to which streams must adjust. On the other hand, streams influence hillslopes in that they act as local base levels; rapid stream downcutting is associated with the development of convex hillslope profiles, while aggradation tends to reduce slope-base gradients and leads to the development of concave profiles (Knighton, 1998).

This 'landscape development' classification of hillslope-channel types has been based on the degree of coupling between the hillslope and the channel, essentially in terms of sediment

transport. This variable degree of interaction between hillslopes and channels can be regarded as a continuum, the two ends of which are represented by 'strongly coupled links' and 'completely buffered links' (Rice, 1994).

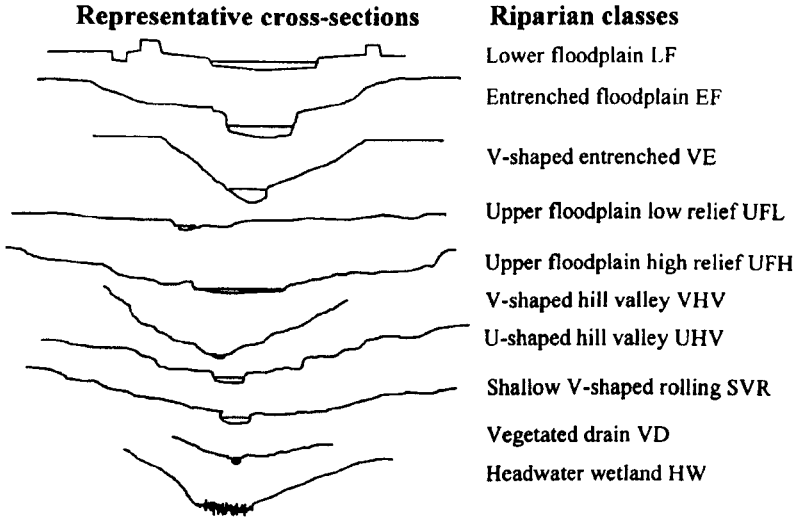

Figure 5.1 Classification of floodplain types (from Quinn et al., *2000).*

Another, related, way of classifying hillslope-channel links is the river continuum concept, which essentially classifies hillslope-channel interactions in terms of network position. In both classifications, the continuum can be given spatial expression: headwater streams, in which river flow, sediment and solute load are closely coupled to hillslope processes; the middle or transfer zone; and the depositional or storage zone, in which river-to-floodplain transfers dominate (Burt, 1997). Although both classifications deal with network position and hillslope-channel form, they differ in the importance they ascribe to each of these properties. In the case of landform development, the classification is based essentially on hillslope-channel profile, and only then implies that certain geometries will occur in certain parts of the catchment. In the case of the river continuum concept, the classification states that the attributes of a particular hillslope-channel unit will depend on where in a catchment the unit occurs, and the implication in this case is that units in a certain part of the network will have a particular geometry.

Implicit in these classifications is the idea that hillslope-dominated units (i.e. those units with a small floodplain) are most likely to occur in headwater reaches, and floodplain dominated units are most likely to occur in lowland reaches. In attempting to cover the spectrum of floodplain types that exist, therefore, it would be instructive to select a headwater riparian

zone and a lowland floodplain for comparison. Within this somewhat crude classification, however, it should be recognised what a much wider range of floodplain types exist, dependent on factors such as climate, underlying geological formation, and so on. An appreciation of the potential scale of the full range of floodplain types can be seen from the diagram of Quinn *et al.* (2000) (Figure 5.1), and this is for just one river. Within the context of floodplains as buffer zones, Quinn *et al.* (2000) then associated each of these riparian classes with different characteristics of slope angle, drainage, clay, slope length and filter width. An idea of the elements that may eventually need to be incorporated into a floodplain classification (with an emphasis here on their function as buffer zones) was also given by Correll (2000); these elements included climate (precipitation, temperature), geological configuration, soils, associated water body, vegetation and site history.

The implication of this is that any two hillslope-dominated (or floodplain-dominated) units may have very different hydrological and chemical transport characteristics, depending on a range of factors other than their position in the landscape. This idea has recently been applied by Montgomery (1999) in the Process Domain Concept for the influence of geomorphological processes in aquatic ecosystems, which recognised that the response of otherwise similar channel reaches can depend upon their geological and geomorphological context. Therefore, whilst recognising the simplicity of the headwater-lowland classification, comparing a headwater and lowland floodplain/riparian zone is something that has not previously been attempted (studies of lowland floodplains being particularly rare), and seems a logical starting point. Additional complexity, in the form of other influencing factors, is something to be incorporated at a later stage.

In addition to the above requirements, field site selection is restricted by the limited availability of suitable data sets. With this in mind, two field sites have been chosen; a lowland floodplain field site on the River Severn, Shropshire, UK, and a headwater riparian zone field site at Sleepers River, Vermont, USA.

5.2.2 River Severn, Shropshire, UK

Hydrological monitoring at this lowland floodplain site has been in operation since June 1997, since which time numerous bankfull flow events and six overbank flow events have occurred, of which four have been well captured by the monitoring system (Table 5.1). The field equipment was originally installed as part of NERC grant GR3/09925, but has subsequently been developed and maintained by this project. The subsurface sedimentology at this site (down to a depth of approximately five metres), has been explored quite extensively and it has been established that the floodplain consists of a gravelly layer overlain by soil of a sandy-clay-loam texture. The transition between these two soil types

occurs at a depth of approximately three to five metres (representing the depth to which a hand-held auger can be used). The broader geological configuration below five metres remains more difficult to explore without more sophisticated machinery, so the depth to which the gravelly layer extends has not been established. At the least, it is clear that this floodplain is not of the type constrained by very shallow bedrock and therefore marks a diversion from the type of fieldsite typically selected for a floodplain investigation (see Section 2.1.5.3). The effect of the soil characterisation below a depth of 5 m, where knowledge of the stratigraphy is more limited, could be explored using the model in the first instance, to save expensive field explorations that may ultimately be unnecessary.

Table 5.1 Summary of River Severn flood event data set.

Event	Date	Duration (hours)	Rainfall total (mm)	Rainfall pattern
Bankfull event A	June 1997	337	106.8	Fairly even throughout the event.
Bankfull event B	Nov 1997	265	30.2	Concentrated at the start of the event.
Bankfull event C	Dec 1997	241	8.8	Fairly even throughout the event.
Flood event D	Jan 1998	1101	96.4	Concentrated at the start of the event.
Flood event E	Mar 1998	451	38.8	One peak near the start and a higher peak near the end.
Flood event F	Oct 1998	1001	114.8	Slightly more rainfall near the start of the event.
Flood event G	Feb 1999	601	61.0	Fairly even throughout the event.

Two broad transects of piezometers (Geotechnical Instruments Vibrating Wire Piezometers: VWP1.1 - 35T) were installed to monitor soil water pressure in the floodplain. The upstream transect (transect S, the spur transect) has four sensors (S1-S4) installed along a line perpendicular to the river, down the hillslope and across the floodplain. The downstream transect (transect H, the hollow transect) has three sensors (H1-H3) within a hillslope hollow and a further sensor (H4) extending onto the floodplain, closer to the river (Figure 5.2). One further piezometer was installed on a stake driven into the river bed in order to provide a continuous measurement of river stage. Soil moisture blocks were also installed but these have not given reliable readings to date and are not considered further. Other instruments at the site record soil temperature (soil temperature probes, Campbell type 107), rainfall (tipping bucket raingauge, Campbell ARG100) and barometric pressure (atmospheric pressure sensor, Campbell PTB101B). Readings are taken automatically from all the sensors at five minute intervals, and an hourly average is stored in two onsite data loggers (one for

each transect; Campbell CR10X). This data set is therefore collected at a very high temporal resolution. More details on the field site establishment and instrumentation can be found in Bates *et al.* (2000).

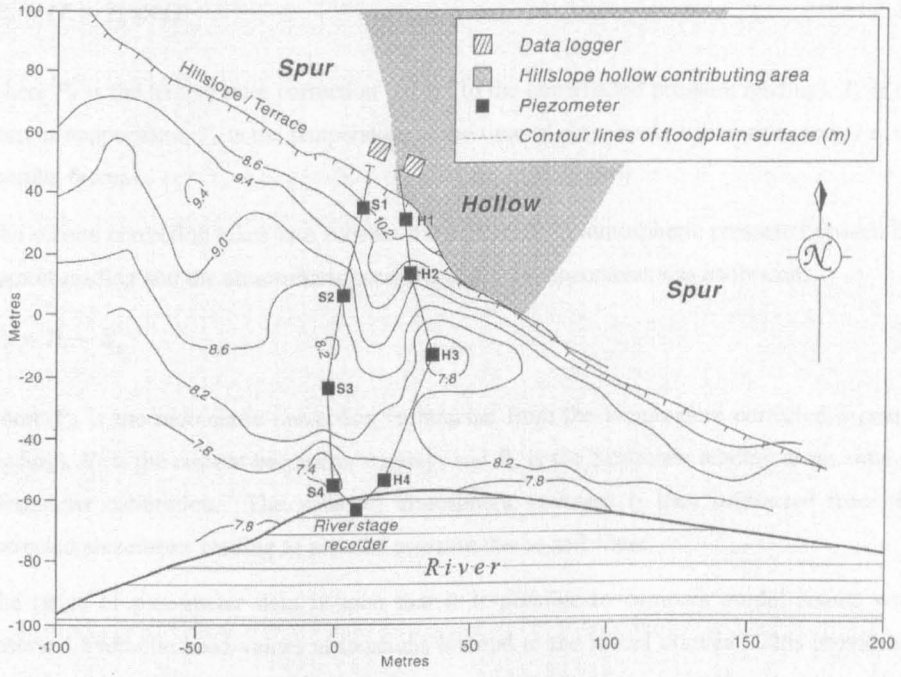

Figure 5.2 Plan of the Leighton field site on the River Severn showing piezometer locations (Burt et al., 2002).

During the period June 1998 to March 1999 the barometric pressure sensor was found to have malfunctioned. The atmospheric pressure readings are important because they are used to correct the piezometer readings for the effects of atmospheric pressure, so an alternative source of these data was required for this period. These data were provided by the British Atmospheric Data Centre (BADC), who granted access to their UK Synoptic Database. Atmospheric pressure readings from the nearest available weather station (Shawbury), approximately 10 miles from the field site, were obtained. In order to check the suitability of this data set, a comparison was made between the Shawbury pressure data and the pressure data from the field site for a period before the field site sensor malfunctioned. This indicated that the two readings usually differed by about ± 1 to 2 millibars, and never by more than ± 4 millibars. A difference of ± 4 millibars corresponds to a soil water pressure measurement of ± 2.9 cm, an acceptable level of error.

The piezometer readings recorded by the datalogger need correcting in order to obtain a value of the pressure due to the soil water. The first correction takes into account the difference in temperature between the current reading and the temperature when the piezometer was calibrated:

$$P_T = (T_1 - T_0) \times \Omega \qquad 5.1$$

where P_T is the temperature correction (added to the uncorrected pressure reading), T_1 is the current temperature, T_0 is the temperature at the time of piezometer calibration, and Ω is the thermal factor.

The second correction takes into account the difference in atmospheric pressure between the current reading and the atmospheric pressure when the piezometer was calibrated:

$$P_B = B_1 - B_0 \qquad 5.2$$

where P_B is the barometric correction (subtracted from the temperature corrected pressure reading), B_1 is the current barometer reading, and B_0 is the barometer reading at the time of piezometer calibration. The value of atmospheric pressure is then subtracted from the corrected piezometer reading to give the pressure due to soil water.

The range of piezometer data is such that it is possible to compare model results with observed hydraulic head values at locations internal to the model domain. This provides a somewhat more rigorous test of model performance than comparison with simple outflow characteristics. This dataset contains no information on chemical transport. This is not seen as a severe limitation considering the emphasis needed on getting a good representation of the hydrological processes as the basic prerequisite for getting the chemical transport right.

> The emphasis is on groundwater quantity, not quality. Probably at least 95% of a problem of contamination would be solved if one knew where the water is really going.
>
> (Morel-Seytoux, 2001)

5.2.3 Sleepers River, Vermont, USA

The Sleepers River Research Watershed in northeastern Vermont, USA, is one of five sites for research on Water, Energy, and Biogeochemical Budgets (WEBB) under the USGS Global Change Hydrology program. This data set comes from a field study conducted in 1996 by Brian McGlynn in the 14 ha headwater catchment W-9B, nested within the intensively instrumented 40.5 ha W-9 catchment. The W-9B catchment is composed of two tributaries (Bx and By) and is entirely forested, largely by mixed northern hardwoods. The elevation in catchment W-9 ranges from 519 to 686 m, and the slopes average 13 per cent.

This study, which was aimed at investigating the flow paths and physical water mixing through hillslope and riparian zones, is reported in McGlynn *et al.* (1999), from which the following field site description has been taken.

Bedrock in the W-9 catchment consists of calcareous granulite interbedded with quartz mica phyllite interbedded. The overburden in the Sleepers River area consists mainly of clay-silt till. The till is an unsorted mix of pebbles and cobbles suspended in a dense matrix of sand, silt and clay. The near-stream zones in the study area consist typically of peat accumulations ranging from sapric to fibric up to 0.9 m in depth overlying dense clay-silt till, which in turn overlies gravelly till of variable depth above bedrock. This near stream profile grades into a more uniform mineral soil further upslope.

Snow cover in the W-9 catchment is present from mid-November to late April and comprises 25-30 per cent of the 1000 mm of annual precipitation. Air temperatures range from –38 to 30 °C, with an annual average of 5 °C. Peak runoff typically occurs during spring melt in mid-April, and minimum flows occur between July and October.

Transect By was instrumented with nested piezometers upstream of the tributary confluence of Bx and By. The study area was characterised by extensive saturated zones on either side of stream By and moderately sloping hillsides farther upslope. Six nests of piezometers were installed along the transect (Figure 5.3). Piezometers consisted of 19 mm PVC pipe open only at completion depths of up to 1.6 m, depending upon local depth to bedrock. Each nest included two or three piezometers. Surface overland flow and shallow subsurface flow were collected in porous cups. One cup was open at the ground surface to capture overland flow. A second cup was perforated between 0.08 and 0.12 m to capture shallow subsurface flow.

Piezometric head values were measured daily in all piezometers with an electronic water level probe. The accuracy of this method was estimated to be approximately ±2 cm. Nested piezometers, including porous cups within surficial organic muck, were sampled daily for calcium, silica, DOC, other major cations, and $\delta^{18}O$ during the 1996 snowmelt period.

Snowmelt water was collected daily from four 1 m^2 plexiglass lysimeters placed above ground surface at various aspects within W-9. Precipitation amounts and intensities were measured with a weighing bucket rain gauge at the meteorological station near the W-9 weir. Data were recorded at one minute intervals on a Campbell CR10 datalogger throughout the study period. Precipitation was sampled on an event basis.

Dynamic cone penetrometer profiles were constructed at and between each nest to determine local depth to bedrock and layering within the soil profile. Soil pits were excavated at the study transect to corroborate determinations made from the dynamic cone penetrometer data.

Hydraulic conductivity values were determined with the Hvorslev water level recovery method in the piezometers (Hvorslev, 1951).

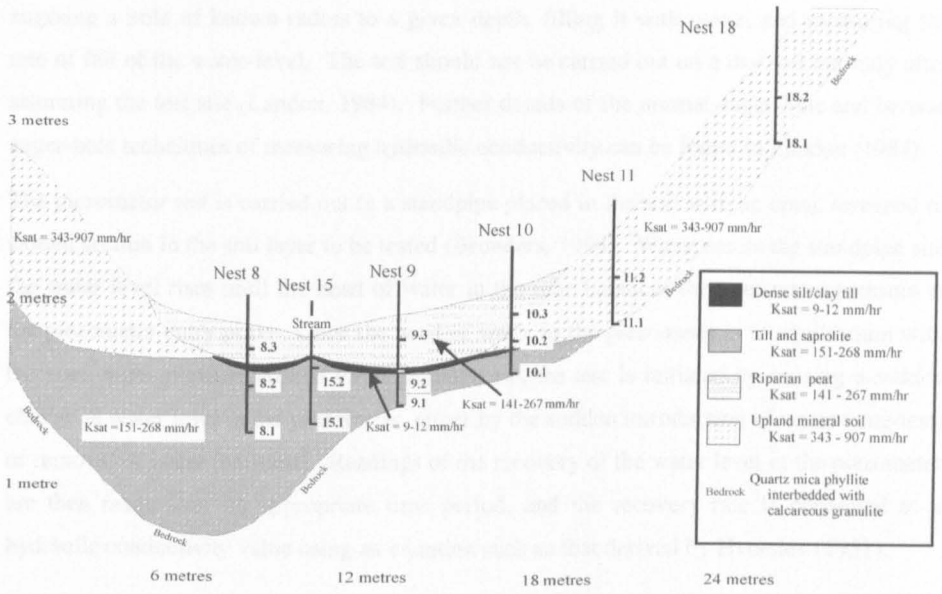

Figure 5.3 Cross section of field installation at Sleepers River, showing location of piezometer nests (from McGlynn et al., *1999).*

The more complex nature of the soil distribution at the Sleepers River fieldsite (in comparison with the River Severn site) provides a more rigorous test of the model capability.

5.2.4 Saturated hydraulic conductivity measurements and potential errors

Several methods are available for the measurement of saturated hydraulic conductivity in soils. These include methods that can be conducted in the field, and those that must be carried out in the laboratory. Obtaining undisturbed cores for laboratory tests is difficult (Landon, 1984). Combined with the fact that such cores are small and may be unrepresentative of the fieldsite soil, it is generally recommended that hydraulic conductivity is measured using one of the field techniques.

The two most commonly used field methods for determining hydraulic conductivity in soils are the auger-hole (or dipwell) and piezometer methods. Other soil methods include the use of infiltration rings, and borehole pumping tests are extensively used in geological formations (Landon, 1984).

Auger-hole tests allow in situ determination of the saturated hydraulic conductivity value in a horizontal direction in a hole of known radius augered to a known depth (Bronders, 1994). During a 'normal' auger-hole test, the rate of water flow into the hole from the surrounding

soil is measured as a function of time, following a sudden water level drop in the auger-hole. The use of the auger-hole method is restricted to areas where a high water table is present. The 'inverse' auger-hole method is an auger-hole test above the water table. It consists of augering a hole of known radius to a given depth, filling it with water, and measuring the rate of fall of the water-level. The test should not be carried out on a dry soil but only after saturating the test site (Landon, 1984). Further details of the normal auger-hole and inverse auger-hole techniques of measuring hydraulic conductivity can be found in Landon (1984).

The piezometer test is carried out in a standpipe placed in the soil with an open, screened or slotted section in the soil layer to be tested (Bronders, 1994). Water enters the standpipe and the water level rises until the head of water in the tube balances the pore water pressure at the piezometer entry point. Once the head of water in the piezometer is in equilibrium with the pore water pressure around the piezometer tip, the test is initiated by causing a sudden change in water level in the piezometer, either by the sudden introduction of water (slug-test) or removal of water (bail-test). Readings of the recovery of the water level in the piezometer are then made over an appropriate time period, and the recovery rate is converted to a hydraulic conductivity value using an equation such as that derived by Hvorslev (1951).

5.2.4.1 River Severn

At the River Severn fieldsite, inverse auger-hole tests were used to estimate soil saturated hydraulic conductivity values. Measurements were taken at five to ten boreholes across the floodplain and averaged to give values of hydraulic conductivity of 1.56×10^{-6} m s^{-1} for the upper sandy clay layer and 2.54×10^{-6} m s^{-1} for the lower, gravelly layer (Bates *et al.*, 2000). Each borehole was thoroughly saturated before testing commenced, and the test was performed at least three times for each borehole. This method was intended to give an indication of the general magnitude of saturated hydraulic conductivity values at the fieldsite. In particular, variations in conductivity throughout the profile could not be investigated as this method gives only an integrated value over the whole depth to which the hole is augered. This may have implications for the value of hydraulic conductivity reported for the lower, gravelly layer of the floodplain soil. It is likely that this method was not ideal for capturing the hydraulic conductivity of the gravelly layer, as the rate of water level drop in boreholes which were augered to the depth of the gravelly layer would have been heavily influenced by water flow through the borehole walls in the upper layer of the soil. It has been hypothesised that the apparent lack of difference in hydraulic conductivity values between the two soil layers may be due to the relatively dispersed nature of the gravels within the fine-grained matrix of the lower layer (Bates *et al.*, 2000), but is likely to have been strongly influenced by the relatively crude nature of the hydraulic conductivity tests.

In addition, it has been noted that in general, field measurements of hydraulic conductivity may underestimate real values. Bonell (1998) notes that one of the main contributions to emerge from environmental isotope studies is the realisation that the effective hydraulic conductivity of small catchments is "much higher than previous estimates from in situ measurements of field saturated hydraulic conductivity using methodologies from soil physics". It is therefore also possible that the values of hydraulic conductivity obtained using the inverse auger-hole test at the River Severn site are underestimates of the true values. Despite the shortcomings discussed here, these observations are felt to be a sufficient guide for initial model analysis, and it is felt that any further data collection needed to refine the soil parameters may be directed by model results.

5.2.4.2 Sleepers River

Hydraulic conductivity at the Sleepers River fieldsite was measured using the piezometer slug-test method of Hvorslev (1951). A number of sources of error can affect the performance of an open standpipe piezometer, including changes in the effective stresses in the soil around the piezometer tip due to removal or displacement of soil during the installation of the piezometer, gas bubbles in the soil or the piezometer, and sedimentation and clogging of the piezometer tip.

Gas bubbles in the soil near the piezometer tip will increase the response time of the piezometer by decreasing the conductivity of the soil. The expansion and contraction of gas bubbles as pore water pressure changes in the soil around the tip will also affect response time by altering the hydraulic conductivity and storage capacity of the soil (Baird and Gaffney, 1995).

Incomplete well development is thought to be a major cause of incorrect measurement of hydraulic conductivity values when using a piezometer slug-test method. Incomplete well development is the failure to remove drilling-related debris (e.g. fine material mobilised by the drilling process) and products of biochemical action from the near-well portions of the formation in which hydraulic conductivity is being measured. Since slug-tests are extremely sensitive to near-well conditions, incomplete well development can result in slug-test estimates that are more reflective of the altered (lower permeability) near-well material (well-skin) than the formation itself (Butler and Healey, 1998). A considerable body of data has been amassed that indicates that the hydraulic conductivity estimate from a pumping test is, on average, considerably larger than the estimate obtained from a series of slug-tests in the same formation. It is suggested that incomplete well development before the slug-test is carried out is a major reason for this difference. Low-permeability well-skins can lead to

slug-test estimates of hydraulic conductivity that may be orders of magnitude lower than the average hydraulic conductivity of the formation in the vicinity of the well screen.

It is possible that hydraulic conductivity measurements made at the Sleepers River field site may be subject to these sources of error. This should be taken into consideration when selecting values of hydraulic conductivity to represent the Sleepers River soils within the model.

5.3 Strategy for model assessment

The model assessment is focused around two floodplain models, based on the two selected field sites. The term model is used in this sense to mean an instance of the generic numerical code that represents a particular site (e.g. the River Severn model or the Sleepers River model). The detailed strategy for model assessment in this study is now outlined according to the following five stages: verification, optimisation, sensitivity, calibration, and validation. These five stages are each carried out twice: firstly for the ESTEL2D code, and secondly for the coupled ESTEL2D-SUBIEF2D code. At each stage, where appropriate, there is a consideration of which aspects of the model are being tested and why, and which aspects of the model output are being compared to assess model performance. The schedule of model runs is then presented, followed by an analysis of the results. These procedures, once completed successfully, should establish the model as having a degree of confirmation that permits exploration with new combinations of parameters, within the range for which the model has been tested, to explore theories about how floodplain hydrological and chemical transport processes operate.

5.3.1 ESTEL2D assessment strategy and results

5.3.1.1 Verification

ESTEL2D has already undergone a number of verification tests, with numerical solutions compared to analytical solutions for a range of dynamic, unsaturated conditions as presented in Tracy (1995). These results are presented in Desitter (1998) and Desitter *et al.* (2000). In summary, these tests indicated an excellent correspondence between the numerical and analytical solutions, hence providing evidence of the quality of the numerical approximation of the ESTEL2D code, and overall software functionality.

5.3.1.2 Optimisation

The effect of model structural parameters including the seepage boundary specification, convergence criterion for the nonlinear iterative scheme, mesh resolution, the accuracy of the iterative schemes, the linear solver of the Richards' equation, the form of the Richards'

equation (*h*-based or mixed), and the choice of soil water retention model were all investigated according to the research design in Table 5.2. The effect of time step size was not investigated as this study made use of the adaptive time step facility that allows time step sizes during a transient simulation to be adjusted dynamically according to the convergence behaviour of the nonlinear iterative scheme (Paniconi and Putti, 1994). The optimisation process was carried out for the River Severn model only. The Sleepers River model was optimised according to the results of the Severn model optimisation.

The boundary conditions for this simulation were as illustrated in Figure 5.4, which also illustrates the dimensions of the domain and the appearance of the high resolution finite element mesh. The importance of allowing a seepage face boundary condition on the upper boundary of the model was investigated as part of the optimisation process. In run 2 (Table 5.2) the seepage face functionality was disabled, and the upper boundary condition was changed to a simple specified flux boundary condition, with a value equal to the rainfall rate.

Table 5.2 Optimisation research design. Those entries in italics indicate which variable has been tested for each run.

Run no.	Seepage	Conv. criterion	Mesh resolution[1]	Accuracy	Linear solver	Scheme of Richards' equation	Soil water retention model[2]
1	Yes	Modified	High	Medium	1	mixed	BC
2	*No*	Modified	High	Medium	1	mixed	BC
3	Yes	*Standard*	High	Medium	1	mixed	BC
4	Yes	Modified	*Medium*	Medium	1	mixed	BC
5	Yes	Modified	*Low*	Medium	1	mixed	BC
6	Yes	Modified	High	*High*	1	mixed	BC
7	Yes	Modified	High	*Low*	1	mixed	BC
8	Yes	Modified	High	Medium	*2*	mixed	BC
9	Yes	Modified	High	Medium	*5*	mixed	BC
10	Yes	Modified	High	Medium	*6*	mixed	BC
11	Yes	Modified	High	Medium	*7*	mixed	BC
12	Yes	Modified	High	Medium	1	*h-based*	BC
13	Yes	Modified	High	Medium	1	mixed	*VG*

[1] High mesh resolution: number of elements = 13117; number of nodes = 6741. Medium mesh resolution: number of elements = 7954; number of nodes = 4133. Low mesh resolution: number of elements = 2092; number of nodes = 1123.

[2] BC = Brooks and Corey, VG = van Genuchten

Three mesh resolutions were investigated: a low resolution mesh with 2.0 m elements, a medium resolution mesh with 1.0 m elements, and a high resolution mesh with a variable element size of 0.5 m at the top of the mesh, degrading to 2.5 m at the base (shown in Figure 5.4). Although piezometer information was only recorded to a depth of approximately 5 m, the mesh was constructed with an extra 20 m of domain below this. In the absence of field information about the lower boundary condition, a no-flow boundary condition was assumed. Moving the lower boundary further away from the region of interest was aimed at reducing the impact of the lower boundary condition on model results.

There were two convergence criteria to specify: one for the nonlinear iterative scheme (Picard scheme), and one for the linear solver. Three levels of accuracy were investigated: high convergence accuracy (1×10^{-8} linear solver, 1×10^{-6} nonlinear iterative scheme), medium convergence accuracy (1×10^{-6} linear solver, 1×10^{-4} nonlinear iterative scheme) and a low convergence accuracy (1×10^{-4} linear solver, 1×10^{-2} nonlinear iterative scheme). The standard and modified Huang convergence criteria for the nonlinear iterative scheme were also tested.

Five different linear solvers were tested, identified in Table 5.2 by their respective codes in the ESTEL2D model. Solver 1 is conjugate gradient, solver 2 is conjugate residual, solver 5 is squared conjugate gradient, solver 6 is conjugate gradient stabilised, and solver 7 is generalised minimum residual. Two schemes for solving the Richards' equation, the *h*-based and the mixed form, were also tested.

Table 5.3 Soil parameters used in the optimisation process.

Soil hydraulic parameter	**Value**
Residual moisture content θ_r	0.0954
Saturated moisture content θ_s	0.41
Brooks and Corey bubbling pressure parameter (h_s) [m]	0.880
Brooks and Corey pore distribution parameter (λ)	0.318
Saturated hydraulic conductivity [m s^{-1}]	2.54×10^{-6}
Specific storage [m^{-1}]	0.0001
Where van Genuchten parameters are used, they have the following values:	
van Genuchten parameter α [m^{-1}]	1.90
van Genuchten parameter n	1.32

To solve the Richards' equation, information on the retention and conductivity curves is required. ESTEL2D can either use a van Genuchten/Mualem relationship (van Genuchten, 1980) or by Brooks and Corey/Burdine relationship (Brooks and Corey, 1964). A Brooks and Corey soil water retention model was selected for use during the optimisation process,

with average parameter values for a clay loam soil type as reported in Cloke (2001) after original statistical distributions given in Meyer *et al.* (1997). The value of saturated hydraulic conductivity, however, was that measured in the field at the River Severn as 2.54 x 10^{-6} m s^{-1}. This saturated hydraulic conductivity value is within the 95 per cent confidence limits calculated for the distribution of clay loam saturated hydraulic conductivity values. Where the van Genuchten soil water retention model was tested, the average van Genuchten parameter values (α and n) for a clay loam soil type were used, also taken from Cloke (2001). These are very close to the values obtained when using the Brooks and Corey – van Genuchten parameter equivalence estimation method of Morel-Seytoux (1996) of $n = \lambda + 1$, and $\alpha = 1/h_s$. The full list of soil hydraulic parameters used during the optimisation process is given in Table 5.3.

The hydrological data set used for the optimisation procedure and sensitivity analysis is from flood event D (Table 5.1) on transect S (Figure 5.2) at the River Severn field site. The initial conditions for these simulations were obtained using a steady state run, during which the boundary conditions were held constant. The value of hydraulic head at $t = 0$ from the hillslope piezometer (S1, Figure 5.2) was used to set the specified head for the left-hand boundary, and the value of hydraulic head from the river stage recorder at $t = 0$ was used to set the specified head for the right-hand boundary (see Figure 5.4 for more details). The flux imposed on the surface for the steady state simulation was originally intended to be a representative regional flux equivalent to the average yearly rainfall of approximately 1000 mm per year, or 3.17 x 10^{-8} m s^{-1}. However, with the parameter combination chosen for the optimisation procedure it was impossible to impose this flux and still obtain a realistic pattern of water flow through the domain, and a smaller value of 3.17 x 10^{-9} m s^{-1} was used instead. However, it is felt that the validity of the conclusions that are drawn from this optimisation procedure, which is assessing model efficiency for a given problem, should not be compromised by this approximation.

The pressure head and moisture content distributions calculated by the steady state simulation were used as initial conditions for the subsequent transient model run. During the transient simulation, the value of hydraulic head from the hillslope piezometer (over the course of the whole flood event) was used to set the specified head for the left-hand boundary, and the value of hydraulic head from the river stage recorder was used to set the specified head boundary condition for the right-hand boundary. The upper boundary flux boundary condition was set using the rainfall rate calculated from rain gauge data collected during the flood event.

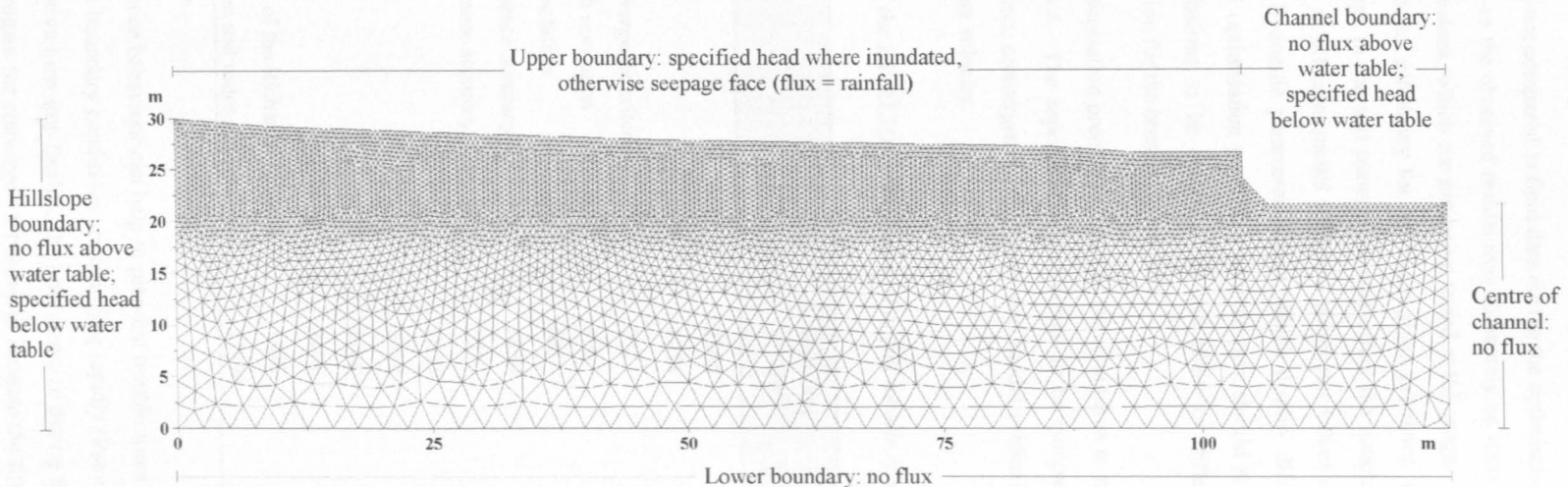

Figure 5.4 Diagram illustrating the Severn model domain used in the optimisation process, and the associated hydrological boundary conditions.

The model results are not compared to field data during the optimisation process, as the fit of the calculated results to the observed results may ultimately be more dependent on the soil hydraulic parameter values, which are not being tested at this stage. This procedure is thus aimed at assessing model efficiency for solving a given problem. It must be considered, however, that a change in the soil parameters may affect the conclusions drawn from the optimisation process, as different model structural parameter values may be better suited to different model soil hydraulic parameter values, which display different degrees of non-linearity. The model optimisation procedure adopted here should at the least enable some general initial conclusions to be drawn about the effect of different model structural attributes, in preparation for the sensitivity analysis.

The results of the optimisation process in terms of the time taken to run each simulation are presented in Table 5.4. The aspects of model output to be compared are mass balance, computational run time, convergence behaviour, and model predictions of pressure head, saturation, and Darcian velocity.

Table 5.4 Results of the ESTEL2D optimisation. For full details of simulation parameters, see Table 5.2.

Run no.	Properties	Run time (seconds)*	Run time as a percentage of base run time
1	Base run	2265	100
2	No seepage	1954	86
3	Standard convergence criterion	NC	--
4	Medium mesh resolution	996	44
5	Low mesh resolution	NC	--
6	High convergence accuracy	3630	160
7	Low convergence accuracy	562	25
8	Solver 2	1600	71
9	Solver 5	2019	89
10	Solver 6	2108	93
11	Solver 7	2114	98
12	h-based form of the Richards' equation	3338	147
13	van Genuchten soil water retention model	25898	1143

* NC = no convergence

Plotting the convergence behaviour can help to pinpoint trouble spots in a simulation, which often occur when the boundary conditions are changing rapidly (Paniconi and Wood, 1993). When using the adaptive time step facility, the time step size during the transient simulation can be used as a surrogate for convergence behaviour because the time step will be smaller

when convergence is more difficult. The mass balance is displayed as the cumulative mass balance error: this is the cumulative lost mass as a percentage of the total mass in the model domain. Where graphs of model variables over time are displayed, they describe the pattern of change at one point in the domain (at x = 50 m, y = 27 m). This point is approximately halfway along the domain in the x-direction, and close to the top of the domain, to illustrate both saturated and unsaturated conditions.

Seepage face

The seepage face boundary condition was found to have a significant effect on the prediction of model variables, including pressure head and Darcian velocity. The results in Figure 5.5a show that a large peak in pressure head is particularly noticeable at approximately 28 days into the simulation, with a corresponding response in the x-component of the Darcian velocity.

Further analysis of this point in the simulation revealed that a particular combination of conditions on the upper boundary gave rise to this phenomenon. At this time, during recession of the flood event, the upper left portion of the boundary (near to the hillslope) was unsaturated (specified flux boundary condition), the upper right portion of the boundary was still inundated (specified head boundary condition), but the middle portion of the upper boundary was in a transitional phase. It was no longer inundated, but it was still saturated. Without the seepage face boundary condition, this portion of the upper boundary was still treated as a specified flux boundary, with a flux equal to the precipitation rate. As a large rainfall event occurred at this time, the boundary conditions thus specified allowed rainfall to infiltrate in this part of the domain, which is a physically unrealistic condition.

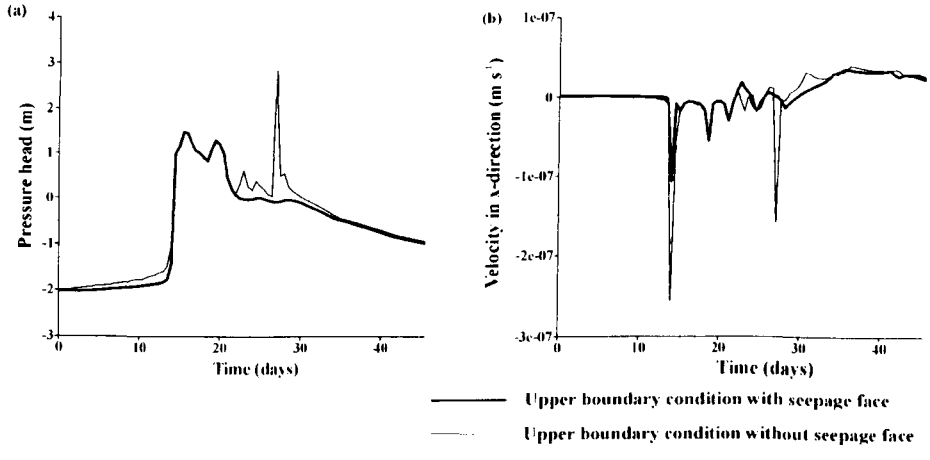

Figure 5.5 Graphs showing the effect of seepage on model results in terms of (a) pressure head prediction and (b) the x-component of Darcian velocity, at the point x = 50 m, y = 27 m.

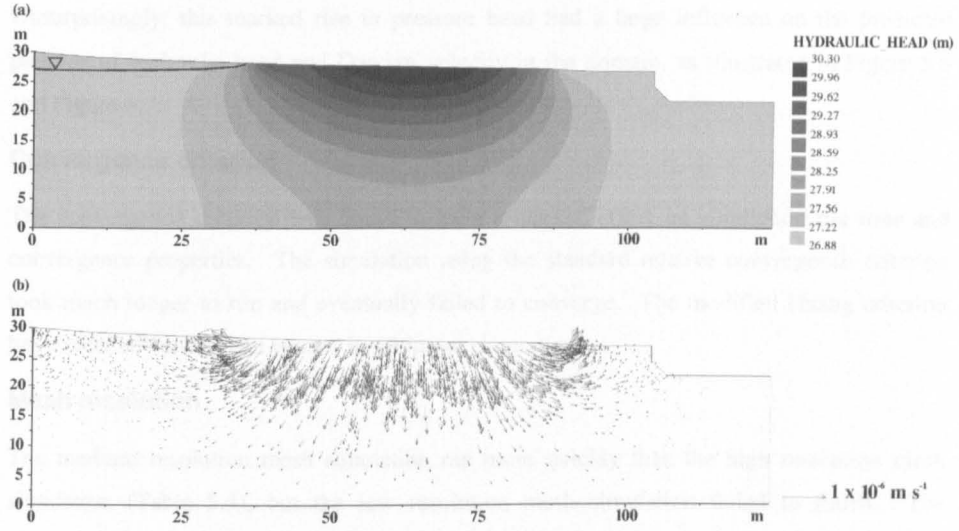

Figure 5.6 Illustration of (a) hydraulic head and (b) Darcian velocity vector patterns at time = 27 days, without a seepage face boundary condition on the upper boundary.

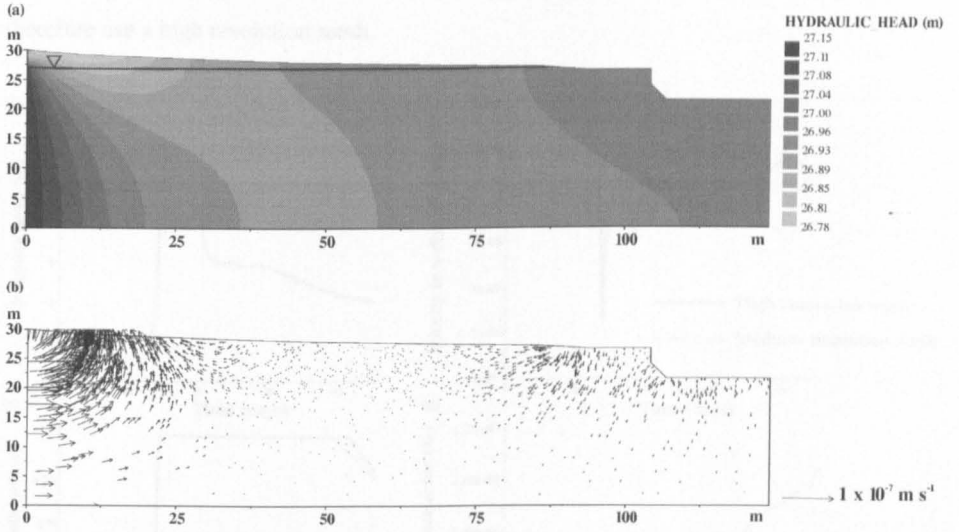

Figure 5.7 Illustration of (a) hydraulic head and (b) Darcian velocity vector patterns at time = 27 days, with a seepage face boundary condition on the upper boundary.

This large influx of water into the domain created a significant and unrealistic peak in the predicted pressure head. With the seepage face boundary condition, this transitional portion of the boundary was treated as a seepage face. In practice this meant that this boundary was treated as specified head, with a value of zero, and rainfall could not infiltrate this part of the boundary, although exfiltration was possible. This illustrates that the seepage face boundary condition fulfils an additional role to just permitting exfiltration of water from the domain; it also prevents the unrealistic situation of water infiltrating through a saturated boundary.

Unsurprisingly, this marked rise in pressure head had a large influence on the predicted patterns of hydraulic head and Darcian velocity in the domain, as illustrated in Figure 5.6 and Figure 5.7.

Convergence criterion

The convergence criterion was found to have a marked effect on simulation run time and convergence properties. The simulation using the standard relative convergence criterion took much longer to run and eventually failed to converge. The modified Huang criterion has a clear advantage and is used in all future simulations.

Mesh resolution

The medium resolution mesh simulation ran more quickly than the high resolution mesh simulation (Table 5.4), but the low resolution mesh simulation failed to finish. The differences between the simulated pressure head, velocity, and saturation were quite small, but the mesh resolution had a significant effect on the mass balance calculation (Figure 5.8). Decreasing the mesh resolution increased the mass balance error. Future simulations therefore use a high resolution mesh.

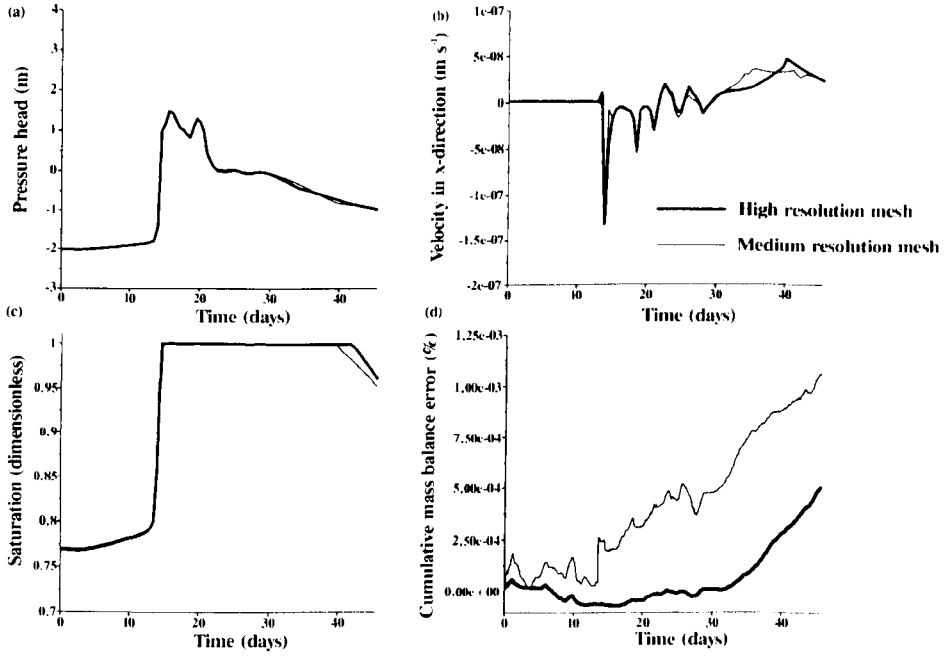

Figure 5.8 Graphs showing the effect of mesh resolution on (a) pressure head, (b) the x-component of the Darcian velocity, and (c) saturation, at the point x = 50 m, y = 27 m, and (d) the cumulative mass balance error.

Convergence accuracy

Solution accuracy had a significant effect on simulation run time. The high accuracy simulation took 60 per cent longer to run than the medium accuracy simulation, and the low accuracy simulation took 75 per cent less time to run. In terms of simulated hydrological variables, there was no discernible difference between the medium and high accuracy results (Figure 5.9), but the low accuracy results were noticeably different. Changing the solution accuracy had a significant effect on the cumulative mass balance error of the simulation, with an increasing level of error associated with lower solution accuracy. In summary, even though the low solution accuracy generated a much faster run time, the increased error in the results makes this level of accuracy unacceptable for future simulations. While the medium accuracy simulation produced greater mass balance errors, there was little difference in the predicted hydrological variables, and it had the advantage of a much faster run time. The medium accuracy level may therefore be preferred over the high accuracy solution, unless a particularly high level of mass balance accuracy is considered necessary.

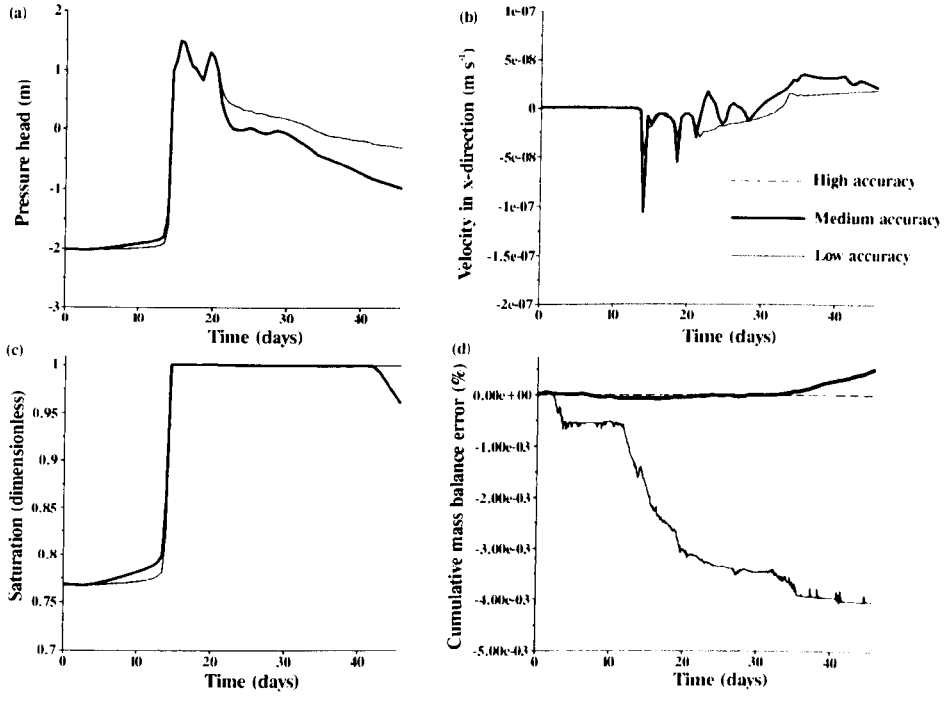

Figure 5.9 Graphs showing the effect of solution accuracy on (a) pressure head, (b) the x-component of the Darcian velocity, and (c) saturation, at the point x = 50 m, y = 27 m, and (d) the cumulative mass balance error.

Solver

The model solvers gave virtually identical model results in terms of hydrological variable predictions. The only differences between the solvers were in terms of run time and cumulative mass balance error (Figure 5.10). The only solver that gave a significantly faster run time than solver 1 (the base run solver, conjugate gradient) was solver 2 (conjugate residual), but this also gave the greatest mass balance error. In fact, all the solvers tested during the optimisation procedure gave greater mass balance errors than solver 1, and solver 1 will therefore be used for all future simulations.

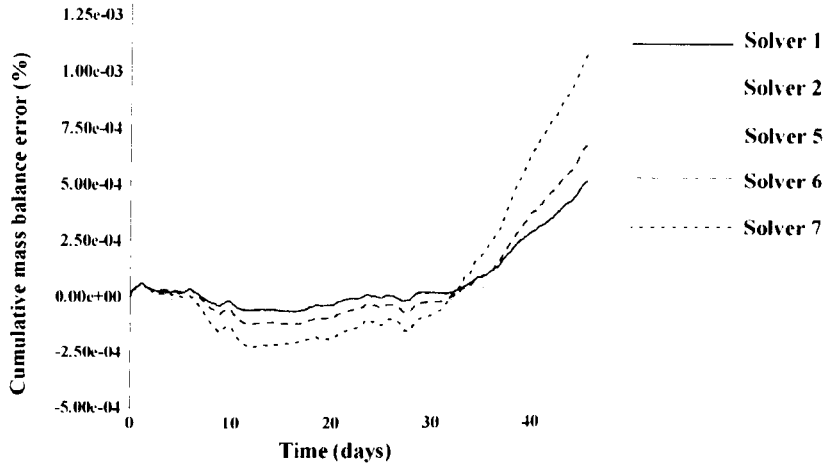

Figure 5.10 Graph showing the effect of model solver on cumulative mass balance error.

Form of the Richards' equation

The form of the Richards' equation had no effect on the prediction of hydrological variables, but it had a significant effect on the run time, and also on the mass balance error. The *h*-based form of the Richards' equation took 47 per cent longer to run than the mixed form of the equation. The convergence behaviour of the model during the two simulations was explored using the time step size as a surrogate for ease of convergence (Figure 5.11). Both simulations used an adaptive time stepping strategy, where the time step is adjusted according to the convergence behaviour of the model. Therefore, a reduced time step size indicates more difficulty in solution convergence. The initial time step was specified as one second, and the maximum time step was specified as 3600 seconds. Figure 5.11a clearly illustrates the differences between the two simulations; the simulation using the mixed form of the equation used a maximum time step of 3600 seconds throughout the run, whereas the simulation using the *h*-based form of the equation often used a much smaller time step.

The *h*-based form of the equation resulted in a much greater mass balance error (Figure 5.11b). It can be seen from Figure 5.11c that most of the error accumulated during one part of the simulation, which corresponded to a period where the boundary conditions were changing particularly rapidly. It is clear that the mixed form of the Richards' equation has a great advantage over the *h*-based form in terms of run time and mass conservation. It is also worth noting that the mixed form of the equation has been demonstrated to be perfectly mass conservative (Celia *et al.*, 1990). In these optimisation cases, however, the solution is not perfectly mass conservative. Some further testing has indicated that this may be because perfect mass conservation is only applicable in unsaturated conditions i.e. where no part of the domain is fully saturated.

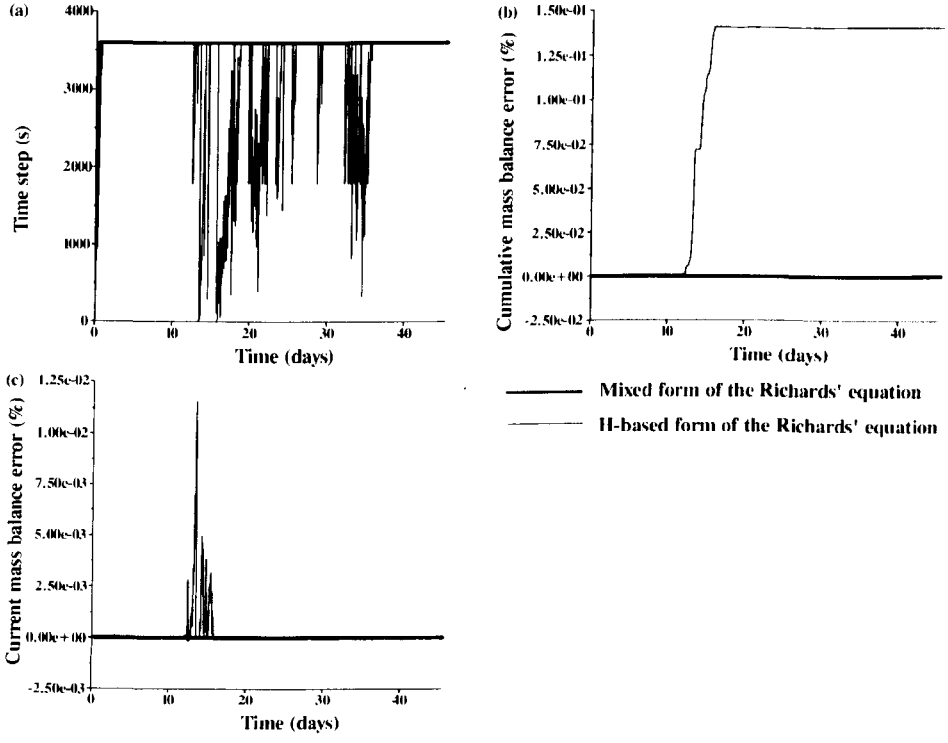

Figure 5.11 Graphs showing the effect of the form of the Richards' equation on (a) time step, (b) cumulative mass balance error, and (c) current mass balance error.

Soil water retention model

Testing the effect of using the Brooks and Corey soil water retention model and the van Genuchten model was the last part of the optimisation process. Even though the parameters were selected in such a way as to achieve parameter equivalence, Figure 5.12 clearly shows the differences between the two models. This difference actually alters the physical problem being solved, and therefore the results of the simulations using the two different models are

not directly comparable. However, it was the only way to gain some kind of insight into the performance of the two model types.

The simulation using the van Genuchten model took 11 times longer to run than the simulation using the Brooks and Corey model (Table 5.4). This is related to the difference in the shape of the $\theta(h)$ and $k_r(h)$ curves of the two soil water models, and the impact that this has on the accuracy, stability, and rate of convergence of the numerical solution. The choice of analytical function for $\theta(h)$ can significantly affect the predicted $k_r(h)$ function obtained with the statistical pore-size distribution models (Vogel *et al.*, 2001). One reason for this is that the predicted conductivity function is extremely sensitive to small changes in the shape of the retention curve near saturation. This sensitivity is a major cause of the sometimes significant differences between predicted $k_r(h)$ functions obtained with the Brooks and Corey and van Genuchten retention functions. The differences are especially apparent in fine-textured soils which can exhibit extreme non-linearity in $k_r(h)$ close to saturation when the van Genuchten equations are used. In this case, the 'equivalent' van Genuchten parameters produce a much steeper $k_r(h)$ curve near saturation in comparison with the Brooks and Corey parameters (Figure 5.12b).

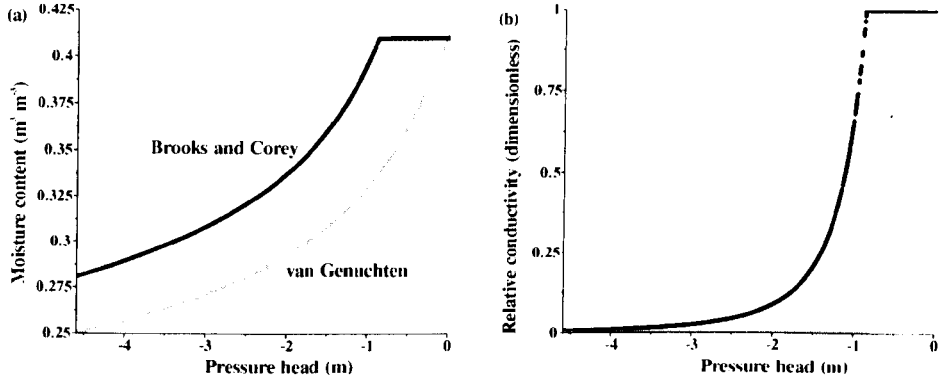

Figure 5.12 Graphs showing two soil water retention models of an average clay loam soil; (a) moisture content versus pressure head $\theta(h)$ and (b) relative conductivity versus pressure head $k_r(h)$.

The non-linear nature of the van Genuchten conductivity function can cause serious numerical convergence problems for van Genuchten parameter n values close to 1 (Vogel *et al.*, 2001). Tests of the Picard and Newton iterative schemes by Paniconi and Putti (1994) revealed that conductivity curves that are most strongly nonlinear cause the greatest convergence difficulties. In addition, the convergence difficulties caused by the strong nonlinearities in some of the $k_r(h)$ curves were compounded in the test case illustrated in Paniconi and Putti (1994) by the presence of a water-table and an extended saturated zone,

exactly the situation that was modelled during this optimisation process. In particular, the steep and near-discontinuous gradients around $h = 0$ result in sharp changes in $k_r(h)$ and its derivative across the saturated-unsaturated interface. In the simulations reported for this optimisation process, changing to the van Genuchten soil water function increased the difficulty of the problem by increasing the gradient of the $k_r(h)$ curve, and hence increased the run time.

It must be appreciated that changing the shape of the soil water retention and conductivity curves, whether by changing the parameters of one soil model or changing between soil models, actually changes the physical problem that the model is solving. It is therefore difficult to say whether the differences in model prediction (e.g. pressure head, saturation) and performance (cumulative mass balance error) as illustrated in Figure 5.13 are strictly due to the choice of soil model, or just a reflection of the change in the shape of the soil water retention curves that result from making this choice.

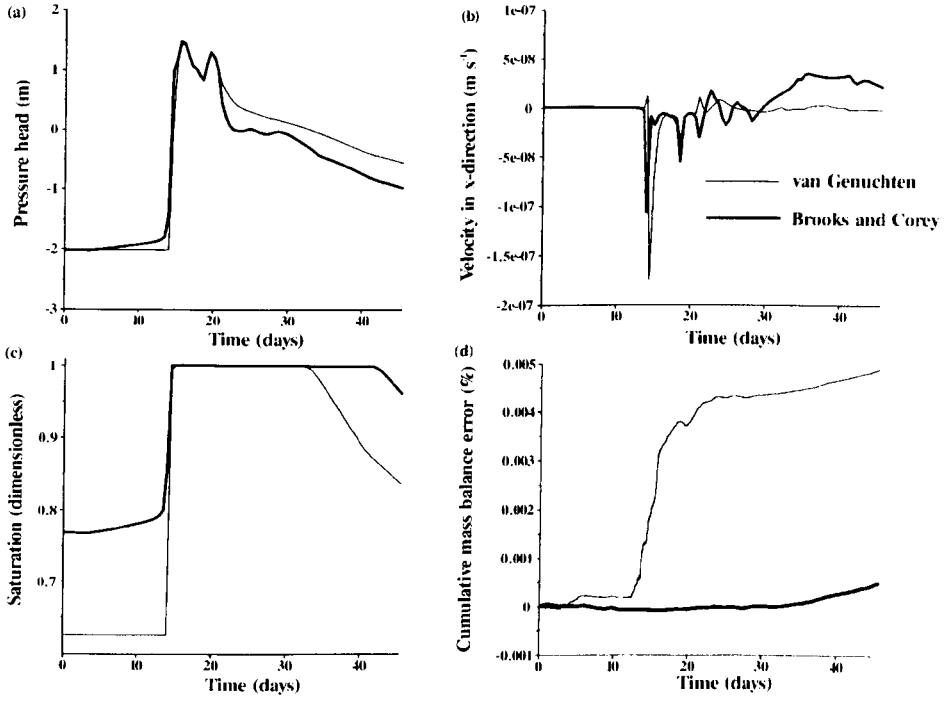

Figure 5.13 Graphs showing the effect of soil water retention model on (a) pressure head, (b) the x-component of Darcian velocity, and (c) saturation, at the point x = 50 m, y = 27 m, and (d) cumulative mass balance error.

As there are no measured soil water retention data for the field sites used in this study, it is impossible to say which soil water model is more appropriate from the perspective of which model is better fitting to field data. Future model runs will therefore use the Brooks and

Corey model on the basis of run time and ease of convergence, while appreciating that the chosen form of the function could potentially impact upon the prediction of model hydrological variables.

In summary, the optimised model has the following attributes: a seepage face boundary condition on the upper boundary, high mesh resolution, medium convergence accuracy, conjugate gradient solver (solver 1), the mixed form of the Richards' equation, and the Brooks and Corey soil water retention function.

5.3.1.3 Sensitivity analysis

The sensitivity of the model performance to various input parameters and boundary specifications will be tested in this section. This will be carried out for the River Severn and Sleepers River models, without reference to observed field data. These model runs will use the model structural parameters as determined during the optimisation procedure. The sensitivity analysis will begin with testing the River Severn model, and the effect of initial conditions, soil hydraulic parameters and boundary conditions on model results.

Initial conditions

> It is extremely rare that detailed knowledge of the distribution of water in a hydrological domain is available at an appropriate time to serve as the start of a model simulation: nor, indeed, is it expected that this information will become routinely available in the near future.
>
> (Wood and Calver, 1992)

Table 5.5 Sensitivity analysis research design for testing the response of the dynamic simulation to the generation of initial conditions in the River Severn model.

Run number	Top boundary flux used for setting initial conditions ($m\ s^{-1}$)*
1	3.17×10^{-6}
2	3.17×10^{-7}
3	3.17×10^{-8}
4	3.17×10^{-9}
5	No flux

* This uses the clay loam soil parameters as given in Run 1 of Table 5.6.

This part of the assessment procedure tested model sensitivity to the generation of initial conditions. The initial conditions for the River Severn ESTEL2D model representation were created using a steady state simulation. For the steady state model run, the value of hydraulic head from the start of the flood event ($t = 0$) from the hillslope piezometer was used to set the specified head for the left-hand boundary, and the value of the river-stage

recorder at $t = 0$ was used to set the specified head for the right-hand boundary (see Figure 5.4 for more details on boundary condition specification). This effectively fixed the level of the water-table at the hillslope and channel boundaries. In addition, for this initial steady state run, some positive flux of water was specified as the upper boundary condition. Although the values of specified head for the hillslope and channel boundaries were based on field-measured values, the choice of the surface flux was somewhat more arbitrary, although it was aimed at reflecting the antecedent conditions relevant to the hydrological event being simulated. The schedule of model runs is listed in Table 5.5. The pressure head and moisture content distributions resulting from these five steady state runs were then used as the initial conditions for a subsequent transient simulation. This part of the sensitivity analysis therefore looked at the response of the dynamic simulation to different values of upper boundary flux used in the steady state run which established the initial conditions.

As the specified upper boundary flux (of the steady state simulation) increased in magnitude, it had an impact on the hydraulic head distribution (Figure 5.14), and associated flow direction and magnitude. At a flux of 3.17×10^{-6} m s^{-1}, a region of high hydraulic head was created in the centre of the domain that available field piezometer data suggested was unrealistic. When these steady state simulation results were subsequently used as the initial conditions for the transient model run, the results indicated that the initial conditions did not impact on model output very far into the transient simulation. However, if the upper boundary flux in the steady state simulation was high, the pressure head and saturation at the start of the transient simulation were initialised as artificially high values (Figure 5.15). These artificially high values persisted for up to 3 days into this 45 day transient simulation. Paniconi and Wood (1993) tested various distributions of initial conditions for a simulation of catchment hydrological processes. In their case, varying the initial conditions did not have as great an effect on the model results as variations in surface saturated hydraulic conductivity.

Further tests have indicated that the value of the upper boundary flux used to generate the initial steady state that is associated with an unrealistic hydraulic head pattern in the initial conditions (see Figure 5.14a) is dependent on the value of saturated hydraulic conductivity; for a lower value of saturated hydraulic conductivity, the unrealistic pattern of hydraulic head (Figure 5.14a) will be produced with a smaller initial specified flux value. This means that for the following sensitivity analysis of soil hydraulic parameters, the initial conditions may have to be slightly different for each value of saturated hydraulic conductivity that is tested. This, however, should not affect the comparison between the simulations, as long as the specified flux is not so large as to generate the 'unrealistic' patterns.

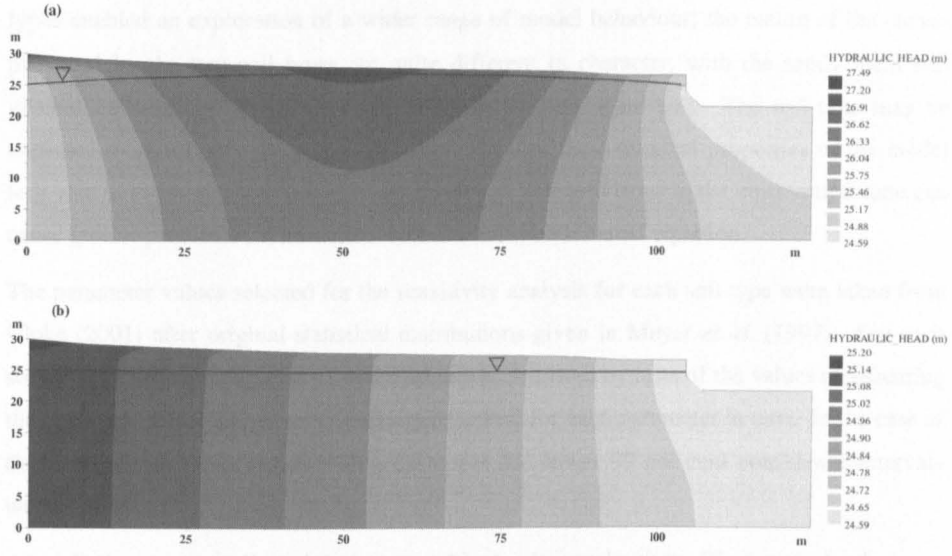

Figure 5.14 Diagrams illustrating the effect of initial upper boundary flux on the generation of hydraulic head distribution and water-table elevation during the steady state run: (a) 3.17 x 10^{-6} m s^{-1} and (b) 3.17 x 10^{-8} m s^{-1}.

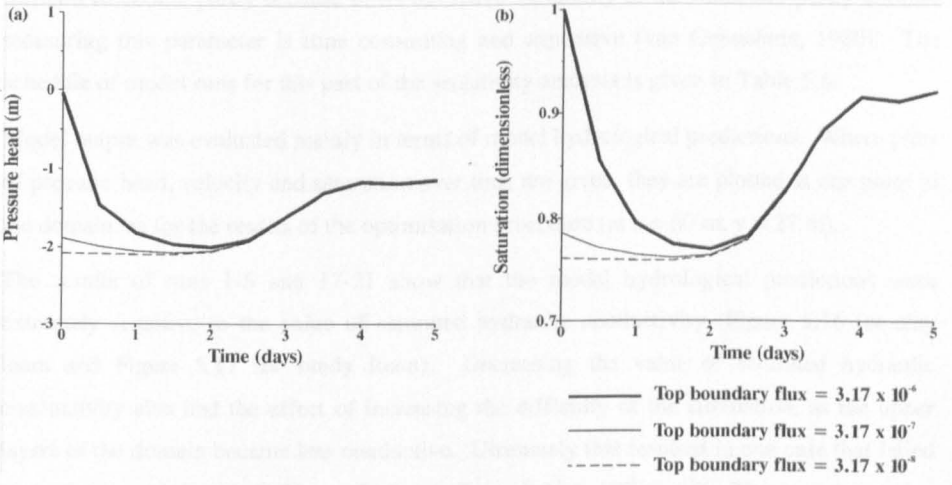

Figure 5.15 Graphs showing the effect of the upper boundary flux used to set up the initial conditions on (a) pressure head and (b) saturation predictions over time at the point x = 50 m, y = 27 m, during the subsequent transient simulation.

Soil hydraulic parameters

The soil hydraulic parameters tested in this section of the sensitivity analysis were saturated hydraulic conductivity (K_{sat}), saturated moisture content (θ_s), residual moisture content (θ_r), and the Brooks and Corey function parameters λ, and air entry value (h_s). Parameter sets describing two different soil types (clay loam and sandy loam) were tested. Both soil types occur in a profile taken in the region of the Severn field site (Brown, 1983). Testing two soil

types enabled an exploration of a wider range of model behaviour; the nature of the curves produced by the two soil types are quite different in character, with the sandy loam soil generally exhibiting much steeper curves than the clay loam soil. The soil type may be expected to affect both the physical results, and also the numerical properties of the model (e.g. rate of convergence), as highly nonlinear soil characteristics in the unsaturated zone can cause greater problems for numerical solutions of the Richards' equation.

The parameter values selected for the sensitivity analysis for each soil type were taken from Cloke (2001) after original statistical distributions given in Meyer *et al.* (1997). For each soil type, the mean parameter values were tested, followed by tests of the values representing the upper and lower 95 per cent confidence interval for each parameter in turn. In the case of the saturated hydraulic conductivity, the upper and lower 99 per cent confidence intervals were also tested.

As preliminary tests indicated that saturated hydraulic conductivity (K_{sat}) might be the most sensitive parameter, this parameter was tested first. Testing this parameter was especially important because reliable estimates of the unsaturated hydraulic conductivity are especially difficult to obtain, partly because of its extensive variability in the field, and partly because measuring this parameter is time consuming and expensive (van Genuchten, 1980). The schedule of model runs for this part of the sensitivity analysis is given in Table 5.6.

Model output was evaluated mainly in terms of model hydrological predictions. Where plots of pressure head, velocity and saturation over time are given, they are plotted at one point in the domain, as for the results of the optimisation procedure (at x = 50 m, y = 27 m).

The results of runs 1-5 and 17-21 show that the model hydrological predictions were extremely sensitive to the value of saturated hydraulic conductivity (Figure 5.16 for clay loam and Figure 5.17 for sandy loam). Decreasing the value of saturated hydraulic conductivity also had the effect of increasing the difficulty of the simulation, as the upper layers of the domain became less conductive. Ultimately this resulted in one case that failed to produce a solution (run 21, sandy loam, K_{sat} = 9.45 x 10^{-8} m s^{-1}). These analyses also indicated a limitation of the mixed form of the equation that had not been noted during the optimisation procedure. Runs 4-5 and 18-21 failed to converge using the mixed form of the equation, but the h-based form of the equation did run in all these cases (except case 21, as mentioned above). For future simulations, the mixed form is used where possible due to its superior mass conservation properties, but where this scheme fails to converge it seems that the h-based form can be used instead to produce a solution.

Table 5.6 Sensitivity analysis research design for soil hydraulic parameter testing for the River Severn model.

Run number	K_{sat} ($m\ s^{-1}$)	θ_s	θ_r	h_s (m)	λ	Specific storage
Clay loam soil						
1*	1.01×10^{-4}	0.41	0.0954	0.880	0.318	0.0001
2	4.39×10^{-6}					
3	9.93×10^{-7}					
4	3.48×10^{-9}					
5	1.51×10^{-10}					
6		0.558				
7		0.262				
8			0.111			
9			0.079			
10				0.208		
11				2.220		
12					0.478	
13					0.158	
14						0.0
15						0.00001
16						0.001
Sandy loam soil						
17*	3.51×10^{-4}	0.41	0.0644	0.177	0.892	0.0001
18	5.13×10^{-5}					
19	1.17×10^{-5}					
20	6.46×10^{-7}					
21	9.45×10^{-8}					
22		0.558				
23		0.262				
24			0.09			
25			0.035			
26				0.062		
27				0.364		
28					1.147	
29					0.637	
30						0.0
31						0.00001
32						0.001

* Runs 1 and 17 may be considered base runs for each soil type. Runs 2-16 and 18-32 will use the parameter values from their respective base runs unless otherwise indicated.

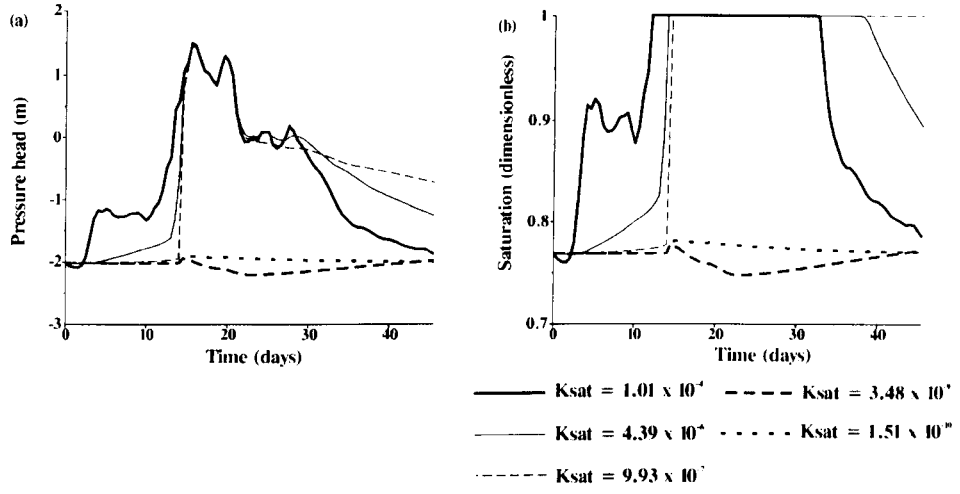

Figure 5.16 Graphs showing the effect of changing the saturated hydraulic conductivity (K_{sat}) of a clay loam soil on predictions of (a) pressure head and (b) saturation, at the point x = 50 m, y = 27 m.

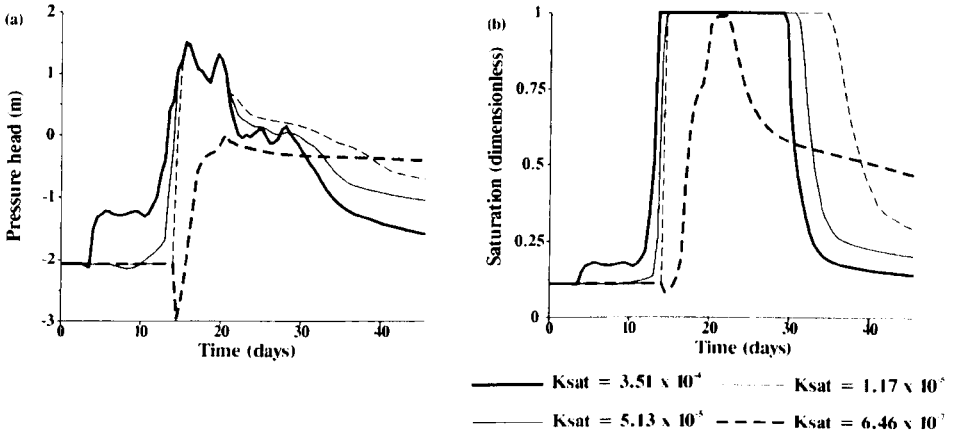

Figure 5.17 Graphs showing the effect of changing the saturated hydraulic conductivity (K_{sat}) of a sandy loam soil on predictions of (a) pressure head and (b) saturation, at the point x = 50 m, y = 27 m.

The differences in the simulated pressure head reflect a changing hydrological response to the overbank flow situation which begins at approximately t = 12 days. This is illustrated in Figure 5.18, which shows what happened during overbank flow (at t = 14 days) for two different saturated hydraulic conductivity values in a clay loam soil. Where the saturated hydraulic conductivity was high (Figure 5.18a), the soil beneath the inundated boundary was quickly saturated, and the water-table moved to the surface. Where the saturated hydraulic conductivity was low (Figure 5.18b), the soil beneath the inundated boundary had a very low conductivity, and did not completely saturate, leading to the formation of a perched water-

table above an unsaturated wedge of soil. This was exacerbated in the case of the sandy loam, where the $k_r(h)$ curve was steeper. The development of this phenomenon also coincided with the time at which some simulations failed to converge, and thus indicates the kind of boundary condition and parameter combination that the numerical model has difficulty in solving.

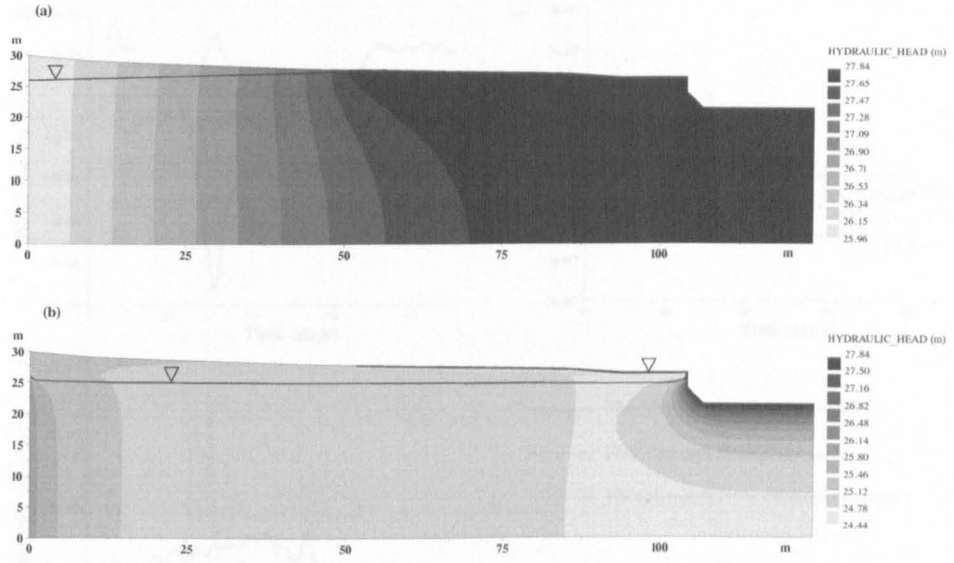

Figure 5.18 Diagram showing the effect of hydraulic conductivity on the development of a perched water-table in a clay loam soil: (a) saturated hydraulic conductivity = 1.01 x 10^{-4} m s^{-1} (no perched water-table), and (b) saturated hydraulic conductivity = 3.48 x 10^{-9} m s^{-1} (perched water-table developed in the floodplain, near the river channel), at time = 14 days.

The patterns of water flux across the boundaries of the model domain were also significantly altered by a change in saturated hydraulic conductivity (K_{sat}). Figure 5.19 shows water flux across the river channel boundary, hillslope boundary, and floodplain surface, for three different values of saturated hydraulic conductivity in a clay loam soil. As this is a two-dimensional (rather than three-dimensional) simulation, the flux calculated by the model is in units of $m^2 s^{-1}$. In presenting the results here, the floodplain transect has been assumed to be of unit width to enable the flux to be presented in units of $m^3 s^{-1}$; the value of the flux does not change, but in this standard format the flux is easier to conceptualise. In addition, the flux is given as a value per unit area of the boundary, hence compensating for the floodplain surface boundary being much longer than the other two boundaries. A positive flux value indicates a flux into the model domain, and a negative flux value indicates a flux out of the model domain.

With a changing value of saturated hydraulic conductivity, the pattern of river bank infiltration remained fairly similar, although the absolute values of flux did change (they were scaled with the K_{sat} value). The pattern of surface infiltration was also similar, with a large peak of infiltration in the middle part of the simulation, corresponding with overbank flow conditions.

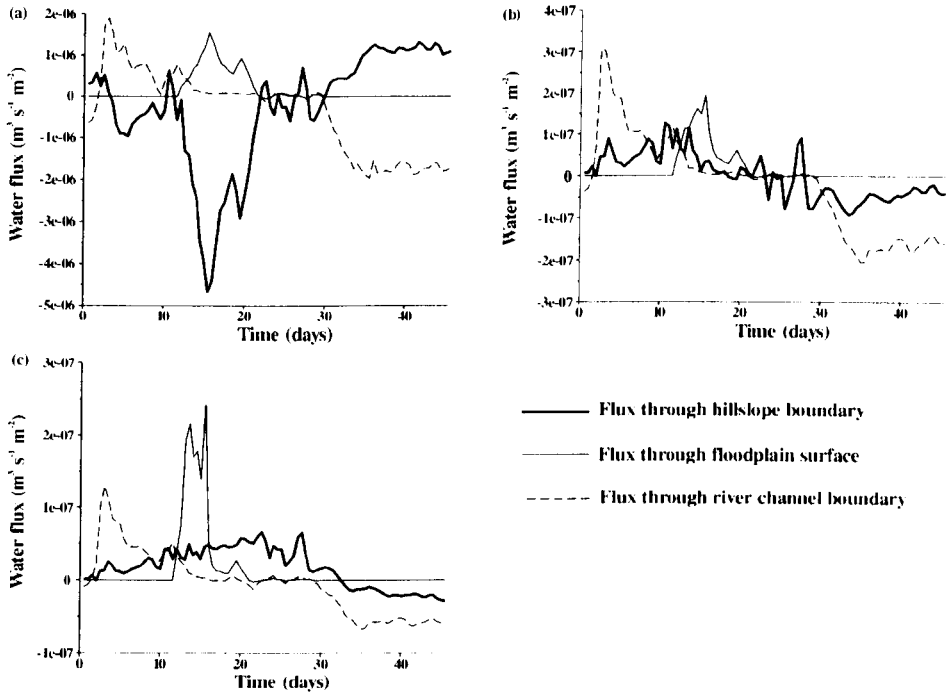

Figure 5.19 Graphs showing the effect of a saturated hydraulic conductivity of (a) 1.01 x 10^{-4} m s^{-1}, (b) 4.39 x 10^{-6} m s^{-1}, and (c) 9.93 x 10^{-7} m s^{-1} of a clay loam soil on predictions of flux through the boundaries of the model domain.

The pattern of flux though the hillslope boundary, however, changed quite significantly as the value of saturated hydraulic conductivity changed, and was not a simple scaling of the fluxes according to the value of K_{sat}. This shows that the change in hydrological behaviour of the system (as highlighted by the earlier perched water-table example) resulting from the change in hydraulic conductivity can also impact upon the magnitude and timing of water fluxes through the floodplain. This would have an associated impact on the timing of chemical transport through the floodplain.

The simulations using the ranges of other soil parameters only resulted in very subtle changes in the simulated water fluxes across the boundaries of the domain, insignificant when compared to the effect of the change in K_{sat}.

The range of values of residual moisture content tested during this sensitivity analysis, for both clay loam and sandy loam, resulted in no noticeable differences in the predicted hydrological variables. Changes in the values of the other soil hydrological parameters: saturated moisture content, and Brooks and Corey parameters λ and air entry value h_s, did have noticeable effects on the simulated hydrological variables. The results of these sensitivity simulations are presented in Figure 5.20 to Figure 5.25. Changing the value of saturated moisture content, for both clay loam and sandy loam soil, made only a very small difference to the predicted pressure head at x = 50 m, y = 27 m (Figure 5.20 and Figure 5.21). However, this change obviously had a big impact on the predicted moisture content over time. This effect was more pronounced for the sandy loam soil for which the soil water retention curves were generally steeper. Thus, a unit change in pressure head resulted in a much greater change in moisture content in the sandy loam soil, as compared with the clay loam soil.

Changing the value of Brooks and Corey parameter λ had a greater effect on the simulated saturation change over time than the pressure head (Figure 5.22 and Figure 5.23). A smaller value of λ resulted in a shallower $\theta(h)$ curve, with the result that the domain remained at a higher level of saturation for a given pressure head. As in the case of the saturated moisture content, this effect was more noticeable in the sandy loam soil due to the steeper profile of the $\theta(h)$ curve.

Changing the air entry value (h_s) had the greatest effect on hydrological predictions after saturated hydraulic conductivity. As with the other soil hydrological parameters, the effect on saturation change over time was marked, particularly for the sandy loam soil (Figure 5.24 and Figure 5.25). A larger value of h_s resulted in a shallower $\theta(h)$ curve, with the domain remaining at a higher level of saturation for a given pressure head. However, the changes in air entry value also resulted in a significant change in the $k_r(h)$ curve (Figure 5.24c and Figure 5.25c). This produced a noticeable effect on the simulated pressure head over time. In this case, the change in h_s acted like the change in saturated hydraulic conductivity. As illustrated earlier, this reduced the conductivity of the soil near the floodplain surface and therefore restricted the amount of water that could infiltrate through this boundary. Once again, this effect was more marked for the sandy loam soil, where quite a small change in the value of h_s (0.062 m to 0.364 m) created a large difference in the simulated pressure head over the course of the simulation.

The final soil hydrological parameter to be investigated was specific storage. As specific storage is incorporated as an extra parameter in the soil water retention curve, it was expected to have an effect on the prediction of saturation. This is indicated in Figure 5.26, although the effect is relatively small until the value of specific storage reaches 0.001 m^{-1}.

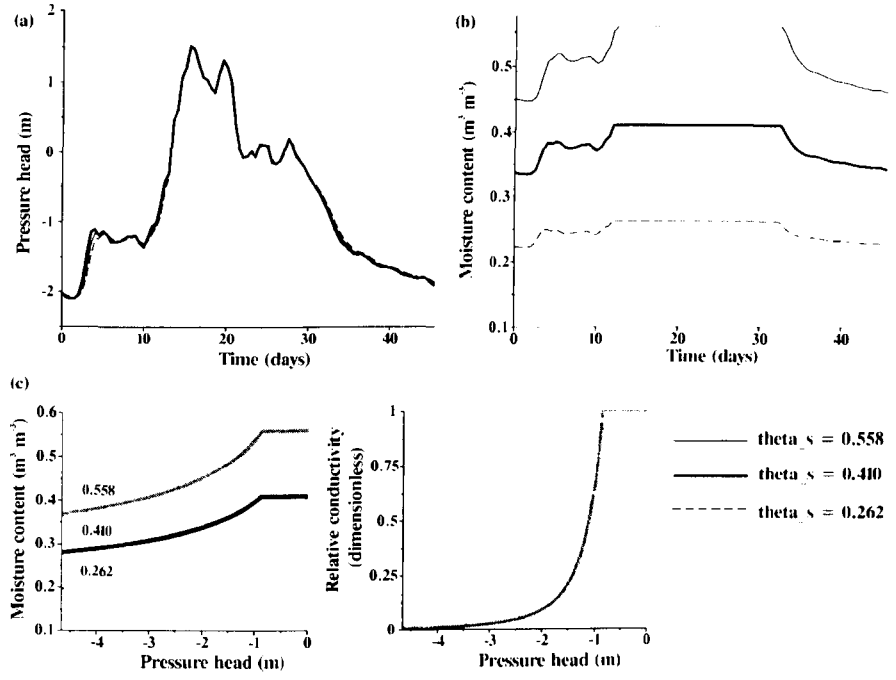

Figure 5.20 Graphs showing the effect of changing the saturated moisture content (theta_s) of a clay loam soil on predictions of (a) pressure head and (b) moisture content, at the point x = 50 m, y = 27 m. The effect on the soil water functions is shown in (c).

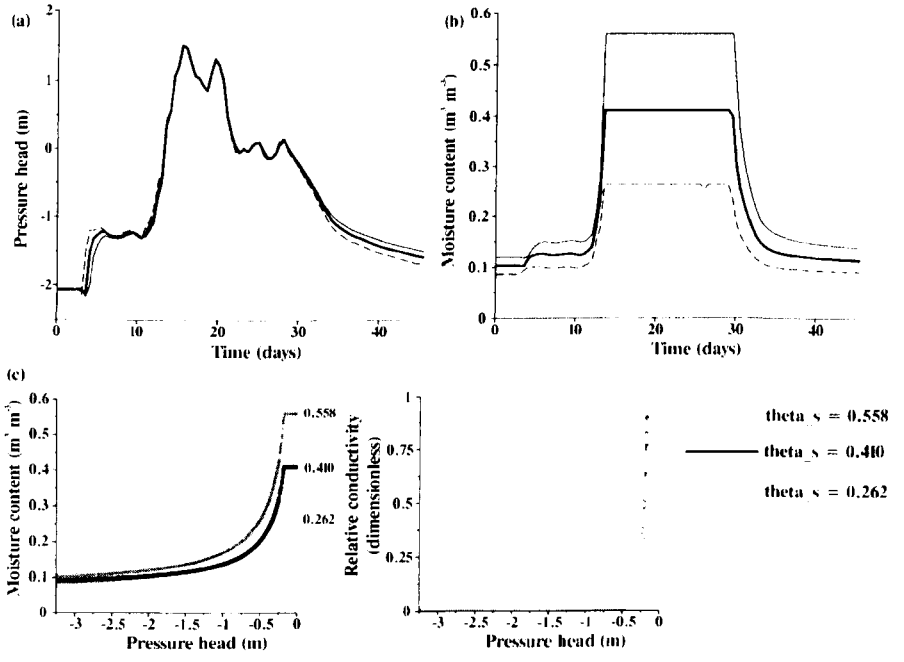

Figure 5.21 Graphs showing the effect of changing the saturated moisture content (theta_s) of a sandy loam soil on predictions of (a) pressure head and (b) moisture content, at the point x = 50 m, y = 27 m. The effect on the soil water functions is shown in (c).

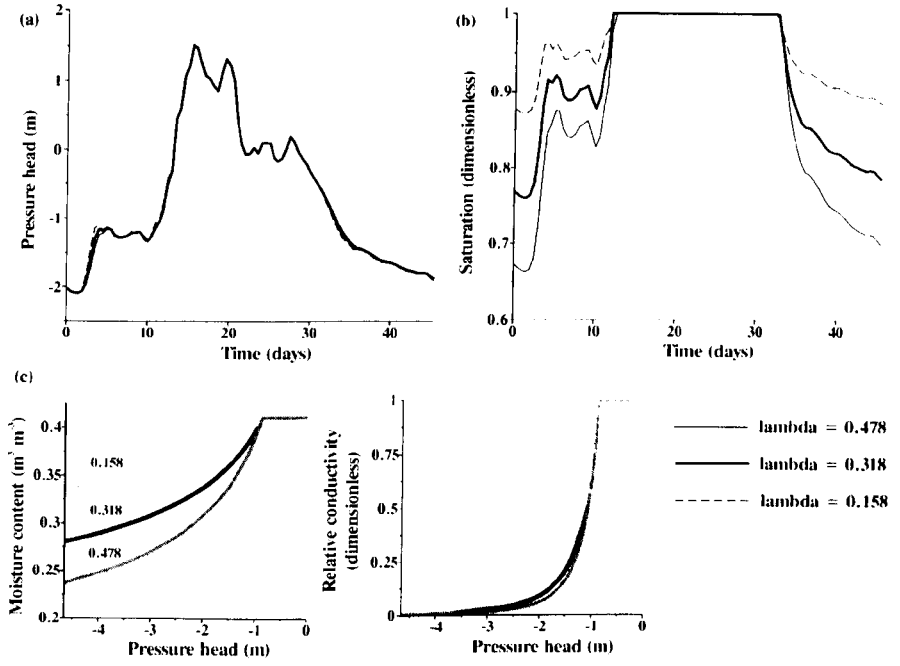

Figure 5.22 Graphs showing the effect of changing the value of lambda of a clay loam soil on predictions of (a) pressure head and (b) saturation, at the point x = 50 m, y = 27 m. The effect on the soil water functions is shown in (c).

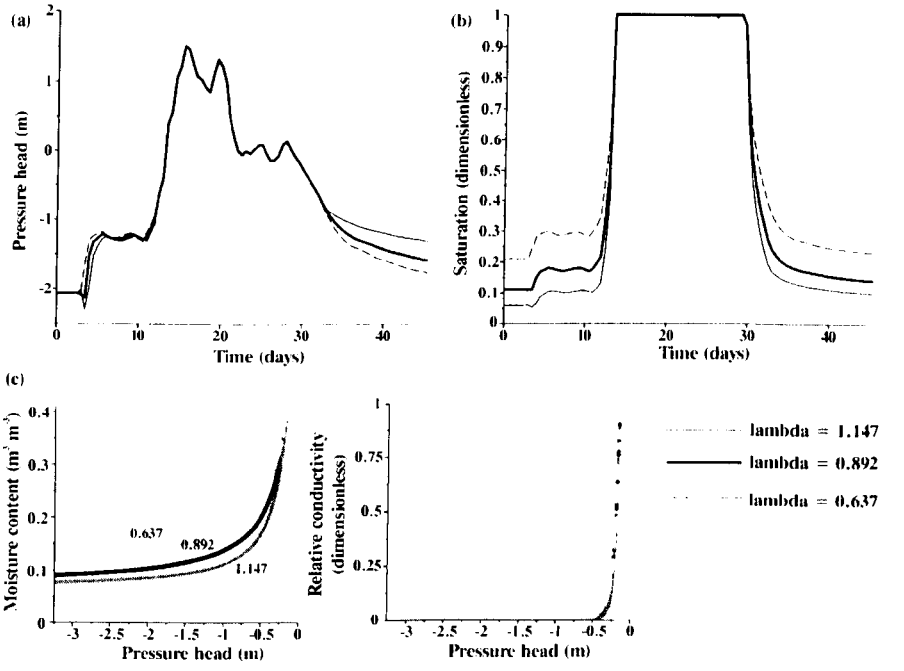

Figure 5.23 Graphs showing the effect of changing the value of lambda of a sandy loam soil on predictions of (a) pressure head and (b) saturation, at the point x = 50 m, y = 27 m. The effect on the soil water functions is shown in (c).

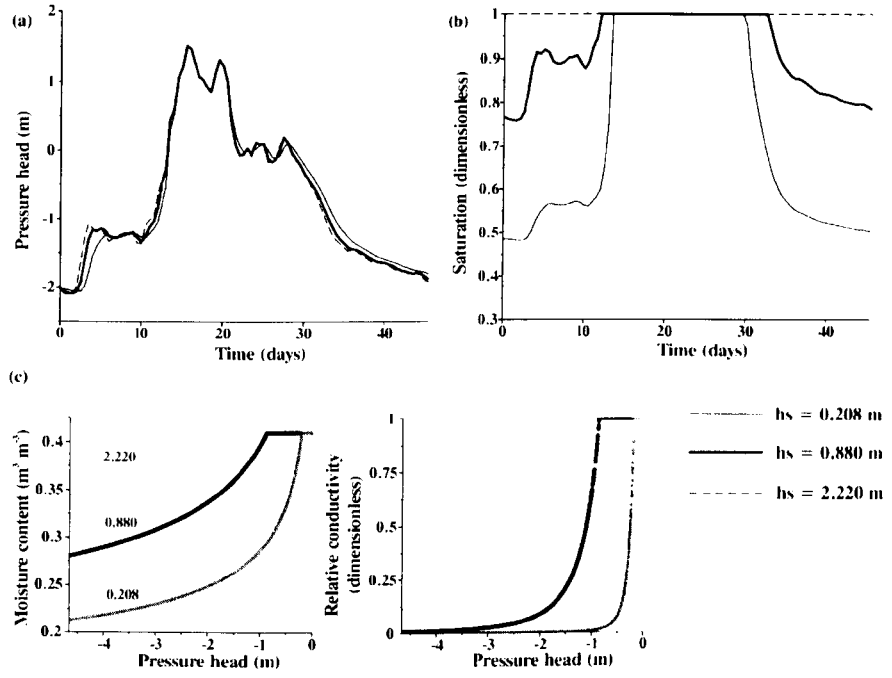

Figure 5.24 Graphs showing the effect of changing the air entry value (h_s) of a clay loam soil on predictions of (a) pressure head and (b) saturation, at the point x = 50 m, y = 27 m. The effect on the soil water functions is shown in (c).

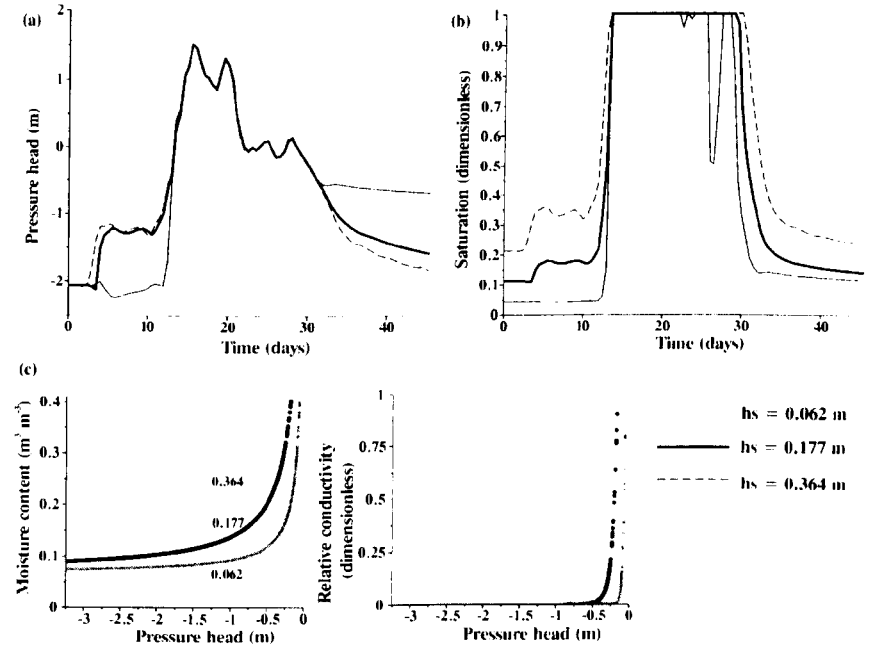

Figure 5.25 Graphs showing the effect of changing the air entry value (h_s) of a sandy loam soil on predictions of (a) pressure head and (b) saturation, at the point x = 50 m, y = 27 m. The effect on the soil water functions is shown in (c).

Part of the idea of introducing a storage parameter to the ESTEL2D model was to maintain the transient behaviour of a simulation under saturated conditions. The indicator of a transient simulation is a change in mass over time. As can be seen from Figure 5.26a, the total mass in the domain was always changing over time, even when the value of specific storage was zero. This indicated that for this simulation of the River Severn floodplain, at no point was the domain completely saturated. There was always a small area of unsaturated soil in the model domain that was enough to keep the simulation transient.

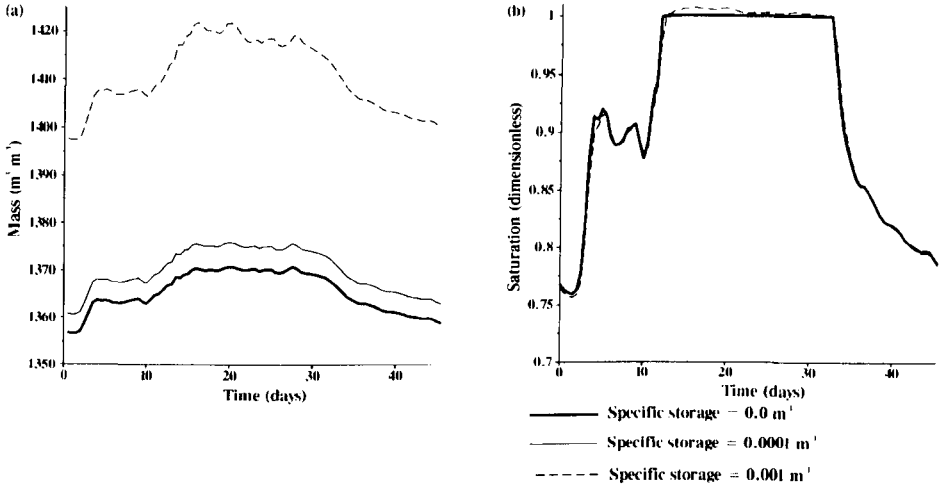

Figure 5.26 Graphs to show the effect of changing the value of specific storage on (a) total mass in the domain and (b) saturation prediction at the point x = 50 m, y = 27 m.

As this was found to be the case, some further model simulations were performed with the aim of assessing the effect of the storage parameter under fully saturated conditions. In order to explore this, the River Severn simulation was re-run for flood event D, but with the value of specified hydraulic head on the hillslope and channel boundaries raised by 5 m. The results clearly showed that in a completely saturated domain, with no specific storage, no change in mass over the course of the simulation was possible (Figure 5.27a). This resulted in the model running, incorrectly, as a series of steady states, rather than as a full transient simulation. Where the specific storage term was introduced, a change in mass became possible. Figure 5.27b also illustrates how the introduction of the storage parameter resulted in a saturation value of over 100 per cent. This small fraction is insignificant when compared with the change in saturation that is possible through desaturation of the soil voids (as described by the soil water retention curve) and only becomes noticeable under highly saturated conditions.

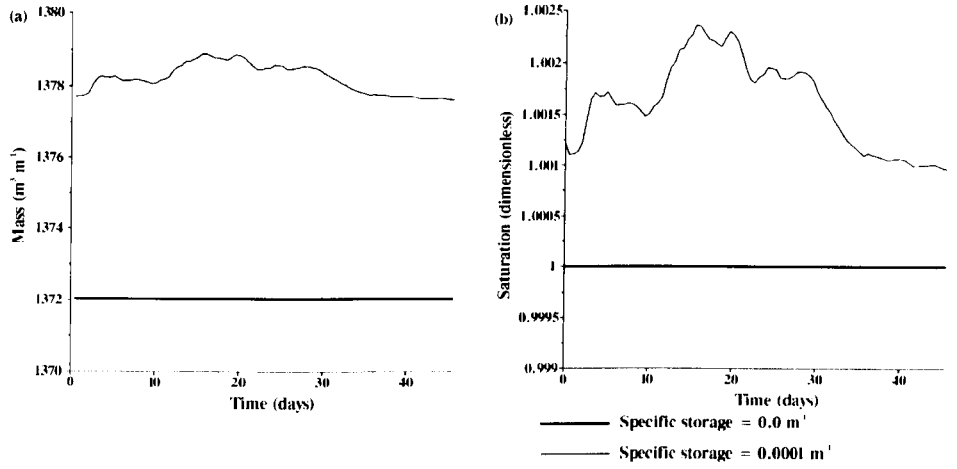

Figure 5.27 Graphs to show the effect of changing specific storage, in a completely saturated domain, on (a) total mass in the domain and (b) saturation at the point x = 50 m, y = 27 m.

Boundary conditions

Following from the investigation into the sensitivity of model performance to changes in the values of soil hydrological parameters, the effect of the choice of boundary condition specification was explored. Errors in boundary condition specification can arise from two main sources: (i) measurement error in the field data used as boundary conditions, and (ii) conceptual errors in how the boundaries are physically characterised. In the hydrological modelling literature, point (i) is sometimes considered, but the effect of point (ii) is not generally investigated. This reflects the fact that field data are often lacking, and that even if the data are available, there are still different ways of specifying the boundary.

> In principle the model can handle any type of boundary condition, but there is often a lack of knowledge and data concerning flow processes across nonsurface boundaries.
>
> (Paniconi and Wood, 1993)

The lower boundary condition of the River Severn domain was specified as no flux. To reduce the influence of this boundary, the mesh was deliberately made 30 m deep, even though the region of interest (and the region where field data were available) was restricted to the upper 5-10 m of the domain. The upper boundary was specified as a seepage face boundary condition, with the specified flux equal to the precipitation rate, where appropriate. The main uncertainty in boundary condition specification therefore occurred when considering the hillslope and channel boundaries.

Several different combinations of specified head and specified flux boundary condition were considered for these boundaries, but ultimately, a specification of a hydrostatic boundary

condition below the water-table, and a no flux boundary condition above the water-table, was found to be the most suitable. Figure 5.28 shows the effect of changing the boundary condition specification at the hillslope boundary. The pressure head pattern illustrated in Figure 5.28a was created using a specified head boundary condition along the whole boundary. This created an unrealistic pattern of pressure head in the upper corner of the domain. The more realistic pressure head pattern in Figure 5.28b was created using a specified head boundary condition below the water-table and no flux above the water-table.

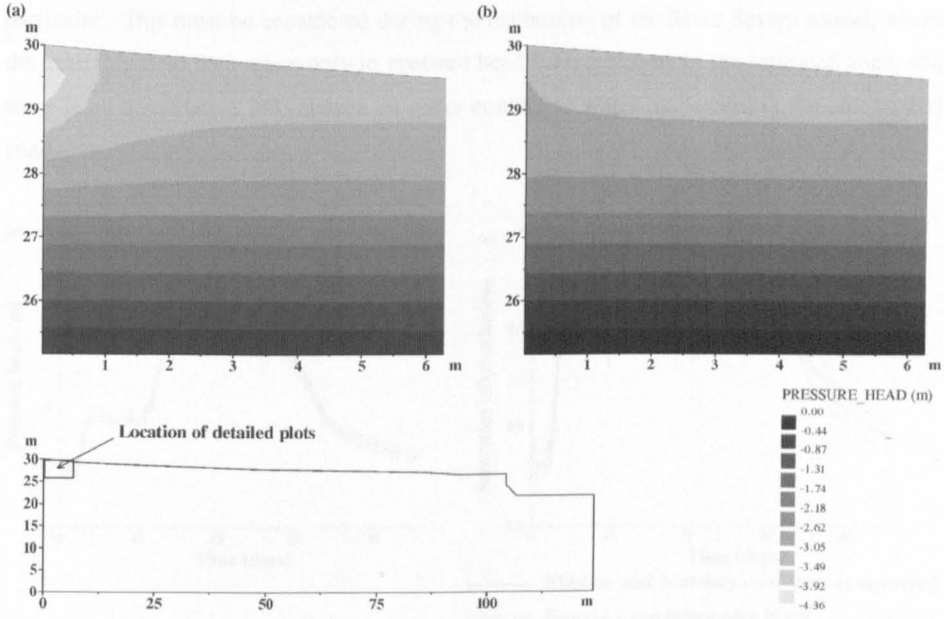

Figure 5.28 Diagrams to show the effect of boundary condition specification on pressure head pattern at the hillslope boundary (sandy loam soil): (a) specified head, hydrostatic boundary condition; (b) no flux boundary specification above the water-table.

This stage of the sensitivity analysis also considered the effect of errors in the value of hydraulic head used in the hillslope and channel boundary condition specification. The maximum error that could be incorporated in the measured value of hydraulic head from the field data was felt to be of the order of ±10 cm. Figure 5.29 shows the effect on the simulated values of pressure head and saturation of changing the boundary input data by ±10 cm. These graphs indicate that the error introduced by uncertainty in the boundary data was probably less than the change in predictions that could be introduced by changing the value of the soil hydrological parameters, in particular saturated hydraulic conductivity. However, the range of possible realistic hydraulic conductivity values for use in representing the River Severn domain can be constrained by the internal piezometer data during the calibration process.

The sensitivity analysis has demonstrated the response of the model to changes in initial conditions, soil hydrological parameters, and boundary conditions. Interestingly, it has demonstrated that certain parameters can have a significant effect on predictions of such variables as saturation extent and change in saturation over time, while at the same time having only negligible effects on the predictions of hydraulic head, and water-table elevation. The wider implication of this is that a modeller can maintain a prediction of hydraulic head that matches well with field data, but with an unrealistic representation of other hydrological conditions within the domain, and within the unsaturated zone in particular. This must be considered during the calibration of the River Severn model, where the available field data relate only to pressure head measurements in the saturated zone, and there is no quantitative information on water content or water movement in the unsaturated zone.

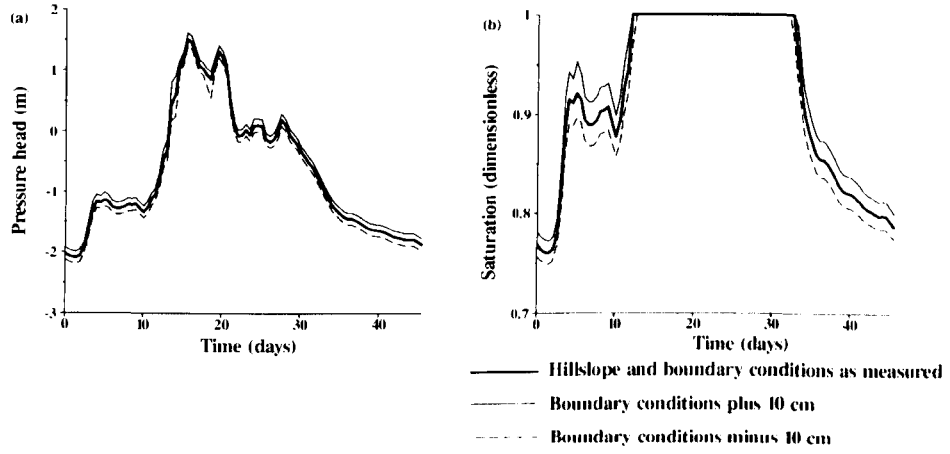

Figure 5.29 Graph to show the effect of uncertainty in the hillslope and channel boundary condition input data on predictions of (a) pressure head and (b) saturation, at the point x = 50 m, y = 27 m.

The sensitivity analysis of the River Severn model has also revealed some circumstances under which the numerical scheme does not converge to a solution. Maintaining numerical accuracy when modelling transient flow in unsaturated, heterogeneous porous media has been recognised as a difficult problem (Mitchell and Mayer, 1998). Characteristics which can lead to slow convergence of the Picard scheme include (a) complex or time varying boundary conditions, (b) steep soil characteristic equations, producing a sharp moisture front with a large drop in conductivity and saturation across the front, (c) an initially dry soil near the surface, and (d) saturated-unsaturated interfaces (Paniconi and Putti, 1994). These can produce ill-conditioned system matrices and adversely affect the convergence behaviour of linear and nonlinear iterative solvers (Paniconi and Wood, 1993). Paniconi and Putti (1994)

found that some of these problems could be alleviated to an extent by using lumped rather than distributed matrices. For a test case involving infiltration into an unsaturated soil slab, mass lumping was able to reduce oscillations at the sharp moisture front, thus resulting in good convergence for the Picard scheme. They also found some improvement with the use of alternative schemes, for example the Newton scheme. However, these types of developments are beyond the scope of this study.

The combination of boundary conditions and soil hydrological properties tested during this sensitivity analysis have provided quite a rigorous test of the model capabilities, covering many of the characteristics which cause difficulties for the numerical scheme. This being the case, it is not surprising that some of the parameter combinations tested led to long run times, or in some cases, non-convergence. The steady state simulations used to set up the initial conditions seem to be especially sensitive to some of these problems. When using the van Genuchten soil water retention function during the optimisation procedure (Table 5.2 and Table 5.3), the model failed to converge in steady state, but the dynamic simulation did run (although it took a very long time to converge). Other modellers have experienced this problem. Romano *et al.* (1999), using a finite element hydrological model (SWMS-2D) and van Genuchten soil water retention function, found that the steady state option failed to converge for any of the test cases they investigated.

Sleepers River

The sensitivity analysis for the Sleepers River model was designed on the basis of the results of the River Severn model sensitivity analysis. This model has four soil types as opposed to the uniform soil used for the River Severn model. Testing every parameter of the soil water retention model for each soil type was felt to be unnecessary, considering the evidence from the Severn sensitivity analysis which indicated that the model output is most sensitive to saturated hydraulic conductivity (K_{sat}). Paniconi and Wood (1993) simulated a small catchment with spatially variable soils, but they only considered spatial variability in saturated hydraulic conductivity, keeping the other parameters of the soil model constant over the catchment. The sensitivity analysis for the Sleepers River model is therefore concerned with the effect of varying K_{sat}, with some additional tests on the effect of changing the boundary condition specification.

The Sleepers River model domain was constructed to lie between piezometer nests 8 and 11 (Figure 5.30). The data at nest 18 (Figure 5.3) were not felt to be reliable enough to form the right hand side boundary. Only the bottom piezometer in this nest was usually below the water-table, and a value of piezometric head was rarely recorded for the upper piezometer. This restricted the hydrological characterisation at this point, making it a less well-defined

position for the model boundary than piezometer nest 11. Figure 5.30b shows the distribution of soil types within the model domain, each of which is associated with a different value of saturated hydraulic conductivity.

The research design for the Sleepers River model sensitivity analysis is given in Table 5.7. Three main aspects of the model parameterisation were tested: the effect of changing the upper boundary specificatin (incorporating a seepage face), the effect of changing the lower boundary specification, and the effect of changing the value of saturated hydraulic conductivity throughout the model domain. The lower boundary was particularly interesting in the Sleepers River case. Unlike the River Severn case, the physical depth to bedrock was well characterised. However, the hydrological conditions and flow pathways at the lower boundary were not well known. The specification of this boundary therefore formed part of the sensitivity investigation.

Table 5.7 Sensitivity analysis research design for Sleepers River model

Run number	**Upper boundary condition**	**Lower boundary condition**	**Saturated hydraulic conductivity m s^{-1}**	
1*	Seepage	No flux	*Average values:*	
			Gravelly till	5.8×10^{-5}
			Dense till layer	2.9×10^{-6}
			Upland mineral soil	1.725×10^{-4}
			Riparian peat	5.65×10^{-5}
2	No seepage			
3	Seepage	Specified flux $= 1 \times 10^{-8}$ m s^{-1}		
4		Specified flux $= 1 \times 10^{-6}$ m s^{-1}		
5		No flux	Gravelly till	7.4×10^{-5} (max)
6			Gravelly till	4.2×10^{-5} (min)
7			Dense till layer	3.3×10^{-6} (max)
8			Dense till layer	2.5×10^{-6} (min)
9			Upland mineral	2.5×10^{-4} (max)
10			Upland mineral	9.5×10^{-5} (min)
11			Riparian peat	7.4×10^{-5} (max)
12			Riparian peat	3.9×10^{-5} (min)
13				All soils at maximum
14				All soils at minimum

* All runs use the parameters from the base run (1) unless otherwise specified.

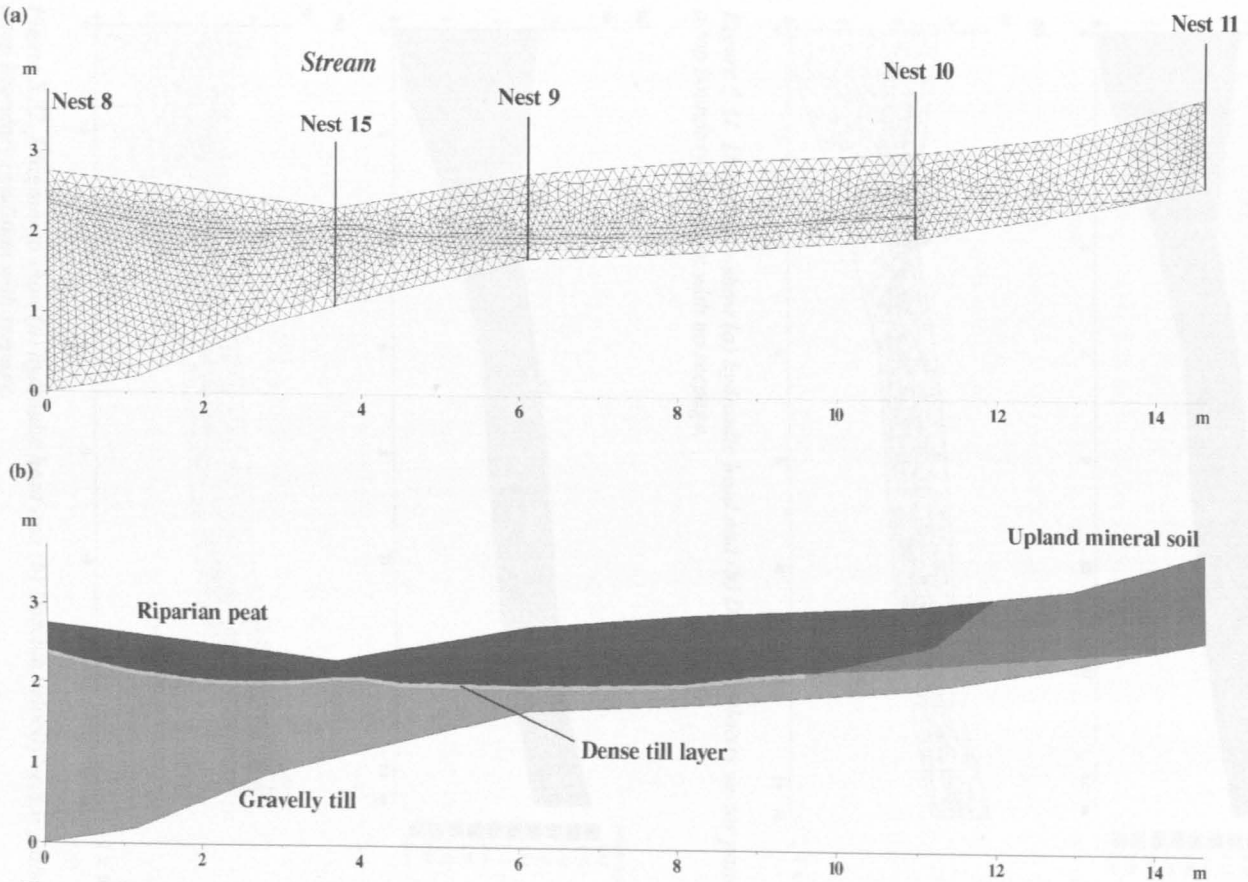

Figure 5.30 Diagram to show (a) Sleepers River finite element mesh, with positions of piezometer nests indicated, and (b) soil distribution.

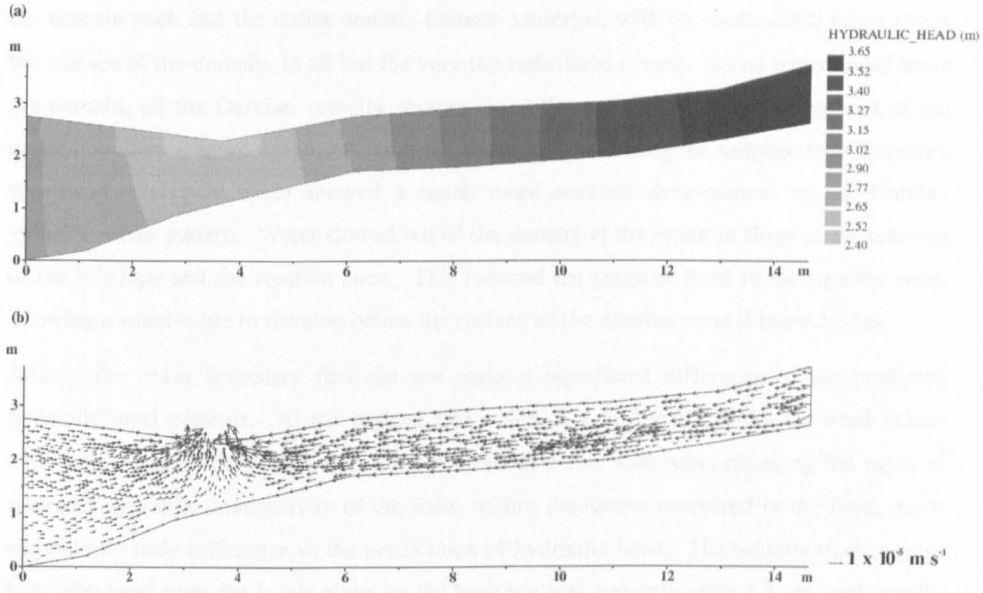

Figure 5.31 Diagram to show (a) hydraulic head and (b) Darcian velocity vector pattern for a top boundary condition with no seepage.

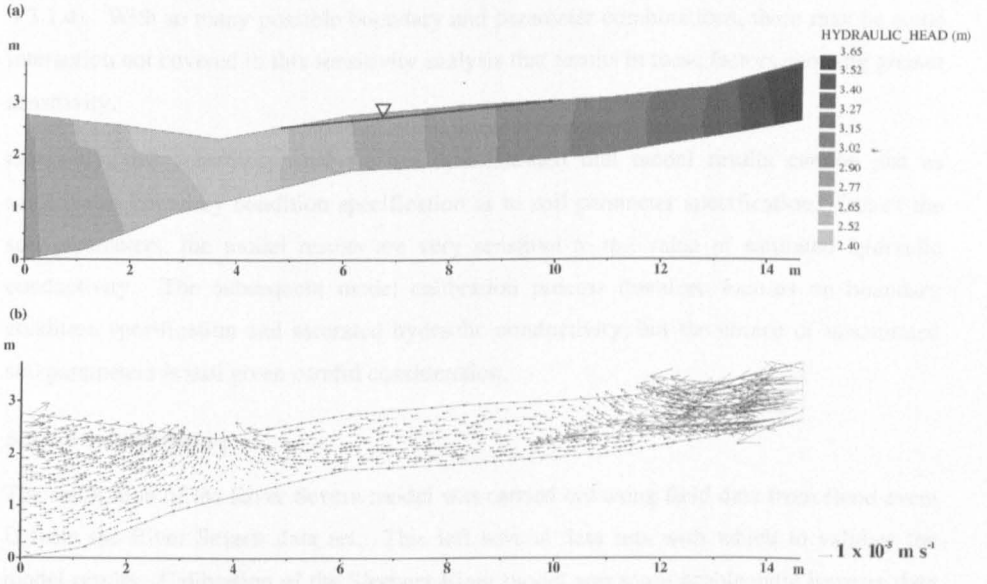

Figure 5.32 Diagram to show (a) hydraulic head and (b) Darcian velocity vector pattern for a top boundary condition with seepage.

As in the River Severn model case, the Sleepers River model was found to be very sensitive to the upper boundary condition specification. Without the seepage face specification, no water was able to leave the domain except at the stream channel, where the boundary condition was defined as specified head (Figure 5.31). This raised the pressure head inside

the domain such that the entire domain became saturated, with the water-table lying above the surface of the domain, in all but the very top right-hand corner. As no water could leave the domain, all the Darcian velocity vectors along the surface followed the contour of the upper boundary (Figure 5.31b). In contrast, the simulation using the seepage face boundary specification (Figure 5.32) showed a much more realistic development of the Darcian velocity vector pattern. Water flowed out of the domain at the break in slope at the junction of the hillslope and the riparian zone. This reduced the pressure head in the riparian zone, allowing a water-table to develop below the surface of the riparian zone (Figure 5.32a).

Adding the lower boundary flux did not make a significant difference to the predicted hydraulic head patterns. At the highest flux value, 1×10^{-6} m s^{-1}, hydraulic head values within the domain changed by a maximum of about 5 cm. Likewise, changing the value of saturated hydraulic conductivity of the soils, within the ranges measured in the field, made surprisingly little difference to the predictions of hydraulic head. The maximum change in hydraulic head from the levels given by the base run was approximately 1.5 cm, and usually the difference was much smaller than this. Interestingly, this still does not discount these factors as being important to the final calibration of the Sleepers River model (see Section 5.3.1.4). With so many possible boundary and parameter combinations, there may be some interaction not covered in this sensitivity analysis that results in these factors showing greater sensitivity.

Generally, this sensitivity analysis has demonstrated that model results can be just as sensitive to boundary condition specification as to soil parameter specification. Out of the soil parameters, the model results are very sensitive to the value of saturated hydraulic conductivity. The subsequent model calibration process therefore focuses on boundary condition specification and saturated hydraulic conductivity, but the choice of unsaturated soil parameters is still given careful consideration.

5.3.1.4 Calibration

The calibration of the River Severn model was carried out using field data from flood event D from the River Severn data set. This left several data sets with which to validate the model results. Calibration of the Sleepers River model was more problematic because data were only available for one event. In an attempt to take account of the need for some validation, the calibration exercise used only half of the available snowmelt event data. The validation then used data from the whole snowmelt event.

Having decided on the most appropriate boundary condition specification during the optimisation and sensitivity analysis procedures, the calibration of the River Severn model focused on the saturated hydraulic conductivity. The simulated hydraulic head was

compared to the observed hydraulic head for the three piezometers on transect S, internal to the model domain; S2, S3 and S4, for a range of saturated hydraulic conductivity values (see Figure 5.2 for location of piezometers in the field, and Figure 5.33 for location of piezometers within the domain). The rest of the soil parameters were specified with values for an average clay loam soil.

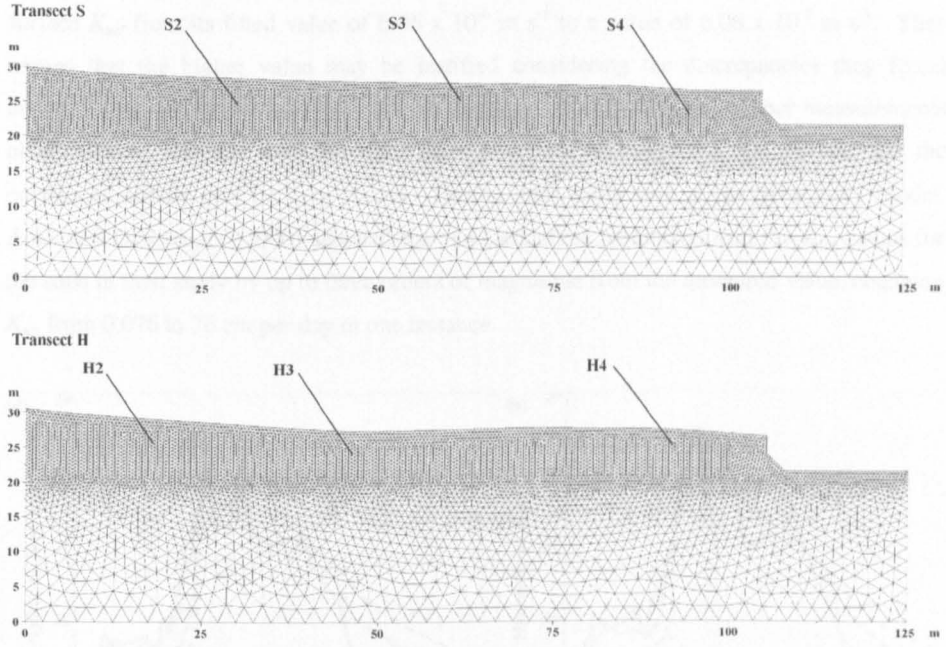

Figure 5.33 Meshes of the two River Severn transects, indicating the location of the piezometers within the domain.

The measured (averaged) values of saturated hydraulic conductivity at the field site ranged from 1.56 x 10^{-6} for the upper soil layer to 2.54 x 10^{-6} m s^{-1} for the lower soil layer. The closest value to this tested during calibration, 5 x 10^{-6} m s^{-1}, produced a fairly unsatisfactory fit to the observed piezometer values, with a smoothed response and a hydraulic head value which was generally too low in the early part of the simulation, and too high at the end (Figure 5.34). This was probably because the hydraulic conductivity of the floodplain soil near the start of the simulation was too low to allow enough infiltration to raise the hydraulic head inside the domain. At the end of the simulation, the conductivity was too low to allow enough water to leave the domain, so the hydraulic head inside the domain remained too high. The value of saturated hydraulic conductivity selected was 5 x 10^{-5} m s^{-1}. This is an order of magnitude greater than the value obtained from field measurements. However, the reliability of these measurements, and how well they represent the floodplain soil, may be questionable, as highlighted in Section 5.2.4. In situ field measurements of saturated

hydraulic conductivity may often be an order of magnitude lower than the average hydraulic conductivity of the formation being measured (Bonell, 1998). Under these circumstances, changing the hydraulic conductivity to better represent the hydrological processes within numerical simulations is a commonly used technique in the hydrological modelling community. For example, Paniconi and Wood (1993) found that to reduce the amount of catchment runoff in their catchment hydrological simulation it was necessary to increase surface K_{sat} from its fitted value of 6.06 x 10^{-6} m s^{-1} to a value of 6.06 x 10^{-5} m s^{-1}. They argued that the higher value may be justified considering the discrepancies they found between near-surface remotely sensed soil moisture observations and deeper measurements obtained from soil core analyses, since these discrepancies suggested that the soil near the catchment surface may be very porous. During their calibration of the SIMULAT model, Aden and Diekkruger (2000) adjusted the van Genuchten parameters and the K_{sat} values for the soils in their study by up to three orders of magnitude from the measured value, changing K_{sat} from 0.076 to 76 cm per day in one instance.

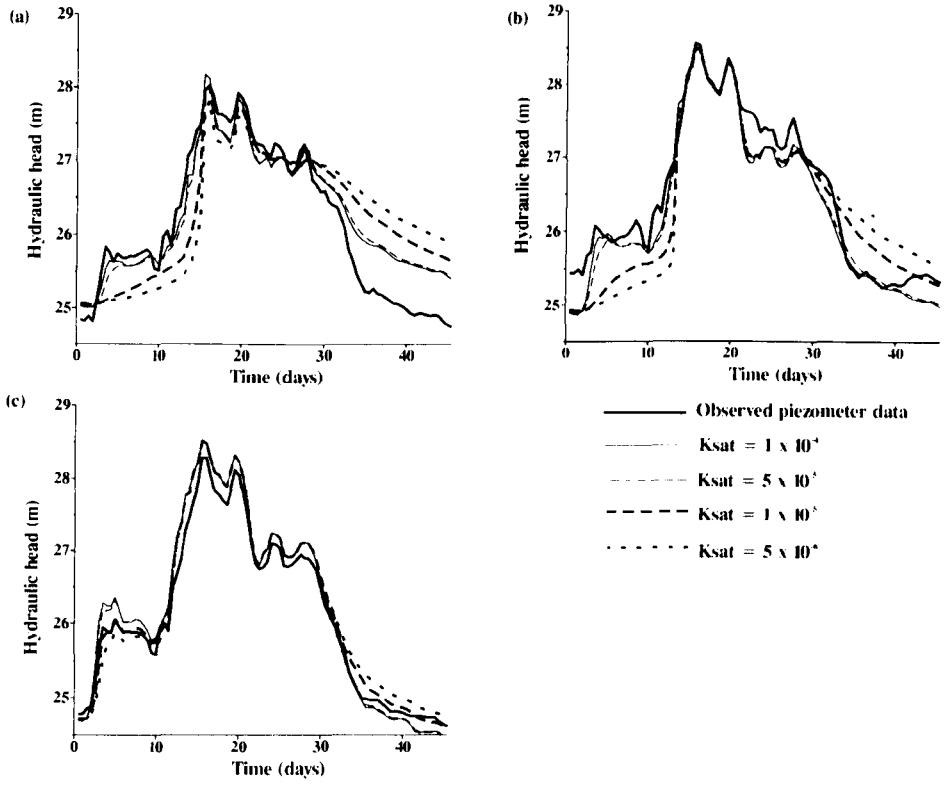

Figure 5.34 Graphs comparing observed piezometer data with simulated results using four different saturated hydraulic conductivity (K_{sat}) values: (a) piezometer S2, (b) piezometer S3, and (c) piezometer S4.

In addition, isotropic soil properties are assumed for the calibrated River Seven model. This assumption is based on field observations of the floodplain material characteristics. The alluvial soil at the field site shows very little vertical stratification beyond the upper 30 cm of organically enriched material. This is a consequence of active channel meandering for this reach of the river leading to periodic reworking of the floodplain sediments.

The calibrated River Severn model assumes fairly wet antecedent conditions, with an initial upper boundary flux of 6.17×10^{-8} m s^{-1}, (which when extrapolated would be equivalent to an average annual rainfall of approximately 1950 mm). As there are no field data to verify the pressure head or saturation extent in the unsaturated zone, these initial conditions could be considered somewhat arbitrary. However, they are felt to be appropriate for this simulation, as this flood event occurred in the winter, after an extended wet period. In addition, the sensitivity analysis has demonstrated that the effect of these initial conditions should not extend far into the main simulation.

Unfortunately, the results from the unsaturated zone could not be validated, but a model representation of this zone that was at least 'realistic' was still sought. This is sympathetic to the notion that sometimes a 'less rigorous' approach to model assessment (Lane and Richards, 2001) may be necessary, or indeed, the only way to proceed. Earlier in this study, it has been demonstrated that a good characterisation of the water-table position and hydraulic head is possible, but this is not sufficient, particularly where the results are to be used for further analysis (i.e. chemical transport analysis). An adequate representation of the Darcian velocity vector field, and moisture content throughout the domain, are vital considerations, even if they cannot be formally validated.

The final calibrated parameters for the River Severn model are given in Table 5.8.

Table 5.8 Final parameter selection for the River Severn model

Soil hydraulic parameter	**Value**
Residual moisture content θ_r	0.0954
Saturated moisture content θ_s	0.41
Brooks and Corey bubbling pressure parameter (h_s) [m]	0.880
Brooks and Corey pore distribution parameter (λ)	0.318
Saturated hydraulic conductivity [m s^{-1}]	5×10^{-5}
Specific storage [m^{-1}]	0.0001

The starting point for the calibration of the Sleepers River model was the base run from the sensitivity analysis (Table 5.7). This used a seepage face boundary condition on the upper boundary, a specified head boundary condition on the left- and right-hand side boundaries,

and a no flux boundary condition along the lower boundary, with average saturated hydraulic conductivity values for each soil type as measured in the field. The results from this model run are illustrated in Figure 5.35, which shows the comparison between the observed and predicted hydraulic head for all five piezometer nests. This diagram shows that the hydraulic head behaviour in piezometer nests 9 and 10 in particular is poorly represented by the model. In addition, the use of a specified head boundary condition fails to capture the dynamic upward or downward water movement at the left- and right-hand side boundaries (nests 8 and 11, Figure 5.35), suggesting that an alternative boundary condition specification may be more appropriate.

The calibration of the Sleepers River model was somewhat more complex than the calibration of the River Severn model, involving consideration of saturated hydraulic conductivity values for all four soil types in the model domain, the flux along the lower model boundary, and the effect of the side boundary specification. To simplify presentation of the results, the final calibrated model will be presented first, followed by the consequences of modifying different aspects of this model configuration. The calibrated boundary conditions used in the Sleepers River snowmelt event simulation are illustrated in Figure 5.36. Figure 5.37 shows the model results using the final boundary conditions and calibrated soil hydraulic conductivity values as given in Table 5.9.

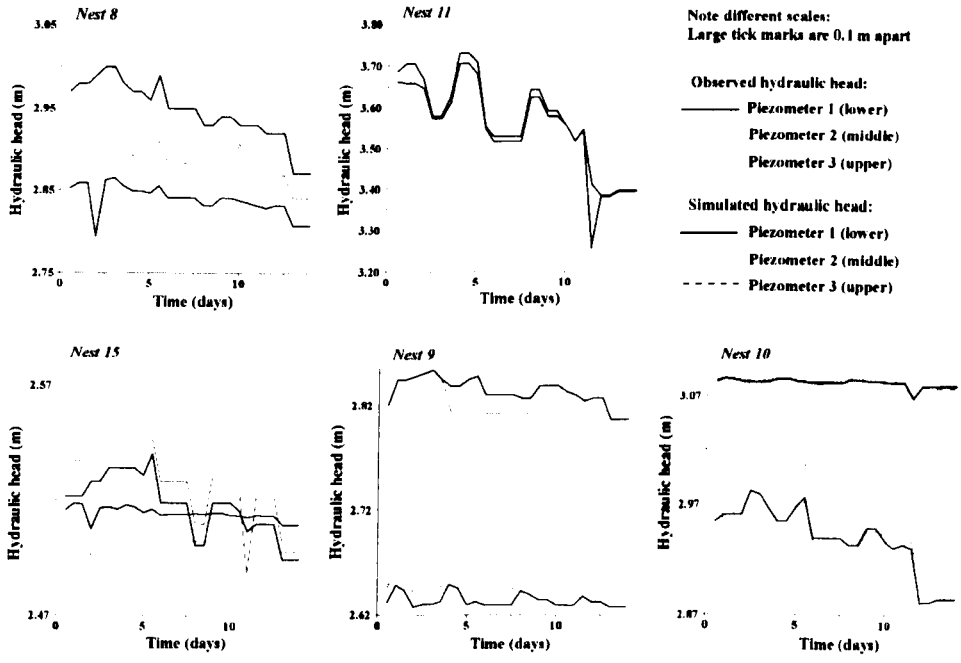

Figure 5.35 Graphs comparing observed (black) and simulated (red) hydraulic head, using average saturated conductivity values as measured in the field.

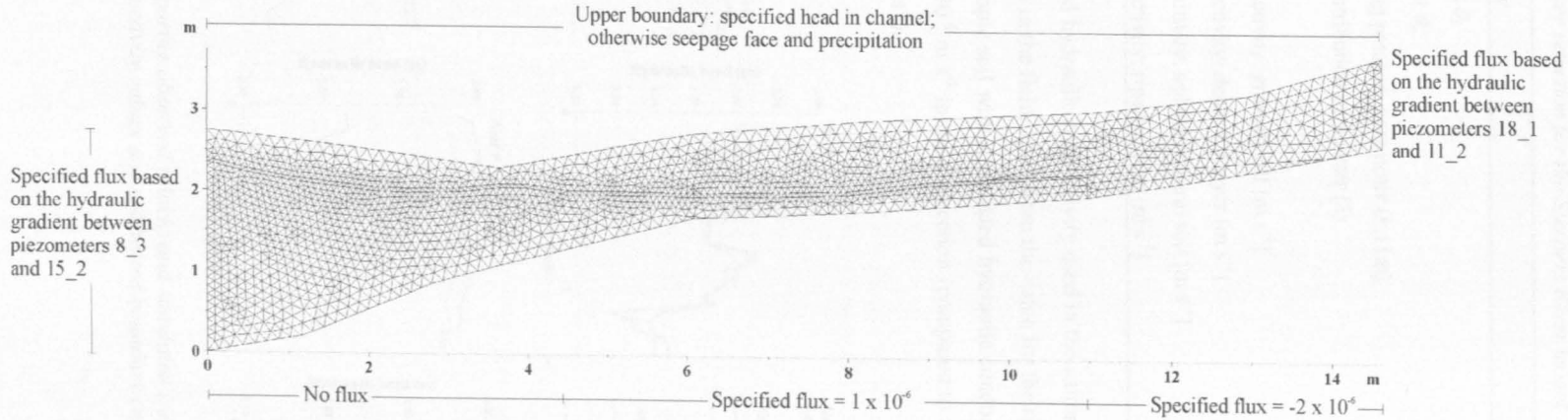

Figure 5.36 Diagram showing the final boundary conditions used in the Sleepers River snowmelt event simulation.

Table 5.9 Final parameter selection for the Sleepers River model

Soil hydraulic parameter	Value
Residual moisture content θ_r	0.0954
Saturated moisture content θ_s	0.41
Brooks and Corey bubbling pressure parameter (h_s) [m]	0.100
Brooks and Corey pore distribution parameter (λ)	0.318
Specific storage [m^{-1}]	0.0001
Saturated hydraulic conductivity: gravelly till [$m\ s^{-1}$]	5×10^{-5}
Saturated hydraulic conductivity: dense till layer [$m\ s^{-1}$]	3×10^{-6}
Saturated hydraulic conductivity: upland mineral soil [$m\ s^{-1}$]	1×10^{-4}
Saturated hydraulic conductivity: riparian peat [$m\ s^{-1}$]	5×10^{-4}, 5×10^{-6}

All the values of saturated hydraulic conductivity used in the calibrated model are within the range of values measured in the field, apart from the value for the riparian peat, which is now represented as an anisotropic soil with a saturated hydraulic conductivity of 5×10^{-4} m s^{-1} in the x-direction, and 5×10^{-6} m s^{-1} in the y-direction (compared to a field measured value of 3.9×10^{-5} to 7.4×10^{-5} m s^{-1}).

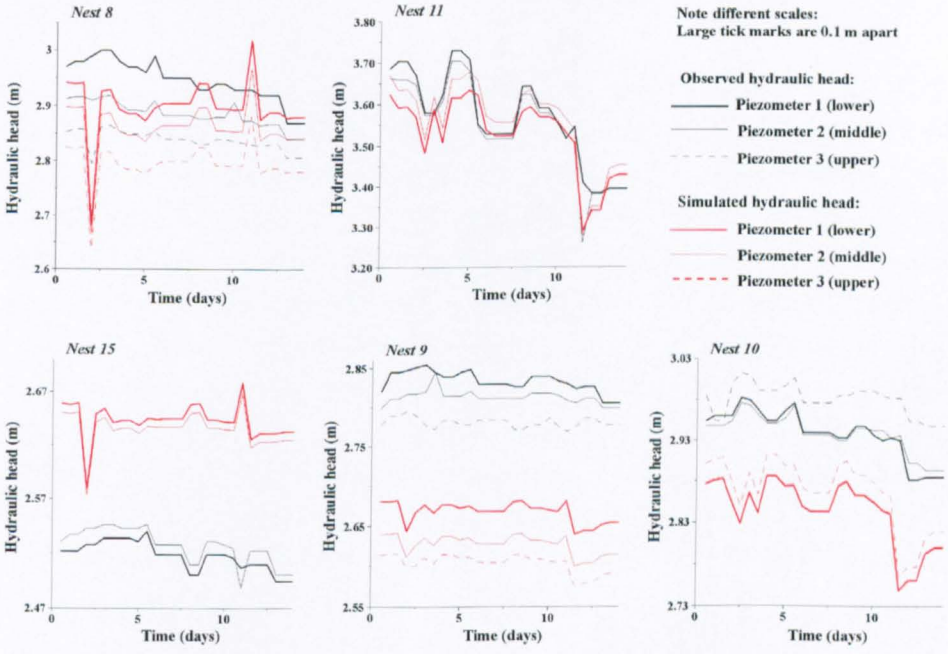

Figure 5.37 Graphs comparing observed (black) and simulated (red) hydraulic head, using calibrated saturated conductivity values and calibrated boundary conditions.

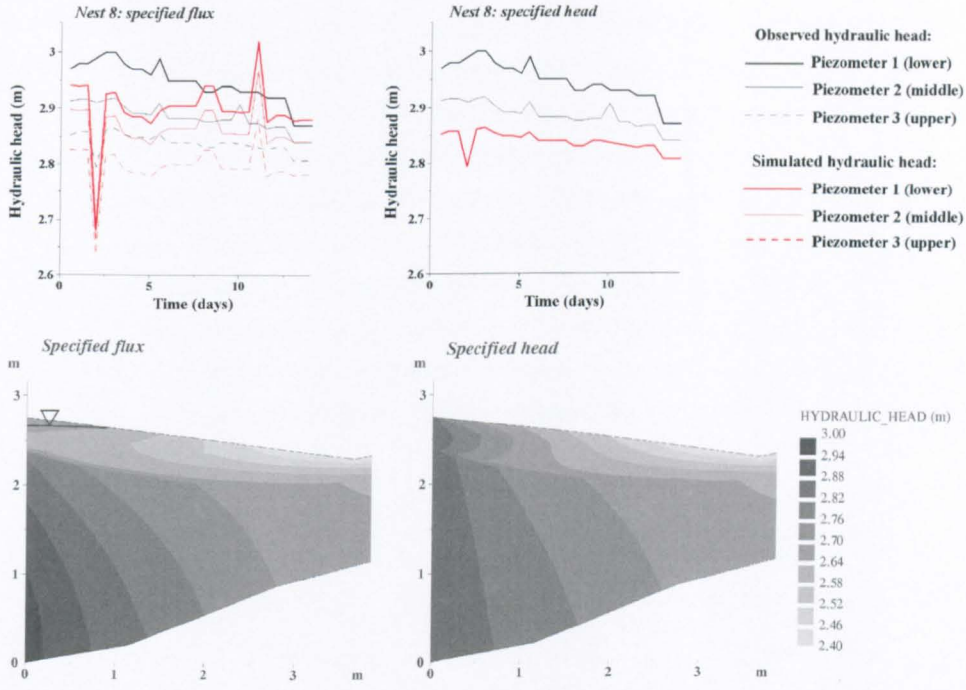

Figure 5.38 Graphs showing the effect of specified flux versus specified head boundary condition on hydraulic head prediction at nest 8, and hydraulic head pattern in the domain near nest 8, at time = 3 days.

The first major change that was made to the Sleepers River model as part of the calibration process was changing the left- and right-hand side boundary conditions to specified flux, rather than specified head. This was because the specified head representation restricted the hydraulic head along the boundary to a hydrostatic condition, where the field data clearly indicated that there was some component of vertical flow as the water crossed this point. The left-hand side flux was specified by calculating the hydraulic gradient between piezometers 8_3 and 15_2, multiplied by the hydraulic conductivity of the gravelly till. The right-hand side flux was specified by calculating the hydraulic gradient between piezometers 11_2 and 18_1 (there were no data for piezometer 18_2), multiplied by the hydraulic conductivity of the upland mineral soil. The situation at the right-hand side boundary is more satisfactorily defined because it involves comparing the hydraulic head at nest 11 with another hydraulic head measurement *outside* the model domain. On the left-hand side boundary, this could not be achieved, because the piezometer nests only extended as far as nest 8. This may help to account for the need to increase the flux on the left-hand side boundary during the calibration (the value estimated from the hydraulic gradient between piezometer 8_3 and 15_2 was multiplied by 4.5). An alternative would have been to truncate the model domain at nest 15, in the stream channel, but this would have excluded an interesting part of the domain from further analysis.

Figure 5.38 illustrates the effect of changing the left-hand side boundary (piezometer nest 8) from a specified head to a specified flux boundary condition. The sharp drop in hydraulic head near the start of the simulation seems to be a result of using piezometer 8_3 as part of the flux calculation, because this drop occurred in piezometer 8_3, but not in 8_2 or 8_1. Although the predicted hydraulic head did not completely match the observed values, changing to a specified flux did achieve the main aim of creating a more realistic *pattern* of hydraulic head in terms of creating upward flow. The striking effect that this had on the pattern of hydraulic head in a wider portion of the domain can also be seen in Figure 5.38. With the specified head boundary condition, this part of the domain was saturated right to the surface. With the specified flux boundary condition, the water-table developed beneath the surface of the riparian zone.

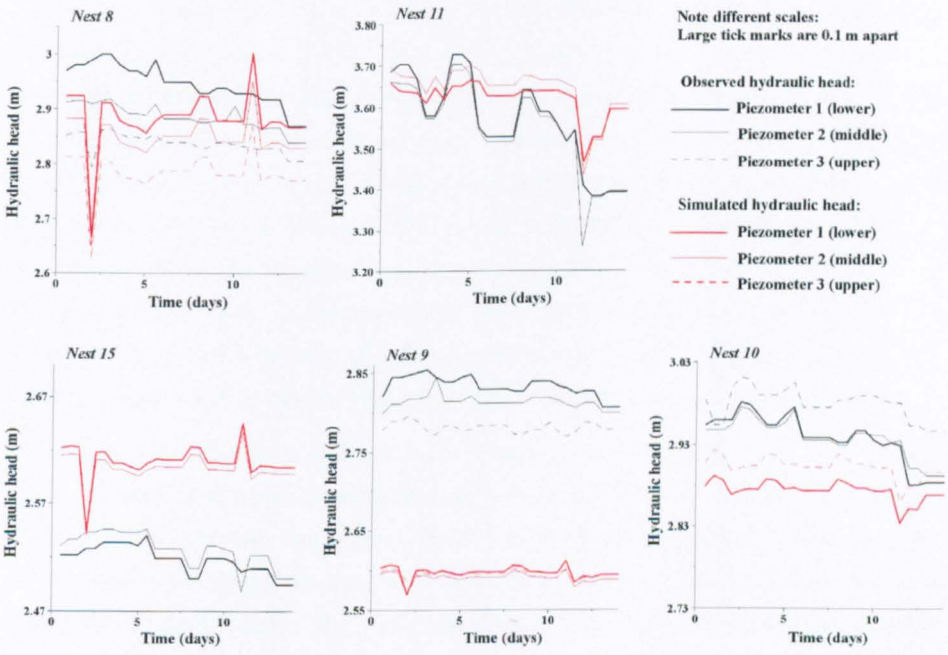

Figure 5.39 Graphs comparing observed (black) and simulated (red) hydraulic head with a no flux boundary condition along the lower boundary.

Improving the representation of the hydraulic head for nests 9, 10 and 11 involved changing the specified fluxes across the lower boundary. During the calibration process it was found that an upward flux in the nest 9 region and a downward flux in the region of nests 10 and 11 (see the boundary condition diagram, Figure 5.36), provided a good representation of the hydraulic head in nests 9, 10 and 11. Figure 5.39 shows the effect of changing the lower boundary condition to zero flux. In comparison with the calibrated results, the hydraulic head at nest 9 was poorly predicted, with virtually no vertical flow. The correspondance

between the observed and simulated hydraulic head at nests 10 and 11 was also weak, as the predicted change in hydraulic head over time was much less dynamic than the behaviour observed in the field.

Although there were no field data to guide the addition of a water flux across the lower boundary, the pattern of flux that has been adopted seems reasonable. It corresponds with the available piezometer data that suggest downwelling from the soil towards the bedrock at the foot of the hillslope where there is a distinct break of slope, and later recharge to the riparian zone in the region of piezometer nest 9.

Improving the representation of the hydraulic head as observed in piezometer nests 9 and 10 involved changing the characterisation of the riparian peat. During the extensive calibration process it was found that an anisotropic saturated hydraulic conductivity of 5 x 10^{-4} m s^{-1} in the x-direction and 5 x 10^{-6} m s^{-1} in the y-direction provided a good representation of the hydraulic head in nests 9 and 10. Figure 5.40, Figure 5.41 and Figure 5.42 illustrate the effect of changing the hydraulic conductivity of the riparian peat to three different, isotropic values, while keeping all other aspects of the simulation the same. At 5 x 10^{-4} m s^{-1} (Figure 5.40), the pattern of flux in terms of the vertical movement of water was poorly represented at nests 9 and 10, and the hydraulic head was 10 to 20 cm too low in each case. At 5 x 10^{-5} m s^{-1} (Figure 5.41), the hydraulic head patterns again showed no evidence of vertical water movement, and this time, the hydraulic head at nest 10 was predicted as approximately 10 to 20 cm too high, and with little variation over the course of the simulation. The hydraulic head predicted at nest 11 also showed a less dynamic response than the observed behaviour.

With a hydraulic head value of 5 x 10^{-6} m s^{-1} (Figure 5.42), the prediction of hydraulic head at nest 9 showed a dramatic improvement, with the correct pattern of upward flow indicated by the predicted hydraulic head pattern. However, the pattern of water flow predicted at nest 10 was then in the wrong direction, flowing upwards instead of downwards, and the values were 20 to 25 cm too high. The predictions of hydraulic head at nests 8 and 15 were also worse in comparison with the measured field data, but this may have been because the flux specified on the left-hand side boundary needed to be altered to take account of the change in hydraulic conductivity of the riparian peat.

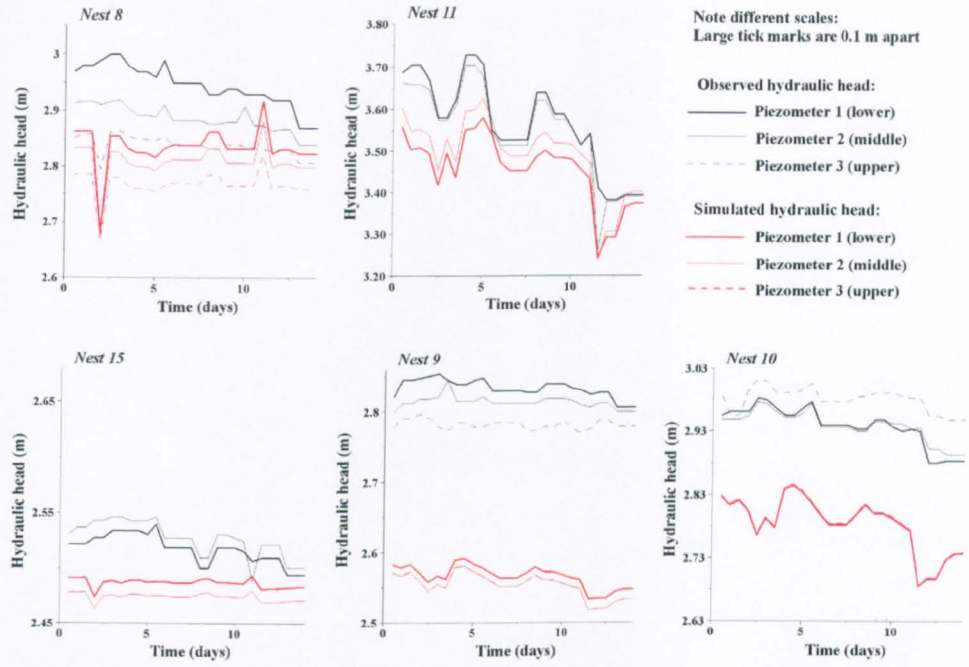

Figure 5.40 Graphs comparing observed (black) and simulated (red) hydraulic head, using a saturated hydraulic conductivity value for the riparian peat of 5 x 10^{-4} m s^{-1}.

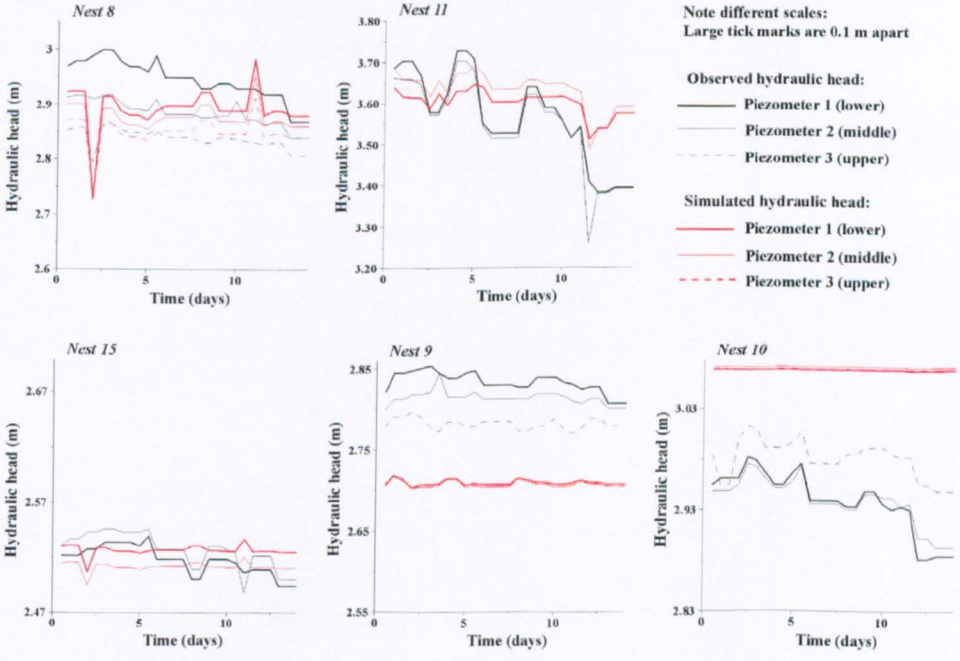

Figure 5.41 Graphs comparing observed (black) and simulated (red) hydraulic head, using a saturated hydraulic conductivity value for the riparian peat of 5 x 10^{-5} m s^{-1}.

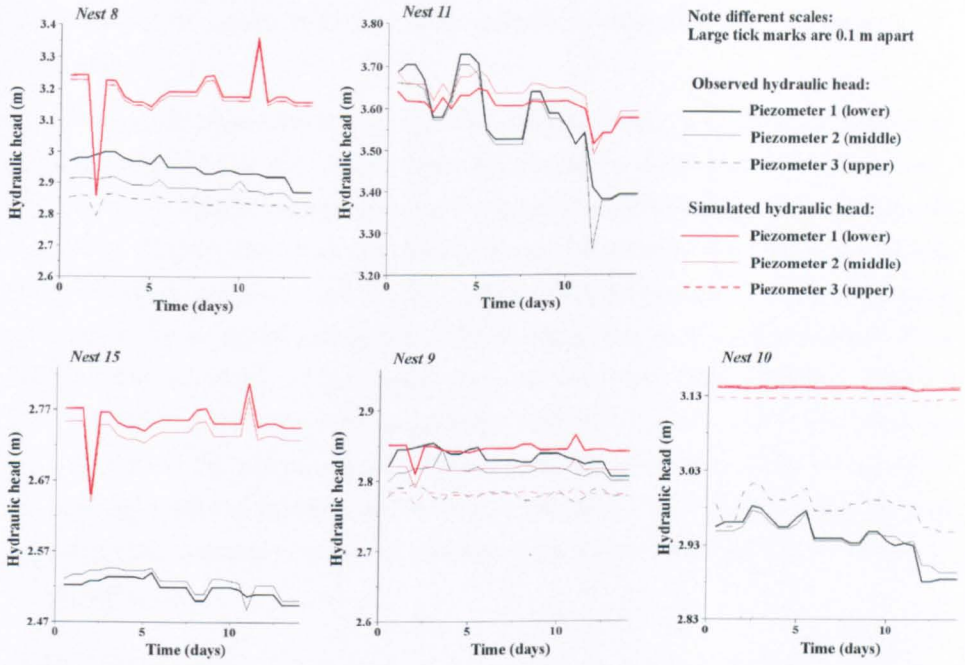

Figure 5.42 Graphs comparing observed (black) and simulated (red) hydraulic head, using saturated hydraulic conductivity value for the riparian peat of 5 x 10^{-6} m s^{-1}.

Considering again the calibrated model results (Figure 5.37), the anisotropic peat representation helped to create the patterns of hydraulic head in nests 9 and 10 that were observed in the field, with upward water flow at nest 9, and downward flow at nest 10. The absolute values of hydraulic head were still 10 to 20 cm too low, but it was felt that this was less important than achieving a good representation of the *pattern* of flow. The anisotropic behaviour of the peat may be explained by the observations of

> ...enlarged openings at the interface between soil layers and many root channels – flow was likely in excess of measured matrix hydraulic conductivity values found with piezometer bail tests...Further, the dense upper till layer at the peat-till interface appeared to inhibit root growth. The resulting concentration of roots at this interface could increase lateral water transmission.
>
> (McGlynn *et al.*, 1999)

There were still some other discrepancies between the observed and predicted hydraulic head patterns; at nest 15, the predicted hydraulic head was about 10 cm too high, and suggesting slight upward flow, as opposed to the slight downward flow suggested by the piezometer data. However, some of these gradients implied by the field data were so small that they could have fallen within the envelope of measurement accuracy (±2 cm), and so further

calibration of the model, away from those reasonable assumptions that were made so far, was resisted.

In summary, the River Severn model has been calibrated using only the value of saturated hydraulic conductivity. The more complex Sleepers River model was calibrated through a combination of changing saturated hydraulic conductivity values, and changing the boundary conditions. Four specific adaptations were necessary: (a) specified flux boundary conditions along the side boundaries, in order to represent correctly the vertical movement of water in these zones; (b) an explicit representation of the seepage face on the upper boundary; (c) an anisotropic representation of the riparian peat, and (d) a spatially variable flux along the lower boundary, down towards the groundwater in the hillslope area, and upwards from the groundwater in the riparian zone. Although model calibration efforts in the wider hydrological modelling literature tend to focus on the soil characterisation, it appears that the boundary conditions can exert just as important a control over the model results as the soil parameterisation.

5.3.1.5 Validation

This section focuses on using data sets that have not been used so far during the model testing. The River Severn model is validated using data from three overbank flood events, listed in Table 5.1 as flood event E, F and G, and two bankfull events, listed as bankfull event A and B, for both transect S and transect H. Validation of the Sleepers River model involves using data from the whole 1996 snowmelt event.

Validation of the River Severn model was carried out by comparing the observed and simulated hydraulic head values at points internal to the model domain, corresponding to the location of piezometers S2, S3 and S4 on transect S, and H2, H3, and H4 on transect H. The location of these points inside the two model domains is illustrated in Figure 5.33.

Generally, the fit between observed and predicted hydraulic head for all the events tested as part of the validation exercise was quite good (Figure 5.45 to Figure 5.44). The fit tended to be worse at the beginning and end of the events, but a proportion of this could be explained by the performance of the vibrating wire piezometers at these times during the flood events. The piezometers were installed as deep as possible using a hand held auger, but even so, during long periods of the year, when the water-table was relatively low, the water-table was below the level at which the piezometers were installed. These piezometers were not designed to record soil water suction; they can only reliably record positive soil water pressures. Therefore, at the beginning and end of the flood events, when the water-table was relatively low, the piezometers may not have been able to record the soil water pressure. An

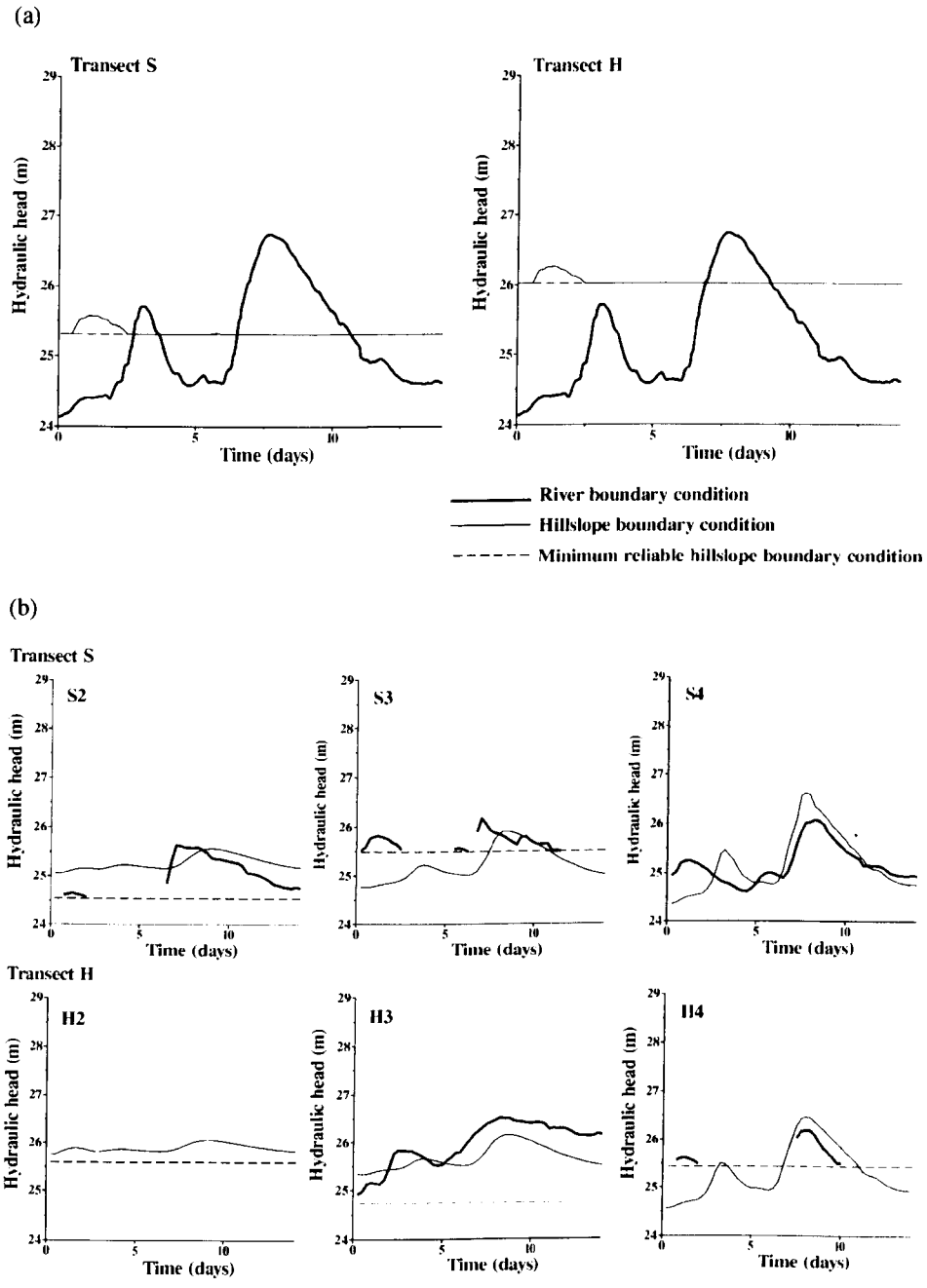

Figure 5.43 (a) Graphs showing boundary conditions for bankfull event A. (b) Graphs comparing observed (thick line) and simulated (thin line) hydraulic head, for transects S and H. Dotted line indicates minimum reliable piezometer measurement.

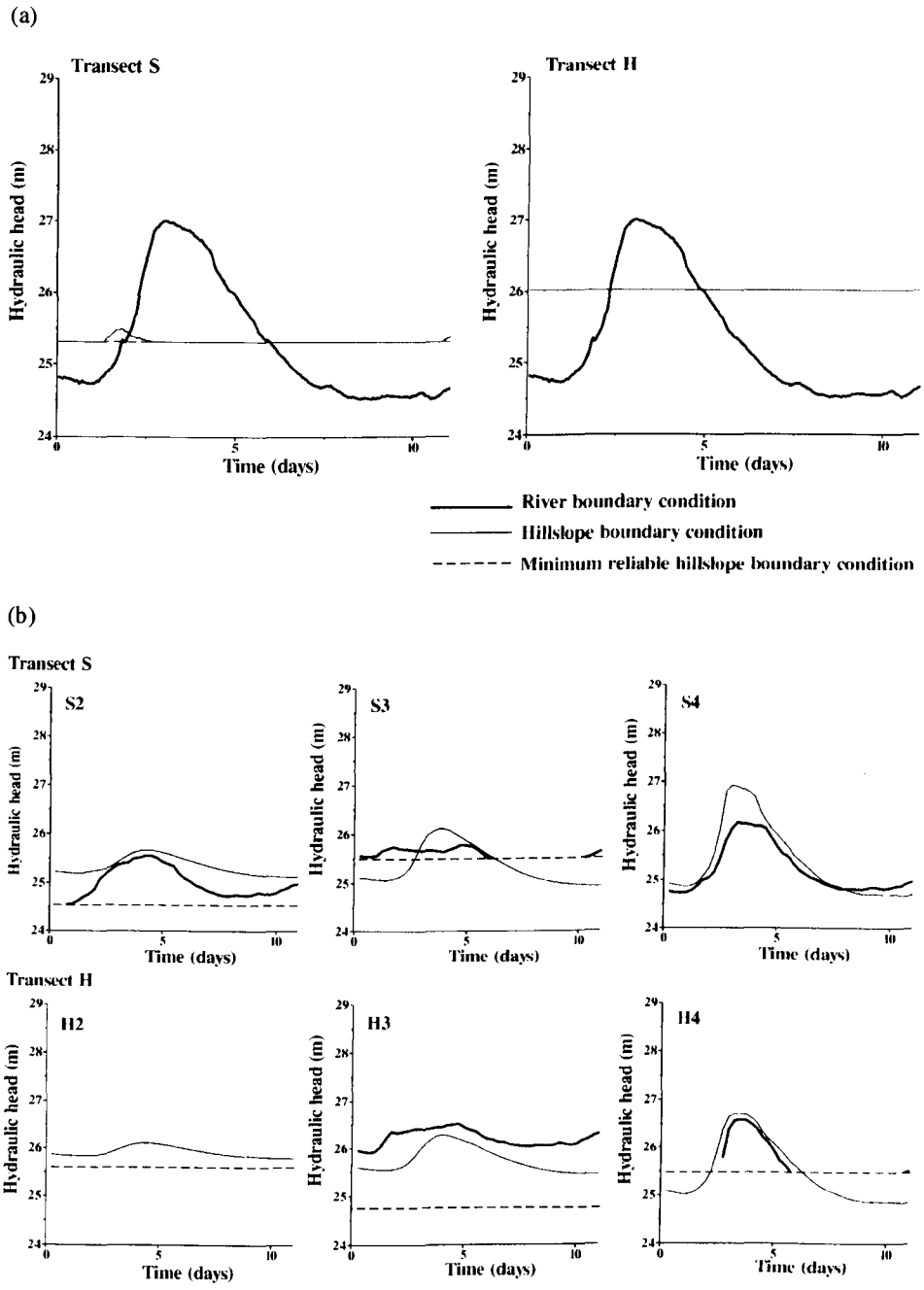

Figure 5.44 (a) Graphs showing boundary conditions for bankfull event B. (b) Graphs comparing observed (thick line) and simulated (thin line) hydraulic head, for transects S and H. Dotted line indicates minimum reliable piezometer measurement.

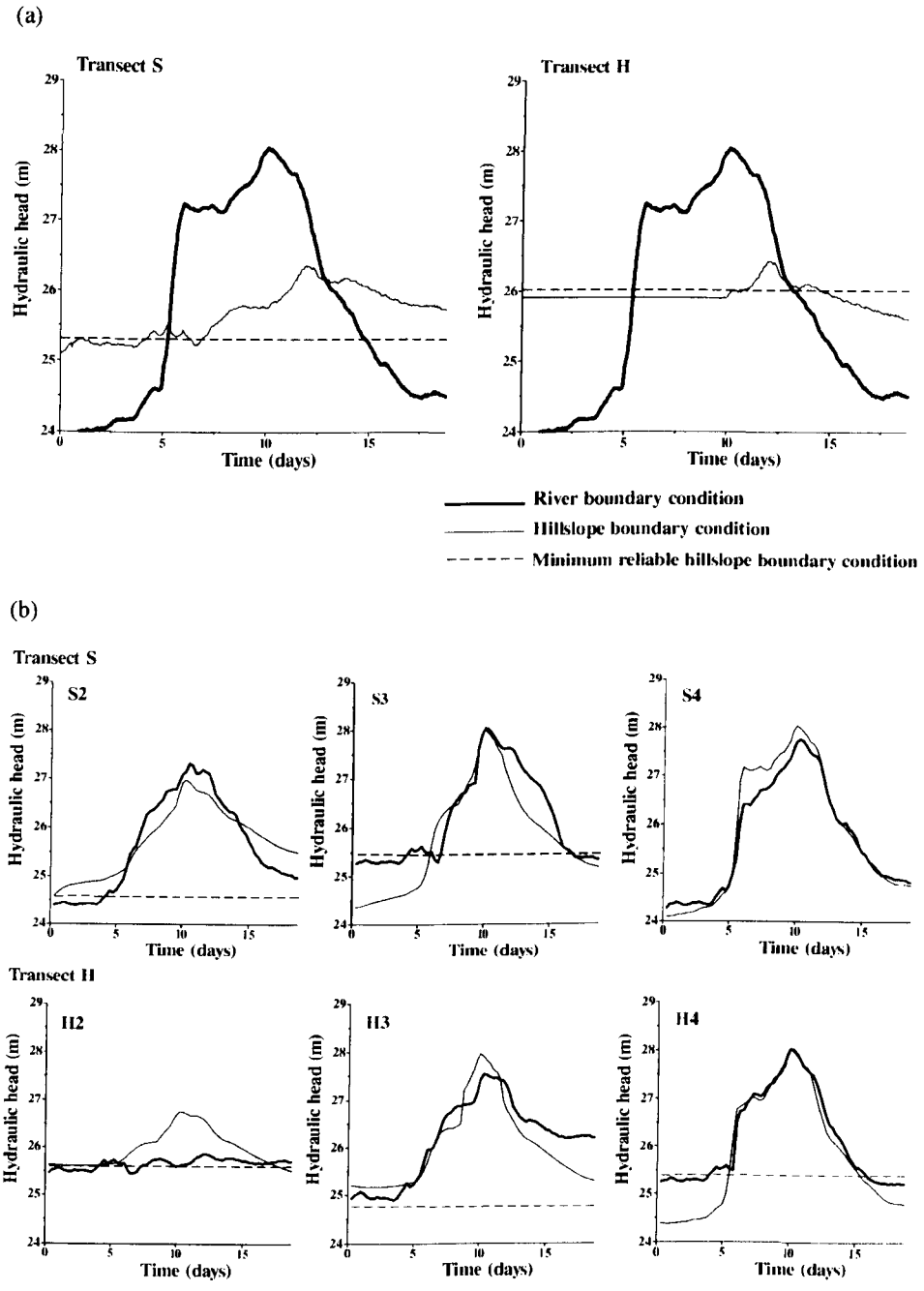

Figure 5.45 (a) Graphs showing boundary conditions for flood event E. (b) Graphs comparing observed (thick line) and simulated (thin line) hydraulic head, for transects S and H. Dotted line indicates minimum reliable piezometer measurement.

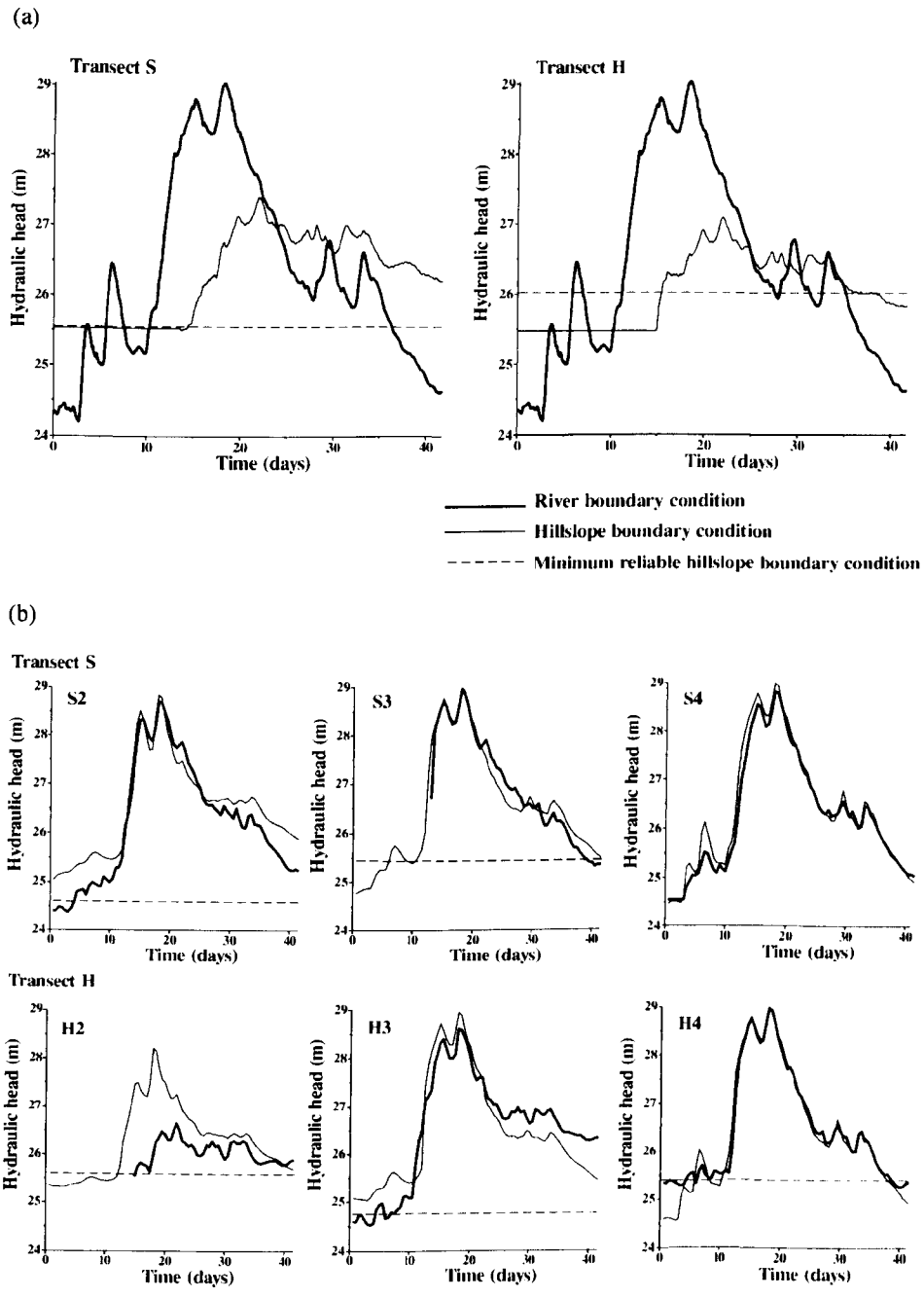

Figure 5.46 (a) Graphs showing boundary conditions for flood event F. (b) Graphs comparing observed (thick line) and simulated (thin line) hydraulic head, for transects S and H. Dotted line indicates minimum reliable piezometer measurement.

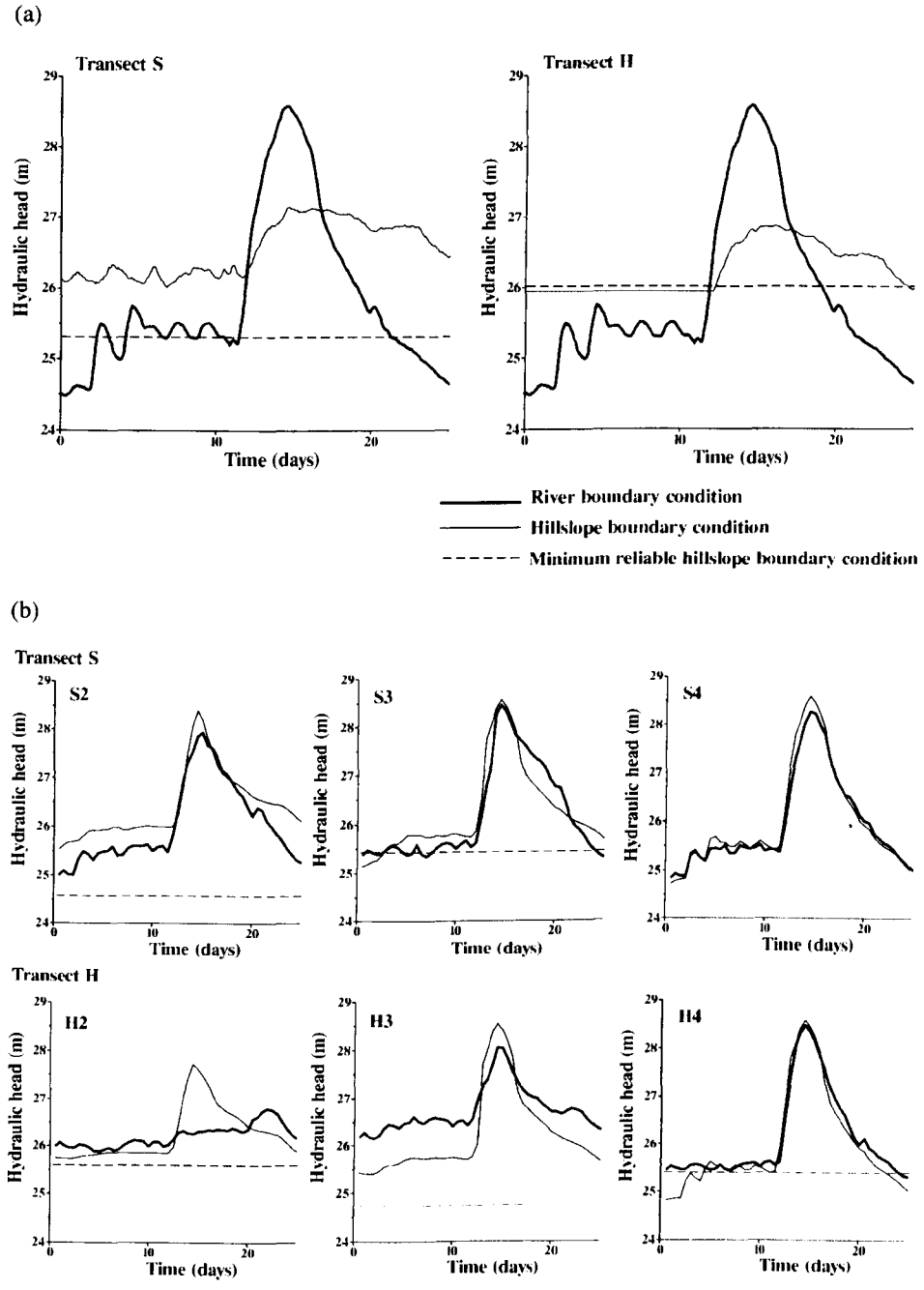

Figure 5.47 (a) Graphs showing boundary conditions for flood event G. (b) Graphs comparing observed (thick line) and simulated (thin line) hydraulic head, for transects S and H. Dotted line indicates minimum reliable piezometer measurement.

additional line has therefore been added to each graph on the validation diagrams, to indicate the hydraulic head value below which the observed piezometer reading may be considered unreliable. The biggest problem that this caused was in specifying the hillslope boundary condition for each transect, as can be seen in the graphs which illustrate the boundary conditions for each validation run (Figure 5.45 to Figure 5.44). For some of these events, the hillslope piezometer did not begin recording until half way through the event. This left the hillslope boundary condition poorly characterised, and perhaps led to some of the discrepancies between observed and simulated hydraulic heads in the piezometers internal to the domain, particularly for those piezometers nearest the hillslope (i.e. S2 and H2).

The results of the Sleepers River validation are illustrated in Figure 5.48, showing model predictions of hydraulic head for each piezometer nest for the full 29 day record of the 1996 snowmelt event.

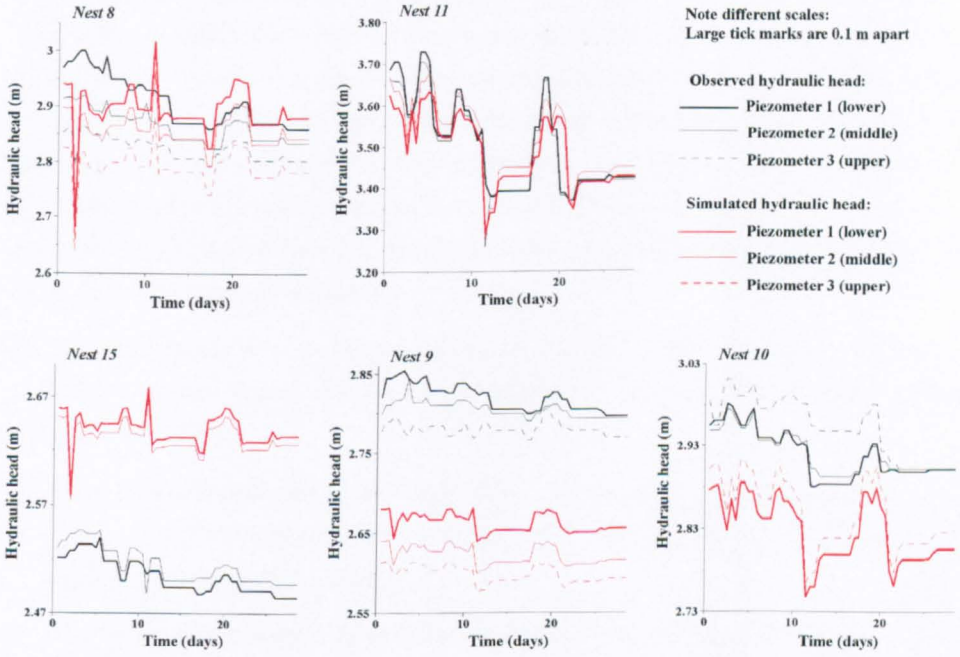

Figure 5.48 Graphs comparing observed (black) and simulated (red) hydraulic head, for the full Sleepers snowmelt event.

The validation for Sleepers River was certainly less rigorous than the River Severn validation, as there was only one event available for both calibration and validation. Although the patterns of hydraulic head (in terms of the direction of water flow) were generally well represented, there were still some significant discrepancies between the observed and predicted hydraulic head values, most notably at piezometer nest 9, where the

absolute difference between modelled and measured hydraulic head was of the order of 20 cm.

Where such discrepancies occur between the model results and field data, it is possible that they may be due to time-lags in the piezometer response to changes in soil water pressure. There are four basic types of piezometer: pneumatic, vibrating wire, closed standpipe and open standpipe (Baird and Gaffney, 1994). Vibrating wire piezometers, as used at the River Severn fieldsite, respond to changes in soil pore water pressure almost instantaneously, and time lag errors are likely to be minimal. Out of all the piezometer designs, open standpipe piezometers, as used at the Sleepers River site, are most likely to be subject to time-lag errors.

Standpipe piezometers take a period of time to register pressure changes because water needs to flow into or out of the instrument for equilibration to occur (Hanschke and Baird, 2001). Depending on the exact design of the piezometer, and the hydraulic conductivity of the soil around the piezometer, such water exchanges may take hours or days, resulting in misleading information on pore-water pressures within the soil (Hanschke and Baird, 2001). Hanschke and Baird (2001) investigated time-lag errors for several combinations of soil type and open standpipe piezometer design. In their experiments, the long response time of some piezometers led to piezometer readings that indicated not only an incorrect rate of flow, but also the wrong pattern of flow (i.e. strong downwardly acting hydraulic gradients instead of upwardly acting hydraulic gradients).

It is also possible that there are errors in the surveyed position of the piezometers. Surveying is subject to several sources of error, which can be classified according to three categories (Ritchie *et al.*, 1988):

- Gross errors: mistakes that cannot be corrected. They can be of any size or nature, and tend to occur through carelessness, for example, writing down the wrong value or reading the instrument incorrectly.
- Systematic errors: errors which follow a logical pattern. They can be theoretically predicted (and therefore corrected), for example, the effect of temperature on tape length.
- Random errors: errors which reflect the limit of precision of the measurement process. They have very definite statistical behaviour and while they cannot be predicted in any single measurement, the effects of random errors can be minimised using statistical procedures (for example, adopting the mean of a set of values).

If such errors occurred during the measurement of the piezometer locations at Sleepers River, and were not corrected, they may have resulted in the recorded location of any given piezometer being slightly above or below its true position, relative to the datum and to other piezometers. This could have two main impacts. First, the measurements of hydraulic head may be slightly too high or too low. For example, if the pressure head in a given piezometer was measured as 5 cm, and the piezometer was believed to be 10 cm above the datum, this would give a hydraulic head value of 15 cm. However, if the location of the piezometer had been measured incorrectly, and the piezometer was really only 8 cm above the datum, this would mean that the hydraulic head value was really only 13 cm: an error of 2 cm. This could be critical in locations such as piezometer nest 15, where the measured hydraulic head values are usually only a couple of centimetres apart, as it could mean the difference between a positive or negative vertical hydraulic gradient (i.e. upward or downward flow). In comparison with a domain on the much larger scale of the River Severn, such errors will be relatively much more important in the Sleepers River domain because of its small size.

The second impact of any surveying errors could be that a piezometer is indicated to be situated in one soil type, whereas in reality it is located in another soil type. This may be particularly relevant for those piezometers located in or near the dense till layer. As this soil type has such different hydraulic properties to the surrounding soil layers, it is expected that the hydrological response of piezometers located within, in comparison with those just above or below this low conductivity layer, will be quite different. This may help to explain some of the differences in observed and predicted hydraulic head for piezometers situated in or close to the dense till layer, for example, piezometers 15_2 and 9_2. In the model they will have been set up to be within one soil type, whereas in reality they may be located in a different soil type, which would dictate a different hydrological response. A realistic representation of these piezometers could therefore never be hoped to be achieved within the model.

The possible existence of such inaccuracies in the Sleepers River piezometer readings makes it difficult to draw conclusions about whether the discrepancies between the measured and modelled hydraulic head patterns are due to errors in the field data, or errors in the modelled representation of the Sleepers River system.

5.3.2 Coupled ESTEL2D-SUBIEF2D assessment strategy and results

5.3.2.1 Verification

SUBIEF2D has been the subject of a verification exercise during development at EDF, although this was for surface water transport problems. Verification of subsurface water

transport using SUBIEF2D was carried out using an analytical solution from the USGS computer code ANALGWST, and reported in a previous chapter (Section 3.4).

5.3.2.2 Optimisation

Optimisation of the model structure of SUBIEF2D involved testing the time step, grid spacing, and scheme for solving the advection-dispersion equation (PSI scheme, Method of Characteristics, and SUPG). The scenario investigated during this optimisation procedure was the same as that used in the verification exercise of Chapter 3, enabling a comparison of the numerical solution with an analytical solution. The rectangular mesh illustrated in Chapter 3 was also used for the simulations reported here (Figure 5.49), in conjunction with a simplified hydrodynamic results file consisting of a constant velocity in the x-direction of 1 x 10^{-4} m s^{-1}. The output to be compared between the model runs is the profile of solute concentration both along the domain (a transect through y = 40 m) and across the domain (a transect through x = 40 m), and the minimum solute concentration.

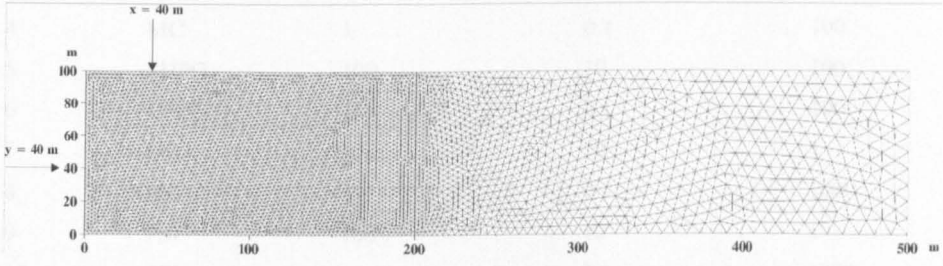

Figure 5.49 Finite element mesh for analytical test case illustrating the point at which transects of solute concentration will be plotted (at y = 40 m and x = 40 m).

The application of finite element methods to solve advection-dispersion problems is subject to local Peclet and Courant number restrictions (Mitchell and Mayer, 1998). These dimensionless numbers incorporate aspects of the problem of spatial and temporal discretisation, which are the subject of this optimisation procedure:

$$Pe = \frac{v\Delta x}{D'} \qquad 5.3$$

$$Cr = \frac{v\Delta t}{\Delta x} \qquad 5.4$$

where v is the average linear velocity [L T^{-1}], D' is the hydrodynamic dispersion [L^2 T^{-1}], Δx is the grid spacing [L], and Δt is the time step [T]. Tests have indicated that for a stable solution, the Peclet number should be less than 2, and the Courant number should be less than 1 (Mitchell and Mayer, 1998).

The effect of grid spacing was explored by changing the value of the dispersion coefficient. This was much easier than changing the mesh, but had the same net effect because the dispersion coefficient is combined with the grid spacing in the Peclet number. This still gave an idea of whether the River Severn and Sleepers River meshes were of a suitable resolution. The time step needed also varies with the grid spacing, with a smaller grid spacing needing a smaller time step to maintain a stable solution. This was also explored by testing the effect of time step on the results with different values of hydrodynamic dispersion. The schedule of model runs is presented in Table 5.10.

Table 5.10 Schedule of model runs for SUBIEF2D optimisation.

Run number	Solver scheme[1]	Dispersivity (m^{-1})		Time step (s)
		Longitudinal (α_L)	Transverse (α_T)	
1	PSI	100	10	100
2	PSI	1	0.1	100
3	MC	100	10	100
4	MC	1	0.1	100
5	SUPG	100	10	100
6	SUPG	1	0.1	100
7	PSI	100	10	1
8	PSI	1	0.1	1000
9	PSI	100	10	1
10	PSI	1	0.1	1000

[1] PSI = Positive Streamwise Invariant scheme; MC = Method of Characteristics; SUPG = Streamwise Upwind Petrov-Galerkin scheme.

The first part of the optimisation procedure involved looking at the performance of the three solver schemes: the PSI scheme, the Method of Characteristics, and the SUPG scheme. With high values of dispersivity (runs 1, 3 and 5, Table 5.10), all the schemes produced smooth decreases in solute concentration along a transect away from the solute source (Figure 5.50), and all produced results which were very close to the analytical solution. However, there was a marked difference between the performances of the solver schemes in terms of negative errors (Figure 5.51). Theoretically, a negative solute concentration is impossible, so a negative concentration produced by a scheme is an error. Both the Method of Characteristics and the SUPG scheme produced significant negative concentrations, down to a minimum of approximately –0.075 mg l^{-1}. In contrast, the PSI scheme produced a smaller error of approximately –0.025 mg l^{-1}. In all three cases, the negative errors persisted for the first 5000 seconds of the simulation, and then reduced to near zero. However, in the case of

the SUPG scheme, at around 9000 seconds into the simulation the negative errors began to increase again (i.e. the minimum concentration value became increasingly negative).

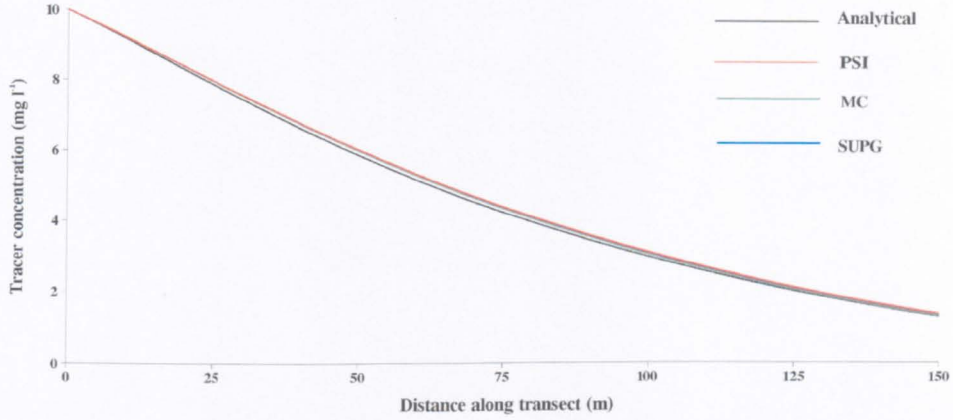

Figure 5.50 Graph illustrating the effect of solver scheme on solute concentration along a transect passing through y = 40 m, after 50 days, with longitudinal dispersivity = 100 m, transverse dispersivity = 10 m.

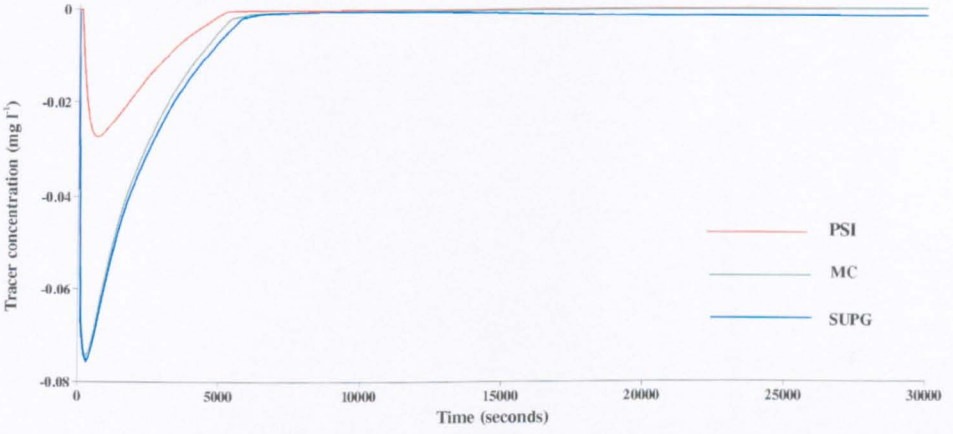

Figure 5.51 Graph illustrating the effect of solver scheme on change in minimum solute concentration over time, with longitudinal dispersivity = 100 m, transverse dispersivity = 10 m

At lower levels of dispersivity, differences between the performances of the three schemes, in terms of the profile of solute concentration, become more apparent (runs 2, 4 and 6, Table 5.10). At this level of dispersivity, both the Method of Characteristics and the PSI scheme showed a significantly different pattern of solute concentration along the transect from that indicated by the analytical solution (Figure 5.52). However, Figure 5.53 shows that the SUPG scheme still suffered from significant negative concentration errors. At this lower level of dispersivity, the SUPG scheme had the greatest errors, followed by the Method of

Characteristics. After 30 000 seconds, the errors in the SUPG scheme levelled out to a near constant –0.004 mg l^{-1}, but the PSI scheme showed virtually no negative errors throughout the simulation..

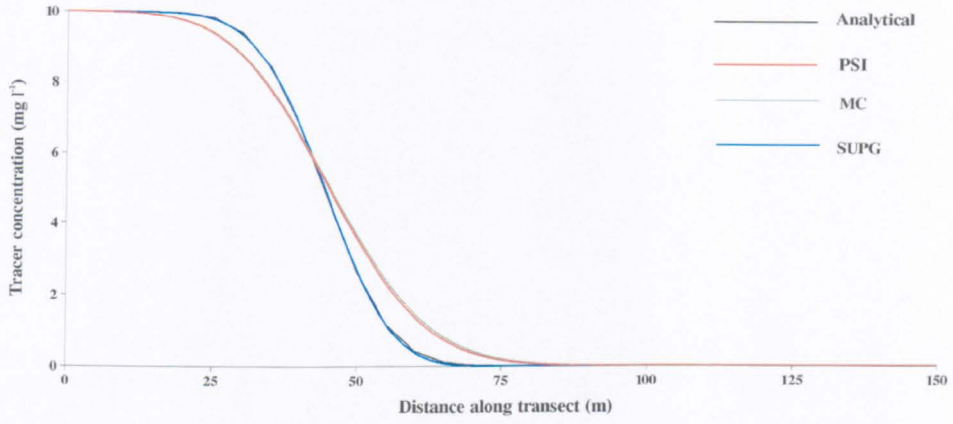

Figure 5.52 Graph illustrating the effect of solver scheme on solute concentration along a transect passing through y = 40 m, after 50 days, with longitudinal dispersivity = 1 m, transverse dispersivity = 0.1 m.

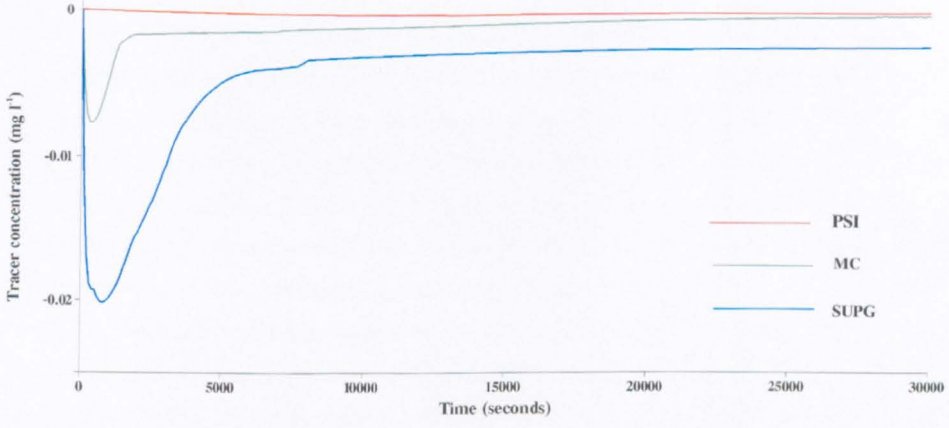

Figure 5.53 Graph illustrating the effect of solver scheme on change in minimum solute concentration over time, with longitudinal dispersivity = 1 m, transverse dispersivity = 0.1 m

A profile of solute concentration plotted across the domain, passing through x = 40 m, gives a further indication of how well the results from each of the solver schemes correspond to the analytical results (Figure 5.54). The SUPG scheme produced the least smooth profile of solute concentration across the domain, with notable increases in tracer concentration at 20 m and 60 m, at the edge of the tracer plume. The PSI scheme produced the smoothest profile, and had the highest concentration at 40 m, which better matched the *pattern* of the

analytical solution, even though the *magnitude* of the solute concentration across the profile was not always so well fitting.

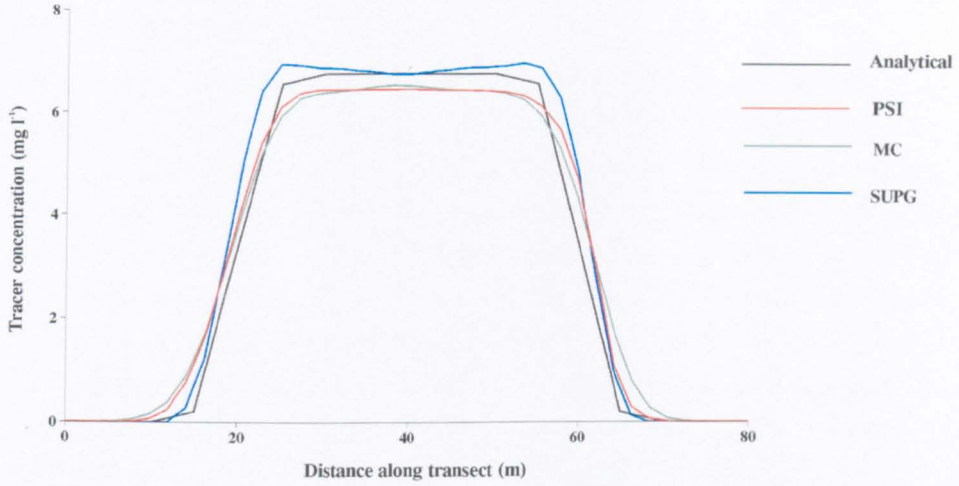

Figure 5.54 Graph illustrating the effect of solver scheme on change in maximum solute concentration over time, with longitudinal dispersivity = 1 m, transverse dispersivity = 0.1 m.

Numerical solutions of the advection-dispersion equation commonly suffer from inaccuracies in the solution, including oscillations in the computed concentration profile, and numerical errors that cause a smearing of the concentration front (numerical dispersion). To ensure numerical stability and minimise numerical dispersion, the cell Peclet number should be no greater than 2 (Equation 5.3). For all the simulations reported here, the Peclet number was well below 2. However, increasing element size (decreasing dispersivity), even where the Peclet number was very small, clearly did introduce inaccuracies in the solution, and increased numerical dispersion in particular. To minimise numerical difficulties when the coefficient of dispersion is small, it has been noted that small space increments are necessary (Anderson, 1979). However, there is a limit to the element density that it is reasonable to work with without an unacceptable increase in simulation time, or reaching the limit of the mesh generation software.

The results of these simulations are in accordance with the established properties of these schemes. In particular, the PSI scheme is known to be monotonic (so it is less prone to producing negative concentrations, or concentrations which are too high), but it is more likely to suffer from problems of numerical diffusion (or 'false' diffusion). On the other hand, the SUPG scheme is less diffusive (as evidenced by the profile of solute concentration in Figure 5.52), but is not monotonic, so if problems occur the scheme can give negative concentrations. It is therefore clear that each scheme has its advantages and disadvantages.

Making any significant developments in terms of advection-dispersion solver schemes is clearly beyond the scope of this project, but this optimisation process has at least highlighted potential problems with the choice of solver that should be taken into consideration when interpreting later results.

The next part of the optimisation process looked at the effect of time step size on the solution. This was carried out for the two different sets of dispersivity values: 100 and 10 m, and 1 and 0.1 m, for the PSI scheme only. The PSI scheme was tested over a range of time step sizes, between 1 and 1000 seconds, but for both high and low dispersivity values, time step size made no difference to the model results in terms of predicted solute concentration. A stable solution over this range of time steps may be expected because for all these simulations, the Courant number remained well below a value of 1. Of course, changing the time step size over this range had a significant effect on the time taken to run the simulation: the simulation using a one second time step took approximately three hours to run; the simulation using a 100 second time step took approximately 20 minutes to run, and the simulation using a 1000 second time step took approximately 1.5 minutes to run. Clearly, there is no advantage to be gained from using a very small time step, but a time step of 100 to 1000 seconds will generate acceptable results without unduly increasing simulation times.

Solute mass balance results

It appeared that there was a large error in the mass balance results of the SUBIEF2D simulations, so the reason for this was investigated further, once again using the analytical domain. The parameters used in this simulation are listed in Table 5.11.

Two simulations were run: one with dispersion values as listed in Table 5.11, and one with dispersion values set to zero. The time step used for both simulations was 200 seconds. Assuming that the domain is of unit width, the imposed flux of solute across the boundary F_i (g s^{-1}) (due to advection only) can be calculated as follows (Equation 5.5):

$$F_i = A.c_0.v_x.\theta \qquad 5.5$$

(for definition of symbols, see Table 5.11). The solute flux for this model specification was calculated to be 0.00119 g s^{-1}.

Despite the change in the values of dispersion, the value of the prescribed flux in the mass balance calculation always remained the same, at 0.00119 g s^{-1}. This showed that the mass balance calculation in SUBIEF2D does not take account of the flux of solute due to dispersion. This would probably not have been so noticeable in the original application of SUBIEF2D, for surface water transport problems, where the transport due to advection is generally much greater than the transport due to dispersion, but it becomes much more

noticeable in low velocity, groundwater flow cases. This means that the dispersive part of the flux is treated in the mass balance calculation as part of the error. The mass balance of these simulations cannot therefore be reliably quantified.

Table 5.11 Schedule of model runs for SUBIEF2D solute mass balance investigation.

Parameter		**Value**
Aquifer width	W	100 m
Lower limit of solute source	Y_1	20 m
Upper limit of solute source	Y_2	60 m
Area of boundary across which solute is imposed	A	42.5 m^2
Volumetric moisture content	θ	0.4 $m^3\ m^{-3}$
Average linear flow velocity in the x-direction	v_x	7.0×10^{-6} m s^{-1}
Average linear flow velocity in the y-direction	v_y	0.0 m s^{-1}
Longitudinal dispersivity	α_L	57.14 m
Dispersion along the flow	D_L	4.0×10^{-4} $m^2\ s^{-1}$
Transverse dispersivity	α_T	18.57 m
Dispersion across the flow	D_T	1.3×10^{-4} $m^2\ s^{-1}$
Solute concentration at source	c_0	10 mg l^{-1}

Further to this, the simulations revealed that even when dispersion was set to zero, where a perfect mass balance calculation would be expected, there was a significant error in the solution. After a run of 4000 seconds, the final mass in the domain should have equalled 4.76 g, providing that no tracer left the domain (and the domain was deliberately made large, and the simulation kept short, to ensure this). In fact, the final mass reported in the domain was 193.63 g, an excess of 188.87 g. This was despite the error on each time step being of the order of 1×10^{-14} g. Closer inspection of the results revealed that this error was entirely introduced during the first time step of the simulation, when a mass of 189.104 g was introduced into the domain, instead of 0.238 g (0.00119 g s^{-1} x 200 s).

The finite element technique works by linear interpolation of solute concentration across the elements. When the tracer concentration of 10 mg l^{-1} was introduced at the boundary (at the first time step), it produced a linear interpolation of solute concentration across the boundary elements between 10 mg l^{-1} (at the boundary) and 0 mg l^{-1} (the initial concentration inside the domain). So, although the tracer concentration was correct at the boundary, and correct at the first node inside the boundary, the distribution of tracer across the boundary element was incorrect, and generated the error in solute mass balance (Figure 5.55).

This error was also a problem when the imposed concentration at the boundary suddenly decreased. Although there was no analytical solution for comparison for this scenario, the problem can be seen in Figure 5.56. Figure 5.56a shows the pattern of solute concentration after 2000 seconds of the low dispersivity simulation. By this time, the concentration across the boundary element extended from 10 mg l^{-1} to 1.6 mg l^{-1}. Figure 5.56b shows the pattern of solute concentration at the next time step (2200 seconds), after the imposed solute concentration at the boundary was reduced to zero. The solute gradient was then linearly interpolated between zero on the boundary, and 1.6 mg l^{-1} inside the domain, which resulted in a sharp (and incorrect) drop in solute mass in the domain.

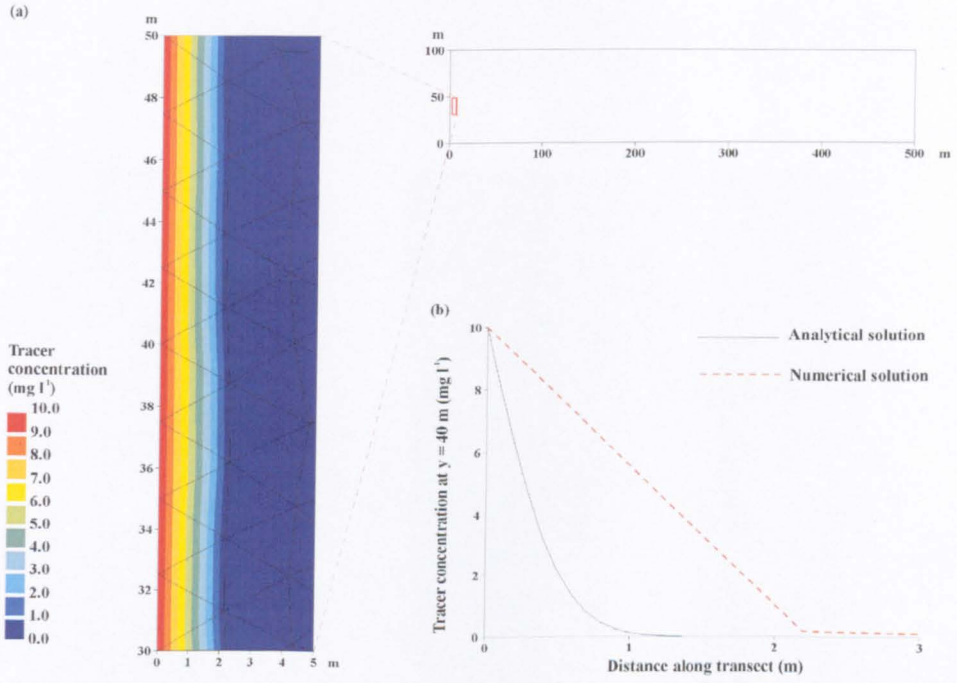

Figure 5.55 Diagram illustrating the generation of errors in solute mass balance in SUBIEF2D calculations. a) Pattern of solute concentration at the boundary after one timestep. b) Comparison of analytical solution and numerical solution after one timestep (200 seconds).

Reducing the element size at the boundary would reduce the magnitude of this problem but it would never be circumvented completely, and the increase in mesh density required may eventually render the system of model equations too large to be easily solved. This problem will cause difficulties during later interpretation of mass balance results, particularly between domains and between tracers, because the magnitude of the error will vary according to the length of the boundary domain involved, the dispersion parameters, and the element size at the boundary.

This global (domain wide) error in solute mass is introduced at the boundaries. It increases in magnitude as the dispersivity decreases (at higher dispersions, a linear interpolation becomes a more appropriate approximation to the true tracer dispersion within an element), and as the concentration gradient increases. As the concentration gradient across the boundary element is likely to be highest at the time in the simulation when flow is first directed into the domain across the boundary (or later in the simulation when flow is re-directed into the domain after a period of outflow across the boundary), this large increase in solute mass over the course of one time step may be revealed as a sharp jump in total mass in the domain. This sharp change will appear significantly larger than the succeeding changes in mass per time step. This may give the potential for a correction to be made to the solute mass balance output at the end of the simulation; this will be explored in Chapter 6 for the River Severn and Sleepers River domains individually.

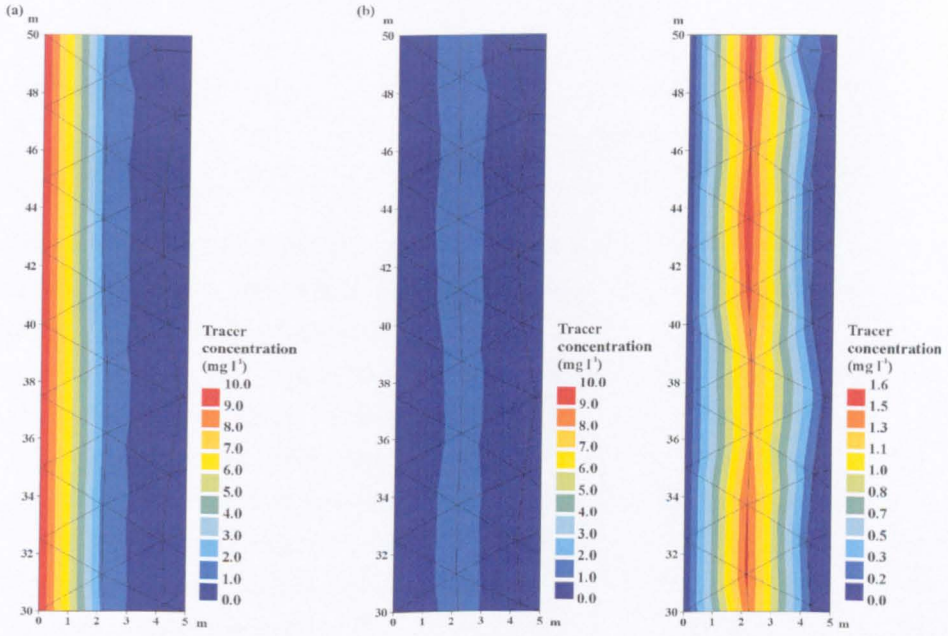

Figure 5.56 Pattern of solute concentration at the left hand boundary of the analytical mesh after a) 2000 seconds, with an imposed solute concentration at the boundary of 10 mg l^{-1}, and b) 2200 seconds, after the imposed solute concentration at the boundary has been reduced to zero. Note that the pattern of solute concentration in b) is plotted twice, on two different scales.

Error in the SUBIEF2D simulation is primarily introduced by this mechanism. To an extent, it can be taken into account during interpretation of the results, but it cannot be eliminated. Interpretation of the solute mass balance results must therefore be undertaken with caution. This error in the simulation has a much more negligible effect on the pattern of solute

concentration within the domain, and this aspect of the model output can be interpreted more reliably.

5.3.2.3 Sensitivity analysis

The River Severn model was used to assess the sensitivity of the SUBIEF2D results to two aspects of model configuration: (a) sensitivity to dispersivity, and (b) sensitivity to parameterisation of the soil hydraulic properties.

Table 5.12 Schedule of model runs for ESTEL2D-SUBIEF2D sensitivity analysis.

Run no.	Dispersivity (m)		Diffusion D* ($m^2 s^{-1}$)	Soil type	K_{sat} ($m s^{-1}$)
	Longitudinal	Transverse			
1	0.1	0.01	5×10^{-10}	Clay loam	5×10^{-5}
2	1.0	0.1	5×10^{-10}	Clay loam	5×10^{-5}
3	10.0	1.0	5×10^{-10}	Clay loam	5×10^{-5}
4	0.1	0.01	5×10^{-10}	Clay loam	1×10^{-4}
5	0.1	0.01	5×10^{-10}	Sandy loam	1×10^{-4}
6	0.1	0.01	0.0	Sandy loam	1×10^{-4}

Dispersivity values are difficult to estimate. It is well established that the magnitude of dispersivity changes, depending on the scale under consideration. For example, laboratory measurements of dispersivity yield values in the range of 10^{-2} to 1 cm, while field measurements can be as high as 10 to 100 m for regional aquifer studies (Anderson, 1979; Freeze and Cherry, 1979). During this sensitivity analysis, three sets of dispersion parameters within this broad range were tested (Runs 1-3, Table 5.12). Transverse dispersivity is typically 5-20 times smaller than longitudinal dispersivity (Freeze and Cherry, 1979), and this is also reflected in the choice of dispersion parameters for the sensitivity analysis, where the transverse dispersivity is specified as 10 times smaller than the longitudinal dispersivity (Table 5.12). The major ions in groundwater have diffusion coefficients in the range 1×10^{-9} to 2×10^{-9} $m^2 s^{-1}$ at 25°C (Freeze and Cherry, 1979). In porous media, these values are reduced by 50 to 99 per cent due to the effect of the solid phase of the porous medium on the diffusion; the value selected for this sensitivity analysis was 5×10^{-10} $m^2 s^{-1}$ (50 per cent of 1×10^{-9} $m^2 s^{-1}$).

To test the sensitivity of the SUBIEF2D results to uncertainty in the hydrological representation of the domain, three different River Severn hydrological results files for flood event D were used as input to the SUBIEF2D code: two using a clay loam representation of the soil (with two different values of saturated hydraulic conductivity), and the other using a

sandy loam representation (Runs 1, 4 and 5, Table 5.12). These three representations were chosen because they gave very similar predictions of hydraulic head, which matched the observed hydraulic head values to a reasonable degree, and yet the characterisation of water fluxes through the domain and representation of the unsaturated zone for each simulation was quite distinct. Each simulation used a 200 second time step.

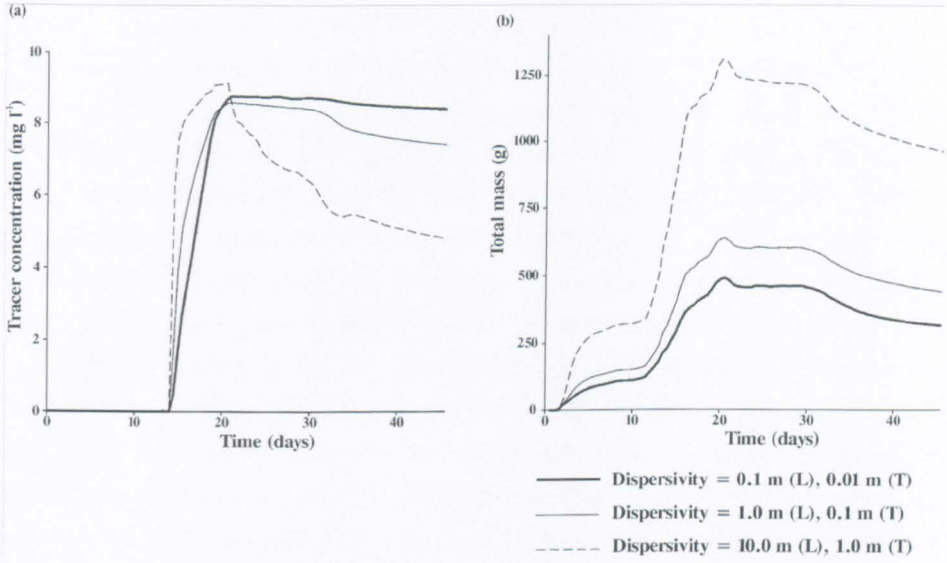

Figure 5.57 a) Change in solute concentration over time at the point x = 50 m, y = 27 m and b) change in total solute mass in the domain over time, for three different values of dispersivity.

Figure 5.57a shows how solute concentration changed over time at one point in the domain (x = 50 m, y = 27 m), approximately halfway between the hillslope boundary of the floodplain and the river, and close to the floodplain surface. After approximately 20 days (by which time the river water had extended over the floodplain surface), the solute concentration for all values of dispersivity had reached a peak. This peak was slightly higher for the highest dispersivity values. Differences in solute concentration resulting from the three levels of dispersivity were more noticeable as the river stage began to drop. Even though input of solute from the river ceased after 20 days of the simulation, the solute concentration hardly decreased where the dispersivity values were low. Where dispersivity values were higher, the solute concentration decreased more rapidly. However, although the concentration may have been lower, Figure 5.57b shows that at the higher level of dispersivity, a much greater mass of solute was introduced to the domain.

Figure 5.58 shows how the level of dispersivity affected the pattern of solute concentration in the domain at the end of the 45.5 day flood event simulation. At low levels of dispersivity, the plume of solute was restricted to the upper 5 m of the domain. As the level

of dispersivity increased, the solute plume became increasingly smoothed at its margins, and the concentration within the plume decreased. At the highest level of dispersivity, the solute plume extended much deeper into the domain. Changing the value of diffusion (run 6, Table 5.12) had no visible effect on the model output in terms of solute concentration or total solute mass.

Figure 5.59 shows the effect of soil hydraulic properties on a) the change in solute concentration over time at one point in the domain, and b) change in total solute mass over time. In comparing the two simulations using clay loam soil properties, it can be seen that as the value of saturated hydraulic conductivity decreased, the total solute mass introduced to the domain decreased, and the solute concentration at a point was also slightly lower. In comparing the two simulations with saturated hydraulic conductivity of 1×10^{-4} m s^{-1}, it can be seen that the sandy loam soil allowed a greater mass of solute to infiltrate the domain than the clay loam soil. Even though the saturated hydraulic conductivity was the same, the difference in conductivity in the unsaturated region (as generated by the soil model properties) allowed water and solute to move more rapidly through the sandy loam soil. This also meant that after the flood peak had passed, and solute was dispersing through the domain, the solute concentration decreased to a greater extent in the case of the sandy loam soil than the clay loam soil. This is reflected in Figure 5.60, which shows the pattern of solute concentration in the domain at the end of the flood event. In the case of the sandy loam soil, more solute had infiltrated and dispersed deeper into the domain than in the case of the clay loam soil.

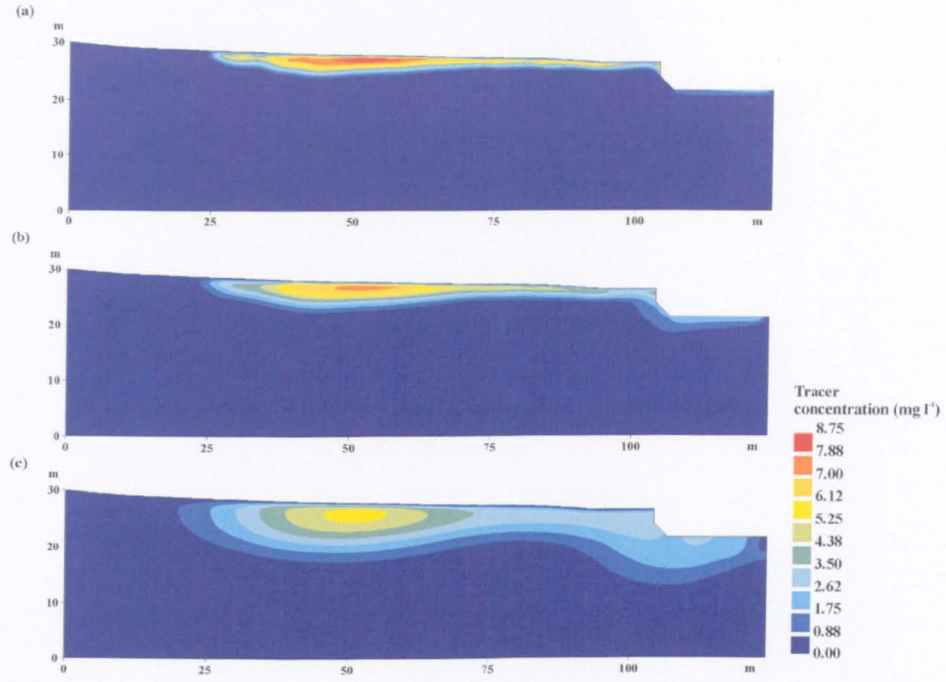

Figure 5.58 Pattern of solute concentration in the domain at the end of the 45.5 day flood event simulation with a) low dispersivity (run 1), b) medium dispersivity (run 2) and c) high dispersivity (run 3).

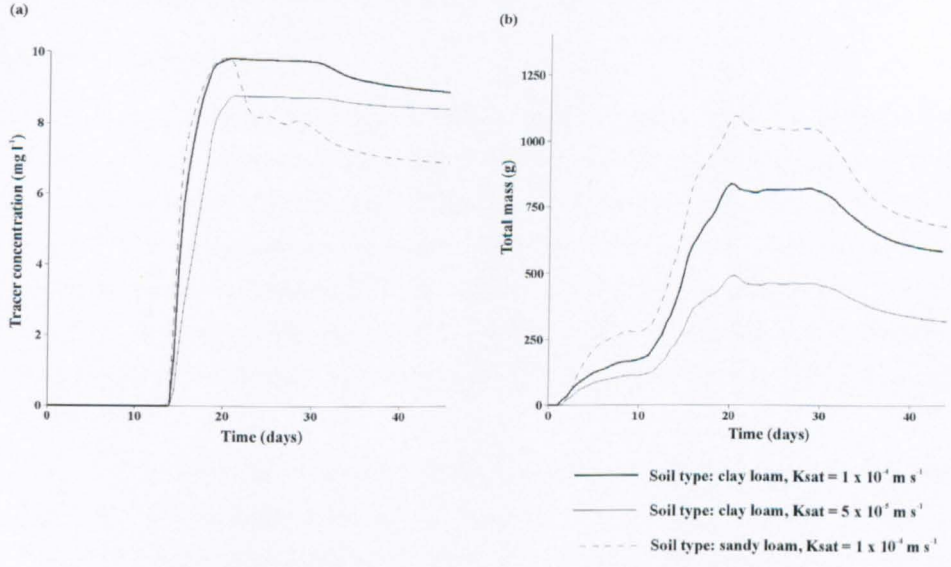

Figure 5.59 a) Change in solute concentration over time at the point x = 50 m, y = 27 m and b) change in total solute mass in the domain over time, for three different soil type/saturated hydraulic conductivity combinations.

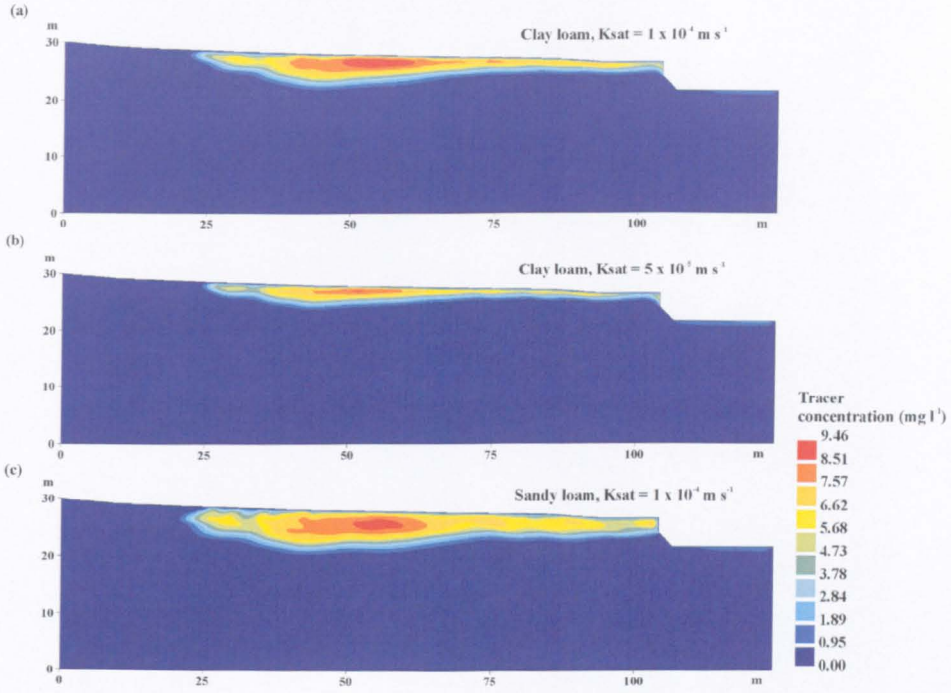

Figure 5.60 Pattern of solute concentration in the domain at the end of the 45.5 day flood event simulation with a) clay loam soil, saturated hydraulic conductivity = 1 x 10^{-4} m s^{-1} (run 4), b) clay loam soil, saturated hydraulic conductivity = 5 x 10^{-5} m s^{-1} (run 2) and c) sandy loam soil, saturated hydraulic conductivity = 1 x 10^{-4} m s^{-1} (run 5).

5.3.2.4 Calibration

As the extent of field site chemistry data was limited, the testing of the SUBIEF2D model subsequent to the optimisation process and sensitivity analysis was restricted to a calibration exercise only, instead of the preferred calibration and validation process. The chemistry data set came from the Sleepers snowmelt event of 1996. During the course of this event, the piezometer nests were sampled for $\delta^{18}O$ on seven occasions. Oxygen-18 has been chosen for this study because it can be modelled without further assumptions about chemical transformation; it is actually a component of the water, reflecting the water source and mixing history.

The boundary conditions for this simulation were set up according to the illustration in Figure 5.61. The measured concentrations at several piezometer locations were used as the basis for the chemical boundary conditions. The temporal concentration profiles used as input to the simulation are illustrated in Figure 5.62 to Figure 5.65.

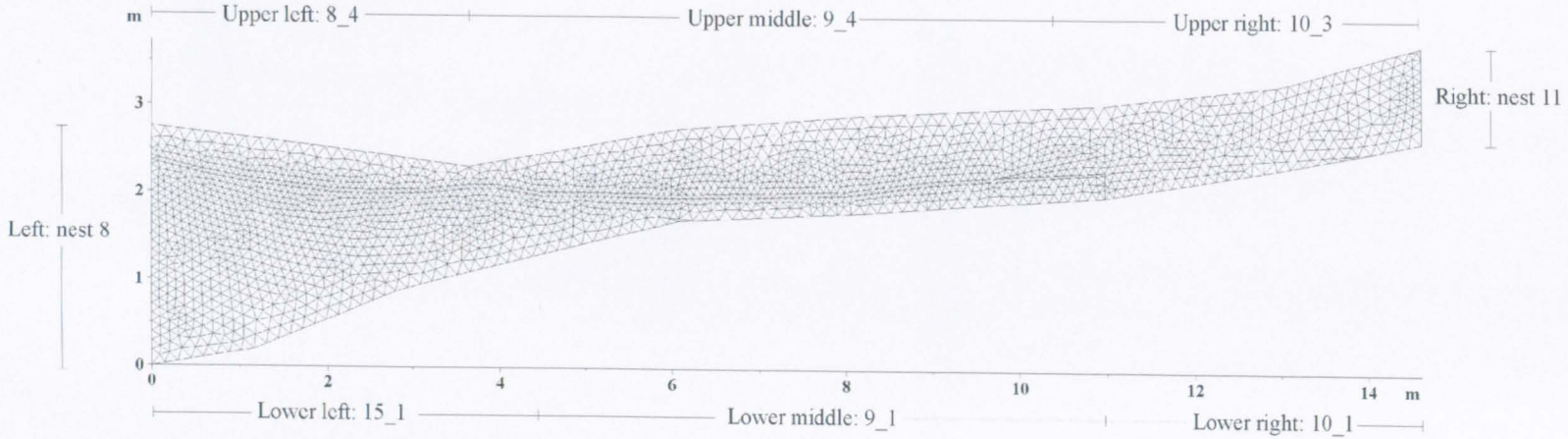

Figure 5.61 Diagram indicating the chemical boundary conditions used for the Sleepers River SUBIEF2D simulation.

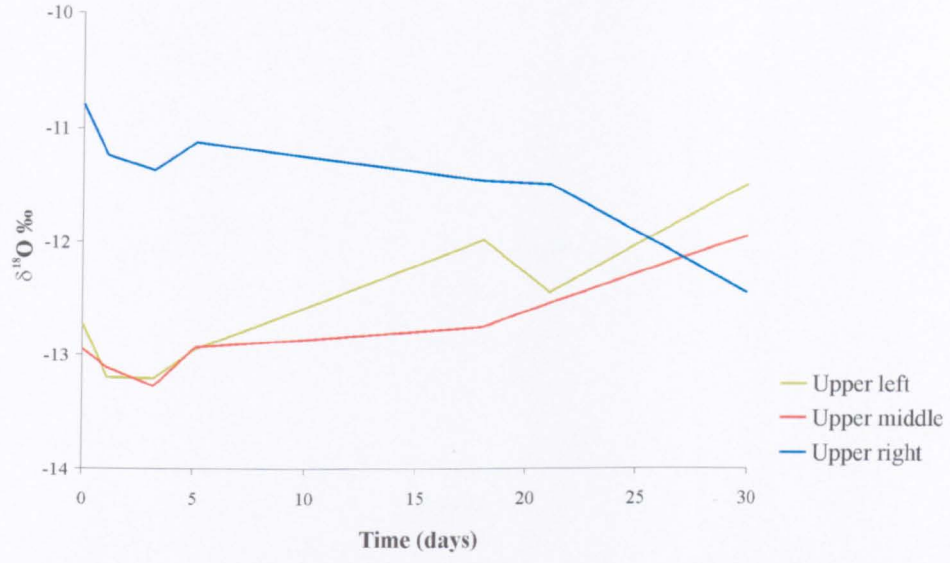

Figure 5.62 Graph illustrating the $\delta^{18}O$ boundary conditions imposed at the upper boundary of the Sleepers River domain for the snowmelt event SUBIEF2D simulation.

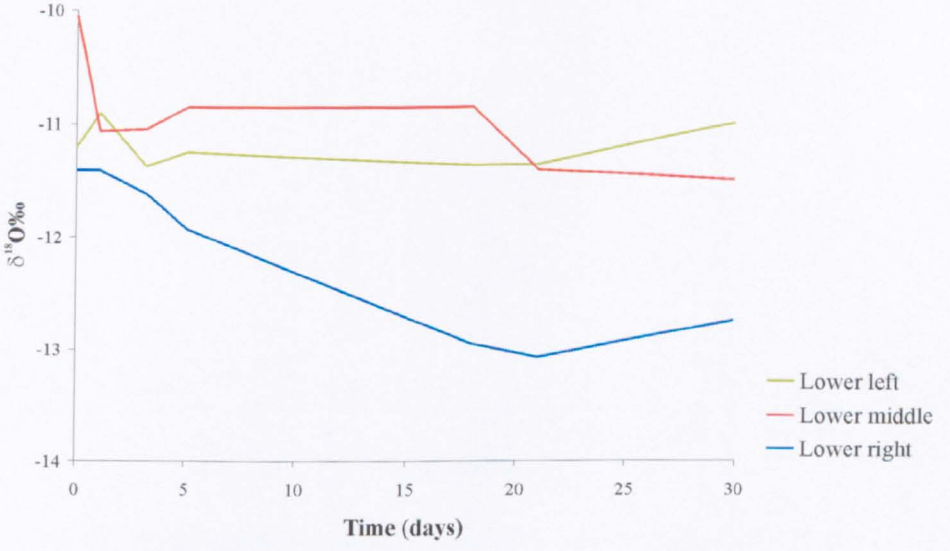

Figure 5.63 Graph illustrating the $\delta^{18}O$ boundary conditions imposed at the lower boundary of the Sleepers River domain for the snowmelt event SUBIEF2D simulation.

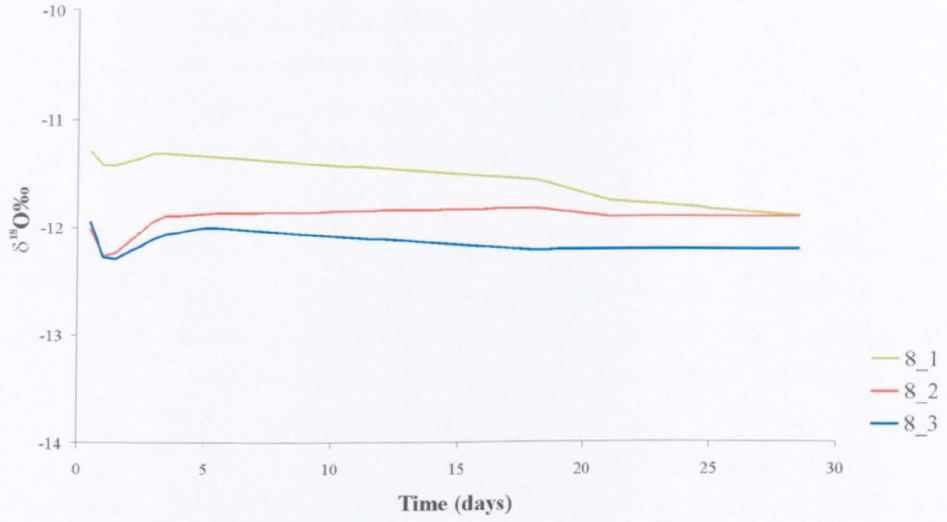

Figure 5.64 Graph illustrating the $\delta^{18}O$ boundary conditions imposed at the left hand side boundary of the Sleepers River domain for the snowmelt event SUBIEF2D simulation.

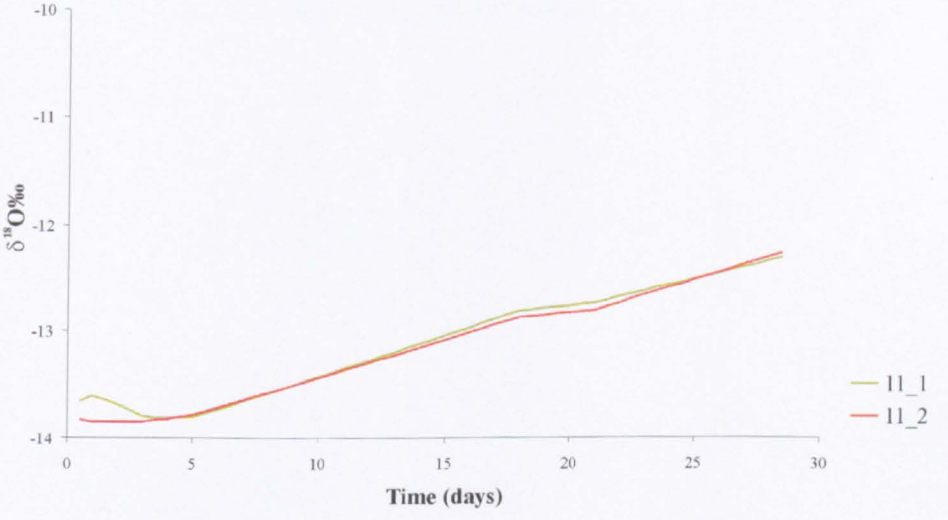

Figure 5.65 Graph illustrating the $\delta^{18}O$ boundary conditions imposed at the right hand side boundary of the Sleepers River domain for the snowmelt event SUBIEF2D simulation.

The concentrations on the right and left hand boundaries were set by the concentrations measured in nests 8 and 11. The concentrations along the upper and lower boundaries of the domain were divided into three sections: right, middle and left. The surface concentration on the left was set according to the concentration of $\delta^{18}O$ measured in shallow piezometer 8_4 (a porous cup installed 8-12 cm below the soil surface). The surface concentration in the

middle was set according to the concentration measured in shallow piezometer 9_4. The surface concentration on the right was set according to the concentration in piezometer 10_3. The concentrations of groundwater input were based on the concentrations measured in the piezometers closest to the bedrock in nest 15 (lower left), nest 9 (lower middle) and nest 10 (lower right).

The concentrations within the domain at the start of the simulation were initialised using an interpolation routine. First, each piezometer point within the domain was allocated with the concentration measured in that piezometer at the start of the event. The concentration was then interpolated between these points to initialise the concentration throughout the whole domain.The results of the simulation are shown in Figure 5.66 to Figure 5.68. These graphs show the observed and simulated $\delta^{18}O$ concentrations over the 29 day snowmelt event. The simulated concentrations of $\delta^{18}O$ in nest 15 were of the right magnitude (–11.5 to –11.0 ppt) but did not reproduce the observed change in concentration with depth (the concentration in piezometer 15_2 should have been less negative than the concentration in piezometer 15_1, Figure 5.66). This may reflect the failure to capture the correct pattern of water flow in the hydrological simulation, where simulated flow was directed slightly upwards, instead of following the observed, downward movement of water.

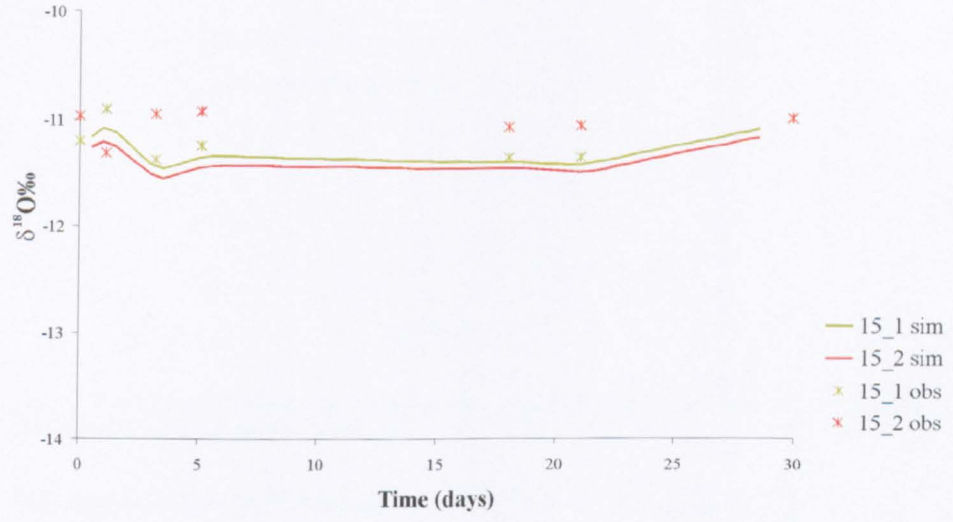

Figure 5.66 Graph comparing observed (stars) and simulated (lines) $\delta^{18}O$ concentrations for nest 15 of the Sleepers River domain.

The concentrations in nest 9 were reasonably well replicated in the fact that the vertical pattern of chemical concentration was correct (the concentration of $\delta^{18}O$ became less negative with depth, Figure 5.67). The reproduction of the pattern of $\delta^{18}O$ concentration

change over time varied between the three piezometers. Piezometer 9_1 was well replicated because the boundary concentration of groundwater input directly beneath it was the concentration observed in piezometer 9_1. The pattern of concentration change over time was also well modelled for piezometer 9_2, but the modelled concentration was too negative. This may have been a result of some uncertainty over the location of this piezometer, and whether it was located above or below the dense till layer. Its response should have been much closer to that of piezometer 9_1 (the lower piezometer in the nest). In the model it was located in the riparian peat, which gave it a modelled response closer to piezometer 9_3, which was also in the riparian peat.

The concentrations in nest 10 were also well replicated in that the concentration varied with depth in the correct manner, becoming more negative with depth (Figure 5.68). The simulated concentrations in each piezometer were, however, closer together than the observed concentrations.

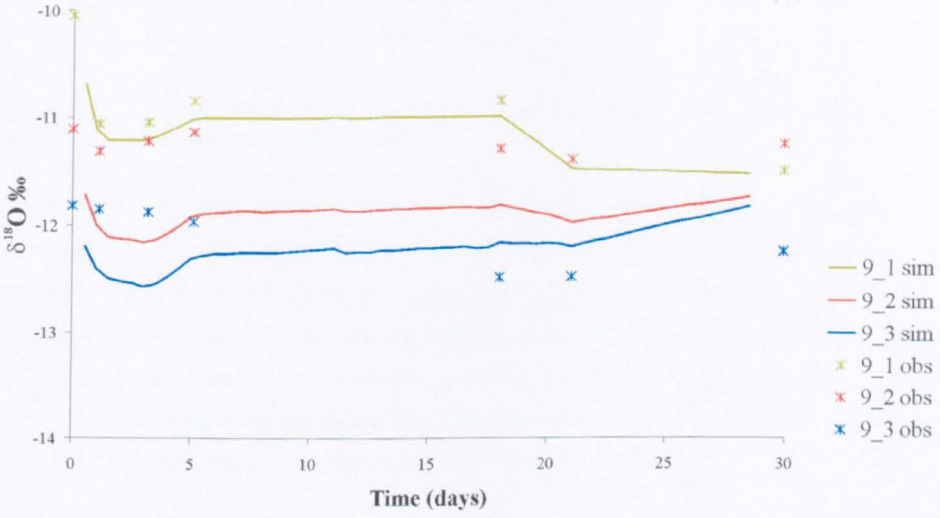

Figure 5.67 Graph comparing observed (stars) and simulated (lines) $\delta^{18}O$ concentrations for nest 9 of the Sleepers River domain.

The observed pattern of $\delta^{18}O$ concentration was almost identical in both piezometer 9_2 and 15_2, although the concentrations were slightly less negative in piezometer 15_2. This is interesting because the concentrations in these piezometers were not particularly well reproduced by the model, and they were both situated in or close to the dense till layer in the field. This suggests that there may be some hydrological connectivity between the two piezometers that was not well captured by the model. In turn, this may be because the positions of these piezometers relative to the dense till layer is crucial and has not been

characterised properly, either during field measurement or during the finite element mesh construction. The possibility of the discrepancy being due to surveying errors was discussed in Section 5.3.1.5.

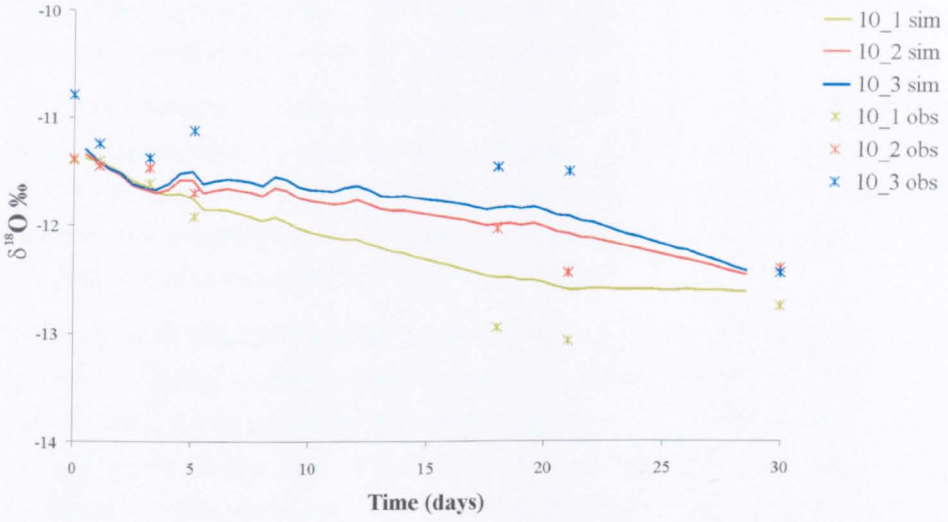

Figure 5.68 Graph comparing observed (stars) and simulated (lines) $\delta^{18}O$ concentrations for nest 10 of the Sleepers River domain.

In summary, replication of the observed $\delta^{18}O$ data has been complicated by the uncertainty in the hydrological field data caused by possible time-lag errors in the piezometer measurements of pressure head, and surveying errors in the location of the piezometers. This exercise has served to illustrate the difficulties in generating a detailed hydrological and chemical transport model representation of such a complex upland riparian zone. Further interpretation of these results, in terms of implications for the understanding of floodplain hydrological processes, will be explored in the following chapter.

5.4 Chapter summary

This chapter has presented the rationale for, and the results of, an extensive programme of model assessment. Several key aspects of the model assessment procedure have been discussed. The choice of output parameters to compare and analyse during model testing is important, because it can potentially have a big impact on the conclusions of the assessment process. This chapter has highlighted how analysis of model results based on only one state variable (e.g. pressure head, water-table elevation) could disguise problems or unrealistic behaviour in other aspects of model performance. In this case, a faithful representation of pressure head distribution is a necessary, but not sufficient, pre-requisite for accurate simulation of chemical transport. Therefore, even though the data required for validating

water fluxes and saturation extent are lacking, the modeller must be prepared to look beyond one simple hydrological indicator (e.g. water-table elevation) to consider whether the wider elements of the hydrological picture (e.g. saturation extent, seepage face development) at least appear intuitively realistic. This brings some 'softer' evaluation techniques to the assessment procedure in the form of hydrological expertise.

This chapter has also demonstrated how model results can be just as sensitive to boundary condition specification as to soil parameter specification. Although this may seem somewhat intuitive, the potential impacts of boundary condition assumptions on model results have received little consideration in the hydrological modelling literature; most attention is generally devoted to the impacts of parameter representation.

The coupled ESTEL2D-SUBIEF2D model has now undergone a rigorous assessment procedure, including extensive validation using high temporal resolution flood event data from a lowland floodplain, and hydrological and isotopic snowmelt event data from a highly complex upland riparian zone. This has fulfilled stages three and four of the research methodology outlined in Section 2.2.2. This gives confidence that the model is working as intended, and can be used to investigate new combinations of parameters to explore theories about how floodplain hydrological and chemical transport processes operate. These theories will be investigated during a set of hypothetical scenario simulations in Chapter 6 and Chapter 7.

6 Exploring Floodplain Hydrological and Chemical Transport Processes

During Chapter 5 an extensive programme of model assessment was undertaken. This gives confidence in the ability of the model to represent floodplain hydrological and chemical systems, and permits an extension of this study into consideration of new parameter combinations in order to explore floodplain processes.

> Even a partially validated model may tell us more about processes than continued and unfocused empirical investigation.
>
> (Bates and Anderson, 2001)

These hypothetical tests employed in this chapter are, in practice, an extension of the sensitivity analysis of Chapter 5, and will form the fulfilment of the fifth and final stage of the research methodology outlined in Section 2.2.2: investigate floodplain hydrological and biogeochemical dynamics through further model development and use a range of hypothetical scenarios to investigate the hypotheses outlined in Section 2.2.1.

This chapter will begin by looking at the process inference that can be drawn from the model sensitivity and validation results presented in Chapter 5. Thus far, these results have only been discussed with reference to model operation issues, not in terms of the information they provide about process operation in floodplain environments. These process implications will then be explored more fully using a hypothetical tracer to investigate more specific hypotheses.

6.1 Initial process inference from model assessment results

The ESTEL2D and coupled ESTEL2D-SUBIEF2D model validation simulations used in Chapter 5 can now be explored in more detail to look at process inference in the floodplain zone. The use of the numerical model is important because it enables the visualisation and interpretation of water flow paths and fluxes, which cannot be revealed by the field piezometric data alone. The general patterns of water flow during a flood event are described in the following section.

6.1.1 Description of River Severn flow processes

At the start of a flood event, the hydraulic gradient is established in a hillslope to river direction. Water flows into the floodplain from the hillslope and out of the floodplain via the river bed and banks into the river channel (Figure 6.1a).

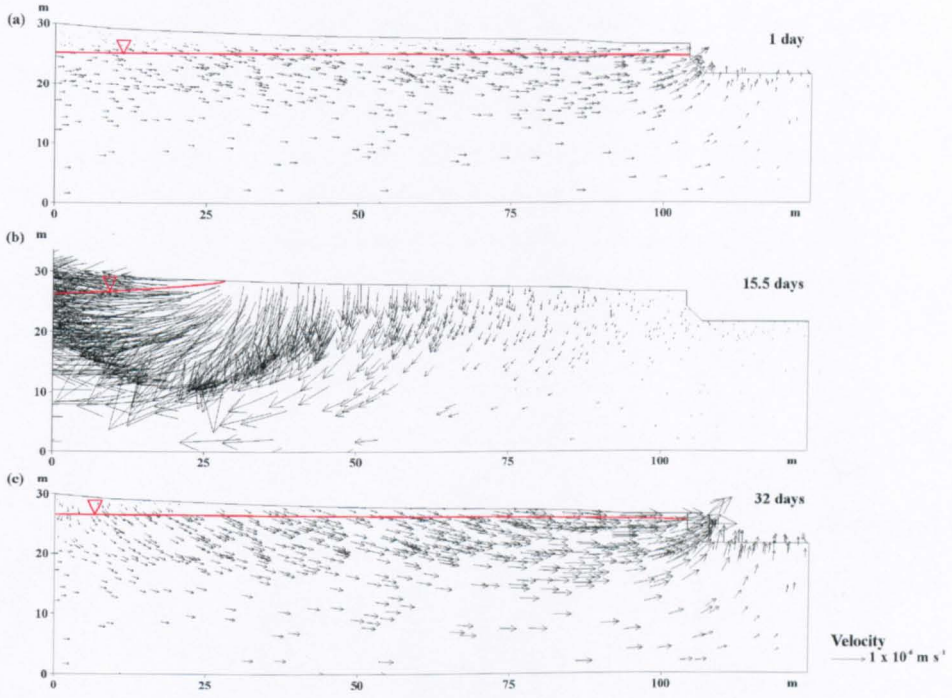

Figure 6.1 Darcian velocity vector patterns during flood event D on transect S at (a) 1 day, (b) 15.5 days, and (c) 32 days. Red line shows the position of the water-table.

At this point the water-table is up to 5 m below the floodplain surface. As the river stage begins to rise, the hydraulic gradient is reversed, and water begins to flow in a river-to-hillslope direction through the floodplain. As channel flow goes overbank and begins to inundate the floodplain surface, a steep hydraulic gradient is produced at the floodplain surface that generates high velocity water flow into the floodplain across the floodplain surface. This infiltrating water is directed towards the hillslope at depth as a result of the overriding river-to-hillslope hydraulic gradient (Figure 6.1b). This region of high velocity water flow moves towards the hillslope as the region of inundation extends across the floodplain towards the hillslope. By comparison, the region near the river channel is subjected to decreasing water velocities. At this time the water-table extends to the surface to meet the inundation surface; the model results, in conjunction with the measured piezometric data, indicate no unsaturated wedge beneath the inundated section of floodplain.

As the water stage falls in the channel, the hydraulic gradient once again reverses and water flows in a hillslope-to-river direction (Figure 6.1c).

While the velocity vector diagrams indicate the pattern of water movement within the floodplain, it is also interesting to look at the magnitude of water fluxes through the model boundaries. Figure 6.2 illustrates water fluxes through the model boundaries during two flood events, E and F. The first diagram in each pair shows the water flux for the whole length of the boundary (imagining that the two dimensional domain is of unit width allows the expression of water flux in units of $m^3\ s^{-1}$ rather than the less intuitive $m^2\ s^{-1}$). The second diagram gives an idea of the water flux per unit length of the boundary, bearing in mind that the length of the hillslope boundary is an artefact of the model domain discretisation, and the channel boundary in the model is an approximation and really only represents half the true channel boundary. The labelling convention in these diagrams is such that positive values of water flux represent flux into the floodplain, and negative values represent fluxes out of the floodplain.

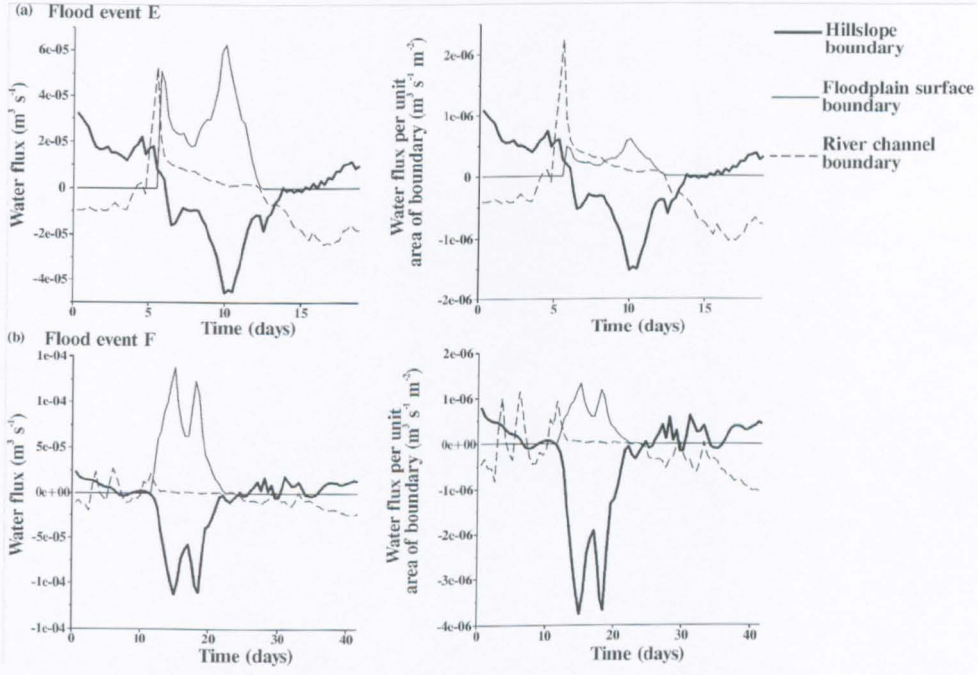

Figure 6.2 Flux of water across model boundaries for (a) flood event E and (b) flood event F.

These flux diagrams confirm the patterns indicated by the Darcian velocity vector diagrams. They also give an indication of the magnitude of water flux across each floodplain boundary, but as the magnitude of water flux is sensitive to errors in the saturated hydraulic

conductivity parameterisation, the interpretation of actual flux values is made with caution. At the beginning and end of the event, there is a flux of water out of the domain across the river channel boundary. This is generally matched by a flux of water into the domain through the hillslope boundary. Superimposed on this general pattern can be seen some small scale fluctuations in the flux across the river channel boundary and hillslope boundary, which reflect responses to localised changes in hydraulic gradient. During flood event F, the relationship between the river channel boundary fluxes and hillslope boundary fluxes is different at the beginning and end of the event. At the beginning of the event, before the main period of inundation, there are small scale fluctuations in the flux across the river channel boundary which are not reflected in fluxes across the hillslope boundary (Figure 6.2b). At the end of the event (post-inundation) these small scale fluctuations occur in both the hillslope and river channel boundary fluxes, with an increase in the influx of water across the river channel boundary corresponding with an increase in the outward flux of water across the hillslope boundary, and vice versa. This probably reflects the more highly saturated condition of the floodplain at the end of the event, which means that local changes in hydraulic head can be transmitted much more rapidly across the floodplain to the opposite boundary. In contrast, at the beginning of the event, there is a significant lag time before the effect of an event in one part of the domain is felt in another.

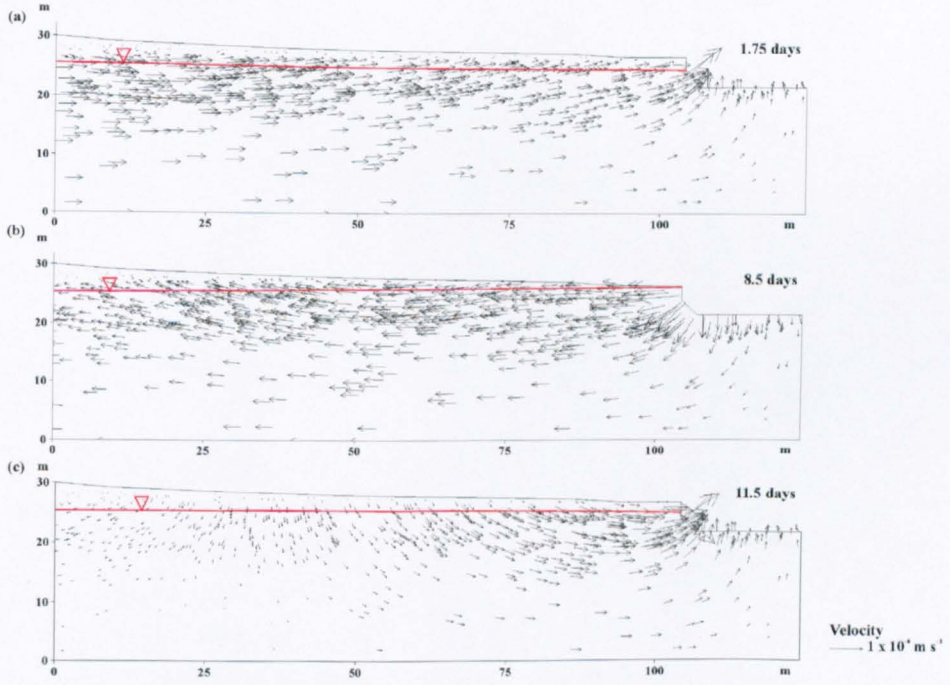

Figure 6.3 Darcian velocity vector patterns during bankfull event A on transect S at (a) 1.75 days, (b) 8.5 days, and (c) 11.5 days. Red line shows the position of the water-table.

During the overbank part of the flood event, there is a significant flux of water across the floodplain surface. At the start and end of the simulation the rainfall flux through the floodplain surface is so small in magnitude in comparison with the rest of the water fluxes that it does not show up on the diagram. The timing of this flux of water through the floodplain surface during the overbank part of the flood event corresponds to the timing of a significant flux out of the floodplain through the hillslope boundary. The near-synchronous nature of these fluxes may be a reflection of the near-saturated nature of the floodplain material at this time. During this period of the flood event, the flux of water though the channel bed and banks becomes negligible, reflecting the very low velocity vectors seen at this time in the earlier diagram (Figure 6.1b).

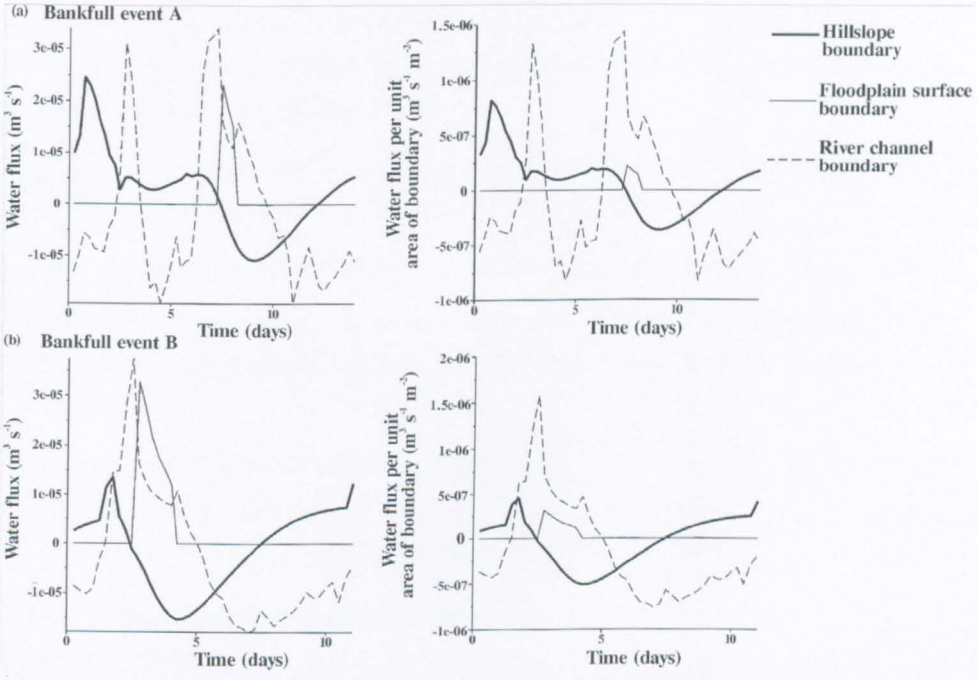

Figure 6.4 Flux of water across model boundaries for (a) bankfull event A and (b) bankfull event B.

An interesting comparison can be made between the overbank flood events and the bankfull flood events. In terms of water flux through the floodplain boundaries, the infiltration through the floodplain surface during the bankfull flood events is, unsurprisingly, quite small (this is indicated particularly well by the flux per unit area diagrams, Figure 6.4). The response of the water flux across the river channel and hillslope boundaries is more revealing. In the case of the bankfull events, the peak in loss of water from the floodplain across the hillslope boundary does not match the peak in infiltration of water into the

floodplain across the river channel boundary, whereas in the case of the overbank flood event, these two fluxes are almost synchronous, for example, at peak inundation (10 days) during flood event E (Figure 6.2a). Once again, this probably reflects the difference in degree of saturation of the floodplain in these two cases. Under the more fully saturated overbank flood conditions, the effect of the water infiltrating across the river channel boundary is transmitted much more rapidly to the hillslope boundary than under less saturated, bankfull flood conditions, because as the level of saturation decreases, the effective hydraulic conductivity also decreases.

6.1.2 Analysis of River Severn flow processes

Analysis of the results of the River Severn model runs can begin by reference to some initial simulations of this fieldsite reported in Bates *et al.* (2000). This will draw on ESTEL2D results as obtained during the model assessment process (Chapter 5) that will be used to look at process inference in this floodplain zone.

The Bates *et al.* (2000) paper made three main process inferences, which will be examined here in the light of the simulations carried out thus far in this study:

1. The unsaturated zone in the floodplain is not significant during overbank flood events.
2. Floodplain water movement is predominantly a 2D lateral process during flood events, although 3D processes may become more significant towards the beginning and end of the event.
3. Groundwater ridge formation takes place during overbank flood events, and this process appears to be distinctly different from the groundwater ridging operating on hillslopes, with flow being directed towards the hillslope rather than the channel.

6.1.2.1 Importance of the unsaturated zone

The inference that the unsaturated zone in the River Severn floodplain is not significant was drawn on the basis of soil hydraulic parameters that were inadvertently prescribed incorrectly. The study of Bates *et al.* (2000) used a van Genuchten soil water retention model to describe the floodplain soil, but the value of α, which is comparable to the inverse of the air entry value of the Brooks and Corey model, was inadvertently prescribed 10^4 times too small (in the case of the loamy sand, 0.0004 m^{-1} instead of 4.0 m^{-1}). This is equivalent to introducing a capillary fringe of 2500 m instead of 0.25 m. As the zone above the water-table is approximately 5 m wide at its greatest extent, this very small α value results in the entire domain being virtually 100 per cent saturated at all times, and the interpretation of the results was based on simulations where there was effectively no unsaturated zone.

This conclusion must now be re-evaluated in the light of new simulations in this study which make use of more appropriate model parameters. The new simulations indicate a more realistic pattern of water flow in the domain, with horizontal flow in the saturated zone, and vertical flow in the unsaturated zone, which is also of a smaller magnitude due to the reduced hydraulic conductivity in this area (e.g. Figure 6.1a).

The sensitivity analysis revealed a sensitivity to soil hydraulic parameters which naturally was not discovered in the previous study. Of particular note is the sensitivity to the value of saturated hydraulic conductivity (K_{sat}). In the Bates *et al.* (2000) simulations, changing K_{sat} made no difference to the predicted hydraulic head. In addition, although the water fluxes across the boundaries of the domain were scaled according to the value of K_{sat}, the *pattern* of water flux was not affected. The introduction of the more realistic representation of the unsaturated zone changes these findings completely.

With changing K_{sat}, the predicted pressure head within the domain changes noticeably (Figure 6.5, reproduced from Chapter 5). This basically reflects a change in the way the water moves through the unsaturated zone, and hence a change in process operation associated with the change in K_{sat}. As K_{sat} decreases, the hydraulic conductivity in the unsaturated zone becomes too low to allow all the precipitation that is imposed on the surface boundary of the domain to infiltrate. This means that the predicted hydraulic head at the beginning of the flood event does not rise as quickly as has been observed in the field. At very low values of K_{sat}, the onset of overbank flow during a flood event is associated with the development of a perched water-table near the river channel, extending across the floodplain as the extent of floodplain inundation increases. This is because the hydraulic conductivity in the unsaturated zone near the floodplain surface is too low to allow water to percolate to the water-table. It is therefore possible to distinguish between two separate behaviour types during overbank flow, which can be turned on and off by changing the value of K_{sat}; situations where a perched water-table develops, and situations where the main water-table quickly rises to the floodplain surface. These two situations are characterised by very different patterns of hydraulic head within the domain. On the basis of field measurements of hydraulic head it is therefore possible to judge which outcome is more likely. In the River Severn case, the predicted hydraulic head associated with the perched water-table formation is not at all like the observed hydraulic head; the predicted hydraulic head values therefore indicate that the water-table rises quickly after floodplain inundation, implying a relatively high value of K_{sat}.

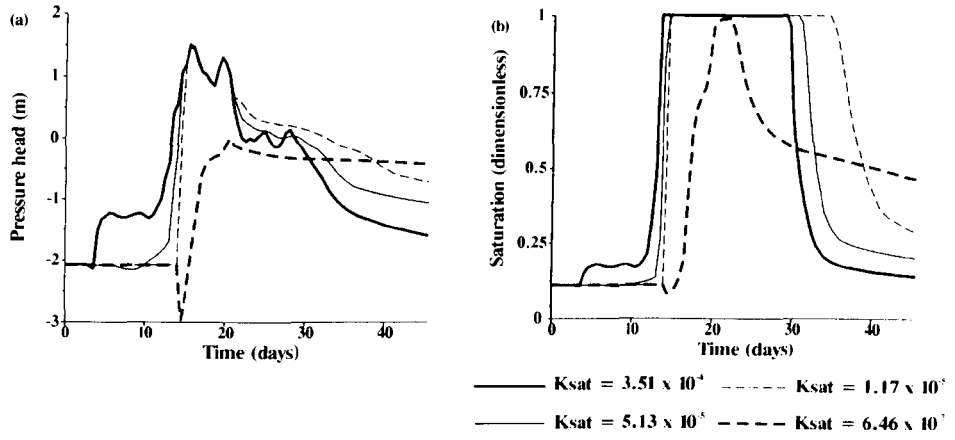

Figure 6.5 Graphs showing the effect of changing the saturated hydraulic conductivity (K_{sat}) of a sandy loam soil on predictions of (a) pressure head and (b) saturation, at the point x = 50 m, y = 27 m. Reproduced from Chapter 5.

The earlier simulations of Bates *et al.* (2000) essentially provide an example of how the floodplain system would behave if it were totally saturated. These results indicate that changing the value of K_{sat} would have no effect on the pattern of water fluxes through the domain, although the absolute magnitude of the fluxes would be scaled with the value of K_{sat}. The results presented in this study show that with a more realistic representation of the unsaturated zone, K_{sat} does have a big influence on the pattern of water fluxes. The pattern of flux though the hillslope boundary is quite different between different values of saturated hydraulic conductivity, and is not a simple scaling of the fluxes according to the value of K_{sat}. As the same behaviour was not observed in the fully saturated case of Bates *et al.* (2000), this indicates that the unsaturated zone does have an important role to play in the hydrological operation of this lowland floodplain environment. Changing the value of K_{sat} essentially changes the process operation of the unsaturated zone.

An additional implication of the whole domain being saturated in the Bates *et al.* (2000) simulations is that with no proper treatment of storage, the transient simulations essentially operated as a series of steady states, instead of demonstrating truly transient behaviour. The reason for this behaviour was outlined in Chapter 4. The fundamental feature that distinguishes transient fluid flow from the steady state case is the phenomenon of change in stored fluid mass (Narasimhan, 1979), so as the moisture content reached saturation in the Bates *et al.* (2000) simulations, no changes in water storage could occur.

The incorrect soil parameter specification was also observed to have a significant impact on simulation time, and on the rate of convergence of the numerical solution. Where soil conditions are unsaturated, the non-linearities of the soil water retention model can hinder rapid model convergence. In the Bates *et al.* (2000) simulations the domain was fully

saturated, so the non-linearities of the unsaturated zone were avoided, and the simulations ran quickly and converged easily to a solution. In the simulations reported in this study, the presence of an unsaturated zone (up to 5 m in depth) in the domain generally made the simulations much slower, and many more problems of numerical stability and convergence were encountered. For example, the simulation of a 45 day flood event was reported by Bates *et al.* (2000) to take 21 minutes. A simulation of the same flood event in this study, using a van Genuchten soil water retention model, took over 7 hours to run (see Table 5.4).

6.1.2.2 2D and 3D floodplain flow processes

The inference that the River Severn floodplain water movement is predominantly a 2D process was made by comparing the observed and predicted hydraulic head profiles. These seemed to indicate that the fit between observed and simulated hydraulic head was generally good, and a more complex, 3D approach to the problem was not justified. More specifically, however, it seemed that the fit was better during the peak of the flood event, but that there tended to be larger discrepancies between the observed and predicted data towards the beginning and end of the event. For example, in Figure 6.6 this effect is particularly noticeable for piezometers S3 and H4. This was taken to indicate that 3D processes may have greater significance at the beginning and end of flood events (Bates *et al.*, 2000). However, a reappraisal of the field data during the course of this study has indicated that the poor fit may be due to less reliable pressure head measurements at the beginning and end of flood events. These times correspond to periods of lower water-tables, when the level of the water-table may in fact fall below the level of the piezometers. As the vibrating wire piezometers installed at the River Severn fieldsite are only designed to record positive pore water pressures, the piezometer output may well become unreliable at these times.

The hydraulic head value at which this happens for each piezometer is indicated in Figure 6.6. It can clearly be seen that in the case of the two poorly fitting results (S3 and H4), the value of hydraulic head taken as 'measured' in fact corresponds to the minimum value that it was possible to measure reliably with that piezometer. This does not discount the possibility of an element of 3D flow at the beginning and end of the flood event, but the error introduced by the unreliable piezometer measurements must at least contribute to the discrepancy that is observed. In general, the evidence is that groundwater flow during flood events is 2D lateral across the floodplain and that a profile model oriented perpendicular to the channel will be parallel to the main groundwater flow path.

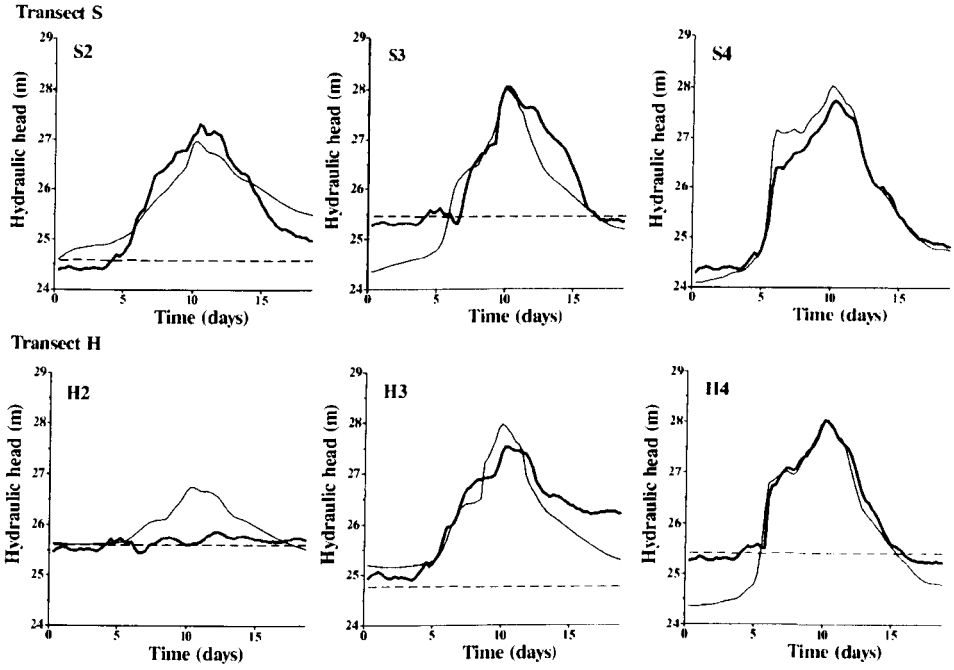

Figure 6.6 Graphs comparing observed (thick line) and simulated (thin line) hydraulic head, for transects S and H. Dotted line indicates minimum reliable piezometer measurement. Reproduced from Chapter 5.

6.1.2.3 Groundwater ridging effects

The new simulations indicate the development of a strong 'groundwater ridge' at the inundation front which is in agreement with the findings of the Bates *et al.* (2000) simulations. The Darcian velocity vectors indicate a strong influx of water through the floodplain surface near the inundation front, directed towards the hillslope at depth (Figure 6.7). This is a direct result of the hydraulic gradient imposed by the boundary conditions, and is in contrast to the classic view of a groundwater ridge in a hillslope-channel section (with no intervening floodplain), where the groundwater ridge causes flow to develop in a hillslope-channel direction (Sklash, 1990).

The newly developed, coupled model in this study will now be used to explore whether "such flows may even result in a movement of surface water into hillslope areas" (Bates *et al.*, 2000). By introducing a hypothetical tracer into the river water, the infiltration and movement of this water through the floodplain can be examined.

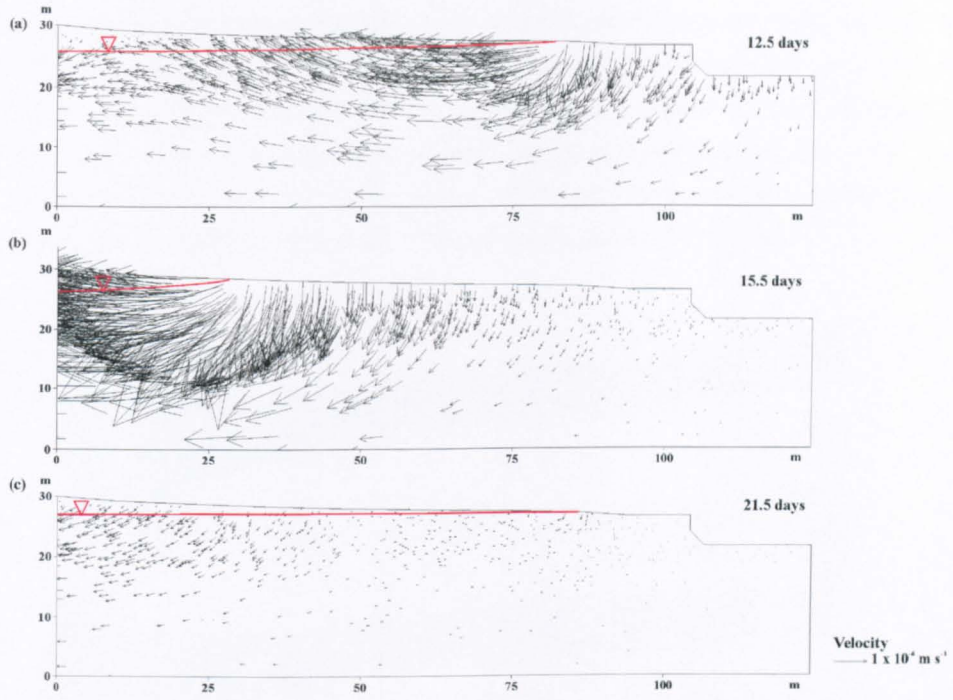

Figure 6.7 Groundwater ridge development during flood event D at (a) 12.5 days, (b) 15.5 days and (c) 21.5 days. Red line shows the position of the water-table.

6.1.3 Sleepers River

Initial analysis of the Sleepers River model runs can begin by reference to some initial process implications reported in McGlynn *et al.* (1999), which were based on field data alone. This analysis will draw on the ESTEL2D and coupled model results from the model assessment procedure described in Chapter 5.

The use of a numerical model to explore the Sleepers River field data allows the 2D patterns of water movement and $\delta^{18}O$ concentrations within the domain and how these change over time to be seen, which aids the understanding of the system. On a basic level, it expands the visualisation of the system, beyond that which can be inferred from the piezometric and solute field data alone. The hydrological and chemical transport modelling of this system will be discussed together, because as the $\delta^{18}O$ is essentially a perfect tracer for the water flow (it is part of the water molecule itself), an interpretation of the $\delta^{18}O$ concentrations allows us to infer the pathways of water flow.

The ESTEL2D results indicated that the changes in hydraulic head and water-table elevation over the course of the modelled snowmelt event at Sleepers River are subtler than the changes simulated for the River Severn. This starts to hint at the differences in processes that may be introduced by a change in system scale and configuration. Figure 6.8 shows

relatively small changes in hydraulic head, with the greatest variation being seen on the hillslope at the right hand boundary. The deflection in the hydraulic head contours which can be seen in Figure 6.8 results from a combination of boundary condition specification and, importantly, the distribution of different soil types implemented in this model, and particularly the influence of the riparian peat. The model results correspond well with the pattern and magnitude of fluctuations in hydraulic head observed in the field.

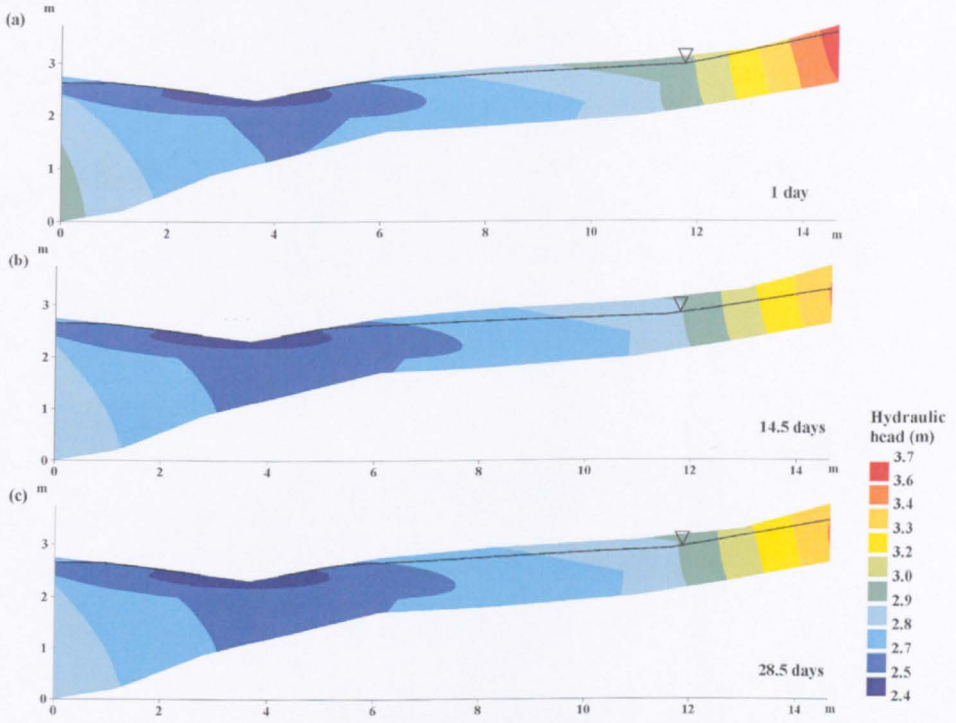

Figure 6.8 Patterns of hydraulic head at Sleepers River at (a) 1 day, (b) 14.5 days, and (c) 28.5 days. Black line shows the position of the water-table.

Except very locally, there is no inundation of the riparian zone by stream water. This results in a marked difference in hydraulic head pattern when compared with the lowland floodplain environment of the River Severn, as there is no reversal of the hydraulic gradient between the hillslope and the stream channel. This can be seen in Figure 6.8 where the hydraulic head is consistently highest in the hillslope region and lowest in the channel region, resulting in a constant hillslope to river flow direction. While the hydraulic gradient reversal is not significant for the upland riparian zone, the influence of seepage through the surface of the riparian zone is indicated by the model to be much more important than for the lowland floodplain. The seepage face can also be seen to be dynamic; the length of the surface boundary across which seepage occurs expands and contracts over the course of the event.

These inferences are consistent with the idea that upland zones are areas of water generation, and that the picture for lowland zones is complex, as the floodplain may act as a water source and a water sink. This preliminary analysis begins to reveal the more detailed processes behind these ideas, and the subsequent hypothetical tracer scenarios will expand upon this by indicating how these hydrological processes impact upon water mixing and chemical transport and transformation.

In terms of chemical transport, the model assessment procedure indicates that the simulated patterns of $\delta^{18}O$ concentration provide a reasonably good fit to the values of $\delta^{18}O$ concentration observed in the piezometer nests. In particular, the model simulates the correct vertical stratification of $\delta^{18}O$ concentrations as indicated by the concentrations observed in the field. This being the case, it enables us to look at the boundary conditions (in terms of $\delta^{18}O$ concentration, as well as hydrological boundary conditions) that were needed to create the simulated pattern of $\delta^{18}O$ within the domain, and examine the consequences of these boundary conditions for water sources and flow paths in the field situation.

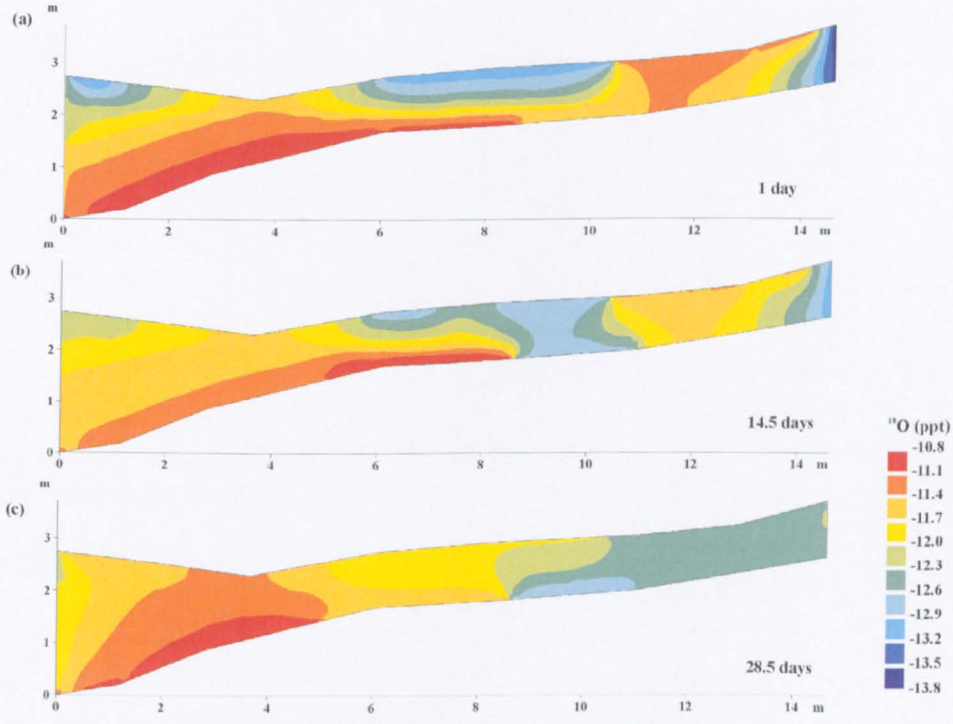

Figure 6.9 Patterns of $\delta^{18}O$ at Sleepers River at (a) 1 day, (b) 14.5 days, and (c) 28.5 days. As an approximation, the red end of the key indicates groundwater and the blue end of the key indicates snowmelt derived water.

At piezometer nest 10 (see Figure 5.3 and Figure 5.30 for location of piezometers), the $\delta^{18}O$ concentrations observed in the field were the most problematic to explain. The water lower in the profile (10_1) had a relatively lighter (more negative) composition than the water higher in the profile (10_3). This was the opposite to what was expected given that the groundwater in the system (and therefore the water found in piezometer 10_1) was expected to be relatively heavy (i.e. less negative), and that the input on the surface (and therefore in piezometer 10_3) was expected to be snowmelt derived and therefore relatively light.

So, the modelling process forced a consideration of how the vertical concentration pattern observed in nest 10 could be inverted in comparison with what was expected. To produce the observed pattern of $\delta^{18}O$ concentration in nest 10 required an input of relatively light water at the lower boundary in this region, and relatively heavy water at the surface. The process operation that this implies is a delivery of new, lighter, (snowmelt derived) water from upslope at the lower boundary. This would also fit with the downward water flux needed at the lower boundary in the hillslope region during the hydrological simulation. This water has moved into the soil in the hillslope area (discharge) and then moves back into the soil from the bedrock in the region of nest 10 (recharge). The relatively heavy (less negative) water found at the top of the profile could indicate the influence of rainfall events, as it is known that the rainfall was isotopically heavier than the snow. At this time in the season the ground was clearing of snow cover, which may have left more of the ground surface open to direct precipitation. This suggests that it might not be appropriate to apply one overall value of snowmelt $\delta^{18}O$ over the whole transect, as the $\delta^{18}O$ of the water infiltrating through the surface may vary according to how much of that water is derived from rain or snow. In addition, local exfiltration and reinfiltration of hillslope water along the surface could cause variation in the local input of $\delta^{18}O$ in the region of nest 10; this exfiltration is clearly indicated by the Darcian velocity vector pattern at the foot of the hillslope in the hydrological simulation results. This confirms the interpretation of hillslope water penetrating to depth at the hillslope-riparian interface (McGlynn et al., 1999); the model highlights this interface and its sensitivity to hillslope inputs.

The wider implications of this example are that the model can help to bring into sharp focus those areas of a system where process understanding is weak and where there are greatest uncertainties over field processes. The nature of the modelling process is such that those aspects of field data that are most difficult to explain, and the related uncertainties over field processes, must be confronted, because *something* has to be prescribed on every boundary. Where there is uncertainty, the model can be used to explore the consequences of different options, but ultimately, a decision must be made. The model highlights some of the critical spatial zones in the riparian-hillslope interaction.

6.2 Scenario testing: statement of hypotheses to be tested

After this preliminary phase of analysis, the coupled model was used to extend these initial advances in process understanding. To achieve this, a series of hypotheses about floodplain hydrological and chemical transport processes, based on the literature reviews and findings of this study thus far, were tested through the simulation of scenarios using a hypothetical tracer. The use of the term floodplain here is intended to denote both floodplain systems in lowland regions, and riparian zones in headwater regions.

Water moving through floodplains is believed to come from several different sources. Hillslope inputs may be more likely to be significant under low river flow conditions, when the hydraulic gradient may be expected to be in the hillslope-river direction. Riverine inputs may be expected to increase in importance during high flow conditions, and water may be exchanged with the floodplain through the bed and banks of the channel, or via overbank flow and infiltration through the floodplain surface. As has already been demonstrated, these processes are likely to vary with the scale and configuration of the floodplain system.

With regard to the floodplain chemistry, several scenarios can be envisaged. It is likely that chemical sources will vary during the course of a flood event. Depending on the pathway of water movement at any one time, chemicals may pass through the floodplain from hillslope sources, or pass into the floodplain from the river. The concentration of chemicals in each of these water sources is likely to be temporally variable. For example, the 'flushing' of chemicals stored in the soil after an extensive dry period may lead to a significant solute pulse being delivered to the floodplain, either by the river or via the hillslope, and the timing of this pulse may have important implications for chemical transport and transformation within the floodplain. The residence time of chemicals within the floodplain soils is an important factor in chemical transport and transformation that is heavily influenced by the soil hydraulic conditions. Establishing what happens when waters of different origin and different chemical concentration meet in the floodplain, and where the chemicals end up (i.e. whether they remain resident in the floodplain or are exported to the river) remains unclear.

Once a computer simulation model has been satisfactorily tested, it could be applied to an almost infinite combination of conditions. Very extensive volumes of information may thus be created. As with the model assessment, it is essential that an appropriate research design, which meets the aims, requirements and scope of the desired application be well structured and defined (Howes and Anderson, 1988). It is important that the model should only be applied within the range of the theory from which it has been developed (Howes and Anderson, 1988). With this in mind, the broad concepts of floodplain hydrological and

chemical transport processes outlined above have been narrowed down into specific hypotheses to be addressed during the remainder of this study:

1. The scale of the hydrological event (overbank flood, bankfull flood and low flow event) controls floodplain water and solute source, flow path and residence time.
2. The scale of the floodplain zone (headwater riparian zone versus lowland floodplain) controls floodplain water and solute source, flow path and residence time.
3. Other factors (such as carbon content and distribution, temperature and soil hydraulic characteristics) are important in controlling solute transport and transformation.

Hypotheses 1 and 2 will be explored in Chapter 6. Hypothesis 3 will be explored in Chapter 7.

6.3 Hypothesis One: scale of hydrological event controls floodplain water and solute, flow path and residence time

In this part of the study, the River Severn model was used to assess the effect of different hydrological events on water source and residence time in the floodplain. The River Severn model was selected as the associated field data cover a range of hydrological events on which to base the study.

A hypothetical tracer was introduced at the various points in the model domain to indicate flow paths and residence time of waters of different provenance: hillslope, floodplain or channel. A similar hypothetical approach was used by Woessner (2000) who introduced a conservative solute at a concentration of 100 mg l^{-1} into his subsurface model domain along one boundary to delineate groundwater and surface water and zones of mixing.

This approach allowed a comparison of the delivery of water and solute under overbank flow, bankfull flow and low flow conditions. It also enabled an examination of the significance of the groundwater ridging phenomenon in terms of its impact on the flux of water, and any associated solutes, through the floodplain. The model was used to examine both how the flood event influenced the flux of water through the floodplain surface, but also how the hydraulic gradients induced in the floodplain served to affect the introduction of hillslope inputs to the floodplain.

In order to get an indication of the importance of flood events within the broader picture of floodplain hydrological and chemical transport processes, two of the flood event simulations were extended using a hypothetical hydrological results file which aimed to simulate low flow conditions persisting for three months following a flood event. This was used to look at

the residence time of water and chemicals input from the hillslope within the floodplain, and the potential persistence of chemicals introduced into bank storage during a flood event.

6.3.1 Schedule of model runs

For this set of simulations, three hypothetical tracers were defined: one each to serve as markers for hillslope water, river water, and floodplain water. For the hillslope tracer, at any time when water flow was directed across the hillslope boundary in a hillslope-floodplain direction, tracer was introduced into the domain at a concentration of 10 mg l^{-1}. When the flow direction was reversed, the boundary condition at the hillslope changed to a free flow condition, so the tracer concentration at the boundary was no longer imposed but was a function of the tracer concentration inside the domain.

To introduce a tracer in the river water involved a more complex boundary condition definition, as unlike the fixed length hillslope boundary, the length of the boundary along which the river water could infiltrate varied according to the extent of overbank flow. This specification therefore made use of the variable within the hydrological code which designated a specified head boundary condition, as this corresponded to those regions of the boundary that were subject to inundation by river water. As in the hillslope tracer case, at times when the water flow was directed into the floodplain across the channel or surface boundary, the tracer was imposed at a concentration of 10 mg l^{-1}. When the flow direction was reversed, the boundary reverted to a free flow condition.

In the case of the floodplain water, the tracer was introduced into the domain as four pockets of tracer at a concentration of 10 mg l^{-1}. These were established in the initial conditions file, and no further tracer was added to the floodplain water during the simulation. The aim of this was to establish the pattern of movement, and export, of water that was already in the floodplain at the start of a flood event.

This model configuration was run for the four overbank flood events (D-G) and two bankfull flood events (A and B) for which field data were available for the River Severn (see Table 5.1). This was carried out for both the spur and hollow transect models of the River Severn. In addition, for one overbank flood event (G) and one bankfull event (A), for the spur transect (S), the computation was extended for a hypothetical three-month low flow hydrological event. These simulations used the hillslope and channel boundary conditions as prescribed by the last time step of the flood event simulation, extended into an artificial hydrological results file with constant boundary conditions. These simulations were therefore not strictly speaking low flow events, but they did have a hydraulic gradient across the floodplain that generated water flow in a hillslope-channel direction. Reliable low flow data were not available from the fieldsite due to the problems with piezometer measurements

under low water-table conditions; under these circumstances the level of the water-table fell below the installation level of the piezometers, leading to unreliable measurements. The aim of these simulations was to get an indication of how important the flood events are in comparison with the longer term, low flow situation, and for what length of time hillslope and river derived water from a flood event may remain resident in the floodplain system.

The dispersivity values chosen for these simulations were 1.0 m longitudinal dispersivity (along the flow) and 0.1 m transverse dispersivity (across the flow), based on the results of the sensitivity analysis in Chapter 5. The value of molecular diffusion was 5×10^{-10} $m^2 s^{-1}$.

6.3.2 Results

The results of these simulations will be presented using a range of indicators including graphs of solute concentration, solute mass balance, water fluxes, Darcian velocity vectors, and hydraulic head.

The problems with the interpretation of the solute mass balance results were described in the model assessment of Chapter 5 (Section 5.3.2.2). However, it was felt that solute mass balance would add a useful dimension to the analysis of the hypothetical scenarios, so these results have been included during this part of the study. However, some important points must be taken into consideration when interpreting the solute mass balance results of the River Severn model simulations.

In the case of the hillslope water tracer, the error introduced into the mass balance results was relatively easy to identify. At any point when a steep concentration gradient occurred across the hillslope boundary, this resulted in either the introduction of an excess of solute into the domain, or a loss of an excess of solute from the domain, depending on the direction of the gradient. For example, when solute was first introduced to the domain, the steep concentration gradient between the incoming water and the water in the domain introduced a large positive error in the mass of solute in the domain (i.e. too much solute is introduced). These events showed up as sharp increases or decreases in the total mass in the domain, and were therefore relatively easy to correct. This correction was performed for the hillslope water tracer for each hypothetical simulation, in the manner illustrated in Figure 6.10. However, it must be remembered that the excess tracer that was introduced remained in the domain, and therefore was still affecting the movement of tracer within the domain during the model simulation. Performing this correction also had the effect that it was possible to have a negative total solute mass in the domain in the final diagrams. Comparisons of absolute values of solute mass are therefore inappropriate, but some interpretation of the pattern of change in solute mass over time is felt to be valid and useful.

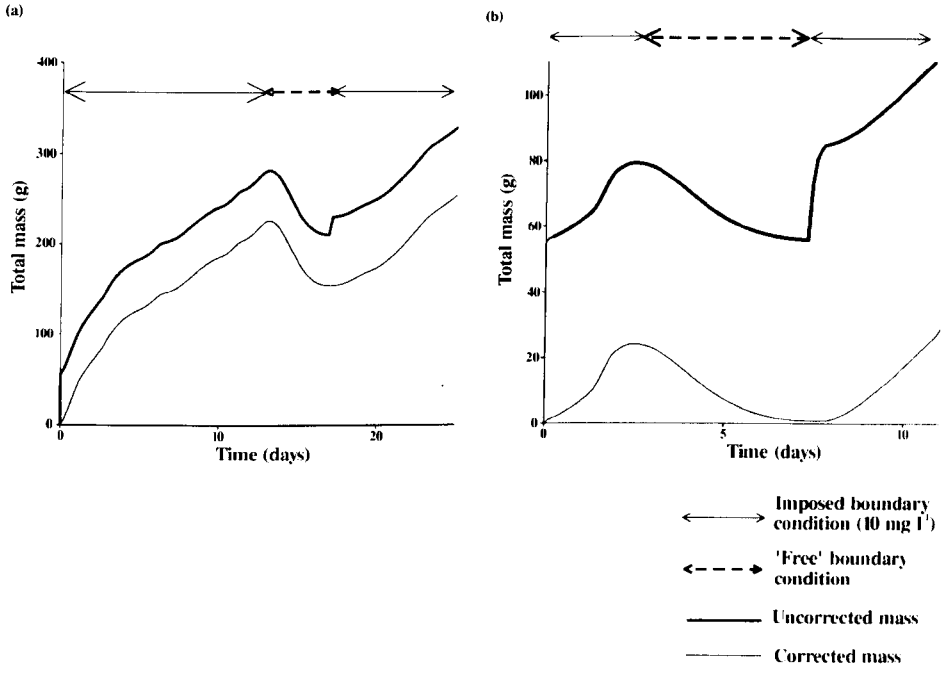

Figure 6.10 Illustration of solute mass balance correction carried out for the hillslope water tracer for (a) flood event G and (b) bankfull event B.

In the case of the river water tracer, the incremental nature of the introduction of solute to the domain as the water gradually inundated the floodplain made it very difficult to identify the excess solute that had been introduced to the domain. Therefore, the solute mass balance for the river water tracer was not corrected. The floodplain water tracer was affected by this problem to a much lesser degree than the other two tracer sources. This was because relatively little of the floodplain water tracer actually crossed the model boundary. The solute mass balance for the floodplain water tracer therefore did not need to be corrected.

The diagrams that show the solute concentration in the River Severn model domain have been cropped to focus on regions of interest. In the case of the river water and floodplain water tracer, this involves showing the upper portion of the domain, down to a depth of 15 m (Figure 6.11). This also more accurately reflects the fact that the lower 20 m of the model domain was added to reduce the impact of the lower boundary condition on the rest of the simulated results, but that field information with which to assess the validity of these results was only available to a depth of 5-10 m. In the case of the hillslope water tracer, the region displayed in the results is the first 25 m of the domain, extending from the hillslope boundary of the model (Figure 6.11). In the following results, not every combination of tracer source and event type is discussed. The discussion is restricted to the situations where new process understanding is developed.

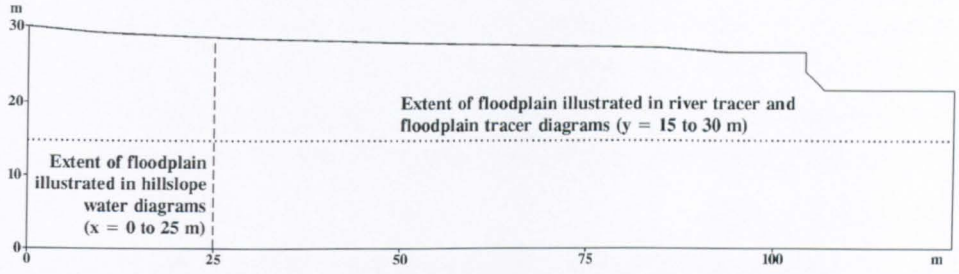

Figure 6.11 Diagram showing the extent of the model domain illustrated in subsequent diagrams of this chapter.

6.3.2.1 River-water tracer: overbank flood event

Figure 6.12 shows the infiltration and movement of a tracer associated with river-derived water in the floodplain, over the course of flood event D, on transect S. As the floodplain was inundated (inundation occurred between day 12 and day 32 of the 45.5 day event), strong hydraulic gradients across the floodplain surface allowed river water to enter the floodplain (Figure 6.12a). Although the extent of inundation later receded, the river water continued to infiltrate to greater depth in the floodplain. Of course, the amount of dispersion illustrated in the model results may have been an over- or under-estimation, as the dispersion parameters were based on literature values rather than field values, but this scenario does at least demonstrate the general pattern of tracer movement.

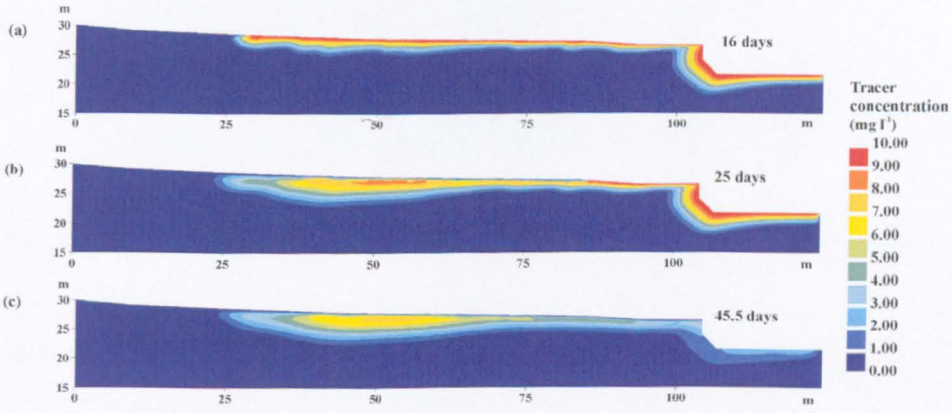

Figure 6.12 Pattern of river water tracer concentration during flood event D on transect S at (a)16 days, (b) 25 days, and (c) 45.5 days.

By 45.5 days (Figure 6.12c) the hydraulic gradient was re-established in a hillslope-to-river direction, and tracer concentration had overall decreased. The decrease in tracer concentration was most marked in the near-stream zone (those areas of the floodplain in closest proximity to the river channel bed and banks), where concentrations had decreased

from 10 mg l^{-1} to 0-2 mg l^{-1}. In contrast, the concentration of tracer near the floodplain surface remained high, at up to 7 mg l^{-1}. This reflects the much lower velocities in the near-surface, unsaturated zone, and indicates that a chemical in river water delivered to this zone in overbank flow has the potential to remain resident in the floodplain for long periods of time.

6.3.2.2 Floodplain-water tracer: bankfull and overbank flood event

Figure 6.13 shows the movement of a tracer introduced to the floodplain before the start of a flood event. Figure 6.13a shows that this hypothetical tracer was initialised in the model as four discrete 'parcels' of tracer, each at a concentration of 10 mg l^{-1}. Figure 6.13b shows the extent of tracer movement after a bankfull flood event. In 14 days, the floodplain tracer had moved little under the influence of advection, although the influence of dispersion can be clearly seen. Clearly, the influence of the bankfull flood event did not extend very far away from the channel in terms of moving tracer that was already present in the floodplain.

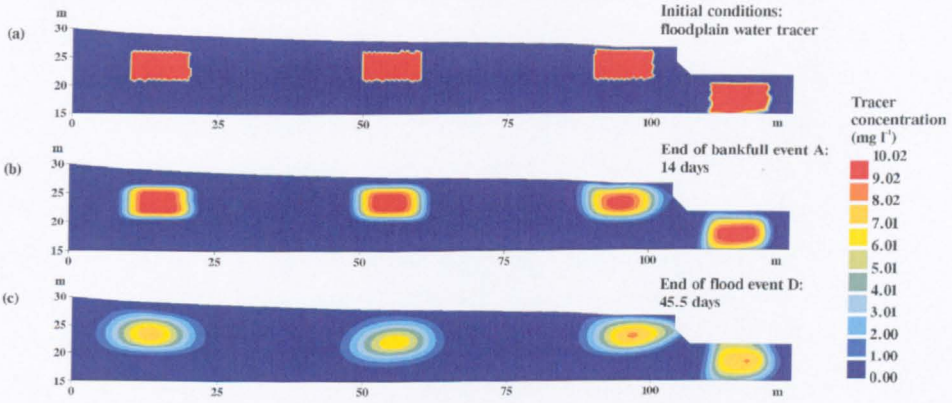

Figure 6.13 Pattern of concentration of floodplain tracer (a) initial distribution, (b) distribution at the end of bankfull event A, and (c) distribution at the end of flood event D.

Figure 6.13c shows the extent of tracer movement after an overbank flood event. In comparison with the bankfull flood event, there was more tracer movement, but much of this was still a result of movement by dispersion rather than advection. Advection may have been expected to play a more dominant role considering the high groundwater velocities that were observed in the near-surface zone during overbank flow events. The greatest influence of this high velocity water therefore seemed to be in terms of the amount of river-derived water that was introduced to the floodplain, as water already present in the floodplain was not transported by this high velocity water. This may indicate that the period of high water velocity was too short, or too localised to the floodplain surface, to effect any significant transport, at all but very shallow depths in the floodplain. The greatest degree of tracer

movement was again seen in the near-stream zone, as was indicated in the case of the river-water tracer (Figure 6.12c).

The following sets of diagrams show the tracer distribution following a period of low flow, with flow in a hillslope-to-river direction. Each diagram has three parts; the tracer distribution at the end of the flood event; the tracer distribution after a 40 day low flow period, and the tracer distribution after a 90 day low flow period. In total, three different events are illustrated: bankfull event A, flood event F, and flood event G. For each event, there is an illustration of the distribution of river-derived tracer, hillslope-derived tracer, and floodplain-derived tracer. These results will be presented grouped according to the tracer source: river-water, hillslope-water and floodplain-water.

6.3.2.3 River-water tracer: flood event vs low flow event

The following three diagrams show the distribution of river-water derived tracer in the floodplain for bankfull event A (Figure 6.14), flood event F (Figure 6.15), and flood event G (Figure 6.16) (note the different concentration scales for each diagram). As may be expected, there was a large contrast in the distribution of tracer between the bankfull flood event and overbank flood events. At the end of the bankfull event (Figure 6.14), tracer had been introduced only in a localised, near-stream region. The tracer introduced near the floodplain surface resulted from a slight inundation of the floodplain close to the channel. After 90 days of the low flow period, the tracer in the near-stream zone (adjacent to the bed and banks) had reduced to a concentration below 0.72 mg l^{-1}, from its initial concentration of 10 mg l^{-1} introduced during the event. The only tracer that remained was in the zone near the floodplain surface, adjacent to the stream. This corresponded with an area of the floodplain which was unsaturated by this time. This indicates the important role that the unsaturated zone could play in tracer transport through the floodplain environment.

As explained earlier, it was very difficult to produce total solute mass diagrams for the river water tracer, due to the incremental nature of the introduction of solute to the domain. However, this was only a problem for the overbank events, where the length of the boundary across which tracer was introduced was constantly changing. A total solute mass graph could be produced in the case of the bankfull flood event (Figure 6.17a). This shows a sharp increase in total mass of tracer coinciding with the rise of the river stage and the water flow changing to a river-to-hillslope direction. When the hydraulic gradient later reverses, after about 11 days, water and solute begin to leave the domain across the river channel boundary. This pattern continues during the 90 day low flow period, with the mass decreasing at a decreasing rate, probably due to the reduction in concentration gradient across the river channel boundary.

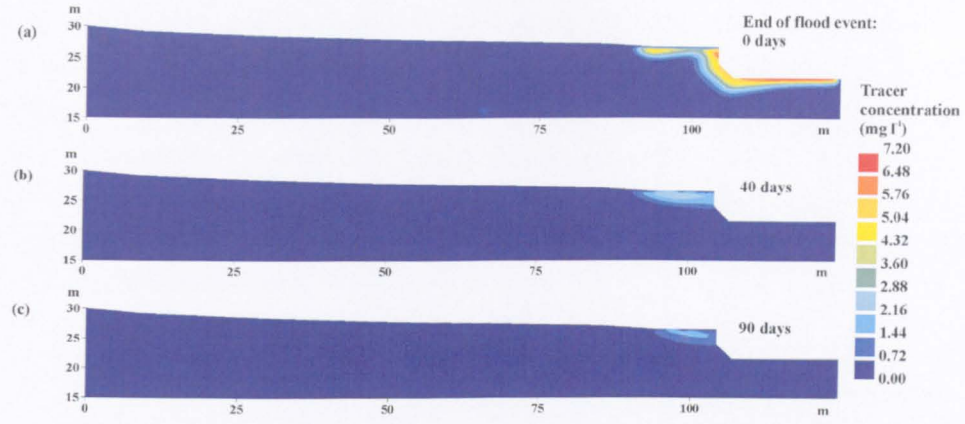

Figure 6.14 Concentration of river water tracer during low flow conditions following bankfull event A at (a) 0 days (end of bankfull event A), (b) 40 days and (c) 90 days.

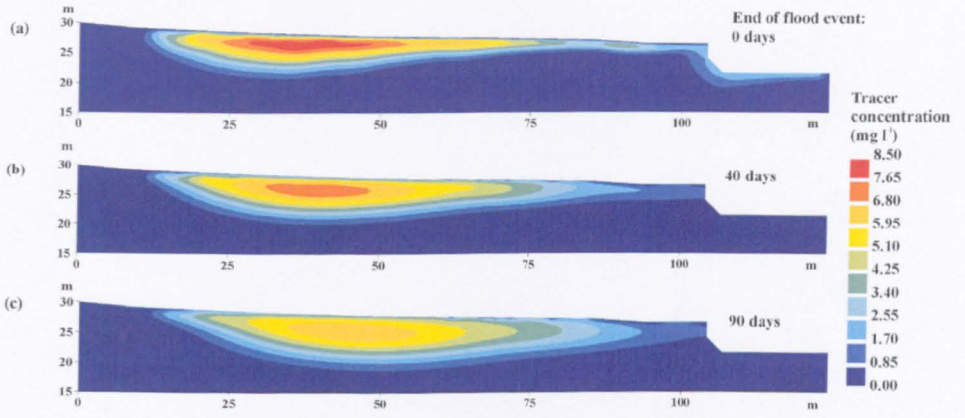

Figure 6.15 Concentration of river water tracer during low flow conditions following flood event F at (a) 0 days (end of flood event F), (b) 40 days and (c) 90 days.

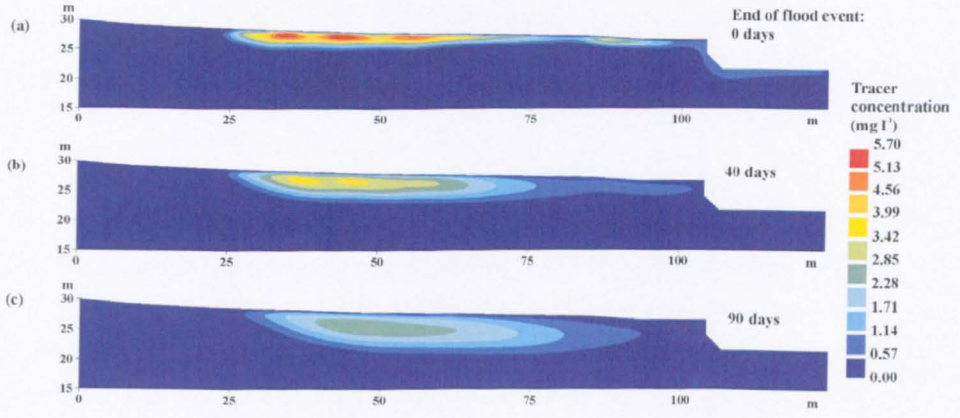

Figure 6.16 Concentration of river water tracer during low flow conditions following flood event G at (a) 0 days (end of flood event G), (b) 40 days and (c) 90 days.

In contrast, during the two overbank flood events the river-water derived tracer was deposited across a much wider area. Although it is difficult to comment on the mass of tracer introduced to the floodplain during the overbank events, it seems reasonable to state that the greater area of deposition of the overbank flood events were associated with the delivery of a much greater mass of river-water derived tracer than the bankfull flood event. The extent of overbank flow meant that there was a much greater surface area over which the tracer could be introduced to the floodplain.

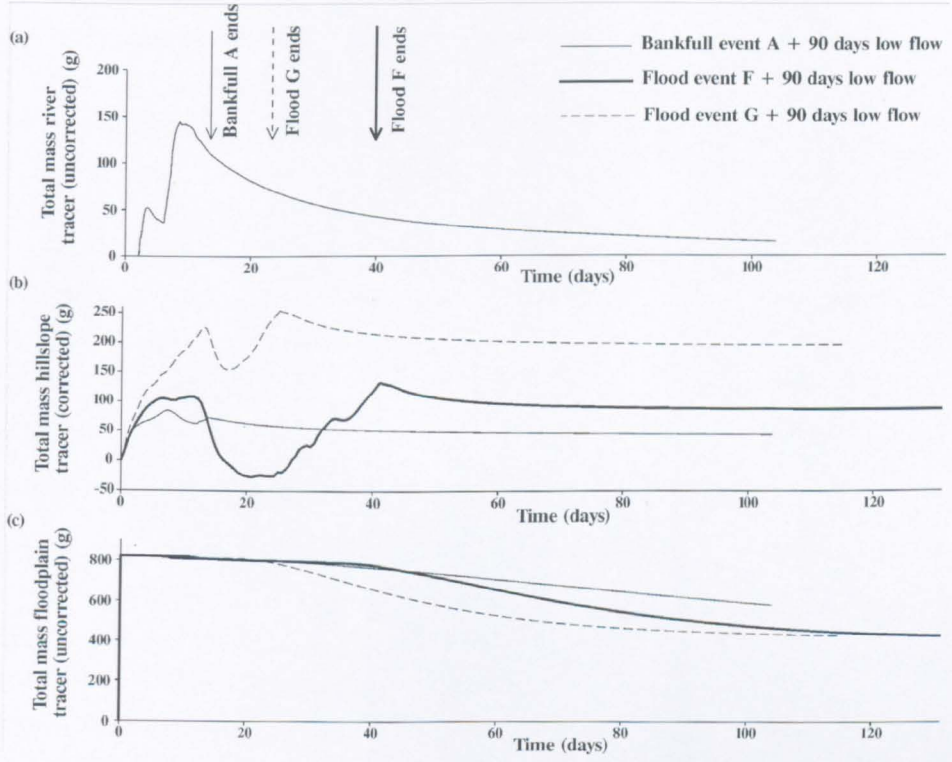

Figure 6.17 Change in mass of tracer during three flood events and subsequent low flow period (a) river water tracer, (b) hillslope water tracer and (c) floodplain water tracer.

The areas of the floodplain which received the highest concentration of river water tracer were those at which the velocity vectors directed into the floodplain remained highest for the longest period of time, which tended to be the region corresponding to the furthest inundation extent. It is clear that a greater mass of tracer was introduced to the floodplain during flood event F in comparison with flood event G. The duration of the flood event G simulation was 601 hours in comparison with 1001 hours for the flood event F simulation. But the crucial part of the event in terms of tracer infiltration was the period of floodplain inundation; for flood event F, this was approximately 12 days, whereas for flood event G, the

flood water only extended overbank for approximately 6 days. This was reflected in the amount of tracer introduced into the floodplain during these two events.

By the end of the overbank flood event, concentrations of river-derived tracer in the floodplain remained high. There was some tracer transport due to advection, in a hillslope-to-river direction, but there was also a significant degree of tracer movement due to dispersion, which acted to move tracer deeper into the floodplain. Once again, the tracer in the near stream zone had reduced to a negligible concentration. It can be seen that even after a considerable period of time under low flow conditions (an arbitrary three month period), there was a significant mass of tracer remaining in the floodplain, at a concentration up to 7.65 mg l^{-1} in the case of flood event F, and 2.85 mg l^{-1} in the case of flood event G. This effect was enhanced by the low water velocity conditions in the unsaturated zone in the upper 5 m of the floodplain. This raises the possibility that precipitation events could take on greater significance for transport of this river-derived tracer in the floodplain during these low flow periods. During the overbank flow events, the effect of rainfall on hydraulic gradients and water velocity near the floodplain surface was found to be negligible in comparison with the effect of the overbank flow. During low flow periods the effect of rainfall in increasing moisture contents and hydraulic conductivity in the unsaturated zone could make a more significant difference to both water and chemical movement in this zone.

6.3.2.4 Hillslope-water tracer: flood event vs low flow event

To set up the hillslope-water derived tracer scenarios, the whole flood event was first run with a specified solute concentration of 10 mg l^{-1} on the hillslope boundary. This specified tracer condition was only applied at times when the water flow was in a hillslope-to-floodplain direction across the hillslope boundary; at times when flow was in the opposite direction, this boundary was specified with a free flow condition. For the subsequent low flow simulation, no tracer was input at the boundary. The aim of this was to see how long the flood event-derived tracer would remain in the floodplain, and what would happen to the distribution of this tracer.

Each of the diagrams of the hillslope water tracer have the same scale of tracer concentration for comparison (Figure 6.18, Figure 6.19, and Figure 6.20). In all cases, it can be seen that by the end of the flood event, a plume of hillslope water tracer has been introduced at the hillslope boundary. During the low flow period, the tracer proceeded to move through the floodplain towards the river channel. In every case, the effect of the unsaturated zone on tracer movement was once again clear; in the upper 5 m of the floodplain, the tracer concentration remained high, as tracer advection and dispersion was low in this low velocity

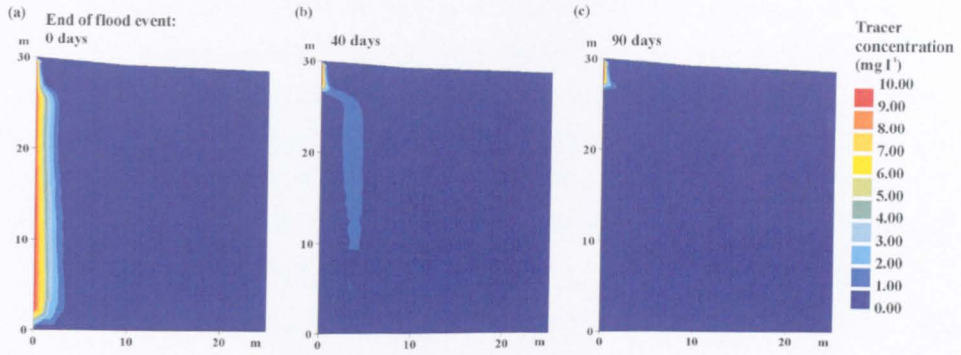

Figure 6.18 Concentration of hillslope water tracer during low flow conditions following bankfull event A at (a) 0 days (end of bankfull event A), (b) 40 days and (c) 90 days.

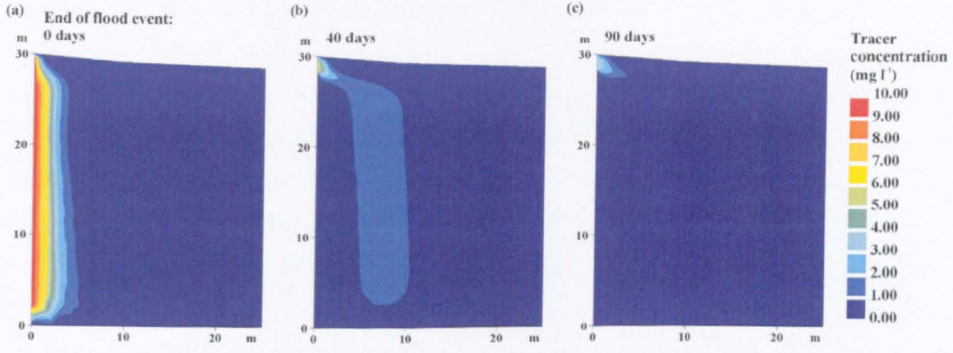

Figure 6.19 Concentration of hillslope water tracer during low flow conditions following flood event F at (a) 0 days (end of flood event F), (b) 40 days and (c) 90 days.

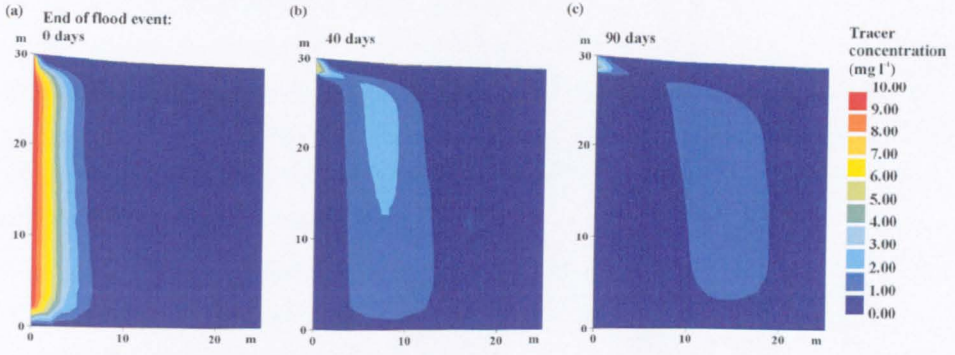

Figure 6.20 Concentration of hillslope water tracer during low flow conditions following flood event G at (a) 0 days (end of flood event G), (b) 40 days and (c) 90 days.

region. In the saturated zone, however, tracer movement was much more rapid, and the tracer dispersed so that after 90 days of low flow conditions, the tracer concentration throughout the saturated zone of the floodplain had reduced from 10 mg l^{-1} to a maximum of 1 mg l^{-1}. It is likely that the differences in tracer concentration between the three flood events partly reflect the duration of each event simulation. Recalling that the tracer was only introduced at the boundary at times when water flow was in a hillslope-to-river direction, the length of pre- and post- overbank period that was modelled in each simulation affected the total mass of tracer introduced to the model domain.

Despite the aforementioned problems with the tracer mass balance description, the mass balance plots in Figure 6.17b start to give an indication of the effect of the hydrological event on the introduction of hillslope water tracer to the domain, and the residence time of this tracer in the floodplain. As noted earlier in the interpretation of solute concentration, the fact that some events had a higher total solute mass than others is not particularly relevant, because this was partly dependent on the length of pre- and post-flood event period that was simulated. However, the *pattern* of change in total solute mass over time is important and can be interpreted more reliably. For every flood event, the change in hydraulic gradient to a river-to-hillslope configuration during peak river flow had an effect as far across the floodplain as the hillslope-floodplain boundary. This is indicated by the drop in total hillslope water-derived tracer mass, at around 16 days for bankfull event A, 20 days for flood event F, and 18 days for flood event G (Figure 6.17b). This can be seen more clearly in Figure 6.21, which shows each of the simulated flood events without the low flow events appended. During the period of overbank flow when the reversal of hydraulic gradient occurs, the total mass of hillslope water tracer began to drop, as the tracer in the floodplain left the domain through the hillslope boundary. In the case of the longest flood events, this period of decreasing tracer mass could last for up to 10 days. When the hydraulic gradient re-established in a hillslope-to-river direction, the input of hillslope tracer resumed. In terms of the introduction of hillslope water tracer to the floodplain in the long term, this 10 day hiatus may not be very significant. But in terms of the potential for interaction between tracer introduced in hillslope flow and river water flow, and in holding back the contribution of non-point source pollutants from the hillslope, the timing of this delivery of hillslope water may take on added importance.

The effect of the reversed hydraulic gradient holding back the hillslope inputs to the floodplain was much more pronounced for the overbank flood events, which may be expected due to the much greater hydraulic head gradients measured over relatively short distances during these events. But these results do seem to support the idea that even bankfull events can hold back the contributions of water (Burt *et al.*, 2002), and in this case

associated chemical tracers, from the hillslope. These results also illustrate that channel processes have the potential to impact on hydrological and chemical conditions right across the floodplain and into the adjacent hillslope.

After the flood event, it appears that any solute that had entered the floodplain from the hillslope was likely to remain resident in the floodplain for a considerable period of time. Even though the concentration of the tracer in the saturated zone reduced to 1 mg l^{-1} or less over the 90 day period, this was because the tracer was dispersing within the floodplain rather than leaving it. This is illustrated by the total solute mass diagram in Figure 6.17b. In the 90 days following the main flood event, the total solute mass hardly decreased. Although the tracer did move across the floodplain towards the river channel, hardly any of the tracer introduced during the flood event actually left the domain.

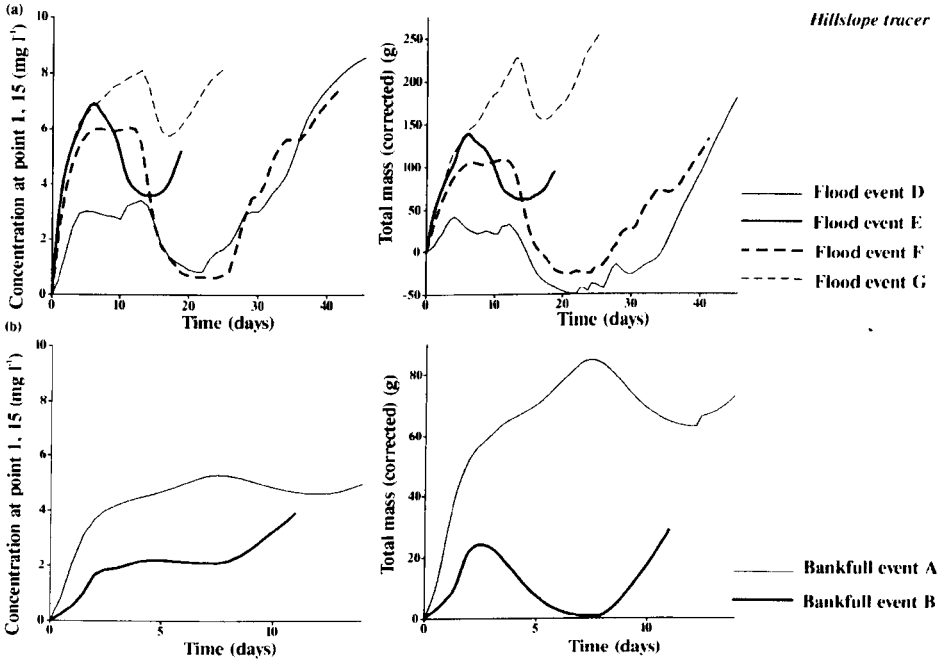

Figure 6.21 Concentration of hillslope water tracer at point x = 1, y = 15 m over time and total mass of hillslope water tracer for transect S for (a) overbank flood events and (b) bankfull events.

6.3.2.5 Floodplain-water tracer: flood event vs low flow event

To set up the floodplain-water tracer scenarios, the flood event simulation was initialised with 'patches' of tracer, as described previously (Figure 6.13a). For the subsequent low flow simulation, no further tracer was added. Once again, the aim of this low flow scenario was

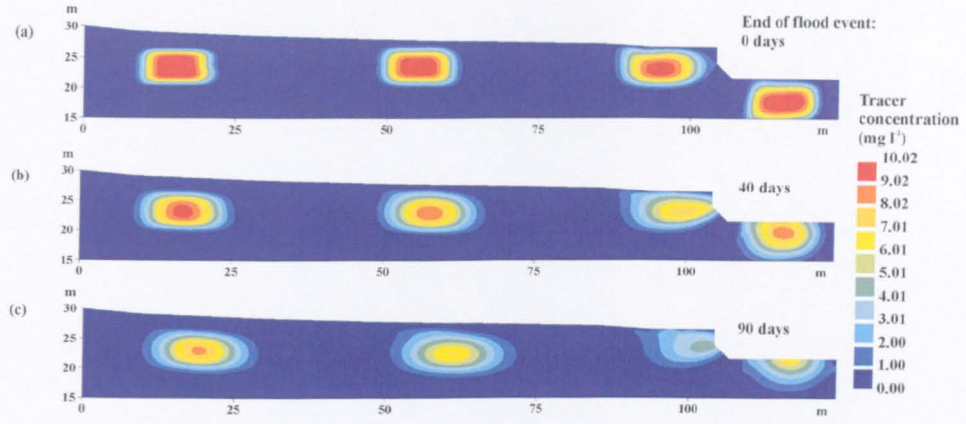

Figure 6.22 Concentration of floodplain water tracer during low flow conditions following bankfull event A at (a) 0 days (end of bankfull event A), (b) 40 days and (c) 90 days.

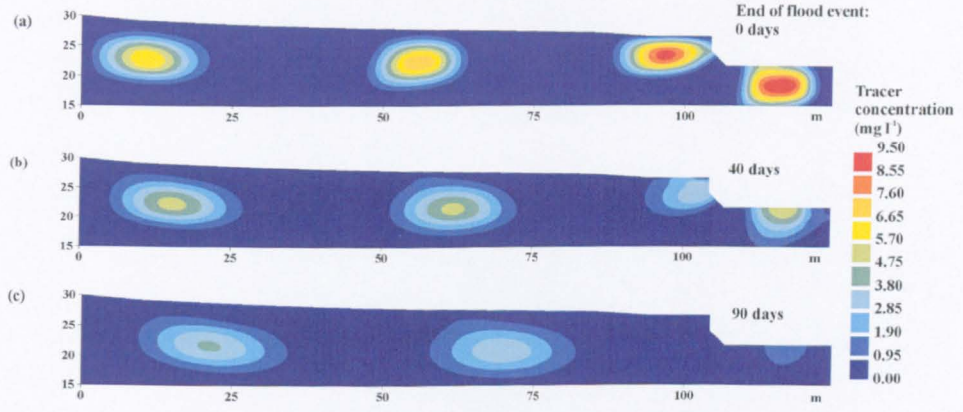

Figure 6.23 Concentration of floodplain water tracer during low flow conditions following flood event F at (a) 0 days (end of flood event F), (b) 40 days and (c) 90 days.

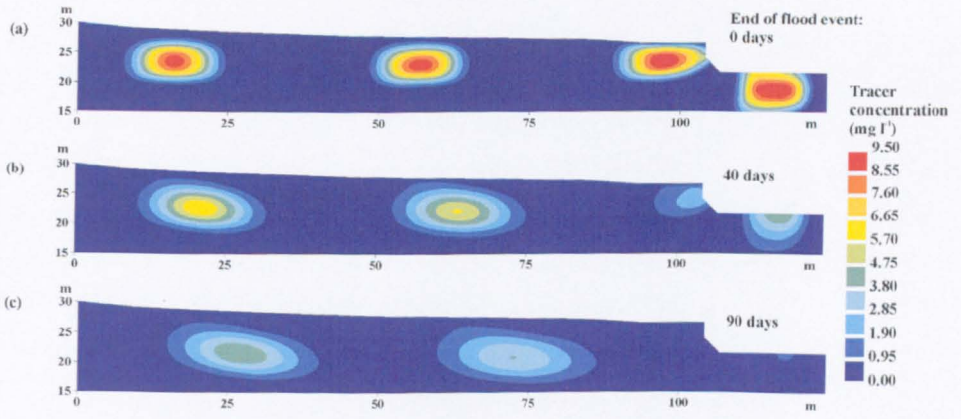

Figure 6.24 Concentration of floodplain water tracer during low flow conditions following flood event G at (a) 0 days (end of flood event G), (b) 40 days and (c) 90 days.

to see what would happen to the distribution of this tracer within the floodplain after the flood event, and how long such a tracer would remain resident in the floodplain. Note that the second two diagrams in the series (Figure 6.23 and Figure 6.24) have a slightly different scale of tracer concentration from the first diagram (Figure 6.22).

By the end of bankfull event A (Figure 6.22a), the floodplain tracer had hardly moved. This partly reflects the fact that the influence of the reversed hydraulic gradient in the unsaturated zone of the floodplain, especially at greater distances from the river channel, was not great enough to cause significant tracer movement. The lack of tracer movement may also reflect the shorter time period of the bankfull event simulation, in comparison with the overbank flood event simulations, particularly as during the subsequent 90 day low flow event, the tracer did disperse to a greater degree. Once again, this dispersion is particularly noticeable in the near stream zone, where solute concentration decreased to 7 mg l^{-1} or less after 90 days (Figure 6.22c). Thus, the reduction in total solute mass illustrated in Figure 6.17c largely reflects the movement of solute from the near stream zone out of the floodplain and into the river channel, while most of the mass of solute which originated in the 'patches' further from the river channel remained in the floodplain.

The effect of the two overbank flood events, in comparison with the bankfull flood event, is actually very similar. The fact that the final concentrations were lower in the case of the two overbank events (Figure 6.23, Figure 6.24) probably reflects the longer period of the overbank flood simulations. As a result of this, by the end of the 90 day low flow period the two near stream tracer patches had reduced in concentration from 10 mg l^{-1} to 5.7 mg l^{-1} or less. The movement of this tracer out of the floodplain and into the stream channel is reflected in the reduction of total solute mass for the two overbank flood events illustrated in Figure 6.17c.

There were some noticeable differences between the two overbank flood events. By the end of flood event G (Figure 6.24a), the two near-hillslope patches still had a concentration of up to 10 mg l^{-1}. By comparison, at the end of flood event F (Figure 6.23a), the two near-hillslope patches had decreased in concentration to 7.6 mg l^{-1} or less, and the shape of the tracer patch had been noticeably modified. This is not simply a consequence of the longer time period of the flood event F simulation leading naturally to a higher degree of dispersion, because the two tracer patches in the near stream zone remained at a high concentration, comparable with those of the flood event G simulation. Compared with flood event G, flood event F has a much longer floodplain inundation period. The previous river-water tracer simulations indicated how tracer infiltrated further into the floodplain at the maximum extent of inundation (Figure 6.15). This region, at a distance of 25 to 50 m from the hillslope boundary in the diagram, experienced saturated conditions and a steep hydraulic gradient,

inducing high velocity water flow for a longer period of time than area of the floodplain directly adjacent to the river channel. This period of high velocity water flow in this region of the floodplain during flood event F was enough to induce more significant movement of the parcels of tracer nearest the hillslope boundary than was observed for flood event G, or bankfull event A.

6.3.2.6 River-water tracer: comparison of transects

The three diagrams, Figure 6.25, Figure 6.26, and Figure 6.27, compare the distribution of river water tracer on transect S and transect H, at the end of three different flood events. Note the different tracer concentration scale on each diagram.

The effect of topography on tracer infiltration is clearly evident in these diagrams. It appears that tracer infiltrates to a greater depth on transect H than on transect S, in the region of transect H characterised by a depression in the floodplain (at a distance of approximately 50 m from the hillslope boundary). As the river water extended across the floodplain during an overbank flood event, the depth of water ponded on the floodplain surface was greater above the depression than on adjacent areas of the floodplain surface, and greater than at the corresponding location on transect S. This resulted in a steeper hydraulic gradient across the floodplain surface, with corresponding higher water velocities, by which mechanism the solute was able to infiltrate further in this region of the floodplain. However, considering the total solute mass diagram (Figure 6.28), which compares the total river water tracer mass of (a) transect S and (b) transect H over all the simulated flood events, it appears that the difference in total solute mass introduced across the whole floodplain is minimal. In the case of bankfull flood events, more tracer was introduced on transect S than transect H. This was because the 'bankfull' events simulated were not totally in bank. When slight overbank flow occurred along the 5 m of the floodplain surface nearest to the river channel, more tracer was introduced to the floodplain on transect S because the elevation of the floodplain is slightly lower in this area on transect S in comparison with transect H.

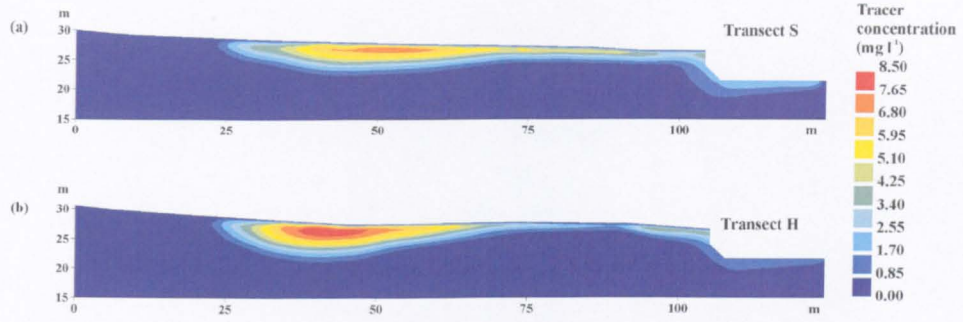

Figure 6.25 Concentration of river water tracer on (a) transect S and (b) transect H at the end of flood event D.

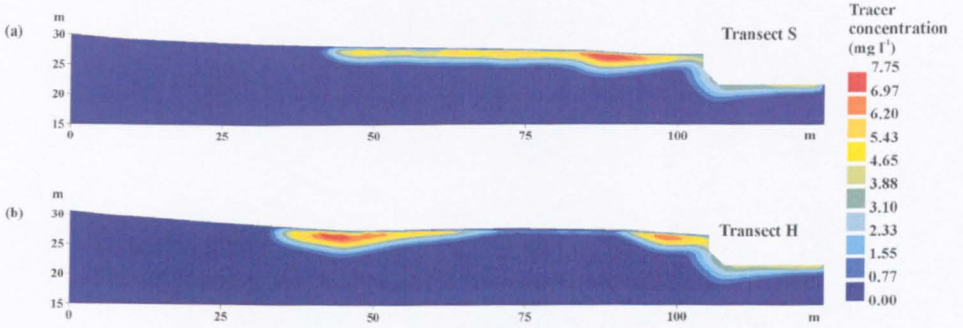

Figure 6.26 Concentration of river water tracer on (a) transect S and (b) transect H at the end of flood event E.

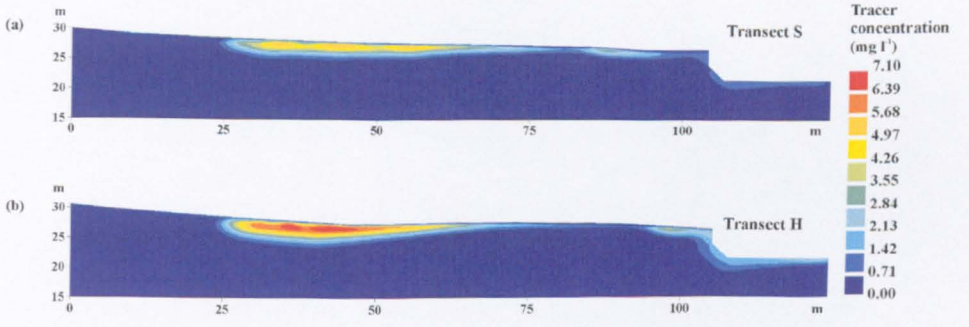

Figure 6.27 Concentration of river water tracer on (a) transect S and (b) transect H at the end of flood event G.

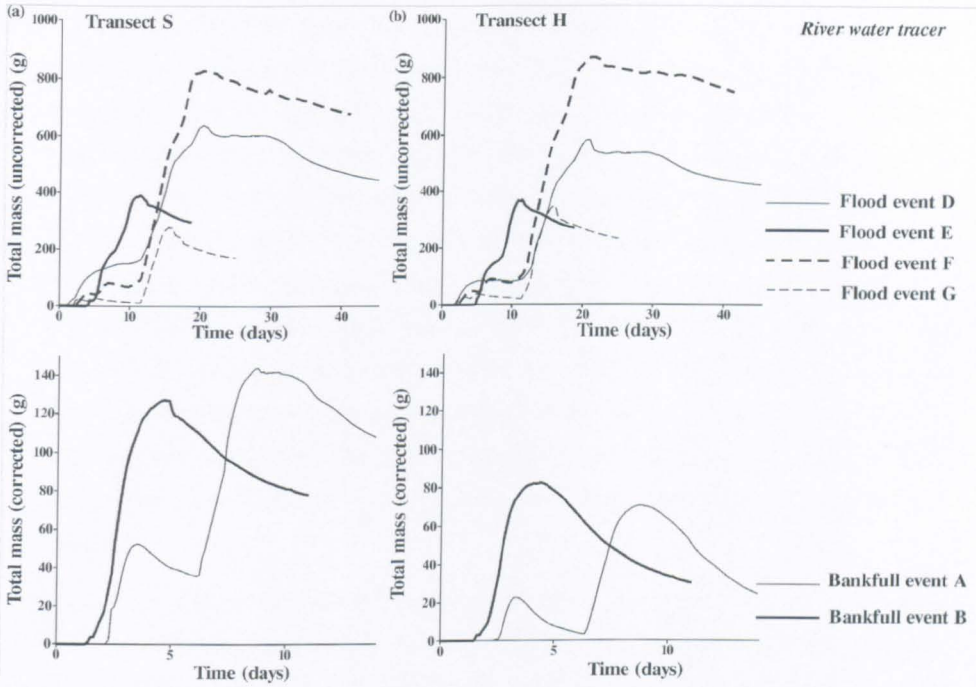

Figure 6.28 Total mass of river water tracer over time for (a) transect S (overbank and bankfull flood events) and (b) transect H (overbank and bankfull flood events).

6.3.3 Summary of hypothesis one

The simulations carried out during this section have allowed a refinement of the initial ideas about processes of water and chemical mixing, residence time, and export in floodplains, and how these processes are affected by hydrological events.

1. During periods of low flow, the main source of water for the floodplain is the hillslope. During the course of a flood event, both overbank and bankfull, the river becomes an important source of water and chemicals. The contribution from the river is greater for an overbank flood event where the river water extends across the floodplain surface. This is the first time that an indication of the relative importance of river and hillslope inputs of water and chemicals has been proposed.

2. Overbank flood events are times of increased hydrological activity and associated chemical movement. In contrast, under low flow conditions, water and chemical movement is much more restricted. This implies that any solute delivered to the floodplain during a flood event has the potential to remain in the floodplain for a long period of time. This is a novel finding with the implication that in the long term, flood events could be extremely important for solute delivery and residence time in the floodplain environment.

3. The unsaturated zone near the surface of the floodplain seems to have special significance. This region experiences very slow water and chemical movement in comparison with the saturated zone. Therefore, any solute delivered to this region (which tends to be solute derived from the river water) could remain resident for a long period of time. Under these circumstances, it is possible that precipitation events occurring between major flood events could take on greater significance by mobilising solute retained in the unsaturated zone. The unsaturated zone has a particular influence on retaining solute at a high *concentration*. In the saturated zone, the tracer concentration decreases much more rapidly, due to dispersion, but overall the *mass* of tracer in the floodplain may still remain high if the tracer does not reach an outflow boundary (for example, the hillslope tracer, Figure 6.18 to Figure 6.20). The indication of the importance of the unsaturated zone is in contrast to the findings of Bates *et al.* (2000).

4. There is no evidence for the movement of river-derived water into hillslope areas, hence refuting the hypothesis of Bates *et al.* (2000). However, both bankfull and overbank flood events have an effect on hydrological behaviour as far away from the channel as the hillslope-floodplain boundary. Hillslope inputs of water and solute can be held back for up to 10 days in the case of an overbank flood event, by the steep hydraulic gradient induced by the flood water. In the context of the long term effect of flood events on floodplain chemical transport, this 10 day interruption of hillslope inputs may not seem very significant. However, more critically, it may affect the potential for interaction between solutes in hillslope-derived water, and solutes in river-derived water.

5. Chemicals already present in the floodplain at the start of the flood event experience varying degrees of movement, depending on the hydrological event. The greatest degree of tracer movement is seen in the near-stream zone, where saturation is consistently higher. Under conditions of steep hydraulic gradients (e.g. across the floodplain surface near the hillslope boundary during flood event F), some floodplain-tracer movement can be initiated. However, significant solute export, from the floodplain to the river channel, does not occur until the flood event ends and low flow conditions are re-established (at which time the floodplain becomes a solute source). It seems that the flood event itself is a period of net input of water and chemicals to the floodplain (i.e. a solute sink). Export of pre-event solute from the floodplain is delayed until after the flood event, which has implications for the timing of solute contributions to river water, and the transfer of this solute through the catchment. The indication of which regions of the floodplain may be subject to greatest solute movement during a flood event is a novel development of this study.

6. Floodplain topography has a localised influence on the infiltration of river-water derived solutes. Depressions in the floodplain are subject to a greater depth of ponded water, and a steeper hydraulic gradient across the floodplain surface, allowing solute to infiltrate to a greater depth. This supports the conclusion of Stewart *et al.* (1998), that infiltration of chemicals into the floodplain surface may be spatially variable, and difficult to characterise using current field-based techniques.

6.4 Hypothesis Two: scale of floodplain zone controls floodplain water and solute source, flow path and residence time

The aim of these simulations was to start to explore the kind of process differences that might be found between upland and lowland floodplain/riparian zones. To do this, the Sleepers River model was run using hypothetical tracers in a similar manner to the River Severn simulations, in order to highlight water flow paths and residence times of water originating from different sources. These results were then compared with the results from the River Severn simulations from hypothesis one (Section 6.2). The conclusions from this section will necessarily be limited by the fact that data are only available from one lowland and one headwater catchment, which cannot hope to be representative of all headwater and lowland catchments. However, this is the first attempt of such a comparison, so however approximate the results, they may at least provide some insight into the kind of differences that can be found, and provide a starting point for future exploration of this issue.

The diagram in Figure 6.29 emphasises the difference in scale that is involved in this comparison. This illustrates the limitations of only studying water flow and chemical transport processes in headwater catchments, as many previous studies have done. The huge difference between the two cross-sections may suggest that it is unrealistic to try to scale up results from a headwater study to a lowland environment; the possibility of different processes operating over such a wide range of hillslope-channel environments is one that should clearly be explored. This reinforces the need for a consideration of lowland hillslope-channel connections, and comparison of lowland/headwater environments, as attempted in this study.

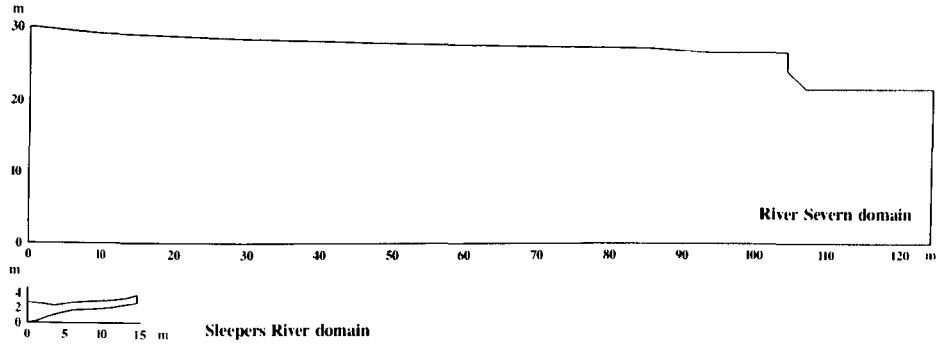

Figure 6.29 Diagram to show the relative scales of the River Severn domain and the Sleepers River domain.

6.4.1 Schedule of model runs

Water sources (and tracers associated with these sources) were divided into eight different regions of the boundary. These regions are labelled one to eight, and are indicated in Figure 6.30.

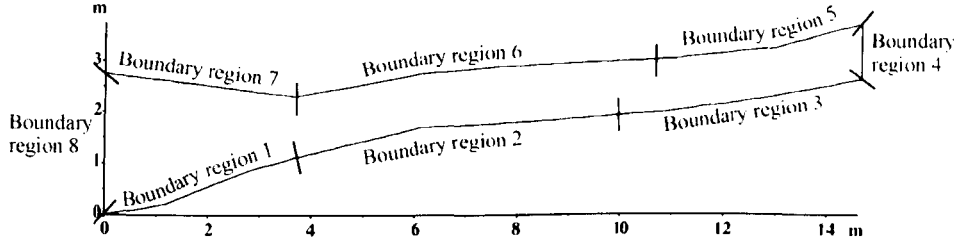

Figure 6.30 Diagram showing the boundary regions along which tracer was introduced to the Sleepers River domain.

At any time when the water flow was directed across the boundary, tracer was introduced into the domain at a concentration of 10 mg l^{-1}, as in the River Severn case. If the flow across the boundary was directed out of the domain at any point, the boundary condition changed to a free flow condition, so the tracer concentration at the boundary was no longer imposed but was a function of the tracer concentration inside the domain, and tracer was able to leave the domain across this boundary. This model configuration was run using data from the 1996 snowmelt event. In addition, the computation was extended for a hypothetical low flow hydrological event. This low flow simulation used the hydrological boundary conditions as prescribed by the last time step of the snowmelt event simulation, extended into an artificial hydrological results file with constant boundary conditions. For the low flow chemical transport simulation, the initial conditions were prescribed as the last time step of the snowmelt event simulation. No additional tracer was added to the domain during

the low flow simulation; the aim of this was to monitor the movement of the existing tracer (introduced during the snowmelt event) through the domain.

Values of dispersivity were specified as 0.1 m longitudinal dispersivity (along the flow) and 0.01 m transverse dispersivity (across the flow). These values were ten times smaller than the values chosen for the River Severn model, to reflect the fact that the Sleepers River domain is smaller than the River Severn domain, and that dispersivity values are thought to be dependent on the scale of the domain (Freeze and Cherry, 1979). The value of molecular diffusion was specified as 5×10^{-10} m^2 s^{-1}.

6.4.2 Results

Results from four out of the eight tracer sources (2, 4, 6, and 8) are illustrated in this section. Each diagram has four parts: (a) the tracer distribution at the end of the snowmelt event (i.e. after 28.5 days of the simulation, after the tracer concentration along the boundary had been specified as 10 mg l^{-1} for the whole snowmelt simulation); (b) after one day of post-snowmelt event low flow conditions (the tracer concentration was no longer specified along the boundary during the low flow event); (c) after 15 days of the low flow event; and (d) the tracer mass in the domain over the course of the simulation, corrected in the manner described in Section 6.3.2.

The maximum tracer mass in the domain varied between the four tracer sources illustrated. This reflects both the differing boundary lengths along which the tracer was introduced, and the length of the flow path that each tracer followed as it was transported to the point of export from the domain. In the case of the tracer introduced on the right-hand side riparian zone boundary (tracer source 6), this also reflects the dynamic nature of flow across this boundary, with flow both into and seepage out of the domain. Generally, once the snowmelt event starts, the mass of tracer in the domain quickly reaches a peak, and then levels out to a fairly constant value (Figure 6.31 to Figure 6.34, part (d)). This constant value is reached when the amount of tracer entering the domain approximately equals the amount of tracer that is leaving. At the end of the event (i.e. when the tracer input stops), the mass of tracer quickly decreases to a negligible value. There are some fluctuations in the tracer mass during the course of the snowmelt event, which reflect the slight changes in water flux into the domain across the boundaries; if the flux decreases slightly, the mass of tracer introduced to the domain at that time will be slightly reduced. These fluctuations are essentially of the same absolute magnitude for each boundary source; the fluctuations for tracer source 6 look more significant (Figure 6.33d), but this is because the total solute mass in the domain is smaller for this tracer.

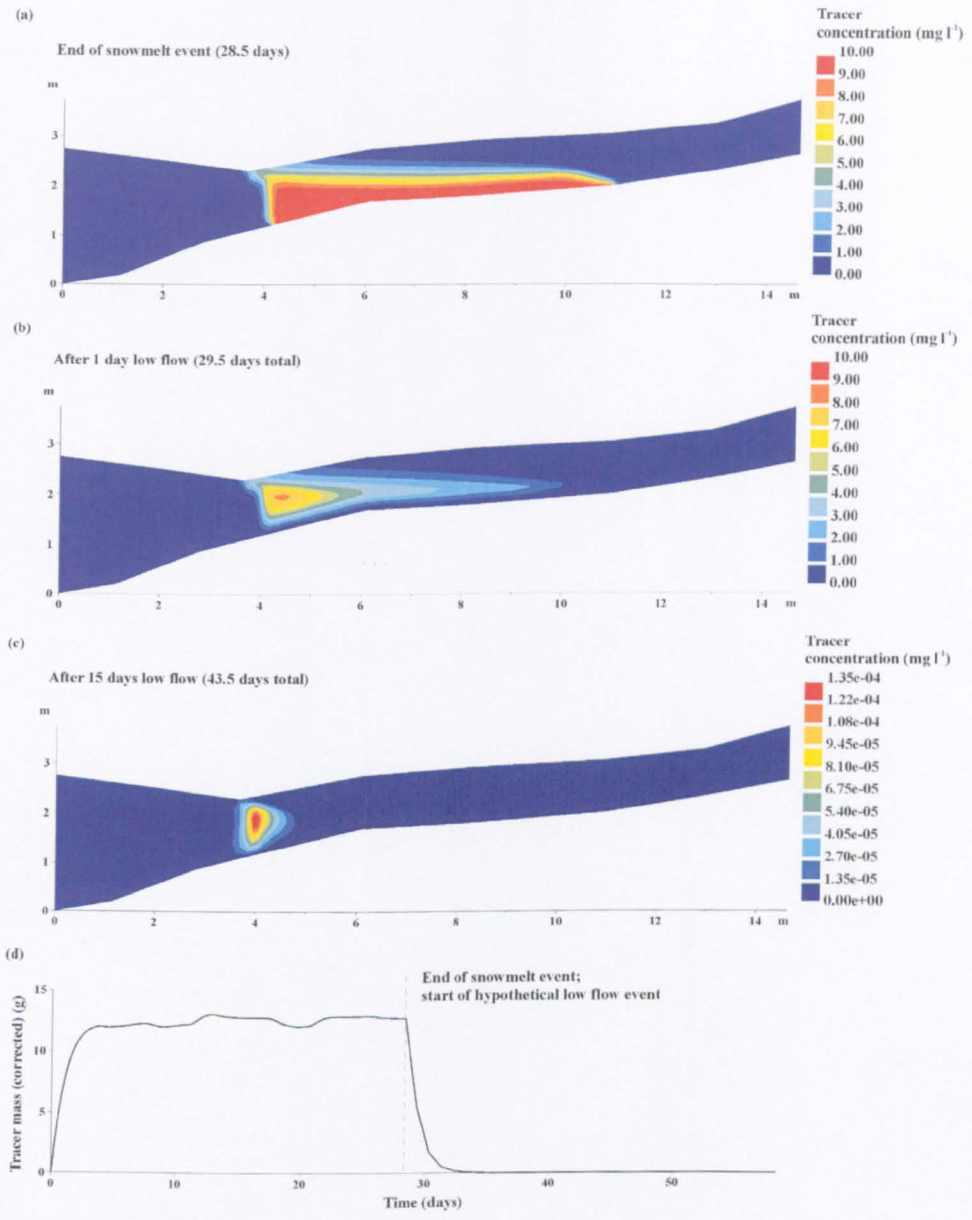

Figure 6.31 Distribution of tracer introduced at boundary region 2 in the Sleepers River domain (a) at the end of the snowmelt event, (b) after 1 day low flow, and (c) after 15 days low flow. Note the different concentration scales. Corrected tracer mass is shown in (d).

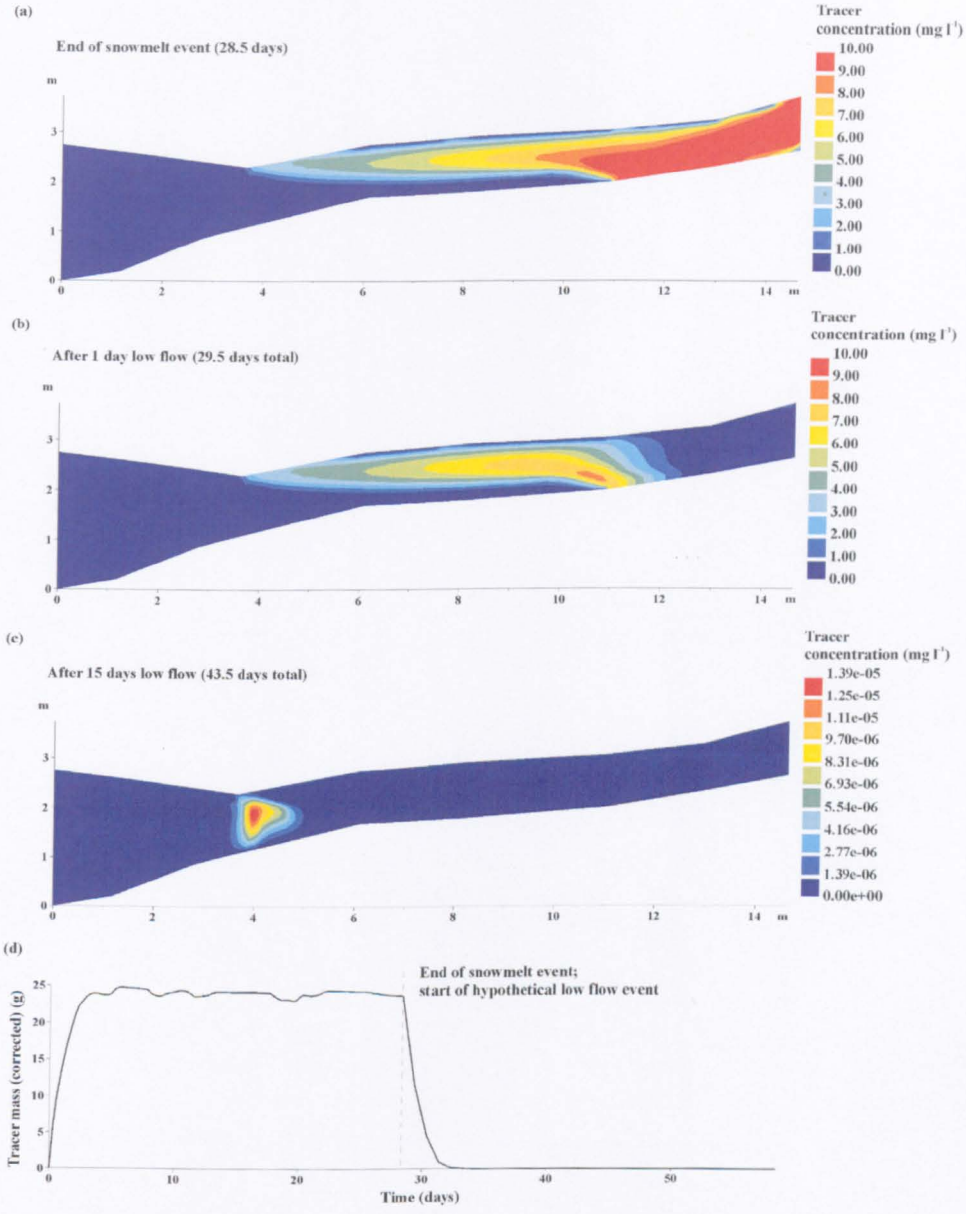

Figure 6.32 Distribution of tracer introduced at boundary region 4 in the Sleepers River domain (a) at the end of the snowmelt event, (b) after 1 day low flow, and (c) after 15 days low flow. Note the different concentration scales. Corrected tracer mass is shown in (d).

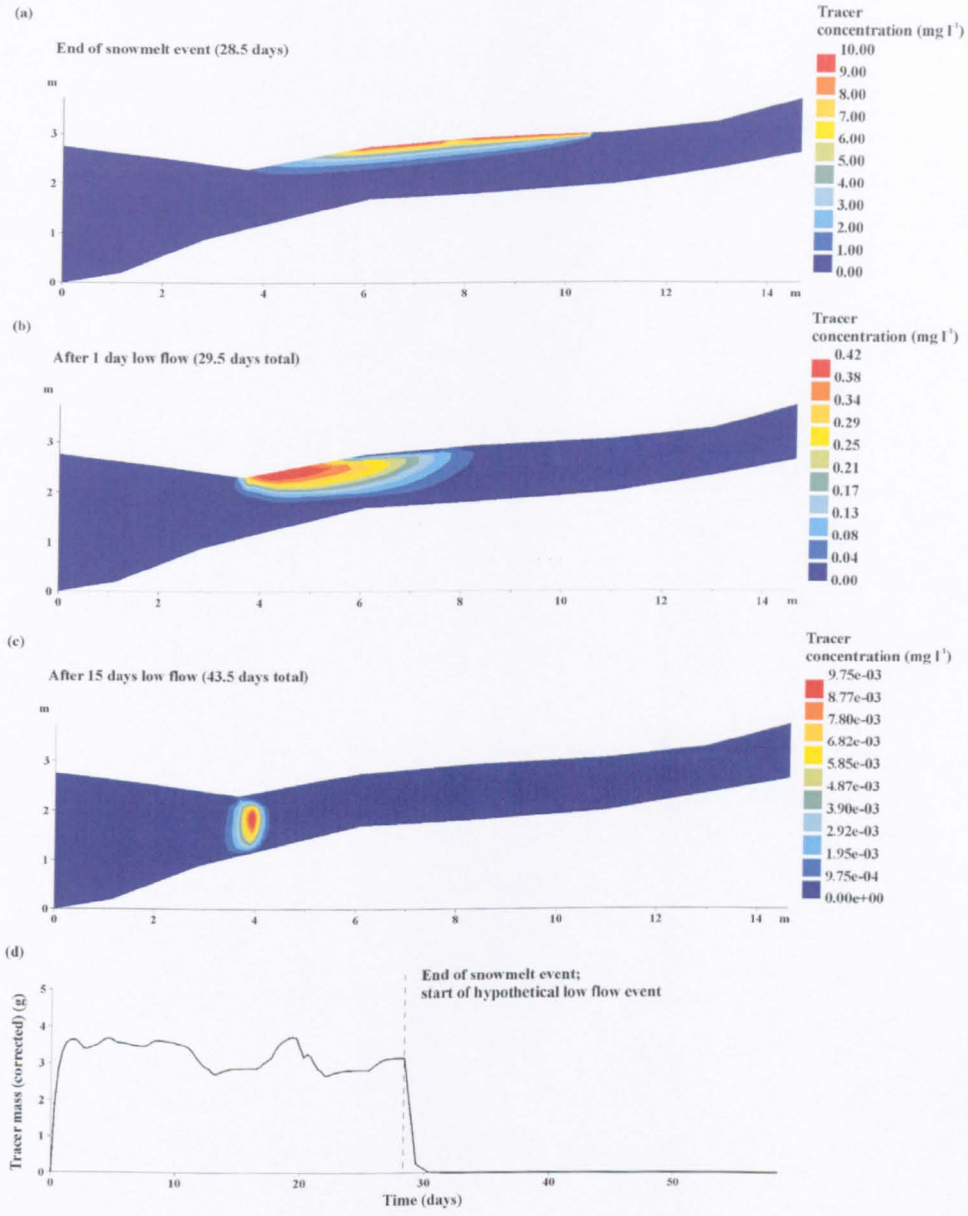

Figure 6.33 Distribution of tracer introduced at boundary region 6 in the Sleepers River domain (a) at the end of the snowmelt event, (b) after 1 day low flow, and (c) after 15 days low flow. Note the different concentration scales. Corrected tracer is also shown in (d).

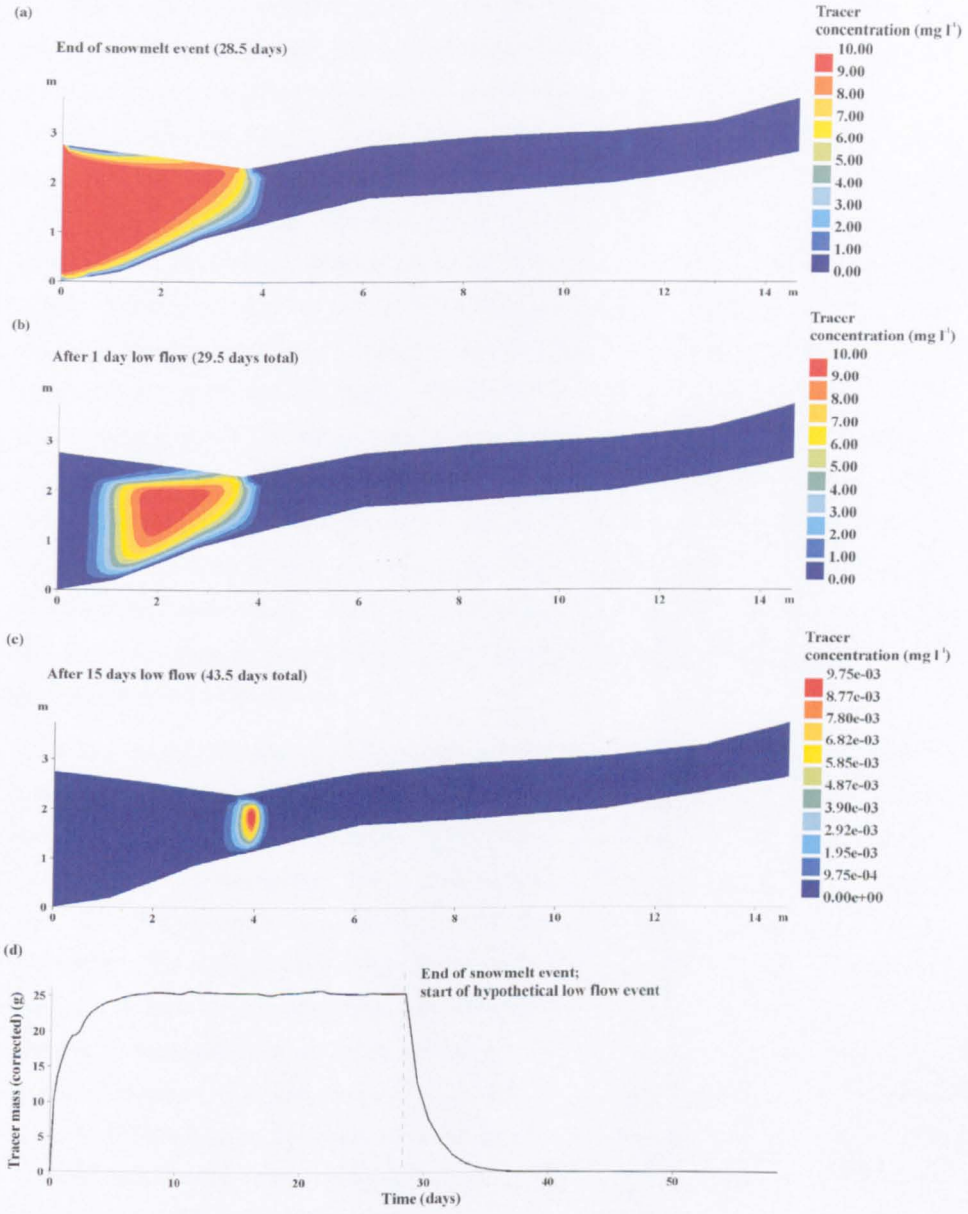

Figure 6.34 Distribution of tracer introduced at boundary region 8 in the Sleepers River domain (a) at the end of the snowmelt event, (b) after 1 day low flow, and (c) after 15 days low flow. Note the different concentration scales. Corrected tracer mass is shown in (d).

The scale and configuration of this upland riparian zone, in comparison with the lowland floodplain, clearly introduces some significant changes in water and transport flow processes, which this hypothetical tracer study helps to demonstrate. First, as the scale of the domain is so much smaller, the movement of the tracer through the domain has to be viewed from a different perspective. The tracer in the Sleepers River domain appears to be transferred more rapidly than in the River Severn case. In fact, the absolute rate of transport is similar, and the apparent difference just reflects the much smaller scale of the Sleepers River domain. However, in terms of chemical residence time this is an important result, as it shows clearly that tracer deposited in the domain during a hydrological event in the headwater riparian zone (in this case, a snowmelt event), can be exported from the domain within a matter of a few days. This is aided in the Sleepers case by the fact that the riparian zone remains almost fully saturated, so transport remains rapid, and there is no accumulation of tracer in the unsaturated zone as occurred on the lowland floodplain during post-flood event low flow. In the lowland floodplain case, the overall mass of tracer in the domain can remain high if the tracer does not reach an outflow boundary; and this may take weeks or months, exacerbated when the soil saturation decreases after the flood event. In the Sleepers River case, the domain is small and tracer introduced to the riparian zone reaches an outflow point within a few hours or days.

In terms of mixing of water of different provenance, there are significant process differences between the two floodplain scales. In the lowland river case, the groundwater ridging phenomenon was found to be important in holding up contributions of water and solute from the hillslope to the floodplain. This process was not found to be operating in the upland case. For this snowmelt event at Sleepers, there was no input of stream water to the floodplain. The configuration of the hillslope-riparian zone-channel and the associated hydraulic gradient is such that the stream water does not flow out on to the riparian zone (there is no overbank flow, as such), and there is no bank storage. Therefore, there is no mixing of hillslope water and river-derived water in the riparian zone, an important process in the River Severn case. However, this study has only investigated one snowmelt event and a hypothetical low flow event at the upland site, and this conclusion may not be valid at all sites and under all hydrological conditions.

In the case of the upland riparian zone, the simulations indicate that (a) contributions from groundwater (along the soil-bedrock boundary) could have an important influence on riparian zone chemistry, and (b) mixing through surface seepage may be more important than at the lowland site. There is a significant input of hillslope water, and also groundwater (from the bedrock) to the riparian zone, which was not evident at the lowland floodplain site (although the rather poor characterisation of the lower boundary in the River Severn case

leaves some uncertainty over this conclusion). Even if the scale of water flowing across the soil-bedrock boundary in the Sleepers River case has been incorrectly specified, there can be little doubt that because the bedrock is much closer to the surface than at the River Severn, whatever happens at this boundary will have a much greater influence on water and chemical flow paths within the riparian zone than at the lowland site. There is more significant (or more noticeable) exfiltration and reinfiltration at the foot of the hillslope and throughout the riparian zone than was found in the lowland floodplain case. This may be evidence of the influence of the shallower depth of the domain (i.e. the closer proximity of the bedrock to the surface) affecting flow paths within the riparian zone. The steeper gradient of the riparian zone and underlying bedrock probably also increases the likelihood of observing exfiltration and reinfiltration of water and associated solutes along the surface of the riparian zone.

Once tracer input has stopped, tracer from each source moves along a well-defined path to the stream channel. The rapid transfer time (in comparison with the size of the domain) means there is little opportunity for dispersion, and the tracer moves in a well-defined plume, retaining a high concentration from the point of input until it leaves the domain. This is in contrast with the lowland floodplain site, where long residence times increase the opportunity for dispersion, resulting in low concentrations of solute within the domain (in the saturated zone), even though the total solute mass remained high.

Tracer introduced along the lower-middle section of the boundary (to the right-hand side of the stream channel, tracer source 2, Figure 6.31) remains in the lower portion of the soil profile. Vertical movement of this tracer is probably limited by the low conductivity of the thin, dense till layer (see diagram of soil distribution, Figure 5.30 in Chapter 5). However, in the region of the stream channel, the distribution of this tracer demonstrates the effect of the sharp upward flow directly beneath the stream channel. Virtually no tracer crosses to the left-hand side of the riparian zone, indicating that this is effectively a no flow boundary. Tracer tends to concentrate in the region directly under the stream channel after several days of low flow conditions, although after 15 days of low flow, the tracer concentration is very low (Figure 6.31c). The distribution of tracer after 15 days of low flow conditions is very similar for all four tracer sources illustrated here.

Tracer introduced along the right-hand side of the boundary (tracer source 4, Figure 6.32) illustrates the contrast in transport between the upper and lower regions of the domain, as separated by the dense till layer. Some of the tracer introduced across this boundary leaves the domain across the lower boundary at the far right-hand side. Most of the remaining tracer is directed to the upper region of the riparian zone, where hydraulic conductivity is generally high. The conductivity in the upper region (the riparian peat) is also higher in the horizontal direction than the vertical, which, in combination with the low conductivity of the

dense till layer, restricts vertical movement of the tracer towards the lower part of the domain.

Although the length of boundary specified for tracer source 2 (lower-middle boundary) is very similar to the length of boundary specified for tracer source 6 (upper-middle boundary), a much smaller tracer mass is introduced to the domain in the case of tracer source 6. This reflects the fact that the upper part of the riparian zone is sometimes not fully saturated, resulting in a lower conductivity (and associated lower rate of tracer transfer) at these times, and that the surface of the riparian zone in this region experiences seepage. At any point along the boundary where flow is leaving the domain, tracer does not enter, so the actual length of boundary across which tracer can cross is significantly reduced. Overall, the paths of tracer movement for tracer entering the domain across this part of the boundary are relatively short, and any tracer that does infiltrate the domain is exported again over a very short distance, either at or near the stream channel, or via exfiltration across the surface of the riparian zone.

Tracer introduced across the left-hand side boundary (tracer source 8) once again illustrates the effect of the no-flow boundary underneath the stream channel (a vertical boundary approximately 4 m from the left-hand side boundary). Tracer movement is restricted to the left-hand side of the domain, and as tracer approaches this no-flow boundary it is deflected upwards so that tracer leaves the domain through the stream bed. Once the input of tracer ceases at the beginning of the low flow simulation, the tracer in the upper portion of the riparian zone, above the dense till layer, leaves the domain very quickly.

6.4.3 Summary of hypothesis two

The simulations carried out in this section can be contrasted with the results from the River Severn simulations of hypothesis one to give an indication of the effect of floodplain scale on water source, flow path and residence time. These results are novel because a comparison of upland and lowland floodplain/riparian zones has not previously been attempted.

1. For the upland riparian zone, over the period studied, the main source of water is the hillslope. In contrast to the lowland floodplain, the river is not a significant water and solute source, as water does not move from the river into the riparian zone under the circumstances investigated here. At the upland site, the hydraulic head varies over a much greater range at the hillslope boundary, in comparison with the variation in stream stage, which means that the hydrological activity at the hillslope boundary therefore has a greater controlling influence on flow paths and flow rates throughout the domain. This is in contrast to the lowland floodplain, particularly during periods of high flow, where the hydrological regime of the river, and associated changes in river stage, have a

much more important controlling effect. The difference in the relative importance of river and hillslope water and solute inputs in upland versus lowland locations is linked to the difference in slope of the land bordering the stream channel, and potentially the underlying geological configuration.

2. Solute delivered to the upland riparian zone has a short residence time in comparison with the lowland floodplain site. Tracer introduced to the upland domain reaches an outflow boundary on the scale of hours to days in comparison with the lowland floodplain which (depending on the tracer source) may take weeks to months. This is mainly due to the much smaller scale of the domain, which means that solute appears to be transferred through the domain much more rapidly, but also because the riparian zone is almost fully saturated throughout the hydrological event studied here. Even after the main snowmelt event at Sleepers River, there are only very small areas of the domain that are not fully saturated. At the lowland site there is the potential for an unsaturated zone up to 5 m thick, which imposes a severe restriction on the transfer of water and solute through this region of the floodplain. The shorter residence time of tracer at the upland site also means that the tracer remains at a high concentration until it is exported from the domain, whereas in the lowland river case, there is a much greater opportunity for dispersion to decrease the tracer concentration.

3. At the upland site, the soil-bedrock interface is known to be much closer to the surface than at the lowland site. The influence of this bedrock boundary on water flow patterns is therefore much greater for the upland riparian zone, and further exploration of this influence could be important. In the Sleepers River case, the possibility of water and tracer being introduced across the lower boundary is important because it is one of the few ways that tracer could be transferred through the lower part of the domain.

4. The heterogeneity of the soil in this upland riparian zone clearly has an important influence on the flow paths of water and chemicals from various sources around the domain. The dense till layer in particular seems to impede vertical movement of chemicals between the upper and lower horizons of the riparian zone. This is not to say that heterogeneities are not present at lowland sites, or that, if present, they are not important. However, because of the rapid transfer times in the smaller scale upland zone, soil heterogeneities could have a proportionally greater influence than at lowland sites. Any chemical not directly delivered to a particular region of the floodplain by advection (because of restrictions imposed by the distribution of different soil types) may never reach this region because of the low potential for dispersion. Conversely, some regions of the domain could effectively become conduits for rapid water and tracer movement.

5. Surface seepage and reinfiltration are more noticeable processes at the upland site than on the lowland floodplain. This may be influenced by the steeper overall gradient of the riparian zone (and also the underlying bedrock) at the upland site, encouraging exfiltration of water along the surface of the riparian zone. At the River Severn site, the gradient of the floodplain surface is very shallow and has little influence on hydraulic head gradients across the domain and associated flow paths, although localised topographical variations do play a role in determining patterns of tracer infiltration into the domain.

6.5 Chapter summary

This chapter has concentrated on using the coupled ESTEL2D-SUBIEF2D model to investigate processes of water and chemical transport in floodplain environments. The modelling strategy employed here has provided information about hydrological flow paths and mixing processes, and chemical residence times, that has not previously been obtained, allowing a new way of visualising and extending the interpretation of the available fieldsite data.

Investigation of floodplain processes has concentrated on two main themes: (a) the effect of the type of hydrological event and (b) the effect of floodplain scale, on water and chemical source, flow path and residence time. This study has given an indication of the relative importance of river and hillslope inputs of water and chemicals to the near-stream zone, and how the scale of hydrological event affects the interaction of these sources. It has suggested the important role of the unsaturated zone in regulating chemical transport through the floodplain, and has generally indicated the areas of the floodplain that are subject to the greatest solute movement. This study has also shown that there are important differences in process operation between the Sleepers River (upland) and River Severn (lowland) sites. These two sites only represent one example of an upland riparian zone and one example of a lowland floodplain respectively, which makes it difficult to draw definite conclusions about the differences between upland and lowland sites in general. However, this is possibly the first time that such a comparison has been attempted, and this investigation has at least highlighted potential areas for further analysis. The results presented here certainly show the importance of expanding the investigation of lowland floodplains; the different processes in operation between headwater and lowland near-stream areas mean that the results of existing smaller scale riparian zone studies cannot simply be scaled up to the larger, lowland floodplains.

The following chapter will explore the potential of the coupled model to look at the importance of other controlling factors (e.g. soil hydraulic characteristics, organic matter

content, and temperature) on chemical transport and transformation, in the case of a non-conservative solute.

7 Exploring Floodplain Biogeochemical Processes

In Chapter 6, the hydrological processes in floodplain systems were investigated using the newly developed and tested numerical code. This has given an indication of the degree of movement and mixing of waters of different provenance, under varying hydrological conditions and between different scales of floodplain.

This analysis will be extended in this chapter to explore floodplain biogeochemical processes. This exploration will focus on denitrification processes in floodplains, as a relevant example of the more general chemical transport modelling capability of this numerical code. An explanation of the denitrification process will be presented, followed by an exploration of the mathematical equations that have been used to represent this process, including a consideration of relevant controlling factors. The exact formulation chosen for implementation in ESTEL2D-SUBIEF2D will then be described. This extension to the numerical code will then be subject to a model assessment procedure, before being used to explore hypothesis three as stated in Chapter 6 (Section 6.2).

7.1 Denitrification in the floodplain environment

Nitrogen transport and transformation, and particularly the denitrification process, have been a focus of field studies in floodplain chemical transport research. This focus has arisen as a result of the idea that floodplains can be used as buffer zones to protect watercourses from non-point agricultural pollutants (e.g. Haycock and Burt, 1993). Specifically, environmentalists see the denitrification potential of floodplain soil as providing a way to prevent excess nitrate concentrations reaching water bodies and causing detrimental water quality effects. In the riparian buffer literature, there are more publications on nitrate removal than any other category of water quality function (Correll, 2000).

This focus on nitrate transport and the denitrification process has resulted in a substantial body of field evidence for factors that are believed to affect denitrification activity. However, these studies remain empirical and site specific, and there has been no substantial effort to generalise these results. Of course, part of the reason for this is the difficulty and expense of conducting denitrification studies in the field. Exploring a wider range of

denitrification scenarios and combinations of controlling factors using a modelling approach therefore seems appropriate and timely. The basic concepts are sufficiently well developed to provide a sound basis for hypothetical scenario testing, and the model will provide a suitable base with which to bring these ideas together and explore them more thoroughly.

In addition, indications from field studies are that the denitrification process is extremely spatially and temporally variable (Johnsson *et al.*, 1991). Current uncertainty about the efficacy of subsurface denitrification as a mechanism of nitrate removal in riparian zones may reflect the difficulty of detecting localised patches of denitrifying activity at depth in these environments (Hill *et al.*, 2000). For example, Hill *et al.* (2000), in a recent study of denitrification activity in a floodplain on a similar scale to the River Severn, suggested that in riparian zones with deep permeable sediments, the ability to remove nitrate (NO_3^-) by denitrification is critically dependent on localised supplies of oxidisable carbon. A distributed model would be a very useful tool with which to explore the heterogeneity of the denitrification process in a way that would be virtually impossible in a field situation.

Denitrification will therefore be the focus of the exploration of floodplain chemical transport and transformations, as an appropriate example of the capabilities of the newly developed model. The next section will begin by setting denitrification within the wider context of the nitrogen cycle, followed by a more detailed consideration of the denitrification process itself. This will include an investigation of the controlling factors, and the formulations available for representing the process in mathematical terms.

7.2 Conceptual model of denitrification

Gains in soil nitrogen occur through the fixation of molecular dinitrogen (N_2) by microorganisms, and from the deposition of ammonium (NH_4^+) and nitrate in rain water; losses occur through vegetation removal, leaching and volatilisation (Figure 7.1). Mineralisation is the conversion of organic forms of nitrogen to ammonium and nitrate. The initial conversion to ammonium is referred to as ammonification; the oxidation of this compound to nitrate is termed nitrification. The utilisation of ammonium and nitrate by plants and microorganisms constitutes assimilation and immobilisation, respectively. Combined nitrogen is ultimately returned to the atmosphere through biological denitrification, thereby completing the nitrogen cycle (Stevenson, 1982).

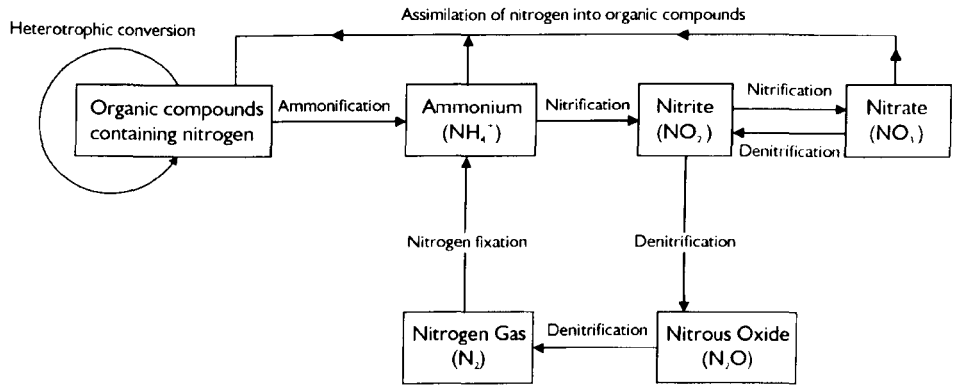

Figure 7.1 A simplified version of the nitrogen cycle showing some of the important biological reactions (from Burt and Haycock, 1992)

Denitrification is the process by which oxidised and ionic forms of nitrogen are transformed into reduced and molecular components (nitric oxide (NO), nitrous oxide (N_2O) and N_2) (Paul and Clarke, 1996). Several intermediates are involved:

$$NO_3^- \longrightarrow NO_2^- \longrightarrow (NO) \longrightarrow N_2O \longrightarrow N_2 \text{ gas}$$

NO is enclosed in brackets as it is not commonly detected as a free intermediate; in fact, for a time there was much debate as to whether it was a true intermediate at all, or merely a by product in the denitrification pathway (Matchett, 1998). Denitrification involves a set of coupled reduction-oxidation (redox) reactions. Redox reactions involve electron transfer between chemical species (Deutsch, 1997). Oxidation occurs if there is a loss of electrons in the transfer process and reduction occurs if there is a gain of electrons. The oxidised component or oxidant is the electron acceptor and the reduced component or reductant is the electron donor (Sparks, 1995). In soils, this transfer process is largely microbiologically mediated (Hénault and Germon, 2000).

Denitrification is understood to occur when facultative anaerobes use nitrate as an alternative electron acceptor to oxygen when oxidising carbon (C) under oxygen-deficient conditions (Grant, 1991). Soluble nitrate is the electron acceptor for denitrification, and soluble carbon is the substrate. A hierarchy exists among the terminal electron acceptors utilised in bacterial respiration. Oxygen is the favoured electron acceptor because it has a higher reduction potential, and has clear precedence over any of the nitrogen oxides as the terminal electron acceptor in the respiration of the majority of the denitrifiers studied to date. When oxygen is not available, the bacteria use the next best electron acceptor available i.e. nitrate. Denitrification is clearly a second choice mechanism for even the most active of the denitrifiers, which vary over a significant range in their demands for rigorousness of exclusion of oxygen before turning to an alternative form of respiration. Anoxia is required

by some (Payne, 1981). It has also been demonstrated that aerobic denitrification is a process that can occur in soils, even though the notion that denitrification is primarily or exclusively an anaerobic process has dominated both theory and practice (Lloyd, 1993).

Denitrification is controlled by a number of factors, such as soil moisture (which influences soil oxygen concentration), nitrate content, temperature and carbon availability, which vary irregularly and substantially in time and space and also interact with each other. Field measurements of denitrification show a corresponding extreme spatial and temporal variability (Hénault and Germon, 2000).

7.2.1 Mathematical models of denitrification

Mathematical modelling approaches to denitrification include chemical kinetics, enzyme- (or biomass-) based kinetics, and empirical equations (Bosatta *et al.*, 1981).

7.2.1.1 Chemical kinetics

Kinetics is the study of time-dependent processes (Sparks, 1995). Chemical kinetics can be defined as the investigation of chemical reaction rates and the molecular processes by which reactions occur where transport is not limiting.

The theoretical expressions for reaction rates as functions of the concentrations of reactants and products are differential equations of the general form (Rolston *et al.*, 1984):

$$-\frac{dA}{dt} = k' A^a B^b .....N^n \qquad 7.1$$

where the order of the reaction is defined as the sum of the exponents (a, b, ..., n) of the concentration terms A, B, ..., N, and k' is the reaction rate coefficient. A first order rate process means that the flow out of the first pool to the second is proportional to the quantity of material remaining in the first pool (Wu and McGechan, 1998). The orders of reactions are experimentally determined (Sparks, 1995). However, whether to use first- or zero- order kinetics with respect to nitrate is currently a matter of debate. To take account of the sensitivity of such transformations to environmental factors such as temperature and soil moisture content, the transformation rate coefficient k' can incorporate a response function for each of these factors.

In Selim and Iskander's (1981) model of nitrogen behaviour in soils irrigated with liquid waste, the denitrification process was considered to be of the first-order kinetic type. Soil environmental conditions such as soil suction, aeration, temperature, organic matter content, and pH were incorporated in the denitrification rate coefficient. Kruh and Segall (1981) treated denitrification as a first-order reaction, where the denitrification rate coefficient was a

function of various factors: temperature, pH, soil moisture, oxygen concentration and availability of electron donors in soil (organic matter). The denitrification routine in the DRAINMOD-N model of nitrogen transformation in soil (Breve *et al.*, 1997) is based on a first-order equation, with rate adjustment factors for soil water content, temperature, and depth (which is treated as a surrogate for carbon availability).

7.2.1.2 Enzyme kinetics

Enzyme kinetics can be seen as an extension of chemical kinetics in which the biological limitations on reaction rates are taken into consideration. Two enzyme kinetic models are often used: the Michaelis-Menten model, and the Monod model. The first model differs from the latter by lack of a growth in microbial population or enzyme concentration while the substrate is being degraded.

The Michaelis-Menten rate law is given by:

$$\frac{dS_b}{dt} = V_{\max} \frac{S_b}{(K_{Sb} + S_b)} \qquad 7.2$$

where S_b is the substrate, V_{max} is the maximum transformation rate, and K_{Sb} is the concentration of S_b at which the transformation rate is half the fastest possible. When S_b is small compared with K_{Sb} the rate is first order with respect to substrate concentration. If S_b is much larger than K_{Sb}, the rate is zero order with respect to S_b.

Michaelis-Menten kinetic modelling of denitrification may take a single or double form:

$$\frac{dN}{dt} = \frac{K_d N}{(K_n + N)} \qquad 7.3$$

$$\frac{dN}{dt} = \frac{K_d N}{(K_n + N)} \frac{C}{(K_c + C)} \qquad 7.4$$

where K_d represents the maximum denitrification rate, N is the concentration of nitrate, C is the concentration of soluble organic carbon, and K_n and K_c are the half-saturation constants for nitrate and carbon transformation respectively (Bosatta *et al.*, 1981). In these comprehensive models it is often necessary to model not only the nitrogen- but also the carbon-cycle, since the latter is usually the rate-limiting nutrient (Bosatta *et al.*, 1981). The maximum denitrification rate can be modified by various non-dimensional reduction factors, representing the effects of environmental conditions, as used in the PHOENIX model of carbon and nitrogen dynamics in grassland soils (McGill *et al.*, 1981).

In Monod kinetic models, the rate of degradation of the chemical is directly coupled to the population dynamics of the microbial degraders. The Monod equation is therefore an

extension of the Michaelis-Menten expression where V_{max} is substituted by a term that takes into account the effect of microbial growth on the substrate S. Since microbes are central to the dynamics of soil nitrogen, it is highly desirable to describe explicitly the activity, growth, and death of the microbes in nitrogen transformations. Van Veen and Frissel (1981) used a Monod-type equation to describe denitrification in their simulation of nitrogen behaviour in soil.

7.2.1.3 Summary of kinetic modelling approaches

The Monod (Michaelis-Menten) kinetic models are theoretically sound and more generally applicable than chemical kinetic models since they are linked to microbial biomass and enzyme-substrate kinetics. Biomass-based models, however, require several parameters that are not commonly measured in soil nitrgoen studies in the field and it is difficult to measure and/or validate microbial biomass. On the other hand, chemical kinetic models require minimal input data and are suitable for low substrate concentrations, but generally do not fit the entire time course of change (Bosatta *et al.*, 1981). Another limitation to chemical kinetic models is that they assume unlimited biological potential, so there are no upper or lower limits on the rate of reaction. Further to the kinetic modelling approaches, empirical rate equations have often been used when cause and effect relations are not known or when there is an advantage in fitting a model to site-specific experimental data. However, empirical models do not have universal applicability as kinetic models do.

7.2.2 Factors affecting denitrification rate

There are several factors that have been shown to affect the rate of denitrification in soils (Stanford *et al.*, 1975):

(i) soil-water relations, as they control rate of oxygen replenishment,

(ii) soil pH and temperature,

(iii) quantity of easily metabolisable organic matter,

(iv) concentration of nitrate.

When modelling the denitrification process using a mechanistic approach, these factors must be incorporated, generally in the form of functions that affect the maximum denitrification rate. For example, in the soil nitrogen dynamics model SOILN, the denitrification model uses response functions to incorporate the effects of soil aeration status e_m, soil nitrate concentration e_{NO3}, and soil temperature e_t (Wu and McGechan, 1998). The denitrification rate is expressed as:

$$\frac{dN}{dt} = K_d e_t e_m e_{NO_3} \qquad 7.5$$

where K_d is the potential denitrification rate and e_{NO3} is a Michaelis-Menten response function of nitrate content. Easily metabolisable organic matter is assumed freely available.

The form of these functions may exert a considerable influence on the model results (Johnsson *et al.*, 1991). In a detailed study comparing the temperature and moisture functions of nine models of carbon-nitrogen transformations in soils, Rodrigo *et al.* (1997) found differences in function values that varied with the range of temperature and moisture considered. In addition, the effects of each of these factors on rates and extent of denitrification in soil are co-dependent and become difficult to examine separately (Payne, 1981).

Under optimum conditions, denitrification proceeds rapidly until the substrate and/or one or more environmental parameters become rate limiting (Bosatta *et al.*, 1981).

7.2.2.1 Soil-water and oxygen content

The relationship between soil water content and microbial processes in soils is complex, since several physical processes that can affect microbial activity vary with soil water content, particularly water movement, gas diffusion, solute diffusion and the survival and movement of micro-organisms. The water function provides a simple way of accounting for the change in oxygen diffusion and storage in the soil as soil-water content changes. This relationship can vary with soil type, depending on the moisture-retention curve, porosity, concentration of organic matter, and pH. Different studies may use different measures of moisture content (soil water potential, relative water content, or percentage of water-filled pore space), depending on the objective of the study. For example, of the four nitrogen dynamics models reviewed by Wu and McGechan (1998), two (SOILN and DAISY) used relative water content in the description of denitrification, and two (ANIMO and SUNDIAL) used soil water tension. The matric potential theoretically allows comparison of soils of different textures; the soil water content can be more useful for describing processes that can limit microbial activity in soils such as nutrient and oxygen diffusion; while the percentage of water-filled pore space is the best indicator of aerobic/anaerobic microbial activity (Linn and Doran, 1984). The percentage of air-filled pores decreases as soil water content increases, resulting in the development of anaerobic conditions. The intuitively obvious connection between moisture content and rate of loss of nitrate nitrogen is substantiated by both field observation and experimental demonstration in the laboratory (Payne, 1981). If other environmental conditions are at optimum levels, denitrification increases as the soil water content increases.

A study by Rolston *et al.* (1984) indicated that model simulations of denitrification are very sensitive to the water function. Some modellers explicitly allow denitrification to occur only when they assume that anaerobic conditions exist e.g. when the pressure head is 15 cm or less or when soil water content is 80 per cent or greater (Bosatta *et al.*, 1981). The soil water content adjustment factor f_W in the DRAINMOD-N model is calculated with the following equations. Denitrification will not occur when the water content in the soil is less than the lower threshold water content θ_{lim}.

$$f_W = 0 \qquad (\theta < \theta_{lim}) \qquad 7.6$$

Denitrification is at a maximum when the soil is saturated.

$$f_W = \frac{(\theta - \theta_{\lim})}{(\theta_{sat} - \theta_{\lim})} \qquad 7.7$$

The soil water function in the denitrification routine of the SOILN model is:

$$e_m = \begin{cases} 0 & (\theta < \theta_{lim}) \\ \left[\dfrac{(\theta - \theta_{\lim})}{(\theta_{sat} - \theta_{\lim})}\right]^{d_1} & (\theta >= \theta_{lim}) \end{cases} \qquad 7.8$$

where θ_{lim} (%) is the threshold water content for denitrification and d_1 is an empirical constant. Suggested parameter values are 2 for d_1, and 17 for θ_{lim} (Wu and McGechan, 1998). The soil water content function e_m is used as an indirect expression of the influence of soil oxygen status on the denitrification rate, increasing from a threshold point θ_{lim}, to a maximum at saturation θ_{sat}. Previous implementations of this function have suggested that denitrification essentially ceases (i.e. e_m approaches 0) below 80 per cent of the saturated water content value, for oxygen can apparently diffuse readily to most microsites of biological activity. The maximum potential for denitrification would occur at complete saturation (e_m = 1), where all the pores are completely filled with water, and the diffusion of oxygen is entirely limited by diffusion through soil-water.

In the NEMIS model of denitrification in soils (Hénault and Germon, 2000), the pore space occupied by water, δ_{WF}, is calculated according to the formula proposed by Linn and Doran (1984):

$$\%\delta_{WF} = 100 \times \left(\frac{\theta_v}{P_t}\right) \qquad 7.9$$

where θ_v is the per cent volumetric water content and P_t the per cent total soil porosity.

The soil water content regulates oxygen availability in soil and thus denitrification. Roughly half the variation in denitrification rates in the field can be explained by soil moisture (Paul and Clarke, 1996). The onset of denitrification occurs at about 60 per cent water filled pore space (Linn and Doran, 1984). Grundmann and Rolston (1987) have stated that denitrification starts when the water-filled porosity exceeds 62 per cent.

7.2.2.2 Soil pH and temperature

Like any other biological activity, the rate of denitrification in soil would be expected to vary directly with temperature, and this expectation has been met repeatedly (Payne, 1981). The rate of biological processes generally increases exponentially as the temperature increases above freezing point, followed by a flattened response until the biological optimum is reached, and a negative response above the optimal temperature. Temperature may also have an indirect effect on denitrification rate by affecting both oxygen solubility and oxygen diffusion in water (Paul and Clarke, 1996). The minimum temperature for denitrification is about 5 °C and the maximum is about 75 °C (Paul and Clarke, 1996). In experiments with Rothamsted clay and sandy loams, activity was minimal at 2-5 °C but progressively increased with rises in temperatures ranging up to 25 °C. From that temperature to 60 °C, denitrifying activity continued to increase slightly, then dropped sharply to inactivity (Payne, 1981).

Most functions describing the effect of temperature on microbial processes are based on the Arrhenius or Van't Hoff laws. The Arrhenius function has a thermodynamic basis, but this may not be useful in a complex system such a soil, where each group of microorganisms is likely to have its own temperature response (Rodrigo *et al.*, 1997). The Van't Hoff function describes the exponential increase in the transformation rate with temperature:

$$f_T = Q_{10}^{(T-T_b)/10} \qquad 7.10$$

where Q_{10} is a constant representing the increase in the transformation rate for a temperature increase of 10 °C, T is the actual soil temperature (°C), and T_b is the base temperature for which microbial activity is defined. This type of temperature function has been used in several denitrification models, including DRAINMOD-N. The reported values of Q_{10} vary widely depending on the substrate, experimental conditions and the temperature range (Rodrigo *et al.*, 1997). Rolston *et al.* (1984) used a Q_{10} value of 2.

The soil temperature response function e_t in SOILN is based on a Q_{10} expression. Alternative equations are used dependent on the temperature range:

$$e_t = \begin{cases} Q_{10}^{(T-T_b)/10} & (T>T_{lim}) \\ \frac{T}{T_{\lim}} Q_{10}^{(T-T_b)/10} & (T<T_{lim}) \end{cases} \qquad 7.11$$

where e_t is the temperature response function, Q_{10} is the response to a 10 °C soil temperature change, T is soil temperature (°C), T_b is the base temperature (°C) at which $e_t = 1$, and T_{lim} is a threshold temperature (°C) below which the temperature response is a linear function of temperature. The coefficients suggested by the Wu and McGechan (1998) are a value of 3 for Q_{10}, a value of 20 for T_b, and a value of 5 for T_{lim}.

In the IMPACT model of nitrogen leaching from soil (Andrews *et al.*, 1997), rates of denitrification are based on daily soil temperature at 30 cm depth, T_{30}:

$$\frac{dN}{dt} = K_d . \varepsilon^{(T_{30}-21)} (NO_3 - N) \qquad (T_{30} \geq 10\ ^{\circ}C) \qquad 7.12$$

In this study, a 10 °C temperature limit and a temperature correction factor ε of 1.07 (after Reddy *et al.*, 1979) were selected.

Rodrigo *et al.* (1997), in comparing the temperature functions in nine carbon-nitrogen transformation models, summarised that selecting an appropriate Q_{10} or base temperature value should be more important than deciding which of the two laws, Arrhenius or Van't Hoff, should be used.

Soil pH may also have an influence on denitrification activity, as most denitrifying bacteria grow best at pH 6-8. Denitrification is capable of proceeding at a much wider range of pH values; it becomes slow but may still remain significant below pH 5 (Paul and Clarke, 1996). An optimum pH is hard to define as it may depend on the species and age of the denitrifiers, together with the nitrate concentration. There are few examples where the effect of pH has been included in denitrification models, which may be because of all the environmental factors that affect denitrification, the condition of suitable pH is most likely to be met.

7.2.2.3 Soil carbon content

As most denitrification is accomplished by heterotrophic bacteria, the process is strongly dependent on carbon availability. There is a general correlation between total soil organic matter content and denitrification potential, but much better correlation occurs with the supply of easily decomposable organic matter. Its decomposition produces carbon dioxide (CO_2) and reduces oxygen (O_2) levels, thus increasing demand for nitrate as an electron acceptor. The type of carbon, and its availability, is therefore another important factor regulating the denitrification rate in soils. Jorgensen and Richter (1992) looked at the

composition of carbon fractions and potential denitrification in peat soils. The negative correlation between potential denitrification and the degree of peat decomposition confirms that the solubility of organic matter is an important criterion for its bioavailability. Stanford *et al.* (1975) found that denitrification rates in a number of diverse soils correlated better with the soluble fraction of soil carbon (the glucose-equivalent) than with total soil carbon. This result is not surprising, because much of the total carbon of soils is highly resistant to decomposition.

The carbon cycle and nitrogen cycle are therefore closely intertwined during the denitrification process (Paul and Clarke, 1996). There is, however, a large variation in the rigour with which the influence of carbon concentration is incorporated in models of denitrification. In the SOILN model, carbon is assumed freely available in the soil and its effect on denitrification rates is therefore not represented at all (Johnsson *et al.*, 1991). Kruh and Segall (1981) use an approach whereby the denitrification rate is expressed as a function of the available carbon in soil, including a decomposition rate constant for the carbon fraction. Rolston *et al.* (1984) incorporate the effect of carbon by hypothesising that denitrification occurs according to a first order reaction with respect to both nitrate and carbon concentrations, giving a second order reaction overall. The more comprehensive soil carbon and nitrogen cycling models can take the calculated value of soluble organic carbon concentration to use directly in calculations of denitrification (Wu and McGechan, 1998).

7.2.2.4 Nitrate concentration

The effect of nitrate concentration on denitrification rate is taken into account according to the type of kinetic algorithm selected. According to Paul and Clarke (1996), at nitrate concentrations exceeding 20 mg N l^{-1} the denitrification reaction is independent of the amount of nitrate present and follows zero-order kinetics. The reaction rate may be determined by the amount of carbon available for metabolism rather than by the nitrate level. At low nitrate concentrations, the kinetics of the reduction appear to be first-order. The Michaelis-Menten models therefore have more general applicability, because they can be applied over the entire range of nitrate concentrations. Choosing a zero-order or first-order chemical kinetics model can restrict the application of the model to conditions of high or low nitrate concentrations, respectively.

The effect of nitrate in the SOILN model is controlled by the half-saturation constant K_n, and soil nitrate concentration, N:

$$e_{NO_3} = \frac{N}{N + K_n} \qquad 7.13$$

This is an example of Michaelis-Menten kinetics. A suggested value for the coefficient K_n is 10 (Wu and McGechan, 1998).

7.3 Implementation in ESTEL2D-SUBIEF2D

In summary, denitrification rates in previous models are apparent as a multiplicative function of (Hénault and Germon, 2000):

1. either a denitrification rate coefficient or a soil potential denitrification rate
2. dimensionless functions to account for water content and temperature effects and
3. either nitrate and available carbon concentrations, or a dimensionless function to account for nitrate effect, the effect of available carbon content then being taken into account through the soil potential denitrification rate.

The denitrification process can be modelled by specifying a maximum denitrification rate and a series of non-dimensional reduction factors. The reduction factors are formulated as '0 to 1' functions, with the independent variable being an environmental (i.e. temperature or moisture) or biological (i.e. C/N ratio, microbial population density) condition influencing the process. The denitrification model implemented in ESTEL2D-SUBIEF2D follows this format, being broadly based on the structure of the denitrification model in SOILN. It also takes advantage of the double Michaelis-Menten representation of the transformation of nitrate, which is appropriate for a wide range of nitrate concentrations, and which allows for explicit representation of the influence of carbon concentration on denitrification rates. This is a significant difference from the SOILN model, which assumes a non-limiting carbon source. The only way that a variable carbon concentration can be incorporated in the SOILN model is by specifying a different potential denitrification rate for different soil layers, reflecting a general trend of decreasing carbon concentration, and hence denitrification activity, with depth. In the light of the hypothesis of authors such as Hill *et al.* (2000) that denitrification activity is limited to specific hotspots within a floodplain soil, linked to the availability of carbon, it was felt to be important to allow a spatially variable concentration of carbon over the whole model domain, which is then incorporated explicitly in the denitrification equation.

Denitrification in SUBIEF2D is therefore modelled as a double Michaelis-Menten process, using a maximum potential denitrification rate that is adjusted by two dimensionless reduction factors:

$$\frac{dN}{dt} = K_d F_W F_T \frac{N}{K_n + N} \frac{C}{K_c + C} \qquad 7.14$$

where N [M L^{-3}] is nitrate (NO_3-N) concentration, C [M L^{-3}] is the dissolved organic carbon (DOC) concentration, K_d [M L^{-3} T^{-1}] is the potential denitrification rate, K_n and K_c [M L^{-3}] are the half saturation constants for nitrate and carbon respectively, and F_W and F_T are dimensionless functions accounting for the effects of soil water content and soil temperature, respectively. The formulation of each function within the denitrification model has been based on examples from the literature and other model approaches to denitrification. The water content function is:

$$F_W = \begin{cases} 0 & \theta \le \theta_{lim} \\ \left(\dfrac{\theta - \theta_{\lim}}{\theta_{sat} - \theta_{\lim}} \right)^{d_l} & \theta_{lim} < \theta < \theta_{sat} \\ 1 & \theta \ge \theta_{sat} \end{cases} \qquad 7.15$$

where θ is volumetric moisture content [L^3 L^{-3}], d_l is an empirical constant, θ_{sat} is the saturated moisture content [L^3 L^{-3}], and θ_{lim} is the limiting moisture content for denitrification activity [L^3 L^{-3}]. Figure 7.2 shows the effect of different values of d_l on the moisture function. The value of volumetric moisture content is supplied from the ESTEL2D hydrodynamic results file. This distributed, high resolution hydrological representation is an important distinction between the SUBIEF2D implementation of denitrification and previous models.

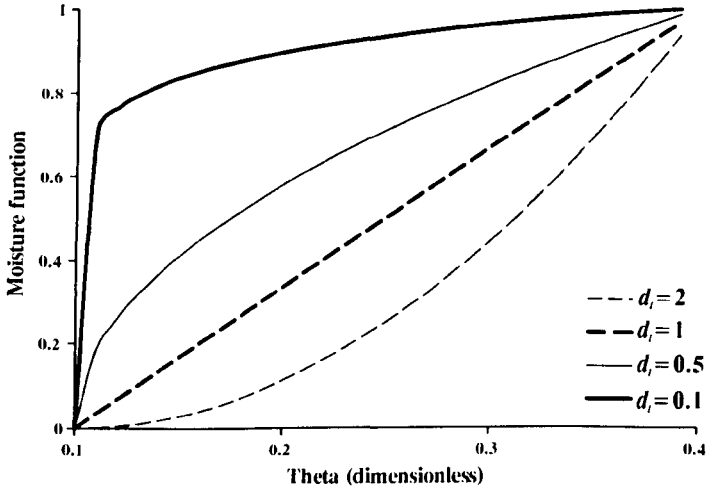

Figure 7.2 Dimensionless moisture function, illustrating the effect of different values of d_l; θ_{lim} = 0.1, θ_{sat} = 0.4.

The temperature function is:

$$F_T = \begin{cases} 0 & T \leq T_{lim} \\ Q_{10}^{(T-T_{opt})/10} & T_{lim} < T < T_{opt} \\ 1 & T \geq \theta_{opt} \end{cases} \qquad 7.16$$

where T is the current soil temperature, T_{opt} is the optimum temperature for denitrification, T_{lim} is the limiting temperature for denitrification, and Q_{10} is the rate of change associated with a 10 °C change in soil temperature. This is a Van't Hoff temperature function. The microbial activity is assumed to be zero below a limiting temperature, which can result in a small discontinuity at this point. Figure 7.3 shows the effect of different values of Q_{10} on the temperature function. Figure 7.4 shows the effect of different values of the half-saturation constant on the Michaelis-Menten function.

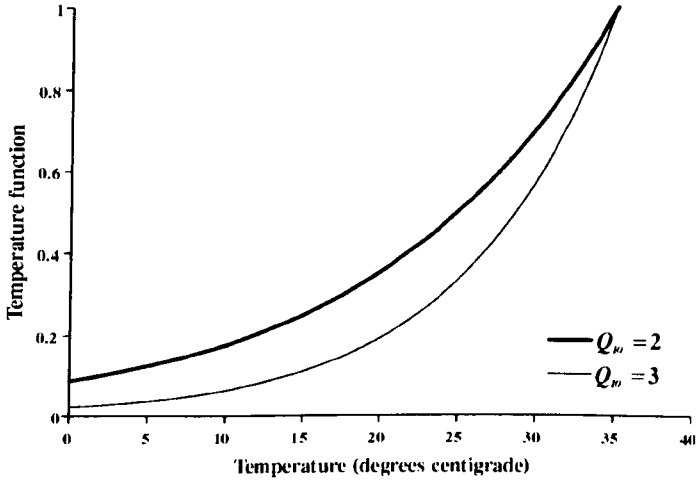

Figure 7.3 Dimensionless temperature function, illustrating the effect of different values of Q_{10}, T_{opt} = 35 °C.

A limitation of this implementation of the denitrification process in SUBIEF2D that the change of carbon concentration over time is not modelled; in effect, the carbon is not used up by the denitrification process. However, at the very least, the incorporation of the carbon function is an advance on previous models (e.g. SOILN). In addition, the finite element formulation facilitates a preliminary examination of the effect of a spatially distributed carbon content throughout the model domain, with a degree of resolution that has not previously been possible. Thus, the present carbon function introduces sufficient complexity for the present application. In addition, the way that the denitrification model has been

implemented is such that a description of carbon utilisation could easily be incorporated once a suitable mathematical representation was found for this purpose.

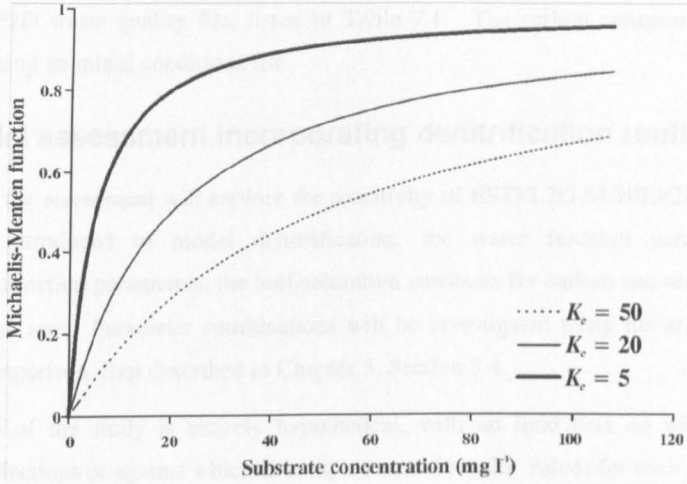

Figure 7.4 Example of the Michaelis-Menten function, illustrating the effect of different values of the half saturation constant.

Table 7.1 Objects used in the SUBIEF2D water quality file.

Object	Description	Denitrification example
State variables	These variables can be chemical components, tracers, etc. A variable V will be a state variable if SUBIEF2D has to compute its variation according to a $dV/dt = \ldots$ equation.	Nitrate concentration.
Computed variables	These variables are computed at each point of the mesh using the values of other variables. It is then possible to write these variables into the SUBIEF results file. In contrast with state variables, computed variables are calculated using a $V = \ldots$. equation.	Water content function, temperature function.
Parameters	These are constants used to parameterise the equations of the model:	
External	External parameters are input data for the model, whose values are likely to be changed by the user during the study. They define a water quality model dictionary. The user can change the external parameter values directly from a water quality steering file.	Denitrification rate constant, half-saturation constant.
Internal	Internal parameters appear in the equations of the model just as computation intermediaries, necessary to make these equations readable.	

The denitrification routine is implemented in SUBIEF2D using the water quality file. This is an input file that allows the user to define the variables that are needed and implement equations to model the transformation rate. Four different classes of objects may be used in the SUBIEF2D water quality file, listed in Table 7.1. The carbon concentration will be initialised using an initial conditions file.

7.4 Model assessment incorporating denitrification routine

This part of the assessment will explore the sensitivity of ESTEL2D-SUBIEF2D to the new parameters introduced to model denitrification: the water function parameters, the temperature function parameters, the half-saturation constants for carbon and nitrate, and the denitrification rate. Parameter combinations will be investigated using the analytical case study for comparison, first described in Chapter 3, Section 3.4.

As this part of the study is entirely hypothetical, with no field data on which to base parameter selections or against which to compare model results, values for each parameter in the denitrification model are based on literature values.

7.4.1 Parameter values for denitrification model

7.4.1.1 Potential denitrification (K_d)

The denitrification potential of a soil has been defined as the amount of NO_2 and N_2O released within a given period when a soil amended with KNO_3 and glucose is incubated anaerobically in the presence of acetylene (Šimek *et al.*, 2000). It is essentially the rate of denitrification under substrate non-limiting conditions. An assay of Denitrifying Enzyme Activity (DEA) characterises the maximum potential denitrifying activity within a given body of soil, and is synonymous with the potential denitrification slurry technique of Smith and Tiedje (1979). Literature values of potential denitrification are not easy to compare because of variations in potential denitrification measurement procedures. It is well documented that different techniques (for example mode of sampling, preparation of soil samples, and treatments) can produce different values of denitrification (Šimek *et al.*, 2000); see Table 7.2 for examples.

Matchett (1998) carried out a study of denitrification on a temperate, lowland floodplain on the River Thame, UK, in an agricultural catchment. Six zones were identified across a 100 m cross section of the floodplain: river [A], oxbow [B], mid-floodplain [C], footslope [D], topslope [E] and scrub [F]. The floodplain vegetation was characterised by rough grass, utilised as improved grazing. The present analysis will make use of potential denitrification data from Matchett (1998) as the characteristics of the River Thame floodplain, in terms of

location within the catchment, climate and land-use, are similar to those of the River Severn, the model of which will be the basis of the denitrification simulations. These data also give a wide range of potential denitrification values on which to base the sensitivity analysis.

The measurement of potential denitrification was obtained under non-limiting physical and chemical conditions: carbon, nitrate, chloramphenicol (which inhibits *de novo* synthesis of reduction enzymes) and water. Values were reported in Matchett (1998) in terms of mass of dry soil ($\mu g\ N\ g^{-1}$ dry soil d^{-1}). These values have been converted to units of mg $N\ l^{-1}$ soil water d^{-1} using values of gravimetric water content; all values will therefore be expressed in terms of concentration in soil water, rather than concentration in dry soil, as required by this modelling approach. This is a rough approximation, but as the range of potential denitrification values is so large, the margin of error involved in this conversion is felt to be relatively insignificant. This is especially true given that the aim of the sensitivity analysis is to test a range of values based on realistic measurements, not any one specific value. A range of potential denitrification values were available from this floodplain site:

(a) measurements taken over a range of depths at site A (river), site B (oxbow) and site C (mid-floodplain) (Table 7.3a);

(b) the average of denitrification measurements taken over the year at each site, A to F (Table 7.3b);

(c) the average of denitrification measurements taken over the site for each month, May 1994 to April 1995 (Table 7.3c).

Table 7.2 Examples of potential denitrification rates obtained using different methods (cited in Bates and Spalding, 1998).

Methodology	**Potential denitrification rate** $mg\ N\ l^{-1}\ d^{-1}$	**Reference**
In situ microcosms amended with varying ethanol-C concentrations.	14-26	Bates and Spalding (1998)
In situ glucose and NO_3^- amended denitrification using acetylene blockage techniques.	0.2 to 3.1	Trudell *et al.* (1986)
Unamended aquifer core sediment microcosms.	5×10^{-3} to 0.5	Smith and Duff (1988)
Amended sediments	~34	
Amended septic drain field sediments	~160	Ward (1985)
Ontario aquifer sediments in a smaller microcosm	0.9 to 3.4	Gillham (1991)

Table 7.3 Potential denitrification rates calculated from Matchett (1998).

(a) measurements taken over a range of depths at site A, B, and C

Site	Potential denitrification $\mu g\ N\ g^{-1}$ dry soil d^{-1}	Gravimetric moisture content $g\ g^{-1}$	Potential denitrification $mg\ N\ l^{-1}$ soil water d^{-1}	Potential denitrification $mg\ N\ l^{-1}$ soil water s^{-1}
Depth: site A (Aug-93)				
5-10	113.80	31.78	358.11	4.14×10^{-3}
20-25	49.18	31.69	155.21	1.80×10^{-3}
27-32	20.87	30.23	69.05	7.99×10^{-4}
40-45	6.03	34.85	17.30	2.00×10^{-4}
70-75	3.26	59.24	5.50	6.37×10^{-5}
Depth: site B (Aug-93)				
5-10	133.70	28.21	473.89	5.48×10^{-3}
20-25	31.68	39.56	80.08	9.27×10^{-4}
27-32	15.53	54.20	28.65	3.32×10^{-4}
40-45	15.89	63.54	25.01	2.89×10^{-4}
70-75	0.99	58.23	1.70	1.97×10^{-5}
Depth: site C (Aug-93)				
5-10	174.18	51.20	340.20	3.94×10^{-3}
20-25	258.99	56.73	456.53	5.28×10^{-3}
27-32	3.33	27.83	11.97	1.39×10^{-4}
40-45	1.84	21.80	8.44	9.77×10^{-5}
70-75	0.09	20.22	0.45	5.21×10^{-6}

(b) annual average potential denitrification values for each site, A to F.

Site	Potential denitrification $\mu g\ N\ g^{-1}$ dry soil d^{-1}	Gravimetric moisture content $g\ g^{-1}$	Potential denitrification $mg\ N\ l^{-1}$ soil water d^{-1}	Potential denitrification $mg\ N\ l^{-1}$ soil water s^{-1}
A	55.85	37.07	150.66	1.74×10^{-3}
B	32.98	46.78	70.50	8.16×10^{-4}
C	90.89	65.20	139.40	1.61×10^{-3}
D	49.46	50.94	97.09	1.12×10^{-3}
E	8.30	22.77	36.45	4.22×10^{-4}
F	0.93	15.74	5.91	6.84×10^{-5}

(c) whole-site average potential denitrification values for each month.

Site	Potential denitrification $\mu g\ N\ g^{-1}$ dry soil d^{-1}	Gravimetric moisture content $g\ g^{-1}$	Potential denitrification mg N l^{-1} soil water d^{-1}	Potential denitrification mg N l^{-1} soil water s^{-1}
May-94	28.14	35.41	79.47	9.20×10^{-4}
Jun-94	82.73	43.39	190.67	2.21×10^{-3}
Jul-94	29.63	24.80	119.48	1.38×10^{-3}
Aug-94	45.33	27.32	165.92	1.92×10^{-3}
Sep-94	52.18	37.81	138.01	1.60×10^{-3}
Oct-94	21.76	36.86	59.03	6.83×10^{-4}
Nov-94	54.57	46.33	117.79	1.36×10^{-3}
Dec-94	45.79	46.14	99.24	1.15×10^{-3}
Jan-95	26.14	42.04	62.18	7.20×10^{-4}
Feb-95	26.71	47.37	56.39	6.53×10^{-4}
Mar-95	56.17	48.78	115.15	1.33×10^{-3}
Apr-95	26.74	40.72	65.67	7.60×10^{-4}

The maximum, minimum, median, upper quartile and lower quartile values of these potential denitrification values were calculated, giving a range of 0.45 to 473.89 mg N l^{-1} soil water d^{-1} (5.21×10^{-6} to 5.48×10^{-3} mg N l^{-1} soil water s^{-1}), and a median value of 79.49 mg N l^{-1} soil water d^{-1} (9.20×10^{-4} mg N l^{-1} soil water s^{-1}). The median value compares favourably with other literature values of potential denitrification rates, as it is of the same order of magnitude (see values in Table 7.4 for comparison). These values were therefore felt to be a suitable basis for the sensitivity analysis.

Table 7.4 Potential denitrification rates: values in soil water were estimated by assuming a gravimetric moisture content of 35% (cited in Šimek et al. (2000)).

Potential denitrification			References
$\mu g\ N\ g^{-1}$ soil d^{-1}	mg N l^{-1} soil water d^{-1}	mg N l^{-1} soil water s^{-1}	
6.6 – 52	18.86-148.57	2.18×10^{-4} to 1.72×10^{-3}	Šimek *et al.* (2000)
21-45	60.00-128.57	6.94×10^{-4} to 1.49×10^{-3}	Yeomans *et al.* (1992)
5	14.29	1.65×10^{-4}	Henrich and Haselwandter (1991)
7	20.00	2.31×10^{-4}	Jarvis and Hatch (1994)

7.4.1.2 Water function

Three parameter values are required for the water function: saturated water content (θ_{sat}), limiting water content (θ_{lim}), and the dimensionless parameter d_l. Johnsson *et al.* (1991), who

used a similar water function in their denitrification model, used a d_l value of 2. The values of d_l that will be tested in this sensitivity analysis are 0.5, 1 and 2. The values of θ_{lim} and θ_{sat} have been chosen to correspond with saturation levels that have been found by several researchers to have particular significance for the denitrification process (for example, Bosatta *et al.* (1981) suggested that several modellers only allow denitrification to occur when the soil water content is 80 per cent or greater). θ_{sat} has been set at a value of 0.6, and values of θ_{lim} of 0.3, 0.39 and 0.48 have been selected, corresponding to saturations of 50, 65 and 80 per cent, respectively (based on a residual moisture content value of zero).

7.4.1.3 Temperature function

Three parameter values are required for the temperature function: optimum temperature for denitrification (T_{opt}), limiting temperature for denitrification (T_{lim}), and the rate of change associated with a 10 °C change in soil temperature (Q_{10}). Firestone (1982) reported that T_{lim} ranges from 2.7 to 10 °C, and that T_{opt} is approximately 65 °C. Bates and Spalding (1998) reported that T_{opt} ranges from 20 to 25 °C. This range in reported T_{opt} values, from 20 to 65 °C, may be a result of the climatic adaptation of the bacteria which mediate the denitrification process (Matchett, 1998). The values of T_{lim} and T_{opt} selected for the sensitivity analysis were 2, 5 and 10 °C for T_{lim}, and 25 and 65 °C for T_{opt}, which reflect the ranges of values identified from the literature.

In terms of Q_{10} values, Johnsson *et al.* (1991) used a value of 3 in their denitrification model, and circa 2 is standard (Matchett, 1998). The values selected for the sensitivity analysis were therefore 2 and 3.

7.4.1.4 Half saturation constant for nitrate (K_n) and carbon (K_c)

Table 7.5 shows a range of K_n values taken from the literature. As they were originally presented in units of μg N g^{-1} soil, they have been converted to the units to be used in this study (mg N l^{-1} soil water) for illustrative purposes, assuming a gravimetric moisture content of 35 per cent. The reported K_n values for soil water vary over four orders of magnitude, from 0.1 to 500 mg N l^{-1} approximately, although most are of the order of 5-35 mg N l^{-1}.

Previous modelling studies have used values of 10 mg N l^{-1} (Johnsson *et al.*, 1991), and 22 mg N kg^{-1} soil (which approximates to 63 mg N l^{-1} soil water assuming a gravimetric moisture content of 35 per cent) (Hénault and Germon, 2000). The sensitivity analysis in this study will test values of 5, 10 and 30 mg N l^{-1}, in keeping with values used in previous modelling studies, and in the range where the majority of measured values lie. As so few modelling studies incorporate the effect of carbon on denitrification, there is a lack of

information about suitable carbon half saturation constants. The values of K_c to be tested during the sensitivity analysis have therefore been based on the selected values of K_n.

Table 7.5 Examples of K_n values from literature sources (cited in Matchett, 1998).

K_n (μg N g^{-1} soil)	K_n (mg N l^{-1} soil water)	Reference
4	11.4	Klemedtsson *et al.* (1997)
117-138	334.3-394.3	Malhi *et al.* (1990)
0.025-0.2	0.07-0.6	Murray *et al.* (1989)
2-5	5.7-14.3	Yoshinari *et al.* (1977)
12-164	34.3-468.6	Matchett (1998)

7.4.1.5 Dissolved organic carbon (DOC)

Hill *et al.* (2000) measured DOC levels in their study of a 100-200 m wide forested floodplain along a fifth order river in Ontario, Canada, in a region of intensive agricultural production. The spatial distribution of DOC concentrations showed a well-defined pattern in the riparian zone. DOC levels in sands at depths of 1.5-5.0 m were usually less than 4.0 mg l^{-1} whereas concentrations were frequently greater than 6.0 mg l^{-1} in peats and interbedded sands and muds. A well-defined zone of high DOC (13-21 mg l^{-1}) concentrations occurred in the upper 1-2 m of the aquifer. Over the whole site, concentrations varied in the range 0-24 mg l^{-1}.

7.4.1.6 Nitrate

The typical values of nitrate found in groundwater are 0.2 to 20 mg N l^{-1}, and an extreme value might be of the order of 70 mg N l^{-1} (Sparks, 1995). In their study of subsurface denitrification in a forest riparian zone, Hill *et al.* (2000) found that groundwater nitrate concentrations entering the riparian zone from the sand plain aquifer ranged from 20-60 mg N l^{-1}. At the plume margins, nitrate concentrations decreased sharply from 12-16 mg N l^{-1} to less than 1 mg N l^{-1}. Groundwater nitrate concentrations in peat and buried channel deposits were usually less than 1 mg N l^{-1}.

Schipper and Vojvodić-Vuković (1998) looked at the effect of porous treatment walls, constructed below the water-table and perpendicular to the groundwater flow, on groundwater nitrate removal. Their study area was on agricultural land on the North Island, New Zealand, and their experimental wall was constructed downslope of a site where effluent applied to land had contaminated groundwater with nitrate. They found nitrate concentrations of up to 50 mg N l^{-1} in some groundwater bores in the study area,

concentrations sometimes exceeding 20 mg N l^{-1} in a stream that flowed through the farm. The average nitrate concentration in the groundwater entering the denitrification wall varied from 5-16 mg N l^{-1}, with individual samples as high as 22 mg N l^{-1}.

Burt *et al.* (1999), in their study of denitrification on the floodplain of the River Thame, UK, found mean nitrate concentrations at this site of 7.7 mg N l^{-1} for the river, 25.91 mg N l^{-1} for a nearby spring, and 1-4 mg N l^{-1} in the groundwater.

7.4.2 Selected parameter values for sensitivity analysis

The final selection of parameter values for the sensitivity analysis is shown in Table 7.6. Where cells are left blank, this indicates that they will take the value given in run number 1, which can be considered as a base run to which the results of further simulations will be compared. All these simulations used a nitrate value of 10 mg N l^{-1}, 10 mg l^{-1} of DOC, and a constant temperature of 15 °C (as used in the model of Johnsson *et al.*, 1991).

Table 7.6 Denitrification parameter values selected for investigation during sensitivity analysis.

Run no	Water function			Temperature function			Carbon function	Nitrate function	K_d
	θ_{lim}	θ_{sat}	d_1	T_{lim}	T_{opt}	Q_{10}	K_c (mg C l^{-1})	K_n (mg N l^{-1})	(mg N l^{-1} s^{-1})
1	0.30 (50%)	0.6	1	5	25	2	10	10	9.2×10^{-4}
2	0.39 (65%)								
3	0.48 (80%)								
4			0.5						
5			2						
6				2					
7				10					
8					65				
9						3			
10							5		
11							30		
12								5	
13								30	
14									5.21×10^{-6}
15									3.10×10^{-4}
16									1.68×10^{-3}
17									5.48×10^{-3}

7.4.3 Sensitivity analysis results

The effect of denitrification on ESTEL2D-SUBIEF2D model results was analysed using the numerical model setup that was used for the analytical comparison in Chapter 3. The results displayed are solute concentration profiles along the domain, at y = 40 m (for mesh design see Chapter 3, Figure 3.7). Figure 7.5a shows the comparison between the analytical solution and the numerical solution under conditions of no denitrification. This illustrates that the numerical solution accords very well with the analytical solution, giving a sound basis on which to analyse the parameter combinations from the sensitivity analysis.

Figure 7.5b illustrates how a change in the limiting moisture content (θ_{lim}) affects the decrease in nitrate concentration away from the nitrate source (at x = 0). At θ_{lim} of 0.48 (equivalent to a saturation of 80 per cent), the decrease in nitrate concentration with distance is virtually indistinguishable from the original simulation that had no denitrification. As the value of θ_{lim} decreases, through 0.39 (65 per cent) to 0.30 (50 per cent), the rate of reduction in nitrate concentration with distance is progressively faster. At a θ_{lim} value of 0.30, virtually all the nitrate has been denitrified by a distance of 25 m from the nitrate source. At a θ_{lim} value of 0.48, nitrate is still present at a significant concentration up to 75 m from the source.

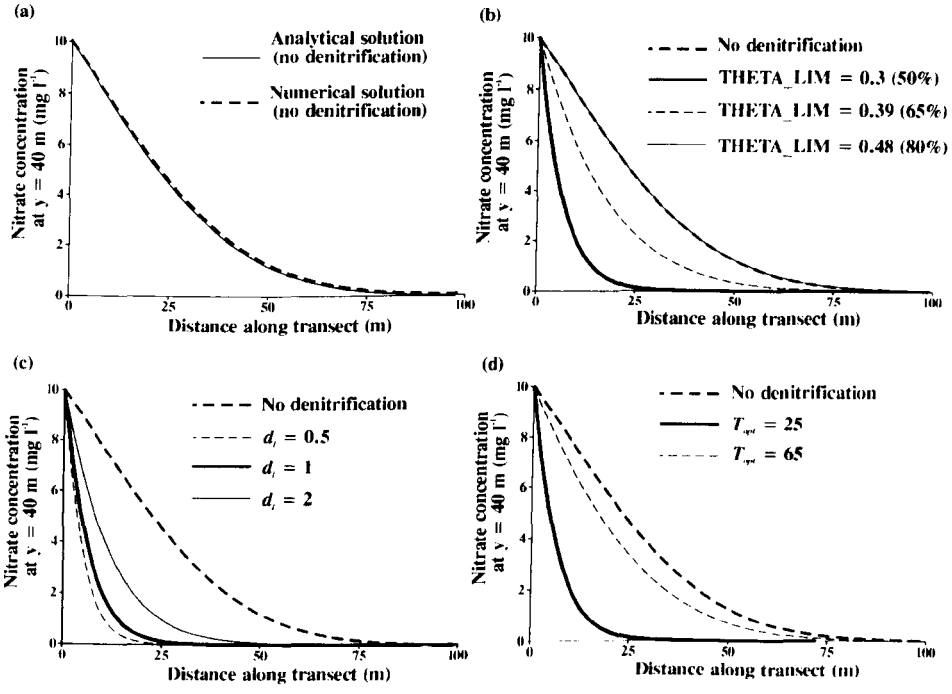

Figure 7.5 Results of sensitivity analysis of denitrification model, illustrated using profiles of nitrate concentration along the analytical transect. (a) no denitrification (comparison of analytical solution and numerical solution), (b) influence of θ_{lim}, *(c) influence of* d_l, *and (d) influence of* T_{opt}.

Figure 7.5c shows the effect of the water function parameter d_l on the rate of decrease in nitrate concentration with distance from the nitrate source. All these simulations were conducted with a θ_{lim} value of 0.30 (50 per cent saturation). With a value of d_l below 1, the nitrate concentration decreases more rapidly with distance from the nitrate source. With a value of d_l greater than 1, the rate of decrease in concentration with distance decreases, so that there is still a significant concentration of nitrate at a distance of up to 50 m from the solute source.

Figure 7.5d shows the effect of changing the value of the optimum temperature parameter T_{opt}. Bearing in mind that the current temperature in all these simulations was kept at a constant 15 °C, changing T_{opt} from a value of 25 to 65 °C has a significant effect on denitrification rates. With T_{opt} at 65 °C, the current temperature is a long way from the optimum, and denitrification rates are correspondingly low; the pattern of decrease in nitrate concentration with distance from the solute source is close to the results of the 'no denitrification' simulation. With a T_{opt} value of 25 °C, the current temperature is relatively close to the optimum, and denitrification rates are correspondingly much greater. Incidentally, changing the value of T_{lim} had no effect on denitrification rate, so the results from those simulations are not illustrated here. This was because the values of T_{lim} tested (2, 5 and 10 °C) were all below the current temperature of 15 °C used in all simulations.

Figure 7.6a shows the effect of changing the value of Q_{10}. Decreasing the value of Q_{10} increases the denitrification rate slightly, but over the range of values suggested by the literature review (2 and 3), the difference in denitrification rate is minor in comparison with some of the other parameters investigated in this study. Figure 7.6b and Figure 7.6c show the effect of changing the half saturation constants for carbon and nitrate respectively. Both show a similar pattern; as the value of the half saturation constant decreases (from 30 to 5 mg N l^{-1}), the rate of denitrification increases. The effect of the half saturation constants obviously depends on the prevailing solute concentration, which is different for DOC and nitrate. This is revealed by the subtle differences that can be seen between the K_c and K_n profiles. In the case of DOC, the concentration remains constant at 10 mg l^{-1} over the entire domain, and for the duration of the event. In the case of nitrate, the concentration introduced to the domain is 10 mg l^{-1}, but this does not remain constant throughout the domain, as the effects of denitrification act to reduce this concentration as soon as the solute starts to move away from the source.

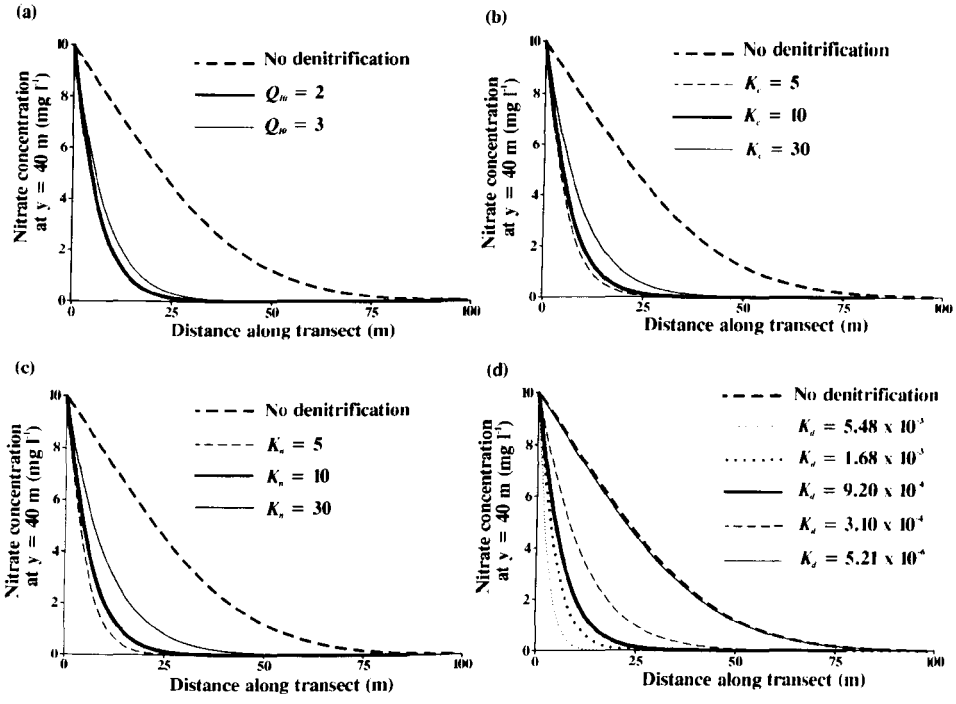

Figure 7.6 Results of sensitivity analysis of denitrification model, illustrated using profiles of nitrate concentration along the analytical transect. (a) influence of Q_{10}, *(b) influence of* K_c, *(c) influence of* K_n, *and (d) influence of* K_d.

The final parameter to be investigated was potential denitrification (K_d). Figure 7.6d shows how the values selected for the sensitivity analysis affected denitrification rates. As expected, as the value of K_d increased, the rate of denitrification also increased. At the smallest value of K_d, 5.21 x 10^{-6} mg N l^{-1} s^{-1}, the rate of denitrification was so low that the profile of nitrate concentration was barely distinguishable from the profile resulting from the 'no denitrification' scenario. At the largest value of K_d, 5.48 x 10^{-3} mg N l^{-1} s^{-1}, the rate of denitrification was very high, so that by the time the nitrate plume reached a distance of approximately 12 m from the solute source, the concentration of nitrate had decreased to a negligible level. Considering that any of these K_d values, which cover a range of three orders of magnitude, could realistically be used in a modelling scenario, this demonstrates the large effect that selection of a particular K_d value could have on simulation results.

In summary, for the ranges tested here the rate of denitrification was most sensitive to changes in the value of potential denitrification (K_d), optimum temperature (T_{opt}), and limiting moisture content (θ_{lim}). The model was least sensitive to changes in the value of Q_{10}. Most importantly, this exercise has demonstrated that the changes in parameter values affected the model in the expected manner.

7.5 Hypothesis Three: other factors (such as carbon content and distribution, temperature and soil hydraulic characteristics) are important in controlling solute transport and transformation

The aim of this section was to show the potential of the model for exploring the effects of other factors that are thought to have an important control on chemical transport through floodplain systems.

The basic set of denitrification model parameters used in the simulations reported in this section were derived from the results of the sensitivity analysis, and are felt to reflect realistic values obtained from literature sources (Table 7.7).

Table 7.7 Base parameter values used during scenario testing of the denitrification model.

Parameter	Value
Limiting moisture content for denitrification activity, θ_{lim} [$L^3\ L^{-3}$]	0.328 (80%)
Saturated moisture content, θ_{sat} [$L^3\ L^{-3}$]	0.41
Empirical constant in water function, d_t [dimensionless]	1
Limiting temperature, T_{lim} [°C]	5
Optimum temperature for denitrification, T_{opt} [°C]	25
Rate of change associated with a 10°C change in soil temperature, Q_{10}	2
Half saturation constant for carbon, K_c [$M\ L^{-3}$]	20 mg l^{-1}
Half saturation constant for nitrate, K_n [$M\ L^{-3}$]	20 mg N l^{-1}
Potential denitrification rate, K_d [$M\ L^{-3}\ T^{-1}$]	9.2×10^{-4} mg N $l^{-1}\ s^{-1}$

7.5.1 Schedule of model runs

The scenarios that are explored in this section concentrate on those factors that are thought to control the denitrification process in floodplain environments. These factors are temperature (for which two different values are tested, representing summer and winter conditions), carbon concentration and distribution within the floodplain, hydrological event, soil hydraulic characteristics (saturated hydraulic conductivity), source of nitrate-rich water (river or hillslope), and the location of the hillslope-floodplain-channel unit within the catchment (headwater or lowland). The characteristics of each model run are listed in Table 7.8.

Simulations 1 to 10 use the River Severn model as a basis. In each of these scenarios, nitrate is modelled from one of two input sources: the hillslope water, or the river water. Where a bankfull or overbank flood event is modelled, the boundary conditions are specified such that when flow is directed across the hillslope boundary, or across the river channel/floodplain surface boundary, into the domain, the nitrate concentration at that boundary is prescribed as 10 mg N l^{-1}. At any time that the direction of water flow reverses, such that water is flowing out of the model domain, the concentration at this boundary is no longer specified (but is a free concentration boundary), and solute is thus able to leave the domain. In run number 3, where the original flood event F is extended for a hypothetical 90 day low flow period, no further nitrate is introduced to the domain after the end of the flood event, but that which is already present in the domain is free to undergo transport and transformation.

Table 7.8 List of scenarios used during testing of hypothesis three.

Run no.	Hydrological event	Dissolved Organic Carbon		Temperature	Saturated hydraulic conductivity*
		Distribution	Concentration (mg l^{-1})	(°C)	(m s^{-1})
1	**Flood event F**	Whole floodplain	High (20)	Winter (6)	5 x 10^{-5} (CL)
2	**Bankfull event A**	Whole floodplain	High (20)	Winter (6)	5 x 10^{-5} (CL)
3	**Extended event F (low flow)**	Whole floodplain	High (20)	Winter (6)	5 x 10^{-5} (CL)
4	Flood event F	Whole floodplain	**Low (3)**	Winter (6)	5 x 10^{-5} (CL)
5	Flood event F	**Surface layer**	**High (20) at surface**	Winter (6)	5 x 10^{-5} (CL)
6	Flood event F	**Patches**	**High (20) in patches**	Winter (6)	5 x 10^{-5} (CL)
7	Flood event F	Whole floodplain	Low (3)	**Summer (17)**	5 x 10^{-5} (CL)
8	Flood event D	Whole floodplain	Low (3)	Winter (6)	**5 x 10^{-5} (CL)**
9	Flood event D	Whole floodplain	Low (3)	Winter (6)	**1 x 10^{-4} (CL)**
10	Flood event D	Whole floodplain	Low (3)	Winter (6)	**1 x 10^{-4} (SL)**
11	Sleepers	Whole domain	High (20)	Winter (6)	SR4
12	Sleepers	Whole domain	**Low (3)**	Winter (6)	SR4
13	Sleepers	**Riparian peat**	High (20) in peat	Winter (6)	SR4

*CL = clay loam soil; SL = sandy loam soil; SR4= Sleepers River distribution of four soil types

Simulations 11 to 13 use the snowmelt event of the Sleepers River model as a basis. In each of these scenarios, nitrate is introduced at the two hillslope boundaries, at a concentration of

10 mg N l^{-1}. As water flow is always directed into the domain across these boundaries, the concentration is specified as 10 mg N l^{-1} for the duration of the snowmelt event.

7.5.2 Results

7.5.2.1 Comparison with conservative tracer

Figure 7.7 shows the distribution of solute within the floodplain after 20 days of flood event F, which is after the main flood peak has passed. The two parts to this figure, (a) and (b), show a comparison of a conservative tracer and nitrate distribution for solute introduced in hillslope water and river water respectively. These simulations have identical initial conditions. In the case of the hillslope water source, the difference appears relatively minor. Near the top of the domain, the concentration and pattern of nitrate is not very different from that observed in the case of the conservative tracer. However, below a depth of 5 m, the concentration of nitrate is negligible, and has certainly reduced to a greater extent than in the case of the conservative solute, which remains at a higher concentration. As the water flow fields are identical in both cases, the reduction in nitrate concentration in this region must be due to favourable conditions for denitrification. The difference observed between the upper 5 m and lower 25 m of the domain probably reflects the contrast in moisture contents (and associated hydraulic conductivity) between these two zones. In the lower part of the domain, high moisture contents keep the hydraulic conductivity near maximum, so solute is rapidly transported away from the source, contributing to lower overall concentrations, while the highly saturated conditions are conducive to rapid denitrification (particularly in this case where carbon concentrations are high throughout the whole domain). In contrast, in the upper part of the domain moisture contents are generally low, restricting solute movement and becoming limiting to the denitrification process.

Nitrate-rich groundwater from the hillslope water source is clearly resident within the floodplain system for a sufficiently long period of time to allow the denitrification process to operate effectively, as Figure 7.8 illustrates. In fact, under the conditions in this scenario, which are highly conducive to denitrification (in particular the high carbon concentration and high moisture content), the mass of nitrate in the domain never reaches such a high level as that of the conservative tracer, and by the end of the flood event/start of the low flow event, there is very little nitrate left in the domain for the denitrification process to act upon.

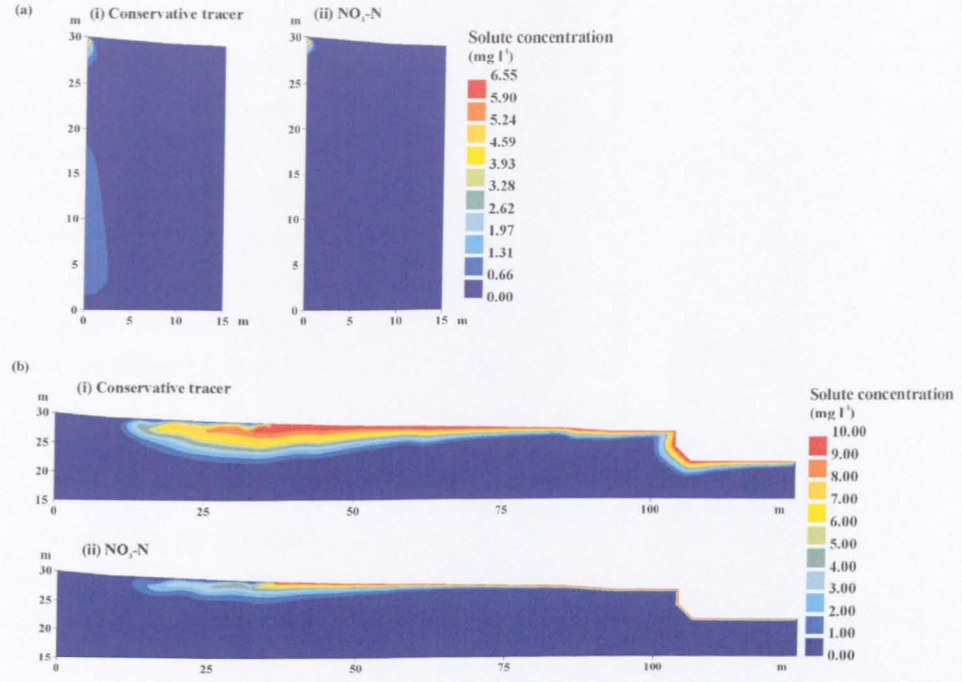

Figure 7.7 Solute distribution: comparison of conservative tracer and NO_3-N for (a) hillslope water source and (b) river water source of solute, after 20 days of flood event F. (Denitrification parameters are as specified in scenario 1, Table 7.8).

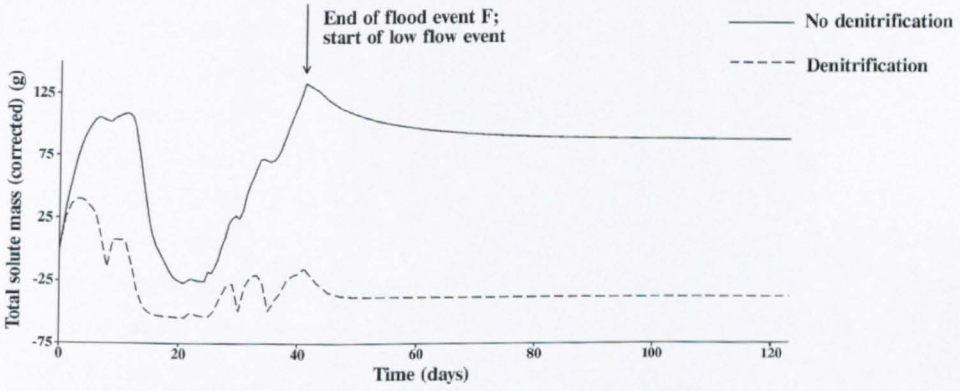

Figure 7.8 Total solute mass: comparison of conservative tracer and NO_3-N for flood event F and subsequent low flow event, for the hillslope water solute source (scenarios 1 and 3; see Table 7.8).

In the case of the nitrate introduced to the domain by the river water, the contrast in pattern of nitrate concentration in comparison with the conservative solute concentration is more marked. Once again, the pattern of saturation seems to be very important. As carbon concentrations are very high, the removal of nitrate from the domain is essentially limited by the moisture content. In the near-stream zone, nitrate is effectively removed as soon as it

enters the domain, as illustrated by the low concentrations of nitrate in this region in comparison with the same region for the conservative solute (Figure 7.7b). The only region of the floodplain where nitrate remains in any significant concentration is near the floodplain surface, and particularly towards the hillslope-floodplain boundary. In this region, high water levels are only maintained for a relatively short period of time. The overbank flow period is long enough to introduce the river-water derived nitrate to the domain almost as far across the floodplain as the hillslope boundary, but the rapid reduction in moisture content in this region (as the river stage drops and the extent of inundation decreases), leaves this patch of nitrate isolated in conditions that are no longer conducive to such rapid denitrification.

7.5.2.2 Effect of hydrological event type

The hydrological characteristics of a site may affect the denitrification process in several different ways: (i) changing the aeration status of the soil, promoting reducing conditions during periods of flooding, (ii) delivery of organic material, which may be a source of both nitrate and carbon, and (iii) delivery of sediment, which may also have an associated organic fraction and may produce a texture favouring denitrifying bacteria. The delivery of water and chemicals is in turn affected by the frequency, duration and seasonality of hillslope runoff and river flood events. This section aims to look at the effect of hydrological event type on the efficacy of the denitrification process.

In terms of hillslope inputs to the floodplain, the pattern of nitrate concentration at the end of overbank flood event F and bankfull event A is very similar (Figure 7.9a and Figure 7.10a). This is influenced by the similar pattern of delivery of nitrate over time to the floodplain for both events, (illustrated by the change in mass over time in Figure 7.11). Although flow is generally in a hillslope to river direction, there is a period during both events when the flow direction is reversed, and any nitrate in the domain can be transported back across the hillslope boundary, in addition to being subject to the denitrification process. By the end of the flood event, nitrate is once again delivered to the floodplain across the hillslope boundary, and will therefore be at a maximum of 10 mg N l^{-1} right on the boundary. The patterns look so similar between the two events because the denitrification rate is very high in both cases; apart from the upper 5 m of the domain, the level of saturation, and all the other denitrification conditions, are the same. Any difference in the amount of nitrate delivered to the floodplain between the two events is masked by the rapid denitrification rate that keeps nitrate concentrations to a minimum.

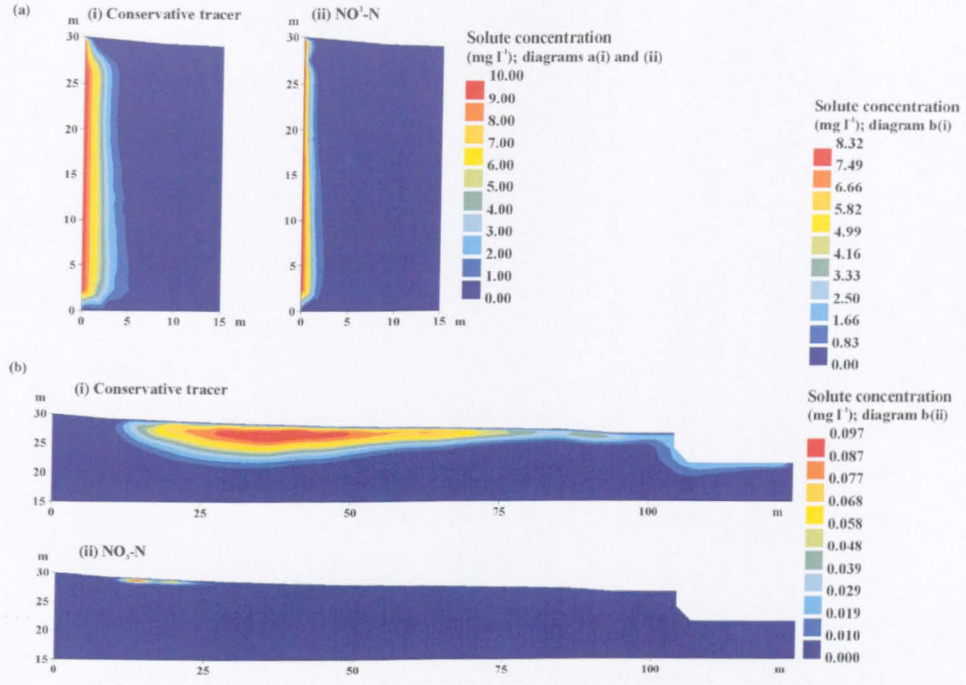

Figure 7.9 Solute distribution: comparison of conservative tracer and NO_3-N for (a) hillslope water source and (b) river water source of solute, at end of flood event F. Note the different concentration scales for the river water solute. (Denitrification parameters are as specified in scenario 1, Table 7.8).

In the case of nitrate delivered via river water, there is an obvious contrast in the distribution of solute between the overbank and bankfull flood event. The difference in the pattern of nitrate concentration at the end of the events is largely due to the difference in the region of the floodplain that the nitrate is delivered to by the river water, and its residence time in the floodplain. In the case of flood event F, virtually no nitrate remains after the 40 day event; a small patch remains near the hillslope, in the surface of the floodplain, where conditions were perhaps slightly less conducive to denitrification (due to lower saturation levels), but even so, the maximum concentration in this region is only 0.097 mg N l^{-1} (Figure 7.9b). In contrast, during bankfull event A, nitrate in river water is not delivered to this region of the floodplain; it remains very localised to the near-stream zone (Figure 7.10b). It appears from these diagrams that denitrification is not so effective in this near-stream region during the bankfull flood event, as the nitrate concentration remains higher than for the overbank flood event, up to a maximum of 0.73 mg N l^{-1}. However, this is because relative to the overbank flood event, by the end of the bankfull flood event the nitrate has been resident in the floodplain for a much shorter period of time. Under conditions conducive to denitrification (particularly the high moisture contents in this region), nitrate introduced to the near-stream bank-storage zone can be denitrified very effectively.

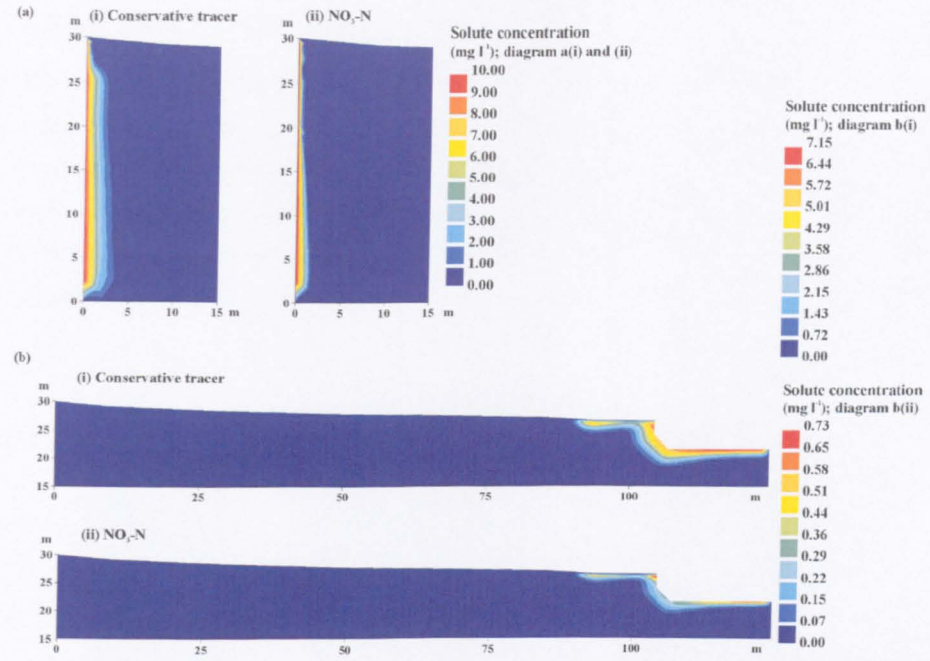

Figure 7.10 Solute distribution: comparison of conservative tracer and NO_3-N for (a) hillslope water source and (b) river water source of solute, at end of bankfull event A. Note the different concentration scales for the river water solute. (Denitrification parameters are as specified in scenario 2, Table 7.8).

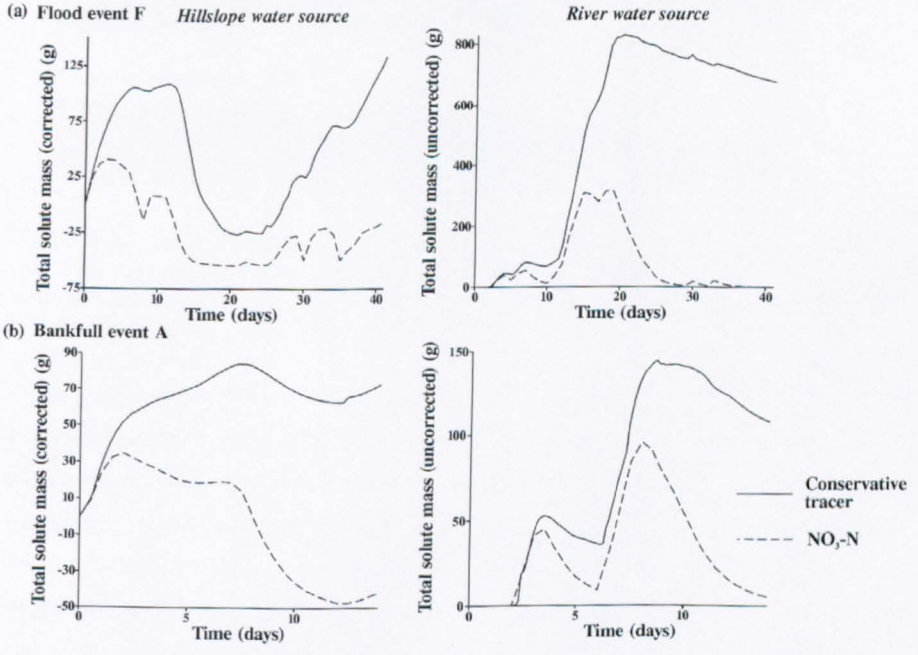

Figure 7.11 Total solute mass: comparison of conservative tracer and NO_3-N for (a) flood event F and (b) bankfull event A, from both the hillslope water and river water solute source. (Denitrification parameters are as specified in scenarios 1 and 2, Table 7.8)

7.5.2.3 Effect of carbon concentration on denitrification

The simulations illustrated so far used a high DOC concentration of 20 mg l^{-1}, effectively meaning that carbon was non-limiting to the denitrification process. However, carbon is generally found at much lower concentrations. Denitrification rates have been found to be highly correlated with carbon concentration (Burford and Bremner, 1975; Reddy *et al.*, 1982); this section looks at the effect of a lower DOC concentration (3 mg l^{-1}) on the denitrification process.

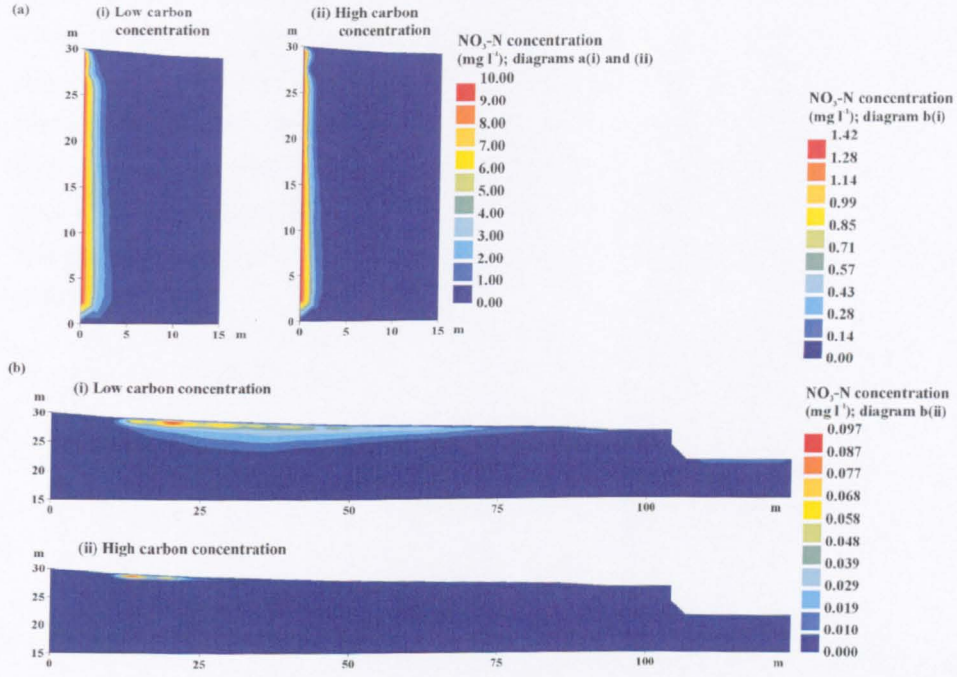

Figure 7.12 Solute distribution: effect of DOC concentration on NO_3-N from (a) hillslope water source and (b) river water source, at end of flood event F. Note the different concentration scales for the river water NO_3-N. (Denitrification parameters are as specified in scenarios 1 and 4, Table 7.8).

Even at quite a low carbon concentration, enough of the other conditions needed for rapid denitrification are present (particularly the high moisture content in most of the domain) to leave nitrate levels at the end of the 40 day flood event relatively low. However, in comparison with the simulation with high carbon concentration, less nitrate is removed (Figure 7.12b). As well as providing a substrate for the denitrification process, carbon also contributes to reduced oxygen levels, as the denitrifier activity consumes oxygen, thereby contributing to reducing conditions which favour rapid denitrification. In the case of the river water derived solute, maximum nitrate concentration at the end of the flood event was

0.097 mg N l^{-1} under conditions of high carbon concentration, and 1.42 mg N l^{-1} under conditions of low carbon concentration (comparison of scenarios 1 and 4, Table 7.8).

Once again, the influence of the unsaturated zone is evident in the results. At a lower carbon concentration, less denitrification takes place overall, but more specifically, the highest concentration of nitrate remains in the uppermost layers of the soil profile, towards the hillslope boundary of the floodplain, where the floodplain is unsaturated for the longest period of time (Figure 7.12b).

Figure 7.13 shows a comparison of the change in nitrate mass over the course of the flood event, for both the hillslope water derived and river water derived solute, under different denitrification conditions. It is clear that given the implementation of the denitrification model in this study, the introduction of carbon at even a very low concentration will generate high denitrification rates (as long as other conditions are non-limiting); the difference in mass between the 20 mg l^{-1} and 3 mg l^{-1} DOC concentration simulations is much smaller than the difference between the 3 mg l^{-1} and no denitrification (effectively no carbon) simulations.

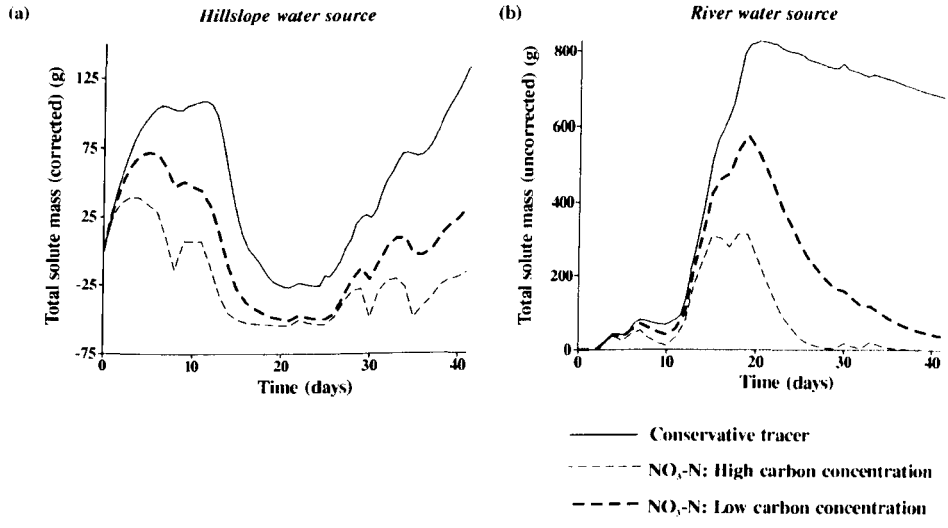

Figure 7.13 Effect of DOC concentration on total NO_3-N mass in the domain for (a) hillslope water and (b) river water NO_3-N source, for flood event F (scenarios 1 and 4; see Table 7.8).

7.5.2.4 Effect of carbon distribution on denitrification

Researchers have come increasingly to realise the importance of not only carbon concentration, but also distribution of carbon deposits, for the denitrification process. Supplies of oxidisable carbon are rarely uniformly distributed throughout the soil profile. In

grassland soils, the potential for loss of nitrogen through biological denitrification is greatest in the surface, root zone (0-25 cm) of mineral soils (Matchett, 1998). However, denitrification can occur within deeper horizons of organic soils; under arable and grassland, significant amounts of organic carbon can be found at depths of 2-3 m. Localised carbon supplies may also occur in buried river channel deposits, or where dissolved organic carbon is transported by groundwater recharge from overlying organic soils to deeper sediments (Hill *et al.*, 2000).

These localised DOC deposits have come to be known as 'hotspots' of potential denitrification activity (Hill *et al.*, 2000). However, these hotspots must occur in (a) hydrologically active areas, to which nitrate is transported, and (b) saturated areas, in order to fulfil this potential.

The distribution of carbon supplies in these simulations is intended to explore the implications of some of these field observations. Hill *et al.* (2000) found a low dissolved oxygen concentration associated with carbon-rich buried channel deposits in the near-stream zone; this has been represented in the simulation by the carbon distribution in Figure 7.14b. The carbon distribution in Figure 7.14c represents the organic layer that is typically found near the surface of soil profiles. The distribution of carbon illustrated in Figure 7.14a is an attempt to simulate a 'carbon wall'. The introduction of such a carbon-rich zone at the hillslope-floodplain boundary is a technique that has been suggested as a way of alleviating nitrate pollution of water courses (Schipper and Vojvodić-Vuković, 1998). During these simulations, distributions (a) and (b) have been combined and are referred to as 'carbon patches'; distribution (c) is referred to as 'surface carbon'.

In the case where the source of nitrate is hillslope water and the carbon is located in the surface of the floodplain, the nitrate is not transported to the zone rich in carbon, and virtually no denitrification takes place (Figure 7.15a(i)). This is clearly reflected in Figure 7.16a, which shows the change in solute mass over the course of the flood event for nitrate from a hillslope water source; there is hardly any discernable difference between the no denitrification case and the surface carbon case. The simulation with the 'carbon wall' shows the potential effectiveness of such a strategy for reducing nitrate concentrations in water from a hillslope source, in this deep alluvial material. In this case, the carbon coincides with saturated conditions below a depth of approximately 5 m to create conditions suitable for rapid denitrification, preventing nitrate from moving across the floodplain towards the river in this region. The mass of nitrate removed in this case (in comparison to the no denitrification case) is illustrated in Figure 7.16a.

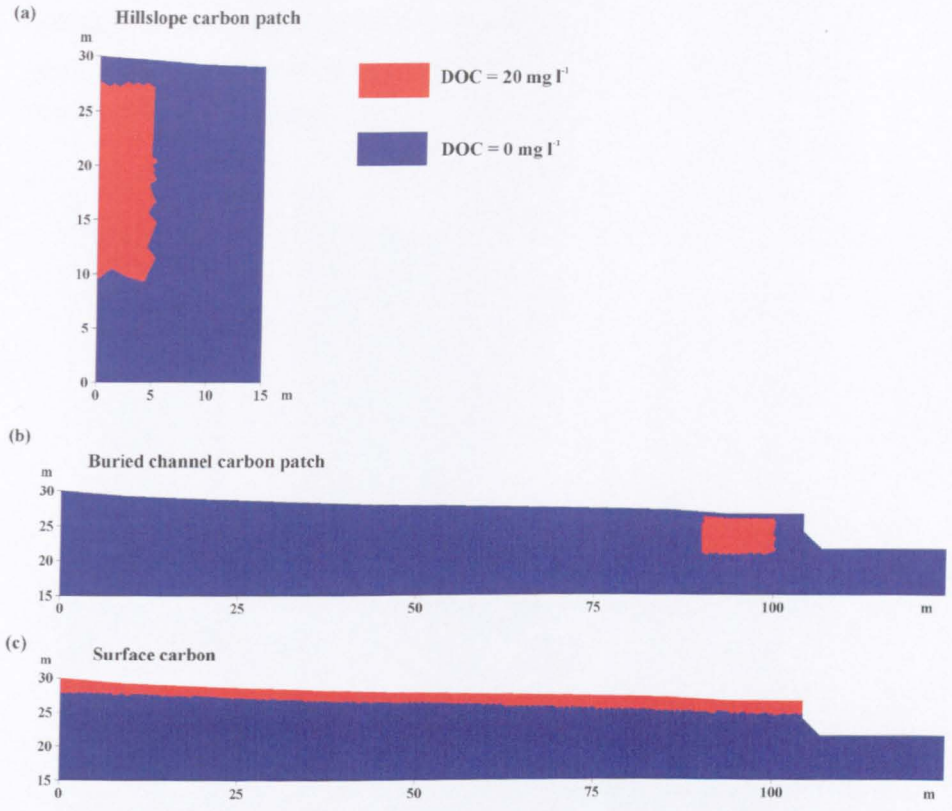

Figure 7.14 Distribution of DOC in (a) scenario 5 (hillslope patch of high DOC), (b) scenario 5 (buried channel patch of high DOC), and (c) scenario 6 (high DOC concentration at floodplain surface).

While the patch of carbon was more effective in promoting denitrification for the hillslope water source of nitrate, the surface carbon deposits were more effective for the river water source. During the overbank flood event, nitrate-rich water is delivered to the surface horizons of the floodplain soil. This of course corresponds with a period of high saturation, a combination that promotes high rates of denitrification. By the end of the flood event, nitrate concentration has reduced to 5.01 mg N l^{-1} or less, compared with a maximum of 8.35 mg N l^{-1} in the scenario with the carbon patches. This shows clearly the importance of carbon interacting with the active hydrological pathway of nitrate delivery. It is not that the near-stream carbon patch is not effective; in fact, in this region the nitrate concentration is reduced to 0.83 mg N l^{-1} or less (Figure 7.15b(ii)). However, because during these overbank flood conditions most of the nitrate is delivered to the floodplain through the floodplain surface and not through the channel bed and banks, most of the nitrate does not interact with the near-stream patch. The contrast is well illustrated by the diagram of change in solute mass over time (Figure 7.16b). If the nitrate was delivered to the floodplain in river water during a bankfull flood event, the influence of the near-stream carbon patch on

denitrification would appear proportionally greater (in comparison with the overbank flood event), as the nitrate would be delivered primarily through the bed and banks; thereby interacting with the carbon source.

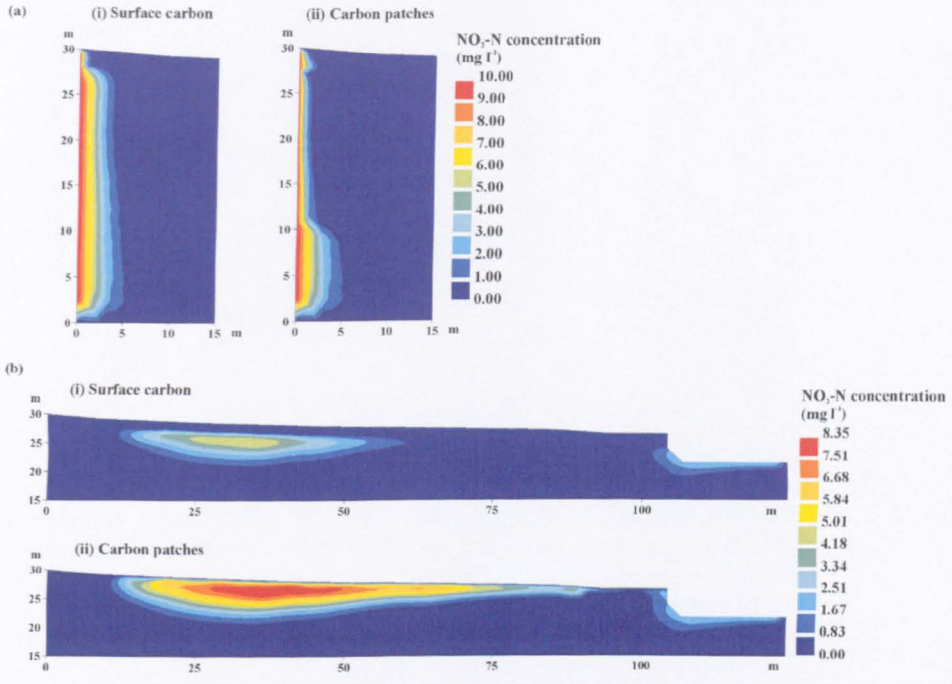

Figure 7.15 Solute distribution: effect of DOC distribution on NO_3-N from (a) hillslope water source and (b) river water source, at end of flood event F. (Denitrification parameters are as specified in scenarios 5 and 6, Table 7.8).

The results of these simulations support the conclusions of Hill *et al.* (2000) that the influence of the depth of permeable riparian sediments overlying aquitards and the location of subsurface deposits formed by fluvial processes may be more important than the width of vegetated riparian strips in understanding the ability of riparian zones to remove nitrates. Deeper nitrate rich groundwater *can* bypass surface carbon deposits in floodplains with deep alluvial sediment, such as the River Severn. The delivery of nitrate to carbon 'hotspots' (Groffman *et al.*, 1996) is fundamental to the denitrification process.

It is easy to see how current uncertainty about subsurface denitrification as a mechanism of nitrate removal in riparian zones may reflect the difficulty of detecting localised patterns of denitrifying activity at depth in these environments. Field campaigns can only sample selectively; if these samples happen to coincide with zones of high carbon concentration, the floodplain may be interpreted as an effective denitrifier, even if these zones are unrepresentative of the floodplain as a whole. On the other hand, studies which find little

evidence of denitrification may simply have missed the critical 'hotspots' of high carbon concentration.

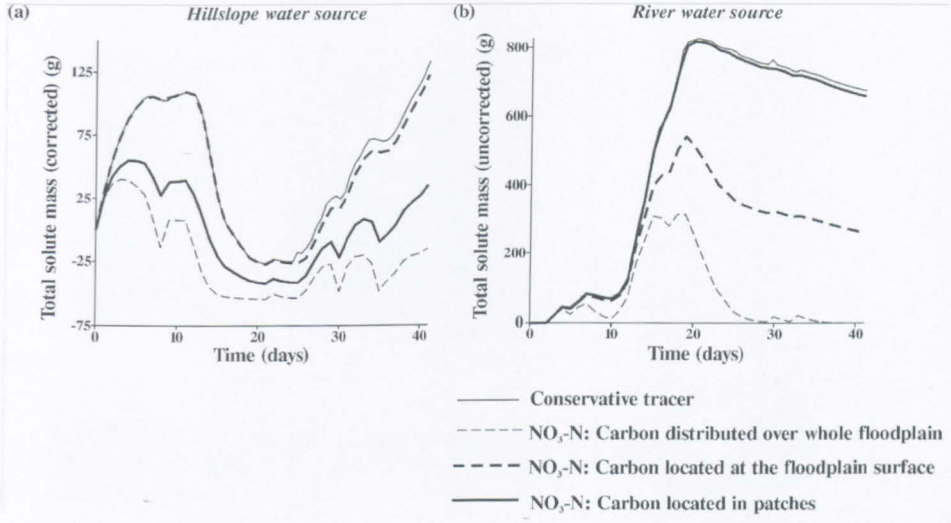

Figure 7.16 Effect of DOC distribution on total NO_3-N mass in the domain for (a) hillslope water and (b) river water NO_3-N source, for flood event F (scenarios 1 and 5 and 6; see Table 7.8).

7.5.2.5 Effect of temperature on denitrification

Seasonality is believed to affect denitrification in many different ways. Seasonal cycles of vegetation growth may contribute to seasonality in the supply of organic material. Hydrological events may be associated with different times of the year; flooding and high water-tables are more characteristic of the winter months, and low flow periods (and short-duration, high intensity convective storms) are more typical of the summer.

Temperature, another important factor in the denitrification process, also has a recognisable seasonal signature. This section aims to explore the effect of temperature on denitrification. Two temperatures were selected for these simulations: 17 °C (summer) and 6 °C (winter), and both were run under conditions of low carbon concentration over the whole domain. These temperatures reflect the soil temperature data collected over a period of four years at the River Severn floodplain field site.

Under the implementation of the denitrification model selected for this study, the change in temperature between 17 °C and 6 °C made only a small difference to the pattern of nitrate concentration in nitrate delivered by hillslope water (Figure 7.17a). The effect of the temperature change on the denitrification of hillslope-sourced nitrate is more noticeable on

the diagram of change in mass over time (Figure 7.18a); clearly, with a higher temperature, there is a greater potential for removal of nitrate mass through denitrification.

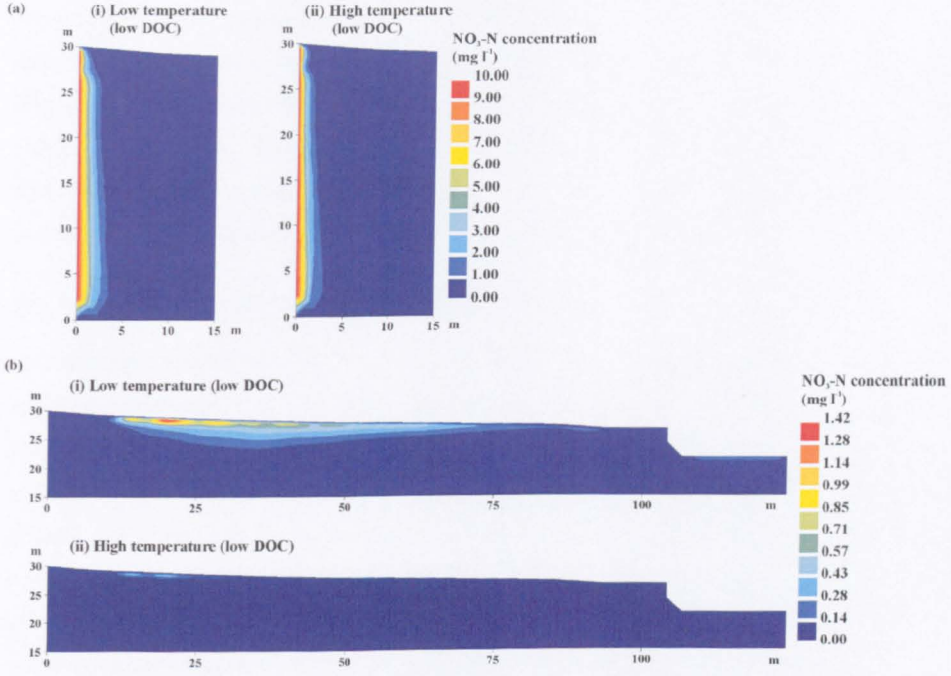

Figure 7.17 Solute distribution: effect of temperature on NO_3-N from (a) hillslope water source and (b) river water source, at end of flood event F. (Denitrification parameters are as specified in scenarios 4 and 7, Table 7.8).

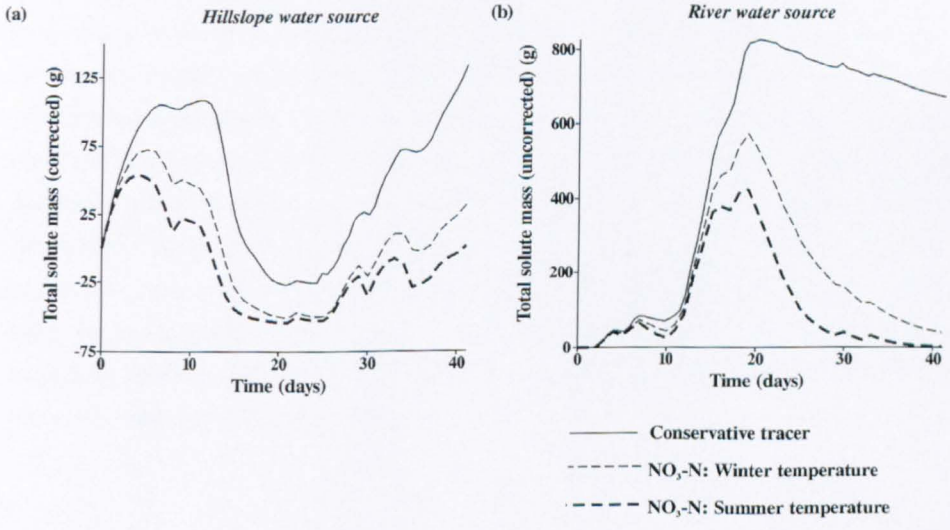

Figure 7.18 Effect of temperature on total NO_3-N mass in the domain for (a) hillslope water source and (b) river water source, for flood event F (scenarios 4 and 7; see Table 7.8).

In the case of the river-water derived nitrate, the effect of temperature on the pattern of nitrate concentration remaining in the floodplain at the end of the flood event appears more marked. However, the concentrations remaining in the case of the river-derived nitrate are overall much lower (a maximum of 1.41 mg N l^{-1}) in comparison with the hillslope water derived nitrate. In the higher temperature simulation, there is virtually no nitrate remaining (Figure 7.17b(ii)). However, this scenario relies on the high temperature coinciding with an overbank flood event, which may be considered unlikely to occur, except perhaps during a summer convective storm. This illustrates once again the complicated nature of the denitrification process, and how one factor cannot be considered in isolation.

7.5.2.6 Effect of soil type on denitrification

Sediment permeability is a factor controlling the transfer of water through the floodplain, and hence could have an important effect on the residence time of solutes transported in association with that water. This section explores the effect of two different values of saturated hydraulic conductivity, and two different soil types (as represented by two different Brooks and Corey soil moisture parameter sets) on denitrification rates. The three River Severn simulations used for the sensitivity analysis of saturated hydraulic conductivity value (using flood event D) were used as the basis of these denitrification simulations. These simulations are listed in Table 7.8 as scenarios 8, 9, and 10.

Figure 7.19 shows the infiltration of the nitrate into the domain after 20 days of flood event D, just after the flood peak, as the river-water derived nitrate is introduced to the floodplain. In the case of the hillslope-water derived nitrate, there is very little difference between the three soil types at this time, except for the most highly conductive (sandy loam) soil, where the nitrate is distributed over a very slightly wider area. Most of the nitrate introduced at the hillslope boundary left the domain as the hydraulic gradient changed to a river-to-hillslope direction. By contrast, at this stage in the flood event, the river-water derived nitrate is distributed at high concentrations over a much wider area, having just been introduced to the floodplain. Clearly, at a higher conductivity (Figure 7.19b(ii)), nitrate is able to penetrate the soil profile to a greater depth than at a lower conductivity (Figure 7.19b(i)). Nitrate infiltrates to the greatest depth under conditions with the highest hydraulic conductivity, and there is no significant difference in the pattern of nitrate concentration between the clay loam and sandy loam soil, at the same conductivity.

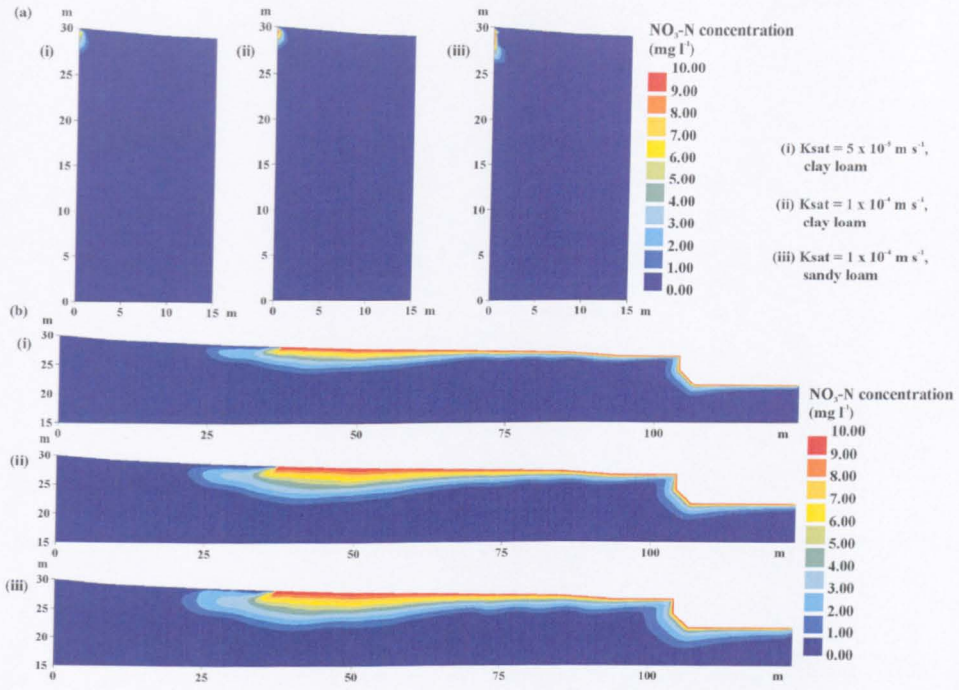

Figure 7.19 Solute distribution: effect of saturated hydraulic conductivity on NO_3-N from (a) hillslope water source and (b) river water source, after 20 days of flood event D. (Denitrification parameters are as specified in scenarios 8, 9 and 10, Table 7.8).

By the end of the flood event, the effect of hydraulic conductivity on the hillslope-water derived nitrate is more noticeable, because the supply of nitrate from this source had been re-established after the flood peak passed. Nitrate penetrates the floodplain to a greater extent where the hydraulic conductivity is greatest: nitrate at a concentration of 1 mg N l^{-1} or greater penetrates to a distance of approximately 4 m at the lower conductivity (Figure 7.20a(i)), and approximately 7 m at the higher conductivity (Figure 7.20a(ii)). For the scenarios considered in this study, hydraulic conductivity has a greater effect on nitrate distribution at the end of the flood event than temperature, but a lesser effect than carbon concentration or potential denitrification rate.

Hydraulic conductivity and soil type also have an effect on the distribution of nitrate at the end of the flood event in the case of the river-water derived nitrate. By the end of the flood event, nitrate concentrations are generally low; reduced to 3.15 mg N l^{-1} or less. The snapshot of the nitrate distribution shown in Figure 7.20b illustrates an important distinction that can be resolved between the effect of hydraulic conductivity, and the influence of soil type.

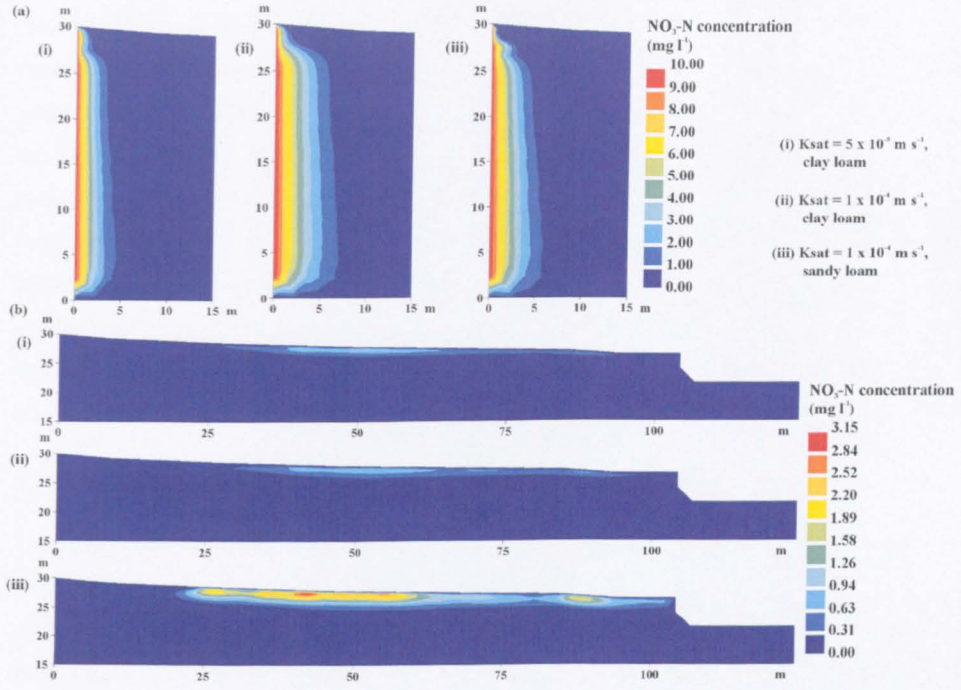

Figure 7.20 Solute distribution: effect of saturated hydraulic conductivity on NO_3-N from (a) hillslope water source and (b) river water source, at end of flood event D. (Denitrification parameters are as specified in scenarios 8, 9 and 10, Table 7.8).

A comparison of Figure 7.20b(i) and Figure 7.20b(ii) indicates that an increase in hydraulic conductivity from 5 x 10^{-5} m s^{-1} to 1 x 10^{-4} m s^{-1} has little influence on the pattern of nitrate concentration. However, a comparison of Figure 7.20b(ii) and Figure 7.20b(iii), which used the same value of hydraulic conductivity but different Brooks and Corey soil moisture model parameters (to represent a clay loam soil and a sandy loam soil, respectively), shows some significant differences in nitrate concentration. These differences are noticeable in the unsaturated zone that forms in the upper 5 m of the soil profile. In this region, the importance of the shape of the moisture content – pressure head (soil water retention curve) and hydraulic conductivity – pressure head relationships is clear. The gradient of both these curves is steeper in the case of the sandy loam soil. This means that the relative conductivity (and hence the hydraulic conductivity) reduces more quickly with an increase in negative pressure head in the sandy loam soil, restricting water and solute movement in the unsaturated zone to a greater degree than in the clay loam soil as the water-table drops. However, most of the nitrate transport occurs when the domain is fully saturated (see Figure 7.19b), at which time the difference in hydraulic conductivity between the two soil types is at its lowest. Therefore, of the two soil relationships, it is likely that the difference in the moisture content – pressure head relationship (the soil water retention curve) is the most significant cause of the differences in simulated nitrate concentration. The difference

between these curves for the two soils is such that moisture content will decrease more rapidly with an increase in negative pressure head in the case of the sandy loam soil. For a given value of negative pressure head, the moisture content will therefore be lower in the sandy loam soil than in the clay soil. This means that the unsaturated zone has a lower moisture content in the sandy loam simulation, which contributes to lower denitrification rates, and higher concentrations of nitrate remaining at the end of the flood event. An additional contributing factor may be the greater penetration of nitrate into the domain in the sandy loam case, although this is not thought to be significant given the great similarity between the concentrations of nitrate introduced to the domain during the flood event in the clay loam and sandy loam simulations (Figure 7.19b(ii) and (iii)).

7.5.2.7 Upland floodplain scenarios

The simulations in this section are aimed at exploring the effect of carbon concentration and distribution on patterns of denitrification in an upland riparian zone (Sleepers River). The results illustrated here are based on scenarios 11, 12 and 13 from Table 7.8. Scenario 11 used a uniformly high DOC concentration over the entire domain (20 mg l^{-1}). Scenario 12 used a uniformly low DOC concentration over the whole domain (3 mg l^{-1}). Scenario 13 used a high DOC concentration (20 mg l^{-1}) in the riparian peat soil zone (near the surface of the domain), and zero DOC concentration in the rest of the domain, which was an attempt to more realistically model the likely distribution of carbon within the domain. All three scenarios were compared to the simulation with no denitrification. Nitrate was introduced at both hillslope boundaries at a concentration of 10 mg N l^{-1}.

As was noted for the conservative tracer simulations, the solute appears to move much more quickly through the upland riparian zone than the lowland floodplain, which is predominantly an artefact of the much smaller size of the upland domain. After 1 day of the snowmelt event, there are some slight differences in the pattern of nitrate concentration between the four scenarios (Figure 7.21). The maximum concentration was 10 mg N l^{-1} in all cases, due to the constant input of nitrate at the hillslope boundaries at that concentration, and in each case, the nitrate was transported away from the boundaries (towards the centre of the domain) to approximately the same distance. The differences between the scenarios were observed in the rate of reduction of nitrate concentration with increasing distance from the boundary. The influence of denitrification can be seen in Figure 7.21b (high DOC concentration) and Figure 7.21c (low carbon concentration); in comparison with the no denitrification simulation, the nitrate decreases more rapidly with distance from the nitrate source. This effect is most marked where carbon concentration is highest (Figure 7.21b).

At this point in the event, there is no discernable difference between the no denitrification case (Figure 7.21a), and the scenario with carbon in the riparian peat zone only (Figure 7.21d). This is because after only one day of the event, the majority of the nitrate has not reached the riparian peat, and has not had the opportunity to interact with the high carbon concentration in this zone.

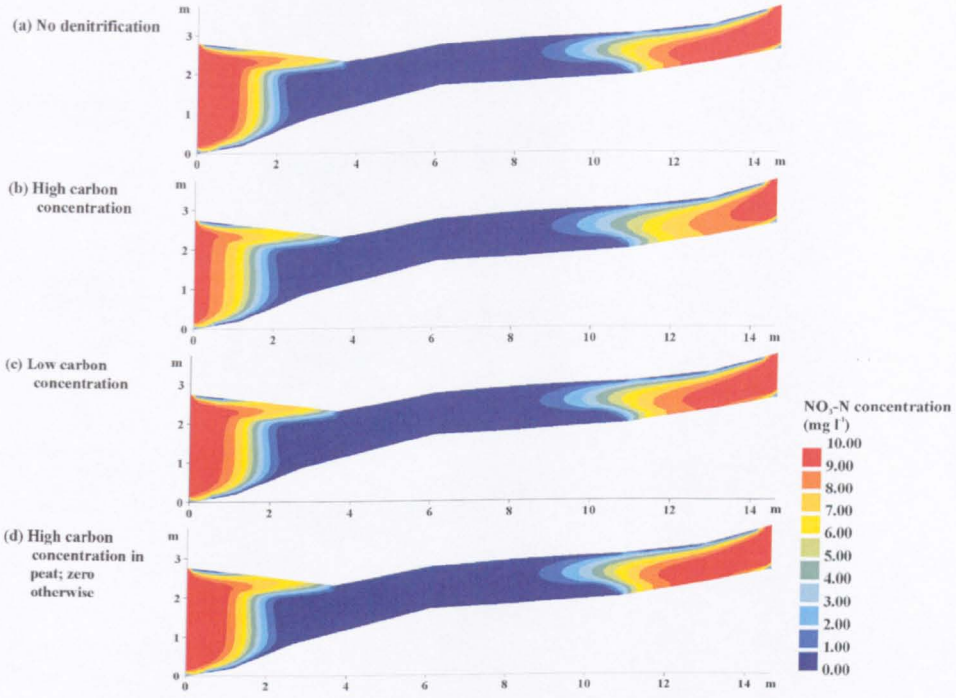

Figure 7.21 Effect of DOC concentration and location on NO_3-N distribution in the Sleepers River domain after 1 day. (a) conservative tracer, (b) high DOC concentration (scenario 11), (c) low DOC concentration (scenario 12), and (d) high DOC concentration in riparian peat only (scenario 13). NO_3-N source is both hillslopes.

After a further two days of the snowmelt event, the differences between the scenarios appear more distinct. As expected, under conditions of high carbon concentration (Figure 7.22b), the decrease in nitrate concentration with distance from nitrate source is greater than under conditions of low carbon concentration (Figure 7.22c). The effect of the high carbon concentration in the riparian peat is still relatively difficult to distinguish (Figure 7.22d), although in comparison with the no denitrification case (Figure 7.22a), slightly lower nitrate concentrations can be seen in the upper soil layer near the left-hand hillslope boundary (1 to 4 m from the left-hand boundary), and in the near stream zone just to the right-hand side of the stream channel (4 to 9 m). This is mainly because the nitrate is transported more quickly through the riparian peat zone (due to higher conductivity values); nitrate concentration therefore builds up in the near-hillslope zone and lower concentrations are found in the

riparian peat area, even before the denitrification process has the opportunity to operate. It is transport rather than transformation which controls the concentration of nitrate in the riparian peat zone.

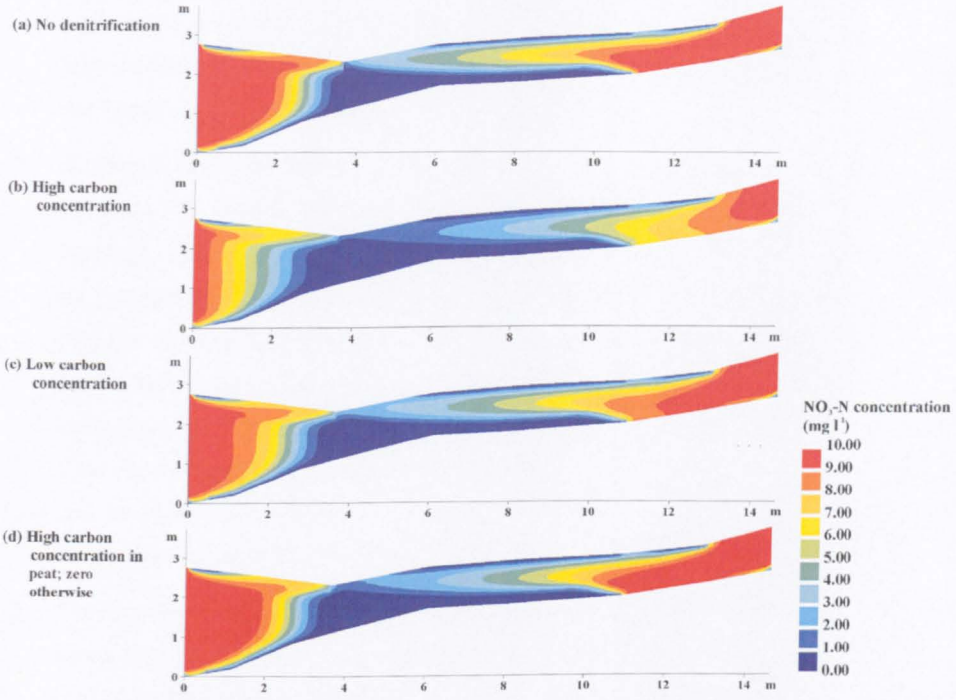

Figure 7.22 Effect of DOC concentration and location on NO_3-N distribution in the Sleepers River domain after 3 days. (a) conservative tracer, (b) high DOC concentration (scenario 11), (c) low DOC concentration (scenario 12), and (d) high DOC concentration in riparian peat only (scenario 13). NO_3-N source is both hillslopes.

7.5.3 Summary of hypothesis three

The simulations carried out in this chapter have explored the effect of a range of factors on chemical transport and transformation in floodplain systems, using nitrate (and the denitrification process) as an example that is particularly relevant to the floodplain environment. The factors that were examined were floodplain hydrological characteristics (scale of event, and delivery of water and nitrate), carbon concentration and distribution, temperature (seasonality) and soil hydraulic characteristics (hydraulic conductivity and soil type, including the influence of the shape of the soil-water retention curve). The results may be summarised as follows:

1. Differences in nitrate concentration observed between the overbank and bankfull flood event on the lowland floodplain related mainly to differences in the region of the floodplain that the nitrate was delivered to, especially in the case of nitrate delivered in

river-water. This in itself is important, because it affects whether the nitrate will have the opportunity to interact with zones of high denitrification potential. Hydrological processes have a more direct influence on nitrate transformation via denitrification by influencing the moisture content of the floodplain soil, and the distribution of zones of high saturation within the floodplain. Hill *et al.* (2000) suggested the importance of hydrological processes for nitrate delivery; this study has extended that idea to consider the impact of specific hydrological event types.

2. If carbon was distributed evenly throughout the domain, then even at a low concentration, significant denitrification occurred (where other factors were non-limiting). This may reflect the implementation of the carbon function in the model, and the fact that the rate of change in denitrification with a change in carbon concentration may not be modelled correctly (particularly as it was difficult to find a literature study from which to select the value for the half saturation constant for carbon, K_c). This point does not greatly affect the interpretation of the carbon distribution scenarios, as whatever the inaccuracy in the modelled relationship between carbon and denitrification rate at higher concentrations, the model does reflect the fact that at zero carbon concentration there will be no denitrification.

3. The location of carbon deposits is very important in determining nitrate concentration throughout the floodplain. The scenarios investigated in this chapter have indicated that critical locations for carbon deposits vary according to the nitrate source. In the case of the lowland River Severn floodplain, a 'carbon wall' introduced at the hillslope-floodplain boundary is effective in reducing the concentration of nitrate entering the floodplain in hillslope-derived water. However, it has no impact on the concentration of nitrate delivered to the floodplain by river water. Near-surface carbon deposits, on the other hand, have relatively little effect on hillslope-derived nitrate concentrations, as the majority of the nitrate from this source flows beneath the carbon-rich zone. However, surface carbon deposits do have a significant effect on the concentration of nitrate delivered to the floodplain by river water during overbank flood events. In the case of the upland Sleepers River model, the influence of high carbon concentrations in the riparian peat is hard to distinguish as the high variability in soil hydraulic conductivity has a significant effect on the areas of the riparian zone that the nitrate is delivered to. Recognition of the importance of the location of carbon deposits within the floodplain follows from studies such as Hill *et al.* (2000). However, this study has extended this finding by indicating that the critical location for carbon deposits varies according to the nitrate source, which in turn is partly dependent on the location of the floodplain/riparian zone in the catchment. This indicates that different management

strategies for diffuse nitrate pollution may be needed in different parts of the catchment: the 'carbon wall' approach may not be suitable under all circumstances.

4. Using the denitrification model implemented for this study, temperature is a secondary factor in determining denitrification rates. It has a relatively minor effect over the range of temperatures studied here (which are felt to reflect temperate climates), and only really has an influence once other limiting factors have been overcome. This study has supported previous ideas about the relative importance of several controlling factors on the denitrification process.

5. Soil hydraulic characteristics have two main effects on nitrate concentration within the floodplain. First, sediment permeability is a factor controlling the delivery of nitrate to the floodplain, and influences how much nitrate is able to infiltrate into the soil profile through the floodplain surface, or flow across the hillslope-floodplain boundary. Second, the shape of the soil water retention curve affects the moisture content of the unsaturated zone, and hence the rate of denitrification.

6. Generally, the areas in which denitrification is rapid may be fundamentally limited by the interaction of hydrological processes (both through nitrate *delivery* and moisture content) and carbon availability. If carbon is mostly available in the upper layers of the soil profile, these are correspondingly the areas that tend towards unsaturated conditions; in this case, water will be the limiting factor. On the other hand, lower layers of the soil are much more likely to be saturated, but in these regions, concentrations of soluble carbon are likely to be lower, leading to a carbon-limited process. Sophisticated understanding of floodplain hydrological processes and distributed representation of carbon deposits, such as achieved in this study, are therefore critical.

7.6 Chapter summary

This chapter has concentrated on using the coupled ESTEL2D-SUBIEF2D model to investigate some of the factors (apart from floodplain scale and hydrological event, investigated in Chapter 6) considered to be important in determining solute transport and transformation in floodplain systems. This work concentrated on nitrate transport and nitrate transformation through denitrification, as this process has received much attention in the floodplain chemical transport literature. In order to test a new set of hypothetical scenarios, a denitrification component for the model was researched, implemented and tested.

In their review of nitrogen movement within riparian systems, Cirmo and McDonnell (1997) highlighted that temporal hydrological variability (high and low flow regimes),

biogeochemical conditions, and antecedent soil moisture, were all believed to be important in controlling nitrogen dynamics. With the background of years of field studies indicating the possibilities for those factors that are most important for the denitrification process, this study has been able to take these initial ideas and use the hypothetical scenario platform to test their relative importance. Despite the many recognised restrictions of modelling, this is a valid and important technique, as it allows all the potential factors to be brought together in a controlled environment in a way that is very difficult in the field.

The results of the these hypothetical scenario simulations have highlighted how large spatial and temporal variations in carbon concentration, nitrate delivery and moisture content in particular can affect denitrification rates and the resulting patterns of concentration of nitrate throughout the floodplain. This supports the conclusion of Hill *et al.* (2000) that denitrification is restricted to narrow zones within the floodplain. A model capable of such high spatial and temporal resolution as the one used in this study has provided the ideal means to capture such variability, in a way which is simply not possible in the field. Field studies of the denitrification process in floodplain environments must be aware of the fact that sampling strategies may not adequately capture this variability.

The interaction of hydrological flow paths (carrying nitrate-rich water) with zones of high denitrification potential (i.e. with high carbon concentration and high moisture content) is indicated to be crucial to the efficacy of the denitrification process. Of course, nitrate not transformed by the denitrification process may still be subject to removal from the floodplain system by other mechanisms not covered in this study, such as plant assimilation.

The next and final chapter will summarise the results of this study as a whole, relating the results to the aims and objectives outlined in Chapter 2. It will go on to indicate the potential for further research in this area.

8 Conclusions

Nature has not made it a priority to make it easy for us to discover its laws.

Albert Einstein (1901)

It has been the aim of this study to a) develop a model of subsurface hydrological and chemical transport processes through both headwater and lowland floodplain systems, and b) use this model to advance process understanding, quantifying the effect of a range of factors on the operation of hydrological and biogeochemical processes in floodplain systems. This concluding chapter considers the success of this study in achieving these aims. Each aim will be considered in turn, reflecting on what has, and has not, been achieved, with a focus on the original aspects of the research. Avenues for future research that have arisen as a result of this work will also be identified and discussed.

8.1 Assessment of aim one

The first aim of this study, as presented in Section 2.2.1, was as follows:

To develop a model of subsurface hydrological and chemical transport processes through both headwater and lowland floodplain systems.

Model development and assessment were the focus of Chapters 3 to 5. The main conclusions of these chapters will be summarised in this section.

8.1.1 Model development

A focal point of this study was to develop a numerical model that would be suitable for modelling subsurface water movement and chemical transport through floodplain systems. This model needed certain fundamental characteristics: two-dimensional formulation to represent the dominant flow processes, finite element discretisation to cope with rapid soil water and chemical movement during simulation of flood events and heterogeneous soil parameterisation, suitability for simulating variably saturated conditions, and flexibility in its implementation of chemical reaction equations. Two existing models, ESTEL2D and

SUBIEF2D, were brought together to produce a coupled model that possesses each of these features. This model development was extended to provide further important features: a unifying treatment of the saturated and unsaturated zones in the form of a specific storage parameter, and the capability of simulating a seepage face boundary condition.

The final model version represents a significant advance on the previous versions of the ESTEL2D and SUBIEF2D codes, as well as on other numerical models. For the first time, all the elements necessary for simulating the highly dynamic hydrological and chemical environment of the near-stream area have been brought together in one model, and it is the first time that such a model has been applied to questions of floodplain subsurface hydrological and chemical transport processes.

The model gave the opportunity to study the high spatial and temporal variability of the near-stream environment. This included, for example, highly dynamic overbank flood events on the lowland floodplain of the River Severn, and the variable carbon distribution in the denitrification scenarios.

8.1.2 Holistic view of floodplain systems

The development of this physically-based model has been an important means of moving away from the view of floodplain system components as a series of 'boxes', towards the more holistic view, with the hillslope and channel as integral parts of the floodplain system as a whole. This is the first time that the whole spectrum of possible inputs (in terms of water and solute sources) to the floodplain system has been modelled. Previous studies have considered hillslope inputs of water and chemicals, but neglected inputs from the river channel (or vice versa), or only considered transfer of river-derived water across the channel bed and banks, but not across the floodplain surface during overbank events. This study brought all these potential sources together so that their relative importance for floodplain hydrological and chemical transport processes, and the factors that affect them, could begin to be assessed.

8.1.3 Fieldwork-modelling strategy

The fieldwork-modelling strategy employed in this study proved to be very powerful. Initial model simulations and testing were guided by data from two fieldsites: one lowland floodplain (River Severn) and one upland riparian zone (Sleepers River). These data were invaluable in the model assessment procedure. In addition, initial theories of floodplain chemical and water movement in these two contrasting floodplain systems were then used as the basis for assessing in what ways the model could most usefully contribute to further understanding of the floodplain system. In turn, the model results have expanded upon these

initial theories, by revealing insights into the floodplain system that could not realistically have been obtained by field studies alone, owing to the high levels of spatial and temporal variability characteristic of this dynamic environment. These findings will be summarised in the discussion of the second aim of the study (Section 8.2).

8.1.4 Headwater and lowland floodplain systems

Many previous studies have concentrated on the near-stream zones of low-order streams, the smaller scale of these systems making it easier to gain a whole-system perspective, from which to understand processes of water and chemical movement. In relation to questions of floodplain scale, this study has contributed considerably to this field of research in two notable ways.

First, it has included a detailed investigation of lowland floodplain processes, including the effect of overbank flood events that had not been considered before. This aspect of the research relied on the lowland floodplain data collected as part of this study at the River Severn fieldsite, which is in itself a body of information unique in its capture of overbank flood events at a high temporal resolution. It also represents one of the first numerical modelling attempts of a very complex headwater riparian zone, both in terms of boundary conditions and soil parameterisation.

Second, this study has attempted an initial comparison of headwater and lowland floodplain systems. The conclusions drawn from this aspect of the study are necessarily limited by the fact that only two field sites were studied (one representing a lowland floodplain, the other a headwater riparian zone), and these examples may not be representative of headwater and lowland floodplains in general, not the mention the whole spectrum of floodplain types that may exist outside these two examples. However, as an initial comparison it seems to have confirmed speculation that moving from the headwater to the lowland floodplain system is not a simple matter of 'scaling-up' processes, as different processes operate at the different scales (these findings will be summarised in Section 8.2). At the least, this study provides a useful starting point for future investigation into the range of processes of floodplain hydrological and chemical transport.

8.1.5 Model use and assessment

The extensive model assessment procedure also gave new insight into some of the more technical aspects of model application. Chapter 5 demonstrated how the choice of output parameters to compare and analyse during model testing is important, because it can potentially have a big impact on the conclusions of the assessment process. Analysis of model results based on only one state variable (e.g. pressure head, water-table elevation)

could disguise problems or unrealistic behaviour in other aspects of model performance. In this study, a faithful representation of pressure head distribution was a necessary, but not sufficient, pre-requisite for accurate simulation of chemical transport. The wider implications of this are that even though the data required for full validation of the system may be lacking (in this study, the lack of information about the unsaturated zone in particular), a modeller must be prepared to look beyond one simple hydrological indicator (e.g. water-table elevation) to consider whether the wider elements of the hydrological picture (e.g. saturation extent, seepage face development) at least appear intuitively realistic. This study therefore lends support to the use of so called 'softer' evaluation techniques in the assessment procedure in the form of hydrological expertise (Lane and Richards, 2001).

The simulations of Chapter 5 also demonstrated how model results could be just as sensitive to boundary condition specification as to soil parameter specification. This is something that has received little consideration in the hydrological modelling literature, as most attention is generally devoted to the impacts of parameter representation on model results.

A thorough model assessment procedure, covering verification, optimisation, sensitivity analysis, calibration and validation, gave confidence in the model results so that the study could move on to the next important stage: use of the model in a range of hypothetical scenarios, to explore theories of water and chemical transport in floodplain systems. This was the subject of the next aim of the study.

8.2 Assessment of aim two

The second aim of this study, as presented in Section 2.2.1, is as follows:

To use this model to advance process understanding, quantifying the effect of a range of factors on the operation of hydrological and biogeochemical processes in floodplain systems.

Processes of water and chemical movement in floodplains were investigated in Chapter 6 and 7, using three main hypotheses as the basis for the design of model simulations. These hypotheses were posed on the basis of findings published in the literature to date, which suggested that certain factors were important to floodplain hydrological and chemical transport processes in some way. However, the details of specific impacts of these factors on floodplain processes, or their relative importance, were not well understood. It was felt that these were important gaps in process knowledge that could be usefully addressed by the newly developed model:

1. The scale of the hydrological event (overbank flood, bankfull flood and low flow event) controls floodplain water and solute source, flow path and residence time.

2. The scale of the floodplain zone (headwater riparian zone versus lowland floodplain) controls floodplain water and solute source, flow path and residence time.

3. Other factors (such as carbon content and distribution, temperature and soil hydraulic characteristics) are important in controlling solute transport and transformation.

The conclusions from each of these hypotheses will be summarised in this section, along with some more general comments about the way the approach used in this study has enhanced process understanding.

8.2.1 New process understanding from hypothetical scenarios

The conclusions from each of the three hypotheses have been summarised in the form of a table (Table 8.1), which illustrates the effect of each factor (hydrological event, scale of floodplain and soil hydraulic characteristics, for example) on the operation of processes in the floodplain environment (namely the source of water and chemicals, hydrological and chemical flow paths, chemical residence time, and nitrate transformation).

The chart identifies some clear differences in process operation for different controlling factors. Under certain combinations of conditions, processes can effectively be turned on and off. The simulations have also given an indication of the relative importance of each factor for the operation of each of these processes, which will be discussed in the following three sub-sections.

8.2.1.1 Scale of hydrological event

In the case of the lowland floodplain, scale of hydrological event is a primary control on the source of water and solutes, hydrological and chemical flow paths, and delivery of solute to different areas of the floodplain. Overbank and bankfull flood events were found to be important in providing a source of water from the river channel, a process that does not happen under low flow conditions. Overbank flood events also deliver water and solutes to a part of the floodplain (the surface soil layers) that low flow events do not. The groundwater ridging effect (and its associated impact on inputs of water and chemicals from the hillslope) was found to be characteristic of both overbank and bankfull events, but not low flow events. However, there was no evidence for the movement of river-derived water into hillslope areas, hence refuting the hypothesis of Bates *et al.* (2000). Flood events are an important time of net input of water and chemicals to the floodplain system; net export is a more important feature of low flow events. This study is the first time that an indication of the relative importance of river and hillslope inputs of water and chemicals to the floodplain has been proposed.

Table 8.1 Summary of the effect of controlling factors on floodplain hydrological and chemical processes.

Controlling factors	Effect of controlling factors on:			
	Water source	**Hydrological and chemical flow paths**	**Chemical residence time**	**Nitrate transformation**
Scale of hydrological event (on a lowland floodplain): *Overbank flood* *Bankfull flood* *Low flow event*	Overbank events: river channel is an important water source to the surface layers of the soil profile. Bankfull events: river water infiltration limited to the channel bed and banks. Low flow conditions: water from hillslope is main water source.	Overbank and bankfull flow conditions: 'groundwater ridge' observed to form in floodplain, whereby flow is directed back towards hillslope from river channel. Water from channel does not move into hillslope, but this phenomenon does control input of water from hillslope during peak flow period, potentially affecting mixing of solutes from hillslope and other sources.	Unsaturated zone near surface of floodplain experiences very slow water and chemical movement in comparison with saturated zone. Solute delivered to this zone (tends to be solute derived from river water during overbank flood events) could remain resident for long period of time. Generally, flood events are periods of net input of water and chemicals to floodplain. Export of pre-event solute is delayed until after flood event.	Scale of hydrological event mainly determines region of floodplain that nitrate is delivered to. Also has a more direct influence on denitrification process by influencing moisture content of floodplain soil, and distribution of zones of high saturation.
Scale of floodplain: *Small, upland riparian zone* *Large, lowland floodplain*	Significant contrast in dominant water source between the two floodplain scales. Lowland case: river is important control, particularly during overbank events. Upland case: relative contribution of hillslope is much greater; river has little controlling influence. This is linked to topography of the sites.	Lowland case: floodplain topography and dynamic river stage changes lead to formation of 'groundwater ridge'. Upland case: this does not occur as land bordering the stream has steeper gradient, and hillslope water stage has dominant control on water flow direction in the riparian zone. Flowpaths in upland riparian zone complicated by more complex soil distribution. Surface seepage and reinfiltration have more noticeable effect on flow paths at upland site.	Solute delivered to upland riparian zone has short residence time in comparison with lowland floodplain site, due to a) smaller size of the domain, and b) more fully saturated conditions of upland riparian zone. Shorter residence time means that solute travels through upland riparian zone at higher concentration; in lowland case, there is greater potential for dispersion to decrease solute concentration.	High variability in hydraulic conductivity of soils at upland site has strong influence on region of riparian zone that nitrate is delivered to. Delivery of nitrate more strongly influenced by event type at lowland floodplain site.
Other controlling factors: *Carbon concentration and distribution* *Temperature* *Soil hydraulic characteristics*	N/A	N/A	Location of carbon deposits very important in determining nitrate concentration throughout floodplain. Critical locations for carbon deposits vary according to nitrate source. Generally, areas in which denitrification is rapid may be fundamentally limited by interaction of hydrology (both through nitrate delivery, and moisture content) and carbon availability. Soil hydraulic characteristics affected delivery of nitrate, and soil moisture content in unsaturated zone. Temperature found to be of secondary importance to denitrification process within the range of temperatures investigated in this study.	

Apart from these primary effects on floodplain processes, the scale of hydrological event has a secondary effect on biogeochemical transformations (denitrification as considered in this study) by controlling the levels of saturation within the floodplain. The unsaturated zone in the upper 5 m of the floodplain is particularly important because it also slows down the advection and dispersion of solute. This implies that any solute delivered to this region of the floodplain during an overbank flood event has the potential to remain in the floodplain for a long period of time. This is a novel finding with the implication that in the long term, overbank flood events could be very important for solute delivery and residence time in the floodplain environment. The indication of the importance of the unsaturated zone is in contrast to the findings of Bates *et al.* (2000). The suggestion of the regions of the floodplain that may be subject to greatest solute movement during a flood event is another original development of this study. Overall, these results support and extend the conclusion of Stewart *et al.* (1998), that infiltration of chemicals into the floodplain surface may be spatially variable, and difficult to characterise using current field-based techniques.

8.2.1.2 Scale of floodplain

The scale of the floodplain was found to have an important influence on the source of water supplied to the system. These results are original because a comparison of upland and lowland floodplain/riparian zones has not previously been attempted. At the lowland site, the river was a significant source of water during flood events. Changes in river stage had an important controlling influence on the direction of flow within the floodplain. This same process was not found in the upland riparian zone. The configuration of the floodplain (in particular, the steeper gradient of the land adjacent to the stream and the underlying geological formation), meant that the river was not a significant source of water to the riparian zone, and the dominant controlling influence on flow paths and flow direction in the riparian zone was water level in the hillslope, not the river stage. In addition, the groundwater ridging effect associated with the flood events on the lowland floodplain, which directed flow away from the channel and towards the hillslope, was not found to occur in the case of the upland riparian zone. Processes of seepage and reinfiltration were found to be more important at the upland site.

The more complex soil distribution at the upland site was found to complicate water and solute flow paths, and solute delivery to different parts of the floodplain. The great disparity in the size of the two floodplains also had a significant effect on chemical residence time; solute was transferred much more rapidly through the upland riparian zone, simply due to its smaller size. This rapid transfer had an additional impact on solute concentration; the longer residence time in the lowland floodplain gave greater opportunity for the solute to disperse,

and for solute concentrations to decrease, even though the total mass of tracer could remain high.

8.2.1.3 Other controlling factors

Other factors, such as carbon concentration and distribution, temperature, and soil hydraulic characteristics, all have an effect on chemical residence time and transformation. However, to a certain extent they all rely on the hydrological characteristics of the floodplain to deliver the solute to an area of the floodplain where they have the opportunity to take effect.

The operation of the denitrification process may be fundamentally limited by the interaction of hydrological processes and carbon availability. Recognition of the importance of the location of carbon deposits within the floodplain follows from studies such as Hill *et al.* (2000). However, the present study has extended this finding by indicating that the critical location for carbon deposits varies according to the nitrate source, which in turn is partly dependent on the location of the floodplain/riparian zone in the catchment. For example, in the case of nitrate delivered to the floodplain via hillslope-derived water, a carbon wall at the hillslope-floodplain boundary may be effective in promoting denitrification, but carbon deposits in the root zone of the floodplain surface will not be, as the hillslope flow will not interact with this region. Temperature was of secondary importance in controlling denitrification.

In general, this study has supported previous ideas about the relative importance of several controlling factors on the denitrification process. Hill *et al.* (2000) suggested the importance of hydrological processes for nitrate delivery; this study has extended that idea to consider the impact of specific hydrological event types. This study has highlighted the importance of achieving a sophisticated understanding of floodplain hydrological processes and distributed representation of carbon deposits, in order to further our understanding of the denitrification process in floodplain environments.

8.2.2 Effect of approach on process developments

The table produced in Section 8.2.1 is a summary of the new process ideas generated by this study. Despite the many difficulties of the modelling approach, not least with concerns about overparameterisation, and the realistic representation of the system in question, this table represents progress that could not have been made without the use of the numerical model. The questions posed here, particularly those that involved high levels of spatial and temporal variability, or extreme hydrological events, could not have realistically have been answered by field studies alone.

The numerical model has essentially been used to extend the interpretation of the existing field data, highlighting areas where understanding of the system is currently weak, and providing new process insight where possible. For example, modelling the complex Sleepers River domain was a challenging test of the modelling approach, but the very process of constructing the model of this site revealed gaps in the understanding of that system that field work alone had not been able to fill. The application of the model was then able to highlight some of the consequences of this lack of knowledge, and suggest the processes that might be happening. This research has demonstrated the potential of the model for hypothetical scenario testing. A range of parameter values and combinations of factors have been tested in a controlled environment, which would be difficult to achieve under field conditions.

8.3 Limitations and suggestions for further work

Further research in this subject area will be able to build on the progress made in model development and process understanding during the course of this study, as well as some of the limitations of the present work.

There are several limitations to the current implementation of the numerical model, which could be investigated as possibilities for future improvement. The sensitivity analysis of the River Severn model revealed some circumstances under which the ESTEL2D part of the numerical model did not converge to a solution. Characteristics which can lead to slow convergence (or non-convergence) of the Picard scheme include (a) complex or time varying boundary conditions, (b) steep soil characteristic equations, producing a sharp moisture front with a large drop in conductivity and saturation across the front, (c) an initially dry soil near the surface, and (d) saturated-unsaturated interfaces (Paniconi and Putti, 1994), all of which were features of the hydrological simulations undertaken in this study. Previous studies have found that some of these problems can be alleviated through the use of mass lumping, or the use of an alternative scheme such as the Newton scheme. While such developments were beyond the scope of this study, they may be worth pursuing to improve future applications of the model.

The mass balance errors of the SUBIEF2D model code certainly placed restrictions on the quantification of chemical transport processes in this study. These errors result from the way solute concentration is interpolated linearly across the elements of the finite element mesh, and are most noticeable at the model boundary when the solute is first introduced to the domain, as this is where the concentration gradient is steepest. An attempt was made to correct this error, where possible, but such a correction was only an approximation. This approximation of the mass of solute in the domain was felt to be worthwhile for this study,

as at least it provided some indication of the solute mass for comparison purposes, but certainly could not be relied upon for quantitative analysis. An improvement to this aspect of the model would certainly be worthwhile, as it would allow more reliable quantification of the solute mass balance of the floodplain system.

Another extension to the solute model which may provide an interesting insight into floodplain water and chemical movement is the addition of a particle tracking routine. The present study has indicated areas of the floodplain into which water from various sources would move, but particle tracking would enable a more robust analysis of these general indications. It would be especially valuable in a case such as the lowland River Severn, where residence times have been indicated to be quite long, as once the solute is highly dispersed, it becomes more difficult to track the progress of the solute using concentration patterns alone. Such an approach would strengthen the initial inferences about solute residence times drawn from this study.

In addition to these developments, the coupled model could also be extended to investigate the transport and transformation of a wider range of chemicals. This could include extending the analysis of nitrate transformation beyond the denitrification process, perhaps including a representation of uptake by vegetation, or other chemical transformation processes. Another avenue to explore, which is of particular relevance to the potential use of floodplains as agricultural buffer zones, would be the transport and transformation of agricultural chemicals such as pesticides (USDA-NRCS, 2000). The choice of chemical transport model for this study is such that extra chemical transport and transformation equations could be implemented relatively easily, once a suitable mathematical description of the processes had been derived.

This thesis explored the effect of three main factors on water and chemical sources, flow paths, and residence time: (i) scale of hydrological event (ii) floodplain scale and (iii) other controlling factors. It is felt that the approach to investigating hypothesis two in particular, which explored floodplain scale, could be improved with the use of artificial geometries and idealised sediment arrangements. The approach adopted in this thesis compared two 'real' floodplain sites; the lowland floodplain of the River Severn and the headwater floodplain of Sleepers River. As the characterisation of the soils at each of these sites was very different (a single, homogeneous soil in the River Severn model, and four soils with different hydraulic properties in the Sleepers River model), it was difficult to isolate those effects on hydrological behaviour that were truly due to scale differences, and those that were due to other differences between the two sites.

Future work could adopt a numerical experimentation approach such as that used by Hanschke and Baird (2001). They constructed a model of an idealised floodplain to test the effect of different piezometer designs and soil types on piezometer response time and resulting hydraulic head readings. By using the theoretical domain, and varying one parameter at a time, Hanschke and Baird (2001) were able to separate clearly the effect of the piezometer design from the effects of the floodplain soil type. In the case of exploring the effect of floodplain scale on water and chemical sources, flow paths and residence time, a theoretical floodplain domain could be constructed, and progressively enlarged while maintaining the same sediment characteristics. Such an approach would allow firmer statements on the potential effects of scale on water flow paths to be made, as any changes in hydrological behaviour would definitely be due to the change in scale, and no other complicating factors.

Further fieldwork (and associated modelling research) could be directed in several interesting areas suggested by this work. A recurring theme throughout this research has been the indication of the importance of the unsaturated zone in determining water and chemical transport in the floodplain. In this study, this effect was most pronounced in the lowland floodplain system, which had an unsaturated zone of up to 5 m at the floodplain surface (the upland riparian zone was almost fully saturated for the duration of the snowmelt event studied here). However, there was no specific field data with which to validate the model results in the unsaturated zone of the lowland floodplain. As this region of the floodplain appears to be so important, future fieldwork efforts may be well spent in investigating the unsaturated zone (for example, measuring soil suctions), and some of the process implications related to it that have been drawn from this study. Future fieldwork could also include investigation of carbon distribution that was found to be significant to the denitrification process, as well as other aspects of floodplain heterogeneity.

On a related note, it was hypothesised during the course of this investigation that the apparent potential of the unsaturated zone to restrict water and solute movement, and hence contribute to extended solute residence times in this region, may be affected by precipitation events which occur after the flood event has passed (i.e. during the low flow periods which characterise the floodplain hydrological regime for the most of the year). The low flow events that were investigated were hypothetical, and included no input of water to the surface of the floodplain as rainfall. This is an area into which the modelling investigation could be extended.

Although modelling of chemical transport has been a focus of this study, only limited chemistry data were available from the field ($\delta^{18}O$ data from the Sleepers River fieldsite, and no chemistry data from the River Severn site). Many of the conclusions of this study have

been made on the basis of literature-derived parameter values, especially for those parameters relating to chemical transport (e.g. dispersion) and transformation (e.g. denitrification model parameters). The decision to use field data to focus on validation of the hydrological rather than the chemical processes has been vindicated, because considerable progress has been made using a thorough understanding of the system hydrological processes as a template for the successful interpretation of chemical transport and transformation processes. However, this line of research may now have reached the stage where some field exploration of chemical movement at the River Severn fieldsite, either through the use of artificially introduced tracers, or investigation of naturally occurring chemicals, would usefully extend the insights that the model has offered.

This research could now be extended to other fieldsites, with the aim of assessing the general applicability of the results presented in this study. The summary table (Table 8.1), and the advances in process understanding it represents, could certainly be used when planning the installation of future floodplain field campaigns to indicate where resources would be best directed.

8.4 Chapter summary

There is a limit to what either fieldwork or modelling alone is able to accomplish, but this research has clearly shown the potential of the combined fieldwork-modelling methodology. The field data and previous body of literature were critical to the success of this approach, because they guided the selection of most important hypothetical scenarios that the model should address. The modelling results may now guide future fieldwork by indicating the processes to look for, and the most important controlling factors to consider. Essentially, this study is seen as one stage in an iterative cycle of fieldwork and modelling; the new process insights inferred by this study can now be taken forward for further testing in the field.

This study has also shown the potential of applying high resolution modelling techniques in hydrology. Such an approach has been long established in hydraulic and groundwater studies, but has been little used in catchment hydrology, despite being available since the 1970s (e.g. Stephenson and Freeze, 1974). Such a modelling approach must be used intelligently to supplement field data, but is capable of driving new research agendas.

In summary, this study has made progress on several levels. A numerical model has been developed which is capable of modelling subsurface water and chemical movement, in the highly dynamic floodplain environment. An identified research need, in terms of the investigation of lowland floodplain systems, has been addressed, and a comparison of headwater and lowland floodplain processes has been attempted for the first time. This has

been carried out within the context of a move towards a more holistic view of the floodplain system, enabling a more comprehensive exploration of the whole range of subsurface flow paths through the system. This moves towards an increased understanding of floodplains as key regulators of hydrological and biogeochemical fluxes through the landscape.

References

Abbott, M. B., Bathurst, J. C., Cunge, J. A., O'Connell, P. E. and Rasmussen, J. 1986a. An introduction to the European Hydrological System – Système Hydrologique Européen, "SHE", 1: History and philosophy of a physically-based, distributed modelling system. *Journal of Hydrology*, 87, 45-59.

Abbott, M. B., Bathurst, J. C., Cunge, J. A., O'Connell, P. E. and Rasmussen, J. 1986b. An introduction to the European Hydrological System – Système Hydrologique Européen, "SHE", 2: Structure of a physically-based, distributed modelling system. *Journal of Hydrology*, 87, 61-77.

Addiscott, T. M. and Wagenet, R. J. 1985. Concepts of solute leaching in soils: a review of modelling approaches. *Journal of Soil Science*, 36, 411-424.

Addy, K. L., Gold, A. J., Groffman, P. M. and Jacinthe, P. A. 1999. Ground water nitrate removal in subsoil of forested and mowed riparian buffer zones. *Journal of Environmental Quality*, 28, 962-970.

Aden, K. and Diekkruger, B. 2000. Modeling pesticide dynamics of four different sites using the model system SIMULAT. *Agricultural Water Management*, 44, 337-355.

Anderson, M. G., Bates, P. D. and Walling, D. E. 1996. The general context for floodplain process research. In: M. G. Anderson, D. E. Walling and P. D. Bates (eds), *Floodplain Processes*. John Wiley and Sons, Chichester, 1-13.

Anderson, M. G. and Burt, T. P. 1990. Process studies in hillslope hydrology: an overview. In: M. G. Anderson and T. P. Burt (eds), *Process Studies in Hillslope Hydrology*. John Wiley and Sons, Chichester, 1-8.

Anderson, M. G. and Rogers, C. C. M. 1987. Catchment scale distributed hydrological models: a discussion of research directions. *Progress in Physical Geography*, 11, 28-51.

Anderson, M. P. 1979. Using models to simulate the movement of contaminants through groundwater flow systems. *Critical Reviews in Environmental Control*, 9, 97-156.

Andrews, R. J., Lloyd, J. W. and Lerner, D. N. 1997. Modelling of nitrate leaching from arable land into unsaturated soil and chalk. 1. Development of a management model for applications of sewage sludge and fertilizer. *Journal of Hydrology*, 200, 179-197.

Aronica, G., Hankin, B. and Beven, K. 1998. Uncertainty and equifinality in calibrating distributed roughness coefficients in a flood propagation model with limited data. *Advances in Water Resources*, 22, 349-365.

Ataie-Ashtiani, B., Volker, R. E. and Lockington, D. A. 1999. Numerical and experimental study of seepage in unconfined aquifers with a periodic boundary condition. *Journal of Hydrology*, 222, 165-184.

Bailey, A. D. 1998. Floodplains and agriculture. In: R. G. Bailey, P. V. José and B. R. Sherwood (eds), *United Kingdom Floodplains*. Westbury Academic and Scientific Publishing, Otley, 11-15.

Baird, A. J. and Gaffney, S. W. 1994. Cylindrical piezometer responses in a humified fen peat. *Nordic Hydrology*, 25, 167-182.

Baird, A. J. and Gaffney, S. W. 1995. A partial explanation of the dependency of hydraulic conductivity on positive pore water pressure in peat soils. *Earth Surface Processes and Landforms*, 20, 561-566.

Bates, H. K. and Spalding, R. F. 1998. Aquifer denitrification as interpreted from in situ microcosm experiments. *Journal of Environmental Quality*, 27, 174-182.

Bates, P. D. and Anderson, M. G. 2001. Validation of hydraulic models. In: M. G. Anderson and P. D. Bates (eds), *Model Validation: Perspectives in Hydrological Science*. John Wiley and Sons, Chichester, 325-356.

Bates, P. D., Anderson, M. G., Baird, L., Walling, D. E. and Simm, D. 1992. Modelling floodplain flows using a two-dimensional finite element model. *Earth Surface Processes and Landforms*, 17, 575-588.

Bates, P. D., Anderson, M. G., Price, D. A., Hardy, R. J. and Smith, C. N. 1996. Analysis and development of hydraulic models for floodplain flows. In: M. G. Anderson, D. E. Walling and P. D. Bates (eds), *Floodplain Processes*. John Wiley and Sons, Chichester, 215-254.

Bates, P. D., Horritt, M. S., Smith, C. N. and Mason, D. 1997. Integrating remote sensing observations of flood hydrology and hydraulic modelling. *Hydrological Processes*, 11, 1777-1795.

Bates, P. D., Stewart, M. D., Desitter, A., Anderson, M. G. and Renaud, J. -P. 2000. Numerical simulation of floodplain hydrology. *Water Resources Research*, 36, 2517-2529.

Bathurst, J. C. 1986. Sensitivity analysis of the Système Hydrologique Européen for an upland catchment. *Journal of Hydrology*, 87, 103-123.

Bear, J. 1972. *Dynamics of Fluids in Porous Media.* Elsevier, New York.

Bear, J. and Verruijt, A. 1987. *Modeling Groundwater Flow and Pollution.* D. Reidel Publishing Company, Dordrecht.

Bencala, K. E. 1993. A perspective on stream-catchment connections. *Journal of the North American Benthological Society*, 12, 44-47.

Beven, K. 1985. Distributed models. In: Anderson, M. G. and Burt, T. P. (eds), *Hydrological Forecasting.* John Wiley and Sons, Chichester, 405-435.

Beven, K. 1989. Changing ideas in hydrology – the case of physically-based models. *Journal of Hydrology*, 105, 157-172.

Beven, K. J. 2000. Uniqueness of place and process representations in hydrological modelling. *Hydrology and Earth System Sciences*, 4, 203-213.

Beven, K. and Binley, A. 1992. The future of distributed models: model calibration and uncertainty prediction. *Hydrological Processes*, 6, 279-298.

Beven, K. and Germann, P. 1982. Macropores and water flow in soils. *Water Resources Research*, 18, 1311-1325.

Biggar, J. W. and Nielsen, D. R. 1976. Spatial variability of the leaching characteristics of a field soil. *Water Resources Research*, 12, 78-84.

Binley, A. and Beven, K. 1989. Modelling heterogeneous Darcian headwaters. In: *British Hydrological Society, 2nd National Symposium, 4-6 September, University of Sheffield, UK.* Institute of Hydrology, Wallingford, 1.17-1.22.

Binley, A. M., Beven, K. J. and Calver, A. 1991. Changing responses in hydrology – assessing the uncertainty in physically based model predictions. *Water Resources Research*, 27, 1253-1261.

Bonell, M. 1998. Selected challenges in runoff generation research in forests from the hillslope to headwater drainage basin scale. *Journal of the American Water Resources Association*, 24, 765-785.

Bosatta, E., Iskander, I. K., Juma, N. G., Kruh, G., Reuss, J. O., Tanji, K. K. and van Veen, J. A. 1981. Soil microbiology. In: M. J. Frissel and J. A. van Veen (eds), *Simulation of Nitrogen Behaviour of Soil-Plant Systems.* Centre for Agricultural Publishing and Documentation, Wageningen, 38-44.

Bren, L. J. 1993. Riparian zone, stream and floodplain issues: a review. *Journal of Hydrology*, 150, 266-300.

Breve, M. A., Skaggs, R. W., Parsons, J. E. and Gilliam, J. W. 1997. DRAINMOD-N: a nitrogen model for artificially drained soils. *Transactions of the American Society of Agricultural Engineers*, 40, 1067-1075.

Bronders, J. 1994. Hydraulic conductivity of a tropical residual soil prone to landslides. *Quarterly Journal of Engineering Geology*, 27, 375-382.

Bronstert, A. 1999. Capabilities and limitations of detailed hillslope hydrological modelling. *Hydrological Processes*, 13, 21-48.

Brooks, R. H. and Corey, A. T. 1964. Hydraulic properties of porous media. *Hydrology Paper No. 3*, Colorado State University, Fort Collins.

Brown, A. G. 1983. Floodplain deposits and accelerated sedimentation in the lower Severn basin. In: K. J. Gregory (ed.), *Background to Palaeohydrology.* John Wiley and Sons, Chichester, 375-397.

Brunet, R. C., Pinay, G., Gazelle, F. and Roques, L. 1994. Role of the floodplain and riparian zone in suspended matter and nitrogen retention in the Ardour River, south-west France. *Regulated Rivers: Research and Management*, 9, 55-63.

Brunke, M. and Gonser, T. 1997. The ecological significance of exchange processes between rivers and groundwater. *Freshwater Biology*, 37, 1-33.

Burford, J. R. and Bremner, J. M. 1975. Relationships between the denitrification capacities of soils and total, water-soluble and readily decomposable soil organic matter. *Soil Biology and Biochemistry*, 7, 389-394.

Burt, T. P. 1997. The hydrological role of floodplains within the drainage basin system. In: N. E. Haycock, T. P. Burt, K. W. T. Goulding and G. Pinay (eds), *Buffer Zones: Their Processes and Potential in Water Protection.* Quest Environmental, Harpenden, 21-31.

Burt, T. P., Bates, P. D., Stewart, M. D., Claxton, A. J., Anderson, M. G. and Price, D. A. 2002. Water table fluctuations within the floodplain of the River Severn, England. *Journal of Hydrology*, 262, 1-20.

Burt, T. P. and Haycock, N. E. 1992. Catchment planning and the nitrate issue: a UK

perspective. *Progress in Physical Geography*, 16, 379-404.

Burt, T. P. and Haycock, N. E. 1996. Linking hillslopes to floodplains. In: M. G. Anderson, D. E. Walling and P. D. Bates (eds), *Floodplain Processes*. John Wiley and Sons, Chichester, 461-492.

Burt, T. P., Matchett, L. S., Goulding, K. W. T., Webster, C. P. and Haycock, N. E. 1999. Denitrification in riparian buffer zones: the role of floodplain hydrology. *Hydrological Processes*, 13, 1451-1463.

Burt, T. P., Matchett, L. S. and Haycock, N. E. 1998. Floodplains as buffer zones. In: R. G. Bailey, P. V. José and B. R. Sherwood (eds), *United Kingdom Floodplains*. Westbury Academic and Scientific Publishing, Otley, 143-151.

Butler, J. J. and Healey, J. M. 1998. Relationship between pumping-test and slug-test parameters: scale effect or artifact? *Ground Water*, 36, 305-313.

Celia, M. A., Bouloutas, E. T. and Zarba, R. L. 1990. A general mass-conservative numerical solution for the unsaturated flow equation. *Water Resources Research*, 26, 1483-1496.

Cey, E. E., Rudolph, D. L., Aravena, R. and Parkin, G. 1999. Role of the riparian zone in controlling the distribution and fate of agricultural nitrogen near a small stream in southern Ontario. *Journal of Contaminant Hydrology*, 37, 45-67.

Chakka, K. B. and Munster, C. L. 1997. Modeling macropore transport of agricultural chemicals on a river floodplain: model formulation. *Transactions of the American Society of Agricultural Engineers*, 40, 1355-1362.

Chescheir, G. M., Gilliam, J. W., Skaggs, R. W., Broadhead, R. G. and Lea, R. 1987. *The hydrology and pollution removal effectiveness of wetland buffer areas receiving pumped agricultural drainage water.* Univ. of N. C., Water Resour. Res. Inst. Rep. 231, Raleigh, N. C., 170pp.

Chestnut, T. J. and McDowell, W. H. 2000. C and N dynamics in the riparian and hyporheic zones of a tropical stream, Luquillo Mountains, Puerto Rico. *Journal of the North American Benthological Society*, 19, 199-214.

Christophersen, N., Neal, C. and Hooper, R. P. 1993. Modelling the hydrochemistry of catchments: a challenge for the scientific method. *Journal of Hydrology*, 152, 1-12.

Cirmo, C. P. and McDonnell, J. J. 1997. Linking the hydrologic and biogeochemical controls of nitrogen transport in near-stream zones of temperate-forested catchments a review. *Journal of Hydrology*, 199, 88-120.

Cloke, H. L. 2001. *Soil Hydrologic Parameters: Information for ESTEL Users.* Internal Report, University of Bristol, UK.

Cooley, R. L. 1971. A finite difference method for variably saturated porous media: application to a single pumping well. *Water Resources Research*, 7, 1607-1625.

Cooley, R. L. 1983. Some new procedures for numerical solution of variably saturated flow problems. *Water Resources Research*, 19, 1271-1285.

Cooper, A. B. 1990. Nitrate depletion in the riparian zone and stream channel of a small headwater catchment. *Hydrobiologia*, 202, 13-26.

Correll, D. L. 1997. Buffer zones and water quality protection: general principles. In: N. E. Haycock, T. P. Burt, K. W. T. Goulding and G. Pinay (eds), *Buffer Zones: Their Processes and Potential in Water Protection.* Quest Environmental, Harpenden, 7-19.

Correll, D. L. 2000. The current status of our knowledge of riparian buffer water quality functions. In: P. J. Wigington and R. L. Beschta (eds), *Riparian Ecology and Management in Multi-Land Use Watersheds.* American Water Resources Association, Middleburg, Virginia, TPS-00-2, 5-10.

Dagan, G. and Bresler, E. 1979. Solute dispersion in unsaturated heterogeneous soil at field scale: I. Theory. *Soil Science Society of America Journal*, 43, 461-467.

Dahm, C. N., Grimm, N. B., Valett, H. M. and Vervier, P. 1998. Nutrient dynamics at the interface between surface waters and groundwaters. *Freshwater Biology*, 40, 427-451.

Davis, S. H., Vertessy, R. A. and Silberstein, R. P. 1999. The sensitivity of a catchment model to soil hydraulic properties obtained by using different measurement techniques. *Hydrological Processes*, 13, 677-688.

Desitter, A. 1998. *Hydro Modelling System: Principal Note and Validation Document Version 1.0.* University of Bristol.

Desitter, A., Bates, P. D., Anderson, M. G. and Hervouet, J. -M. 2000. Development of one, two and three-dimensional finite element groundwater models within a generalized object-oriented framework. *Hydrological Processes*, 14, 2245-2259.

Deutsch, W. J. 1997. *Groundwater Chemistry: Fundamentals and Applications to Contamination.* Lewis Publishers, New York.

Devito, K. J., Hill, A. R. and Roulet, N. 1996. Groundwater-surface water interactions in headwater forested wetlands of the Canadian Shield. *Journal of Hydrology*, 181, 127-147.

Diersch, H. -J. G. and Perrochet, P. 1999. On the primary variable switching technique for simulating unsaturated-saturated flows. *Advances in Water Resources*, 23, 271-301.

Dils, R. M. and Heathwaite, A. L. 1996. Phosphorus fractionation in hillslope hydrological pathways contributing to agricultural runoff. In: M. G. Anderson and S. M. Brooks, *Advances in Hillslope Processes, Volume One.* John Wiley and Sons, Chichester, 229-251.

Domenico, P. A. and Schwartz, F. W. 1990. *Physical and Chemical Hydrogeology.* John Wiley and Sons, New York.

Duff, J. H. and Triska, F. J. 2000. Nitrogen biogeochemistry and surface-subsurface exchange in streams. In: J. B. Jones and P. J. Mulholland (eds), *Streams and Ground Waters.* Academic Press, New York, 197-220.

Dullien, F. A. L. 1979. *Porous Media: Fluid Transport and Pore Structure.* Academic Press, New York.

Dunne, T. 1978. Field studies of hillslope flow processes. In: M. J. Kirkby (ed.), *Hillslope Hydrology.* John Wiley and Sons, Chichester, 227-293.

Dwire, K. A., Kauffman, J. B. and Baham, J. 2000. Relations among redox potentials, water levels, and riparian vegetation. In: P. J. Wigington and R. L. Beschta (eds), *Riparian Ecology and Management in Multi-Land Use Watersheds.* American Water Resources Association, Middleburg, Virginia, TPS-00-2, 23-28.

Feddes, R. A., Kabat, P., van Bakel, P. J. T., Bronswijk, J. J. B. and Halbertsma, J. 1998. Modelling soil water dynamics in the unsaturated zone – state of the art. *Journal of Hydrology*, 69-111.

Fernald, A., Landers, D. and Wigington, P. J. 2000. Water quality effects of hyporheic processing in a large river. In: P. J. Wigington and R. L. Beschta (eds), *Riparian Ecology and Management in Multi-Land Use Watersheds.* American Water Resources Association, Middleburg, Virginia, TPS-00-2, 167-172.

Firestone, M. K. 1982. Biological denitrification. In: F. J. Stevenson (ed.), *Nitrogen in Agricultural Soils.* Agronomy Monograph No. 22, American Society of Agronomy, Wisconsin, 289-326.

Flügel, W. –A. and Smith, R. E. 1999. Integrated process studies and modelling simulations of hillslope hydrology and interflow dynamics using the HILLS model. *Environmental Modelling and Software*, 14, 153-160.

Freeze, R. A. 1971. Three-dimensional transient saturated-unsaturated flow in a groundwater basin. *Water Resources Research*, 7, 347-366.

Freeze, R. A. 1978. Mathematical models of hillslope hydrology. In: M. J. Kirkby (ed.), *Hillslope Hydrology*. John Wiley and Sons, Chichester, 177-225.

Freeze, R. A. and Cherry, J. A. 1979. *Groundwater*. Prentice Hall, New Jersey.

Freissinet, C., Vauclin, M. and Erlich, M. 1999. Comparison of first-order analysis and fuzzy set approach for the evaluation of imprecision in a pesticide groundwater pollution screening model. *Journal of Contaminant Hydrology*, 37, 21-43.

Gardiner, J. L. 1998. Floodplain management in the United Kingdom. In: R. G. Bailey, P. V. José and B. R. Sherwood (eds), *United Kingdom Floodplains*. Westbury Academic and Scientific Publishing, Otley, 17-26.

Gee, D. M., Anderson, M. G. and Baird, L. 1990. Large-scale floodplain modelling. *Earth Surface Processes and Landforms*, 15, 513-523.

Gillham, R. W. 1991. Nitrate contamination of groundwater in Southern Ontario and the evidence for denitrification. In: I. Bogardi and R. D. Kuzelka (eds.), *Nitrate Contamination: Exposure, Consequence and Control*. Springer-Verlag, Berlin, 181-198.

Gilliam, J. W., Parsons, J. E., and Mikkelsen, R. L. 1997. Nitrogen dynamics and buffer zones. In: N. E. Haycock, T. P. Burt, K. W. T. Goulding and G. Pinay (eds), *Buffer Zones: Their Processes and Potential in Water Protection*. Quest Environmental, Harpenden, 54-61.

Gold, A. J., Groffman, P. M., Addy, K., Kellogg, D. Q. and Rosenblatt, A. E. 2000. The role of landscape setting in riparian groundwater nitrate removal. In: P. J. Wigington and R. L. Beschta (eds), *Riparian Ecology and Management in Multi-Land Use Watersheds*. American Water Resources Association, Middleburg, Virginia, TPS-00-2, 113-118.

Gold, A. J., Jacinthe, P. A., Groffman, P. M., Wright, W. R. and Puffer, R. H. 1998. Patchiness in groundwater nitrate removal in a riparian forest. *Journal of Environmental Quality*, 27, 146-155.

Gold, A. J. and Kellogg, D. Q. 1997. Modelling internal processes of riparian buffer zones. In: N. E. Haycock, T. P. Burt, K. W. T. Goulding and G. Pinay (eds), *Buffer Zones: Their Processes and Potential in Water Protection*. Quest Environmental, Harpenden, 192-207.

Grant, R. F. 1991. A technique for estimating denitrification rates at different soil temperatures, water contents, and nitrate concentrations. *Soil Science*, 152, 41-52.

Grayson, R. B., Moore, I. D. and McMahon, T. A. 1992. Physically based hydrologic modelling 2: is the concept realistic? *Water Resources Research*, 26, 2659-2666.

Grimaldi, C. and Chaplot, V. 2000. Nitrate depletion during within-stream transport: effects of exchange processes between streamwater, the hyporheic and riparian zones. *Water Air and Soil Pollution*, 124, 95-112.

Groffman, P. M., Howard, G., Gold, A. J. and Nelson, W. M. 1996. Microbial nitrate processing in shallow groundwater in a riparian forest. *Journal of Environmental Quality*, 25, 1309-1316.

Grundmann, G. L. and Rolston, D. E. 1987. A water function approximation to degree of anaerobiosis associated with denitrification. *Soil Science*, 144, 437-441.

Hakenkamp, C. C., Valett, H. M. and Boulton, A. J. 1993. Perspectives on the hyporheic zone: integrating hydrology and biology. Concluding remarks. *Journal of the North American Benthological Society*, 12, 94-99.

Hanschke, T. and Baird, A. J. 2001. Time-lag errors associated with the use of simple standpipe piezometers in wetland soils. *Wetlands*, 21, 412-421.

Harlin, J. and Kung, C. –S. 1992. Parameter uncertainty and simulation of design floods in Sweden. *Journal of Hydrology*, 137, 209-230.

Harvey, J. W. and Bencala, K. E. 1993. The effect of streambed topopgraphy on surface-subsurface water exchange in mountain catchments. *Water Resources Research*, 29, 89-98.

Harvey, J. W. and Wagner, B. J. 2000. Quantifying hydrologic interactions between streams and their subsurface hyporheic zones. In: J. B. Jones and P. J. Mulholland (eds), *Streams and Ground Waters*. Academic Press, New York, 3-44.

Haycock, N. E. and Burt, T. P. 1993. Role of floodplain sediments in reducing the nitrate concentration of subsurface run-off: a case study in the Cotswolds, UK. *Hydrological Processes*, 7, 287-295.

Haycock, N. E. and Pinay, G. 1993. Groundwater nitrate dynamics in grass and poplar vegetated riparian buffer strips during the winter. *Journal of Environmental Quality*, 22, 273-278.

Haycock, N. E., Pinay, G., Burt, T. P. and Goulding K. W. T. 1997. Buffer zones: current concerns and future directions. In: N. E. Haycock, T. P. Burt, K. W. T. Goulding and G. Pinay (eds), *Buffer Zones: Their Processes and Potential in Water Protection*. Quest Environmental, Harpenden, 305-313.

Hedin, L. O., von Fischer, J. C., Ostrom, N. E., Kennedy, B. P., Brown, M. G. and Robertson, G. P. 1998. Thermodynamic constraints on nitrogen transformations and other biogeochemical processes at soil-stream interfaces. *Ecology*, 79, 684-703.

Hénault, C. and Germon, J. C. 2000. NEMIS, a predictive model of denitrification on the field scale. *European Journal of Soil Science*, 51, 257-270.

Hendricks, S. P. 1993. Microbial ecology of the hyporheic zone: a perspective integrating hydrology and biology. *Journal of the North American Benthological Society*, 12, 70-78.

Hendricks, S. P. and White, D. S. 1995. Seasonal biogeochemical patterns in surface-water, subsurface hyporheic, and riparian ground-water in a temperate stream ecosystem. *Archiv für Hydrobiologie*, 134, 459-490.

Henrich, M. and Haselwandter, K. *1991.* Denitrifying potential and enzyme activity in a Norway spruce forest. *Forest Ecology and Management*, 44, 63-68.

Heppell, C. M., Burt, T. P., Williams, R. J. and Haria, A. H. 1999. The influence of hydrological pathways on the transport of the herbicide, isoproturon, through an underdrained clay soil. *Water, Science and Technology*, 39, 77-84.

Hill, A, R. 1996. Nitrate removal in stream riparian zones. *Journal of Environmental Quality*, 25, 743-755.

Hill, A. R. 1997. The potential role of in-stream and hyporheic environments as buffer zones. In: N. E. Haycock, T. P. Burt, K. W. T. Goulding and G. Pinay (eds). *Buffer Zones: Their Processes and Potential in Water Protection.* Quest Environmental, Harpenden, 115-127.

Hill, A. R. 2000. Stream chemistry and riparian zones. In: J. B. Jones and P. J. Mulholland (eds), *Streams and Ground Waters.* Academic Press, New York, 83-110.

Hill, A. R., Devito, K. J., Campagnolo, S. and Sanmugadas, K. 2000. Subsurface denitrification in a forest riparian zone: interactions between hydrology and supplies of nitrate and organic carbon. *Biogeochemistry*, 51, 193-223.

Hill, A. R., Labadia, C. F. and Sanmugadas, K. 1998. Hyporheic zone hydrology and nitrogen dynamics in relation to the streambed topography of a N-rich stream. *Biogeochemistry*, 42, 285-310.

Hill, A. R. and Lymburner, D. J. 1998. Hyporheic zone chemistry and stream-subsurface exchange in two groundwater-fed streams. *Canadian Journal of Fisheries and Aquatic Sciences*, 55, 495-506.

Holmes, N. T. H. 1998. Floodplain restoration. In: R. G. Bailey, P. V. José and B. R. Sherwood (eds), *United Kingdom Floodplains*. Westbury Academic and Scientific Publishing, Otley, 331-348.

Hornberger, G. M. and Spear, R. C. 1981. An approach to the preliminary analysis of environmental systems. *Journal of Environmental Management*, 12, 7-18.

Howes, S. and Anderson, M. G. 1988. Computer simulation in geomorphology. In: M. G. Anderson (ed.), *Modelling Geomorphological Systems*. John Wiley and Sons, Chichester, 421-440.

Huang, K., Mohanty, B. P. and van Genuchten, M. Th. 1996. A new convergence criterion for the modified Picard iteration method to solve the variably saturated flow equation. *Journal of Hydrology*, 178, 69-91.

Huggenberger, P., Hoehn, E., Beschta, R. and Woessner, W. 1998. Abiotic aspects of channels and floodplains in riparian ecology. *Freshwater Biology*, 40, 407-425.

Hvorslev, M. J. 1951. *Time Lag and Soil Permeability in Ground-Water Observations*. Bulletin No. 36, Waterways Experiment Station, Corps of Engineers, Vicksburg, Mississippi.

Hynes, H. B. N. 1983. Ground water and stream ecology. *Hydrobiologia*, 100, 93-99.

Inamdar, S. P., Mitchell, M. J. and McDonnell, J. J. 2000. Topographic and riparian controls on hydrologic and biogeochemical response of forested catchments. In: P. J. Wigington and R. L. Beschta (eds), *Riparian Ecology and Management in Multi-Land Use Watersheds*. American Water Resources Association, Middleburg, Virginia, TPS-00-2, 137-142.

James, A. 1993. *An Introduction to Water Quality Modelling*. John Wiley and Sons, Chichester.

Jarvis, S. C. and Hatch, D. J. 1994. Potential for denitrification at depth below long-term grass swards. *Soil Biology and Biochemistry*, 26, 1629-1636.

Johnsson, H., Klemedtsson, L., Nilsson, A. and Svensson, B. H. 1991. Simulation of field scale denitrification losses from soils under grass ley and barley. *Plant and Soil*, 138, 287-302.

Jolly, I. D., Narayan, K. A., Armstrong, D. and Walker, G. R. 1998. The impact of flooding on modelling salt transport processes to streams. *Environmental Modelling and Software*, 13, 87-104.

Jordan, T. E., Correll, D. L. and Weller, D. E. 1993. Nutrient interception by a riparian forest receiving inputs from adjacent cropland. *Journal of Environmental Quality*, 22, 467-473.

Jorgensen, R. G. and Richter, G. M. 1992. Composition of carbon fractions and potential denitrification in drained peat soils. *Journal of Soil Science*, 43, 347-358.

Kirkby, M. J. (ed.) 1994. *Process Models and Theoretical Geomorphology*. John Wiley and Sons, Chichester.

Klemedtsson, L., Klemedtsson, A. K., Moldan, F. and Weslien, P. 1997. Nitrous oxide emission from Swedish forest soils in relation to liming and simulated increated N-deposition. *Biology and Fertility of Soils*, 25, 290-295.

Knighton, D. 1998. *Fluvial Forms and Processes: a New Perspective*. Arnold, London.

Konikow, L. F. 1992. The modelling process and model validation – discussion. *Groundwater*, 30, 622-623.

Konikow, L. F. and Bredehoeft, J. D. 1992. Ground-water models cannot be validated. *Advances In Water Research*, 15, 75-83.

Konikow, L. F. and Patten, E. P. 1985. Groundwater forecasting. In: M. G. Anderson and T. P. Burt (eds), *Hydrological Forecasting*. John Wiley and Sons, Chichester, 221-270.

Kruh, G. and Segall, E. 1981. Nitrogen dynamics in soil. In: M. J. Frissel and J. A. van Veen (eds), *Simulation of Nitrogen Behaviour of Soil-Plant Systems*. Centre for Agricultural Publishing and Documentation, Wageningen, 109-125.

Kuczera, G. and Parent, E. 1998. Monte Carlo assessment of parameter uncertainty in conceptual catchment models: the Metropolis algorithm. *Journal of Hydrology*, 211, 69-85.

Lamb, R., Beven, K. and Myrabø, S. 1998. Use of spatially distributed water table observations to constrain uncertainty in a rainfall-runoff model. *Advances in Water Resources*, 22, 305-317.

Landon, J. R. (ed.) 1984. *Booker Tropical Soil Manual*. Longman, New York.

Lane, S. N. and Richards, K. S. 2001. The validation of hydrodynamic models: some critical perspectives. In: M. G. Anderson and P. D. Bates (eds), *Model Validation: Perspectives in Hydrological Science*. John Wiley and Sons, Chichester, 413-438.

Linn, D. M. and Doran, J. W. 1984. Effect of water-filled pore space on carbon dioxide and nitrous oxide production in tilled and nontilled soils. *Soil Science Society of America Journal*, 48, 1267-1272.

Lloyd, D. 1993. Aerobic denitrification in soils and sediments – from fallacies to facts. *Trends in Ecology and Evolution*, 8, 352-356.

Lucille, P. L., Burnol, A. and Ollar, Ph. 2000. Chemtrap: a hydrogeochemical model for reactive transport in porous media. *Hydrological Processes*, 14, 2261-2277.

Malhi, S. S., McGill, W. B. and Nyborg, M. 1990. Nitrate losses in soils – effect of temperature, moisture and substrate concentration. *Soil Biology and Biochemistry*, 22, 733-737.

Maltby, E., McInnes, R. J., Hutchins, M. G. and Hogan, D. V. 1998. Assessment of wetland functioning in the river marginal environment: recent scientific progress and future priorities. In: R. G. Bailey, P. V. José and B. R. Sherwood (eds), *United Kingdom Floodplains*. Westbury Academic and Scientific Publishing, Otley, 153-168.

Marriot, S. B. 1998. Channel-floodplain interactions and sediment deposition on floodplains. In: R. G. Bailey, P. V. José and B. R. Sherwood (eds), *United Kingdom Floodplains*. Westbury Academic and Scientific Publishing, Otley, 43-61.

Matchett, L. S. 1998. *Denitrification in riparian buffer zones*. DPhil Thesis, University of Oxford, UK.

McGill, W. B., Hunt, H. W., Woodmansee, R. G., Reuss, J. O. and Paustian, K. H. 1981. Formulation, process controls, parameters and performance of PHOENIX: a model of carbon and nitrogen dynamics in grassland soils. In: M. J. Frissel and J. A. van Veen (eds), *Simulation of Nitrogen Behaviour of Soil-Plant Systems*. Centre for Agricultural Publishing and Documentation, Wageningen, 171-191.

McGlynn, B. L., McDonnell, J. J., Shanley, J. B. and Kendall, C. 1999. Riparian zone flowpath dynamics during snowmelt in a small headwater catchment. *Journal of Hydrology*, 222, 75-92.

Melching, C. S. 1994. Reliability estimation. In: V. P. Singh (ed.), *Computer Models of Watershed Hydrology*. Water Resources Publications, 69-118.

Mengis, M., Schiff, S. L., Harris, M., English, M. C., Aravena, R., Elgood, R. J. and MacLean, A. 1999. Multiple geochemical and isotopic approaches for assessing groundwater NO_3^- elimination in a riparian zone. *Ground Water*, 37, 448-457.

Mercer, J. W. and Faust, C. R. 1980. Ground-water modelling: an overview. *Ground Water*, 18, 108-115.

Mertes, L. A. K. 1997. Documentation and significance of the perirheic zone on inundated floodplains. *Water Resources Research*, 33, 1749-1762.

Meyer, P. D., Rockhold, M. L. and Gee, G. W. 1997. *Uncertainty Analyses of Infiltration and Subsurface Flow and Transport for SDMP Sites.* US Nuclear Regulatory Commission. Report NUREG/CR-6565.

Miller, D. R., Butler, G. and Bramall, L. 1976. Validation of ecological system models. *Journal of Environmental Management*, 4, 383-401.

Mitchell, R. J. and Mayer, A. S. 1998. A numerical model for transient-hysteretic flow and solute transport in unsaturated porous media. *Journal of Contaminant Hydrology*, 50, 243-264.

Montgomery, D. R. 1999. Process domains and the river continuum. *Journal of the American Water Resources Association*, 35, 397-410.

Morel-Seytoux, H. J. 2001. Groundwater. In: M. G. Anderson and P. D. Bates (eds), *Model Validation: Perspectives in Hydrological Science.* John Wiley and Sons, Chichester, 293-323.

Morel-Seytoux, H. J., Meyer, P. D., Nachabe, M., Touma, J., van Genuchten, M. T., and Lenhard, R. J. 1996. Parameter equivalence for the Brooks-Corey and van Genuchten soil characteristics: preserving the effective capillary drive. *Water Resources Research*, 32, 1251-1258.

Morrice, J. A., Valett, H. M., Dahm, C. N. and Campana, M. E. 1997. Alluvial characteristics, groundwater-surface water exchange and hydrological retention in headwater streams. *Hydrological Processes*, 11, 253-267.

Morton, A. and Suárez, M. 2001. Kinds of models. In: M. G. Anderson and P. D. Bates (eds), *Model Validation: Perspectives in Hydrological Science.* John Wiley and Sons, Chichester, 11-21.

Moulin, C. and Ben Slama, E. 1998. The two-dimensional transport model SUBIEF. Applications to sediment transport and water quality processes. *Hydrological Processes*, 12, 1183-1195.

Moulin, C. and Gailhard, J. 1996. *SUBIEF V3P1 User Manual.* Département Laboratoire National d'Hydraulique, Report HE-43/95/074/B.

Murray, R. E., Parsons, L. L. and Smith, M. S. 1989. Kinetics of nitrate utilization by mixed populations of denitrifying bacteria. *Applied and Environmental Microbiology*, 55, 717-721.

Narasimhan, T. N. 1979. The significance of the storage parameter in saturated-unsaturated groundwater flow. *Water Resources Research*, 15, 569-576.

Narasimhan, T. N. and Kanehiro, B. Y. 1980. A note on the meaning of the storage coefficient. *Water Resources Research*, 16, 423-429.

Narasimhan, T. N. and Witherspoon, P. A. 1977. Numerical model for saturated-unsaturated flow in deformable porous media 1. Theory. *Water Resources Research*, 13, 657-664.

Narasimhan, T. N. and Witherspoon, P. A. 1978. Numerical model for saturated-unsaturated flow in deformable porous media 3. Applications. *Water Resources Research*, 14, 1017, 1034.

Narasimhan, T. N., Witherspoon, P. A. and Edwards, A. L. 1978. Numerical model for saturated-unsaturated flow in deformable porous media 2. The algorithm. *Water Resources Research*, 14, 255-261.

Neuman, S. P. 1973. Saturated-unsaturated seepage by finite elements. *Journal of the Hydraulics Division*, 99, 2233-2250.

Nielsen, D. R., van Genuchten, M. Th. and Biggar, J. W. 1986. Water flow and solute transport processes in the unsaturated zone. *Water Resources Research*, 22, 89S-108S.

Norris, V. 1993. The use of buffer zones to protect water quality: a review. *Water Resources Management*, 7, 257-272.

NRCS, 1997. *Buffer Strips: Common Sense Conservation* [www document]. <http://www.nhq.nrcs.usda.gov/CCS/Buffers.html> (accessed 2 April 2002).

O'Connell, P. E. and Todini, E. 1996. Modelling of rainfall, flow and mass transport in hydrological systems: an overview. *Journal of Hydrology*, 175, 3-16.

Ogden, F. L. and Watts, B. A. 2000. Saturated area formation on nonconvergent hillslope topography with shallow soils: a numerical investigation. *Water Resources Research*, 36, 1795-1804.

Ohrui, K. and Mitchell, M. J. 1998. Spatial patterns of soil nitrate in Japanese forested watersheds: importance of the near-stream zone as a source of nitrate in stream water. *Hydrological Processes*, 12, 1433-1445.

Oreskes, N. and Belitz, K. 2001. Philosophical issues in model assessment. In: M. G. Anderson and P. D. Bates (eds), *Model Validation: Perspectives in Hydrological Science*. John Wiley and Sons, Chichester, 23-41.

Oreskes, N., Shrader-Frechette, K. and Belitz, K. 1994. Verification, validation, and confirmation of numerical models in the earth sciences. *Science*, 263, 641-646.

Padilla, I. Y., Yeh, T. C. J. and Conklin, M. H. 1999. The effect of water content on solute transport in unsaturated porous media. *Water Resources Research*, 35, 3303-3313.

Palmer, M. A. 1993. Experimentation in the hyporheic zone: challenges and perspectives. *Journal of the North American Benthological Society*, 12, 84-93.

Paniconi, C., Aldama, A. A. and Wood, E. F. 1991. Numerical evaluation of iterative and noniterative methods for the solution of the nonlinear Richards equation. *Water Resources Research*, 27, 1147-1163.

Paniconi, C. and Putti, M. 1994. A comparison of Picard and Newton iteration in the numerical solution of multidimensional variably saturated flow problems. *Water Resources Research*, 30, 3357-3374.

Paniconi, C. and Wood, E. F. 1993. A detailed model for simulation of catchment scale subsurface hydrologic processes. *Water Resources Research*, 29, 1601-1620.

Parkin, G., O'Donnell, G., Ewen, J., Bathurst, J. C., O'Connell, P. E. and Lavabre, J. 1996. Validation of catchment models for predicting land-use and climate change impacts. 2. Case study for a Mediterranean catchment. *Journal of Hydrology*, 175, 595-613.

Paul, E. A. and Clarke, F. E. 1996. *Soil Microbiology and Biochemistry*. Academic Press, San Diego.

Payne, W. J. 1981. *Denitrification*. John Wiley and Sons, New York.

Peterjohn, W. T. and Correll, D. L. 1984. Nutrient dynamics in an agricultural watershed: observations on the role of a riparian forest. *Ecology*, 65, 1466-1475.

Petts, G. E. 1998. Floodplain rivers and their restoration: a European perspective. In: R. G. Bailey, P. V. José and B. R. Sherwood (eds), *United Kingdom Floodplains*. Westbury Academic and Scientific Publishing, Otley, 29-41.

Phillips, J. D. 1989. Nonpoint source pollution control effectiveness of riparian forests along a coastal plain river. *Journal of Hydrology*, 110, 221-237.

Pinay, G., Black, V. J., Planty-Tabacchi, A. M., Gumiero, B. and Décamps, H. 2000. Geomorphic control of denitrification in large river floodplain soils. *Biogeochemistry*, 50, 163-182.

Pinay, G. and Burt, T. P. (eds) 2001. *Nitrogen Control by Landscape Structures, Final Report 1997-2000*. Research Project 1997-2000, European Commission DGXII Environment and Climate: ENV4-CT97-0395. 129pp.

Price, D. A. 1997. An integrated approach to modelling floodplain hydraulics, hydrology and nitrate chemistry. *Unpublished PhD Thesis*, University of Bristol, Bristol, England, pp. 250.

Pusch, M., Fiebig, D., Brettar, I., Eisenmann, H., Ellis, B. K., Kaplan, L. A., Lock, M. A., Naegeli, M. W. and Traunspurger, W. 1998. The role of micro-organisms in the ecological connectivity of running waters. *Freshwater Biology*, 40, 453-495.

Quinn, J., Taylor, A., Boyce, W. and Fenton, T. 2000. Riparian zone classification improves management of stream water quality and aquatic ecosystems. In: P. J. Wigington and R. L. Beschta (eds), *Riparian Ecology and Management in Multi-Land Use Watersheds*. American Water Resources Association, Middleburg, Virginia, TPS-00-2, 451-455.

Reddy, K. R., Khaleel, R., Overcash, M. R. and Westerman, P. W. 1979. A non-point source model for land areas receiving animal wastes: mineralization of organic nitrogen. *American Society of Agricultural Engineering*, 22, 863-874.

Reddy, K. R., Rao, P. S. and Jessup, R. E. 1982. The effect of carbon mineralization on denitrification kinetics in mineral and organic soils. *Soil Science Society of America Journal*, 46, 62-68.

Refsgaard, J. 2001. Discussion of model validation in relation to the regional and global scale. In: M. G. Anderson and P. D. Bates (eds), *Model Validation: Perspectives in Hydrological Science*. John Wiley and Sons, Chichester, 461-483.

Refsgaard, J. C. and Knudsen, J. 1996. Operational validation and intercomparison of different types of hydrological models. *Water Resources Research*, 32, 2189-2202.

Rice, S. P. 1994. Towards a model of changes in bed material texture at the drainage basin scale. In: M. J. Kirkby (ed.), *Process Models and Theoretical Gemorphology*. John Wiley and Sons, Chichester, 159-172.

Ritchie, W., Wood, M., Wright, R. and Tait, D. 1988. *Surveying and Mapping for Field Scientists*. Longman Scientific and Technical, Harlow.

Roache, P. J. 1998. *Verification and Validation in Computational Science and Engineering*. Hermosa Publishers, Albuquerque, New Mexico.

Rodrigo, A., Recous, S., Neel, C. and Mary, B. 1997. Modelling temperature and moisture effects on C-N transformations in soils: comparison of nine models. *Ecological Modelling*, 102, 325-339.

Rogers, C. C. M., Beven, K. J., Morris, E. M. and Anderson, M. G. 1985. Sensitivity analysis, calibration and predictive uncertainty of the Institute of Hydrology Distributed Model. *Journal of Hydrology*, 81, 179-191.

Rolston, D. E., Rao, P. S. C., Davidson, J. M. and Jessup, R. E. 1984. Simulation of denitrification losses of nitrate fertilizer applied to uncropped, cropped, and manure-amended field plots. *Soil Science*, 137, 270-279.

Romano, C. G., Frind, E. O. and Rudolph, D. L. 1999. Significance of unsaturated flow and seepage faces in the simulation of steady-state subsurface flow. *Ground Water*, 37, 625-632.

Rubin, J. 1968. Theoretical analysis of two-dimensional transient flow of water in unsaturated and partly unsaturated soils. *Soils Science Society of America Proceedings*, 32, 607-615.

Rulon, J. J., Rodway, R. and Freeze, R. A. 1985. The development of multiple seepage faces on layered slopes. *Water Resources Research*, 21, 1625-1636.

Rykiel, E. J. 1994. The meaning of models. *Science*, 264, 330-331.

Sánchez Pérez, J. M., Trémolières, M., Takatert, N., Ackerer, P., Eichhorn, A. and Maire, G. 1999. Quantification of nitrate removal by a flooded alluvial zone in the Ill floodplain (Eastern France). *Hydrobiologia*, 410, 185-193.

Sargent, R. G. 1982. Verification and validation of simulation models. In: F. E. Cellier (ed.), *Progress in Modelling and Simulation*. Academic Press, London, 159-169.

Schlesinger, S., Crosbie, R. E., Gagné, R. E., Innis, G. S., Lalwani, C. S., Loch, J., Sylvester, R. J., Wright, R. D., Khier, N. and Bartos, D. 1979. Terminology for model credibility. *Simulation*, 32, 103-104.

Schipper, L. A. and Vojvodić-Vuković, M. 1998. Nitrate removal from groundwater using a denitrification wall amended with sawdust: field trial. *Journal of Environmental Quality*, 27, 664-668.

Sear, D. A., Armitage, P. D. and Dawson, F. H. 1999. Groundwater dominated rivers. *Hydrological Processes*, 13, 255-276.

Selim, H. M. and Iskander, I. K. 1981. Modeling nitrogen transport and transformations in soils: 1. Theoretical considerations. *Soil Science*, 131, 233-241.

Šimek, M., Cooper, J. E., Picek, T. and Šantrůčková, H. 2000. Denitrification in arable soils in relation to their physico-chemical properties and fertilization practice. *Soil Biology and Biochemistry*, 32, 101-110.

Sklash, M. G. 1990. Environmental isotope studies of storm and snowmelt runoff generation. In: M. G. Anderson and T. P. Burt (eds), *Process Studies in Hillslope Hydrology*. John Wiley and Sons, Chichester, 401-435.

Smith, C. N. 1998. Calibration, validation and uncertainty estimation in high resolution hydraulic modelling. *Unpublished PhD Thesis*, University of Bristol, UK.

Smith, R. L. and Duff, J. H. 1988. Denitrification in a sand and gravel aquifer. *Applied Environmental Microbiology*, 54, 1071-1078.

Smith, M. S. and Tiedje, J. M. 1979. Phases of denitrification following oxygen depletion in soil. *Soil Biology and Biochemistry*, 11, 261-267.

Sparks, D. L. 1995. *Environmental Soil Chemistry*. Academic Press, San Diego.

Spitz, K. and Moreno, J. 1996. *A Practical Guide to Groundwater and Solute Transport Modelling*. John Wiley and Sons, New York.

Spruill, T. B. and Galeone, D. R. 2000. Effectiveness of riparian buffers in reducing nitrate-nitrogen concentrations in groundwater. In: P. J. Wigington and R. L. Beschta (eds), *Riparian Ecology and Management in Multi-Land Use Watersheds*. American Water Resources Association, Middleburg, Virginia, TPS-00-2, 119-124.

Squillace, P. J. 1996. Observed and simulated movement of bank-storage water. *Ground Water*, 34, 121-134.

Stanford, J. A. 1998. Rivers in the landscape: introduction to the special issue on riparian and groundwater ecology. *Freshwater Biology*, 40, 402-406.

Stanford, G., Vander Pol, R. A. and Dzienia, S. 1975. Denitrification rates in relation to total and extractable soil carbon. *Soil Science Society of America Proceedings*, 39, 284-289.

Stanford, J. A. and Ward, J. V. 1988. The hyporheic habitat of river ecosystems. *Nature*, 335, 64-66.

Stanford, J. A. and Ward, J. V. 1993. An ecosystem perspective of alluvial rivers: connectivity and the hyporheic corridor. *Journal of the North American Benthological Society*, 12, 48-60.

Stanley, E. H. and Jones, J. B. 2000. Surface-subsuface interactions: past, present, and future. In: J. B. Jones and P. J. Mulholland (eds), *Streams and Ground Waters*. Academic Press, 405-417.

Steele, T. D. 1985. Water quality. In: M. G. Anderson and T. P. Burt (eds), *Hydrological Forecasting*. John Wiley and Sons, Chichester, 271-309.

Steenhuis, T., Vandenheuvel, K., Weiler, K. W., Boll, J., Dailparthy, J., Herbert, S. and Samuel Kung, K. –J. 1998. Mapping and interpreting soil textural layers to assess agri-chemical movement at several scales along the eastern seaboard (USA). *Nutrient Cycling in Agroecosystems*, 50, 91-97.

Stephenson, G. R. and Freeze, R. A. 1974. Mathematical simulation of subsurface flow contributions to snowmelt runoff, Reynolds Creek Watershed, Idaho. *Water Resources Research*, 10, 284-294.

Stevenson, F. J. 1982. Origin and distribution of nitrogen in soil. In: F. J. Stevenson (ed.), *Nitrogen in Agricultural Soils*, Agronomy Monograph No. 22, American Society of Agronomy, Wisconsin, 1-42.

Stewart, M. D., Bates, P. D., Anderson, M. G., Price, D. A. and Burt, T. P. 1999. Modelling floods in hydrologically complex lowland river reaches. *Journal of Hydrology*, 223, 85-106.

Stewart, M. D., Bates, P. D., Price, D. A. and Burt, T. P. 1998. Modelling the spatial variability in floodplain soil contamination during flood events to improve chemical mass balance estimates. *Hydrological Processes*, 12, 1233-1255.

Tanji, K. K. 1982. Modeling of the soil nitrogen cycle. In: F. J. Stevenson (ed.), *Nitrogen in Agricultural Soils*, Agronomy Monograph No. 22, American Society of Agronomy, Wisconsin, 721-772.

Todd, D. K. 1955. Groundwater flow in relation to a flooding stream. *Proceedings of the American Society of Civil Engineers*, 81, 628.

Tracy, F. T. 1995. 1-D, 2-D and 3-D analytical solutions of unsaturated flow in groundwater. *Journal of Hydrology*, 170, 199-214.

Triska, F. J., Duff, J. H. and Avanzino, R. J. 1990. Influence of exchange flow between the channel and hyporheic zone on nitrate production in a small mountain stream. *Canadian Journal of Fisheries and Aquatic Sciences*, 47, 2099-2111.

Triska, F. J., Duff, J. H. and Avanzino, R. J. 1993. The role of water exchange between a stream channel and its hyporheic zone in nitrogen cycling at the terrestrial aquatic interface. *Hydrobiologia*, 251, 167-184.

Triska, F. J., Kennedy, V. C., Avanzino, R. J., Zellweger, G. W. and Bencala, K. E. 1989. Retention and transport of nutrients in a third-order stream in northwestern California: hyporheic processes. *Ecology*, 70, 1893-1905.

Troendle, C. A. 1985. Variable Source Area models. In: M. G. Anderson and T. P. Burt (eds), *Hydrological Forecasting*. John Wiley and Sons, Chichester, 347-403.

Trudell, M. R., Gillham, R. W. and Cherry, J. A. 1986. An in-situ study of the occurrence and rate of denitrification in a shallow unconfined sand aquifer. *Journal of Hydrology*, 83, 251-268.

Tychon, B., Vander Borght, P. and De Backer, L. W. 1999. Water and nitrogen transfer study through soils of a small agricultural water catchment. *Water Science and Technology*, 39, 69-76.

USDA-NRCS, 2000. *Conservation Buffers to Reduce Pesticide Losses.* Natural Resources Conservation Service, Fort Worth. 21pp.

Valett, H. M., Hakenkamp, C. C. and Boulton, A. J. 1993. Perspectives on the hyporheic zone: integrating hydrology and biology. Introduction. *Journal of the North American Benthological Society*, 12, 40-43.

Valett, H. M., Morrice, J. A., Dahm, C. N. and Campana, M. E. 1996. Parent lithology, surface-groundwater exchange, and nitrate retention in headwater streams. *Limnology and Oceanography*, 41, 333-345.

van der Peijl, M. J. and Verhoeven, J. T. A. 2000. Carbon, nitrogen and phosphorus cycling in river marginal wetlands; examination of landscape geochemical flow. *Biogeochemistry*, 50, 45-71.

van Genuchten, M. Th. 1980. A closed-form equation for predicting the hydraulic conductivity of unsaturated soils. *Soil Science Society of America Journal*, 44, 892-898.

van Lanen, H. A. J. and Dijksma, R. 1999. Water and nitrate transport to a groundwater-fed stream in the Belgian-Dutch chalk region. *Hydrological Processes*, 13, 295-307.

van Veen, J. A. and Frissel, M. J. 1981. Simulation model of the behaviour of N in soil. In: M. J. Frissel and J. A. van Veen (eds), *Simulation of Nitrogen Behaviour of Soil-Plant Systems.* Centre for Agricultural Publishing and Documentation, Wageningen, 126-144.

Vauclin, M., Vachaud, G. and Khanji, D. K. 1975. Two-dimensional numerical analysis of transient water transfer in saturated-unsaturated soils. In: G. C. Vansteenkiste (ed.), *Computer Simulations in Water Resources Systems.* North-Holland, Amsterdam, 299-323.

Verchot, L. V., Franklin, E. C. and Gilliam, J. W. 1998. Effects of agricultural runoff dispersion on nitrate reduction in forested filter zone soils. *Soil Science Society of America Journal*, 62, 1719-1724.

Vogel, T., van Genuchten, M. Th. and Cislerova, M. 2001. Effect of the shape of the soil hydraulic functions near saturation on variably-saturated flow problems. *Advances in Water Resources*, 24, 133-144.

Voss, C. I. 1984. *SUTRA: A finite element simulation model for saturated-unsaturated fluid-density-dependent groundwater flow with energy transport or chemically reactive species solute transport.* USGS Water Resources Investigations Report 84-4369, Reston.

Wang, H. F. and Anderson, M. P. 1982. *Introduction to Groundwater Modeling.* W. H. Freeman and Company, San Francisco.

Ward, T. 1985. Characterizing the aerobic and anaerobic microbial activities in surface and subsurface soils. *Environmental Toxicology and Chemistry*, 4, 727-737.

Ward, J. V., Malard, F., Tockner, K. and Uehlinger, U. 1999. Influence of ground water on surface water conditions in a glacial floodplain of the Swiss Alps. *Hydrological Processes*, 13, 277-293.

Watts, G. 1997. Hydrological modelling in practice. In: R. L. Wilby (ed.), *Contemporary Hydrology: Towards Holistic Environmental Science.* John Wiley and Sons, Chichester, 151-194.

Wexler, E. J. 1992. *Analytical Solutions for One-, Two-, and Three-Dimensional Solute Transport in Ground-Water Systems with Uniform Flow.* Chapter B7, Techniques of Water-Resources Investigations of the United States Geological Survey, USGS, Denver.

White, D. S. 1993. Perspectives on defining and delineating hyporheic zones. *Journal of the North American Benthological Society*, 12, 61-69.

White, D. S., Elzinga, C. H. and Hendricks, S. P. 1987. Temperature patterns within the hyporheic zone of a northern Michigan river. *Journal of the North American Benthological Society*, 6, 85-91.

Whiting, P. J. and Pomeranets, M. 1997. A numerical study of bank storage and its contribution to streamflow. *Journal of Hydrology*, 202, 121-136.

Williams, R. G., Lowrance, R. and Inamdar, S. P. 2000. Simulation of nonpoint source pollution control using the Riparian Ecosystem Management Model (REMM). In: P. J. Wigington and R. L. Beschta (eds), *Riparian Ecology and Management in Multi-Land Use Watersheds.* American Water Resources Association, Middleburg, Virginia, TPS-00-2, 433-438.

Winter, T. C. 1995. Recent advances in understanding the interaction of groundwater and surface water. *Reviews of Geophysics*, Supplement, 985-994.

Withers, P. J. A. and Jarvis, S. C. 1998. Mitigation options for diffuse phosphorus loss to water. *Soil Use and Management*, 14, 186-192.

Woessner, W. W. 2000. Stream and fluvial plain ground water interactions: rescaling hydrogeologic thought. *Ground Water*, 38, 423-429.

Wondzell, S. M. and Swanson, F. J. 1996. Seasonal and storm dynamics of the hyporheic zone of a 4th-order mountain stream. I: Hydrologic processes. *Journal of the North American Benthological Society*, 15, 3-19.

Wondzell, S. M. and Swanson, F. J. 1999. Floods, channel change, and the hyporheic zone. *Water Resources Research*, 35, 555-567.

Wood, W. L. and Calver, A. 1992. Initial conditions for hillslope hydrology modelling. *Journal of Hydrology*, 130, 379-397.

Wroblicky, G. J., Campana, M. E., Valett, H. M. and Dahm, C. N. 1998. Seasonal variation in surface-subsurface water exchange and lateral hyporheic area of two stream-aquifer systems. *Water Resources Research*, 34, 317-328.

Wu, L. and McGechan, M. B. 1998. A review of carbon and nitrogen processes in four soil nitrogen dynamics models. *Journal of Agricultural Engineering Research*, 69, 279-305.

Yeomans, J. C., Bremner, J. M. and McCarty, G. W. 1992. Denitrification capacity and denitrification potential of subsurface soils. *Communication in Soil Science and Plant Analyses*, 23, 919-927.

Yeh, G. T. and Tripathi, V. S. 1991. A model for simulating transport of reactive multispecies components – model development and demonstration. *Water Resources Research*, 27, 3075-3094.

Yeh, G. T. and Ward, D. S. 1980. *FEMWATER: A Finite Element Model of Water Flow Through Saturated-Unsaturated Porous Media.* ORNL-5567, Oak Ridge National Laboratory, Oak Ridge.

Yoshinari, T., Hynes, R. and Knowles, R. 1977. Acetylene inhibition of nitrous oxide reduction and measurement of denitrification and nitrogen fixation in soil. *Soil Biology and Biochemistry*, 9, 177-183.

Zijl, W. 1999. Scale aspects of groundwater flow and transport systems. *Hydrogeology Journal*, 7, 139-150.